Abstract

Arctic ice masses have rapidly lost mass during the past two decades, coincident with marked climatic and oceanic change. Accelerated ice discharge through marine-terminating outlet glaciers has been a primary contributor to deficits. However, substantial uncertainty exists over the factors controlling Arctic outlet glacier dynamics and their spatial variation. This thesis aims to quantify outlet glacier retreat rates across the Atlantic sector of the Arctic and to assess observed changes in relation to climatic, oceanic and glacier-specific controls. Results from a study region in north-west Greenland recorded dramatic retreat on Alison Glacier, coincident with marked atmospheric warming and sea ice decline. However, retreat rates varied substantially within the region, suggesting that fjord width variability and basal topography were important controls on glacier response to external forcing. The influence of fjord width variability was further explored on Novaya Zemlya, Russian High Arctic, where a statistically significant relationship between total retreat and along-fjord width variation was found and the first empirical categories of this relationship were defined. Here, retreat rates were an order of magnitude greater on marine-terminating outlets than on land-terminating glaciers and accelerated retreat from 2000 onwards was linked to sea ice decline. In a further case study, Humboldt Glacier, northern Greenland, retreated rapidly from 1999, coincident with atmospheric warming. However, retreat rates were an order of magnitude greater on its northern section, due to a major subglacial trough, which strongly modulated its response to external forcing. Overall, during the past decade, outlet glacier retreat was widespread and rapid in the Atlantic Arctic. Although some regional-scale patterns of retreat and response to forcing were evident, retreat rates varied markedly. Fjord width variation was identified as an important and widespread control on outlet glacier retreat, which highlights the need to consider glacier-specific factors when forecasting glacier response to climate change.

Ice-ocean-atmosphere interactions in the Arctic Seas

Joanne Rachel Carr

A thesis submitted in partial fulfilment of the requirements of the University of Durham for the degree of Doctor of Philosophy

December 2013

Department of Geography

University of Durham

Table of Contents

List of Tables

List of Figures

Chapter 1

Chapter 2

Chapter 3

Chapter 4

Declaration

This thesis embodies the results of original research carried out between October 2010 and October 2013. References to existing works are made as appropriate. Any remaining errors or omissions are the responsibility of the author. For each chapter within this thesis, the author carried out the data analysis, led the paper development, wrote the text and created the figures. Co-authors provide editorial input, guidance on the development of research, datasets and/or technical expertise with numerical modelling. A full description of the author contributions to each chapter are detailed in Chapter 1.

J. Rachel Carr

23rd October, 2013

Statement of Copyright

Acknowledgements

First, I would like to thank my supervisors, Dr. Chris Stokes and Professor Andreas Vieli for their help and support with this project. Next, I offer my thanks to my parents, as this thesis would not have been possible without their continuous support and encouragement in all aspects of my life. I would also like to thank my boyfriend for his tolerance and support throughout.

I am grateful to Durham University for funding this project through a Durham Doctoral Studentship and for providing me with the financial means to attend scientific conferences, which have been crucial to my development as a researcher. I also thank the Hatfield Trust, as they have provided valuable financial support for conference attendance. I am grateful to the European Space Agency for granting me access to the data required for the project.

I would like to thank the numerous people in the Geography Department at Durham who have contributed to my Ph.D. project, particularly Dr. Stewart Jamieson for his patient assistance with numerical modelling and Dr. Nick Cox for his help with statistics. I am very grateful to the many scientists from other institutions who provided helpful input on my papers and conference presentations. Finally, I wish to thank the broader community within the Durham University Geography Department for making the last three years a very productive and highly enjoyable time in my life.

Chapter 1: Introduction

1.1. Background & motivation

The Arctic is currently undergoing dramatic environmental change, including rapid glacier retreat, sea ice decline, and marked atmospheric warming [*IPCC*, 2013]. These trends are likely to continue during the 21st century, as Arctic warming is predicted to far exceed the global average and to reach up to 8.3 ºC by 2100 [*IPCC*, 2013]. During the past two decades, Arctic ice masses have rapidly lost mass and contributed substantially to sea level rise [e.g *Gardner et al.*, 2013; *IPCC*, 2013; *Shepherd et al.*, 2012]. The largest single source of mass loss has been the Greenland Ice Sheet (GrIS), where deficits totalled 142 ± 49 Gt a^{-1} between 1992 and 2011 and contributed 0.39 ± 0.14 mm a^{-1} to sea level rise [*Shepherd et al.*, 2012]. Other Arctic ice masses underwent rapid ice loss between 2003 and 2009, specifically northern Arctic Canada (–33 ± 4 Gt a^{-1}), southern Arctic Canada (–27 ± 4 Gt a^{-1}), Alaska (–50 ± 17 Gt a^{-1}), Russian Arctic (–11 ± 4 Gt a^{-1}) and Svalbard (–5 ± 2 Gt a^{-1}) [*Gardner et al.*, 2013]. Given the large potential contribution of Arctic ice masses to contemporary and near-future sea level rise, it is imperative to understand the causes of these dramatic recent losses.

Loss from Arctic masses occurs via two main mechanisms, namely negative surface mass balance (SMB) and accelerated ice discharge from marine-terminating outlet glaciers. SMB is determined by the balance between accumulation of snow at higher elevations and melting at lower altitudes [*Benn and Evans*, 2010]. On the GrIS and Canadian High Arctic, recent negative SMB has predominantly resulted from a marked increase in surface melt rates relative to accumulation [e.g. *Gardner et al.*, 2011; *Rignot et al.*, 2008; *van den Broeke et al.*, 2009; *Zwally et al.*, 2011]. Ice loss can also occur via changes in the dynamics of marine-terminating outlet glaciers, which are fast-moving channels of ice that drain an ice cap or ice sheet and terminate in the ocean [*Benn and Evans*, 2010]. These glaciers are able to respond very rapidly to forcing at their marine boundary [e.g. *Howat et al.*, 2008; *Moon et al.*, 2012; *Vieli and Nick*, 2011]

and can produce large mass deficits over annual to decadal timescales [e.g. *Pritchard et al.*, 2009; *Rignot et al.*, 2008]. Thus, they provide a key mechanism by which Arctic ice masses can respond rapidly and dynamically to climate change. However, substantial uncertainty exists over the main controls on marine-terminating outlet glacier behaviour and this was identified as a primary uncertainty by the IPCC Fourth Assessment Report [*IPCC*, 2007].

Not only do outlet glaciers play a key role in ice sheet stability at short (annual to decadal) timescales, but also at the scale of glacial/interglacial cycles. Almost all ice sheets during the Quaternary are thought to have had substantial marine margins [*Hughes*, 2002], which could retreat by up to several hundred kilometres from the edge of continental shelves during interglacial periods [*Dowdeswell et al.*, 2008b] and provided a mechanism for rapid ice loss and potentially ice sheet collapse [e.g. *Dowdeswell et al.*, 2008b; *Hughes*, 2002; *Hughes*, 1986]. This is consistent with observations of submarine landform assemblages in the Arctic and Antarctic, which record rapid retreat in certain areas (e.g. Marguerite Trough, Antarctica and Traena Trough, Norway), but notably also recorded landforms consistent with both slow (e.g. Bellsund, Svalbard) and episodic retreat (e.g. Larsen A Ice Shelf, Antarctica and Vestfjorden, Norway) [*Dowdeswell et al.*, 2008b].

One potential mechanism proposed to explain the collapse of marine-terminating ice sheets at the end of a glacial cycle was the development of positive feedbacks on ice streams, associated with meltwater input to the bed and/or reduced ice shelf buttressing [*Hughes*, 1986]. Rapid retreat of marine-terminating margins during interglacials, particularly the West Antarctica Ice Sheet (WAIS), has also been linked to instabilities that developed due to the location of the ice sheet grounding line below sea level and on areas of reverse sloping bedrock [e.g. *Joughin and Alley*, 2011; *Mercer*, 1968]. In addition to their potential role in deglaciation, outlet glaciers and ice streams may also influence ice mass stability at millennial timescales. This is exemplified by the Hudson Strait Ice Stream of the Laurentide Ice Sheet, which periodically (~ 7 k.a.)

discharged large volumes of icebergs into the northern North Atlantic [*Heinrich*, 1988] and thus strongly influenced the dynamics of its parent ice mass. Taken together, this evidence highlights the strong influence of marine-terminating outlets on ice sheet behaviour at a range of timescales and underscores the need to investigate the factors controlling their behaviour. The uncertainty over the factors controlling marine-terminating outlet glacier dynamics was the primary motivation for this study. In particular, these controls had previously been assessed on a comparatively small number of study glaciers, mostly on the GrIS. As a result, our understanding of the spatial variation in Arctic outlet glacier retreat rates and their response to forcing was limited. This is very important for understanding future change in the Arctic, as incorrectly extrapolating retreat rates and/or their relationship to forcing can lead to large under- or over-estimates of ice loss and contribution to sea level rise. Consequently, this study compares outlet glacier retreat rates and response to forcing across the Atlantic sector of the Arctic (Section 1.2).

A further motivating factor for the project was the need to investigate the role of local factors, particularly basal topography and fjord width variation, in modulating glacier response to external forcing. Increasing concern over anthropogenic warming from the 1990s onwards and rapid, synchronous retreat in certain areas [e.g. *Howat et al.*, 2008; *Murray et al.*, 2010] led researchers to focus on external controls on glacier retreat, particularly air temperatures. However, the large variability in retreat rates and ice velocities in other regions [e.g. *Carr et al.*, 2013; *McFadden et al.*, 2011; *Moon et al.*, 2012], suggested that factors specific to individual glaciers could substantially influence their behaviour. Importantly, this implies that we may not be able to forecast or interpret glacier behaviour on the basis of climatic or oceanic change alone, but that we also need to account for these glacier-specific factors.

Evidence has also highlighted the influence of glacier-specific factors on ice mass dynamics at millennial to glacial/interglacial timescales and suggests that they may play a key role in determining ice mass stability and non-linear behaviour. A prominent

example is provided by the WAIS, which may be unstable due to its location on a reverse sloping bed [*Hughes*, 1975; *Mercer*, 1968]. Evidence from a range of sources, including geological data [*Mercer*, 1968], diatom records [*Scherer et al.*, 1998] and sea level data [*Bamber et al.*, 2009; *Kopp et al.*, 2009], indicates that the WAIS may have collapsed during the last interglacial, or was at least much less extensive. This illustrates the potential influence of basal topography on ice mass stability and has raised concerns over a similar collapse occur on the contemporary Greenland and Antarctic Ice Sheets, significant portions of which lay below present-day sea level [*Bamber et al.*, 2013; *Joughin and Alley*, 2011; *Morlighem et al.*, 2014]. In addition to basal topographic controls, lateral variations in fjord width also influence glacier dynamics at glacial/interglacial timescales. Studies of retreat since the Last Glacial Maximum (LGM) in West Greenland[*Warren and Hulton*, 1990] and on the Marguerite Bay Ice Stream, Antarctica [*Jamieson et al.*, 2012] demonstrated that temporary stabilisations occurred at lateral constrictions, even on a reverse sloping bed. Glacier-specific factors may therefore influence glacier dynamics and ice mass behaviour on a wide range of timescales, from seasonal to glacial/interglacial periods. As a result, improving our understanding of glacier-specific controls is crucial for accurate interpretation and prediction of glacier response to forcing, and therefore forms a major component of this study.

1.2. Study region

The project study region is broadly defined as the Atlantic sector of the Arctic and is bounded by the co-ordinates 70˚ W to 70˚ E, 85˚ N to 60˚ N (Fig. 1.1). For the purposes of this study, it is referred to as the ‘Atlantic Arctic’. This region was selected for a number of reasons. First, it contains the vast majority of large, marine-terminating Arctic outlet glaciers. Second, it encompasses the area potentially influenced by water of North Atlantic origin, and climatic and oceanic conditions vary substantially across the region. Consequently, the region allows us to assess differences in outlet glacier behaviour and response to forcing for a wide range of climatic and oceanic conditions.

Finally, the region includes a broad range of glacier sizes, fjord geometries and glaciological settings, with the parent ice masses ranging from the scale of an ice sheet to a small ice cap. As a result, glacier response to forcing can be evaluated for a variety of glacier geometries and fjord topographies. The study region includes four main glaciated areas, namely the Greenland Ice Sheet (GrIS), Svalbard (SVB), Novaya Zemlya (NVZ) and Franz Josef Land (FJL) (Fig. 1.1). The glaciological, climatic and oceanic characteristics of these regions are briefly outlined below.

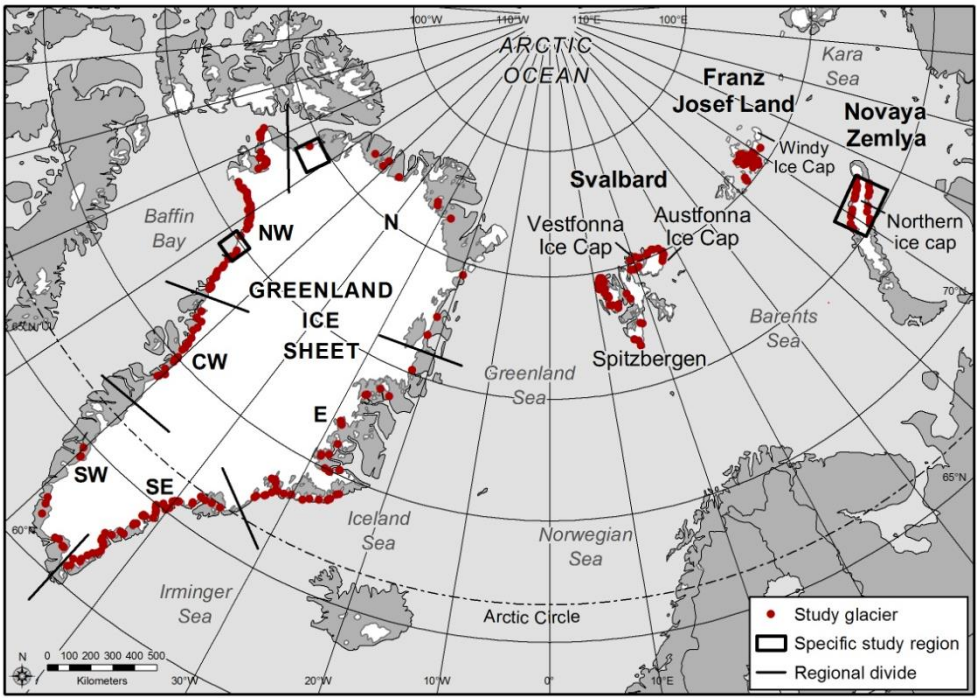

Figure 1.1. Location map, showing major ice masses, specific study regions, regional divides and study glaciers. Black boxes delineate the specific study regions discussed in Chapters 3-5. The regional divides for the GrIS are marked with black dividing lines and study glaciers are symbolised with a red dot.

1.2.1. Greenland Ice Sheet

The GrIS is the largest Arctic ice mass, containing approximately 2.8 million km^3 of ice [*Christoffersen and Hambrey*, 2006]. It has undergone rapid and well publicised ice loss in the past two decades, with recent estimates suggesting that the deficit between 1992 and 2011 totalled 142 ± 49 Gt a^{-1} [*Shepherd et al.*, 2012] and that ice loss accelerated by 21.9 ± 1 Gt a^{-2} between 1992 and 2010 [*Rignot et al.*, 2011]. During this period, the GrIS has experienced rapid glacier retreat, at rates of up to kilometres per year [e.g. *Howat et al.*, 2008; *Joughin et al.*, 2010a; *McFadden et al.*, 2011], and

widespread dynamic thinning and acceleration [e.g. *Moon et al.*, 2012; *Pritchard et al.*, 2009].

The basal topography of the GrIS has recently been mapped using two approaches: compilation of available airbourne ice thickness measurements (Fig. 1.2A) [*Bamber et al.*, 2013] and on the basis of mass conservation (Fig. 1.2B) [*Morlighem et al.*, 2014]. Both datasets suggest that significant portions of the ice sheet interior are located below sea level (Fig. 1.2). Notably, a number of the large outlet glacier basins in northern Greenland, such as Humboldt Glacier, Peterman Glacier and 79 Glacier, all have substantial sections located below sea level and occupy deep troughs that extend far into the interior [*Bamber et al.*, 2013; *Morlighem et al.*, 2014]. Theory suggests that outlets glaciers and ice sheets that are grounded below sea level are unstable and can undergo catastrophic collapse, due to the development of positive feedbacks as the ice front retreats into progressively deeper water [*Hughes*, 1986; *Meier and Post*, 1987; *Mercer*, 1978; *Weertman*, 1974]. However, more recent work has demonstrated that stable grounding line positions can be achieved on a reverse bedrock slope [*Gudmundsson et al.*, 2012; *Jamieson et al.*, 2012; *Nick et al.*, 2010], suggesting that the location of the grounding line on a reverse slope is not necessarily a precursor to rapid retreat.

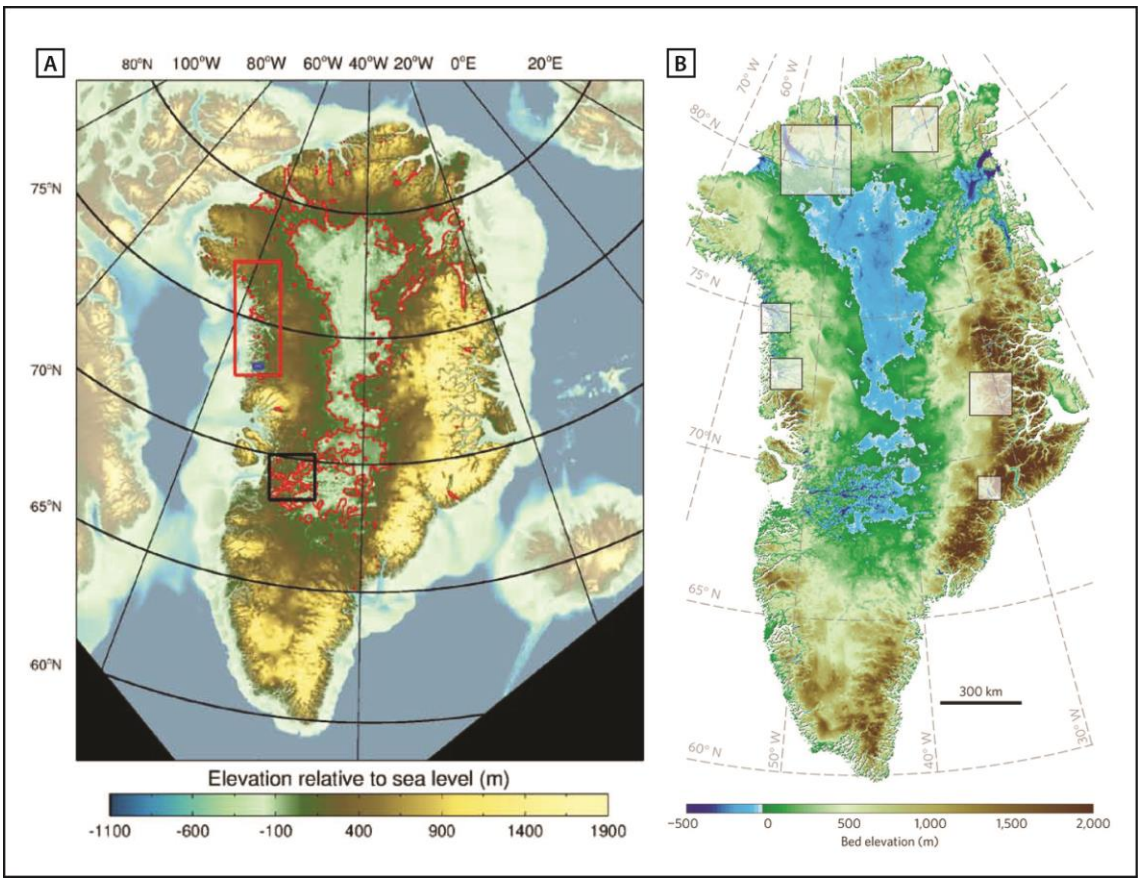

Figure 1.2. Greenland ice sheet basal topography. A) Basal elevations determined from compiled airbourne ice thickness measurements. Areas below sea level are outlined in red. Source: *Bamber et al.* [2013]. B) Basal topography calculated using the mass conservation approach. Areas below sea level are coloured in blue. Source: *Morlighem et al.* [2014].

Marked atmospheric warming has occurred in the region since the 1990s [e.g. *Hanna et al.*, 2008] and the number of extreme warm events was higher in the 2000s than any other period since at least 1890 [*Mernild et al.*, 2013]. Within the context of accelerating sea ice loss across the Arctic [*Stroeve et al.*, 2012], the length of the ice-free season increased markedly around Greenland between 1976 and 2006, particularly in the Davis Strait area (+52 days), Scoresby Sund (+55 days) and western Greenland Sea (+56 days) [*Rodrigues*, 2008; 2009].

Atlantic Water (AW) has been detected in several major GrIS outlet glacier fjords and is thought to have a substantial impact on glacier behaviour [*Christoffersen et al.*, 2011; *Holland et al.*, 2008; *Johnson et al.*, 2011; *Mayer et al.*, 2000; *Straneo et al.*, 2011; *Straneo et al.*, 2010]. AW originally enters the Atlantic sector of the Arctic between

Iceland and Norway and travels north in the West Spitzbergen Current (WSC) (Fig. 1.3). It then re-circulates at the Fram Strait, where it is overridden by cool, fresh Polar Surface Water (PSW) from the Arctic Ocean [*Rudels et al.*, 2005; *Sutherland and Pickart*, 2008]. AW forms a sub-surface temperature maximum within the East Greenland Current (EGC), at approximately 200 to 800 m depth, beneath the PSW [*Rudels et al.*, 2005; *Sutherland and Pickart*, 2008]. The EGC flows southwards along the continental shelf, along with a cool, fresh surface current, named the East Greenland Coastal Current (EGCC) (Fig. 1.3) [*Bacon et al.*, 2002; *Sutherland and Pickart*, 2008]. This current is thought to be primarily driven by glacial runoff [*Bacon et al.*, 2002] and its variability has been linked to recent changes in outlet glacier dynamics in south-east Greenland [*Murray et al.*, 2010]. Warm AW also flows along the Greenland continental shelf in the Irminger Sea, as part of the Irminger Current (IC) (Fig. 1.3) [*Pickart et al.*, 2005; *Sutherland and Pickart*, 2008]. At Cape Farewell, the IC flows beneath the PSW to form a layer of warm (~4.5˚C), modified AW at depths of 200 to 700 m [*Ribergaard et al.*, 2008; *Straneo*, 2006]. These water masses flow northwards as the West Greenland Current (WGC) and gradually mix [*Ribergaard et al.*, 2008; *Straneo*, 2006]. At the Davis Strait, the WGC bifurcates: one branch re-circulates in the Labrador Sea and the other continues northwards along the Greenland coast and into Baffin Bay [*Ribergaard et al.*, 2008; *Straneo*, 2006]. Although forecasting future changes is complex, models suggest that oceanic warming around the GrIS may reach 1.7 to 2 ºC by 2100 [*Yin et al.*, 2012] and marked changes in temperature and salinity have occurred in the region since the 1990s [*Holliday et al.*, 2008; *Stein*, 2005].

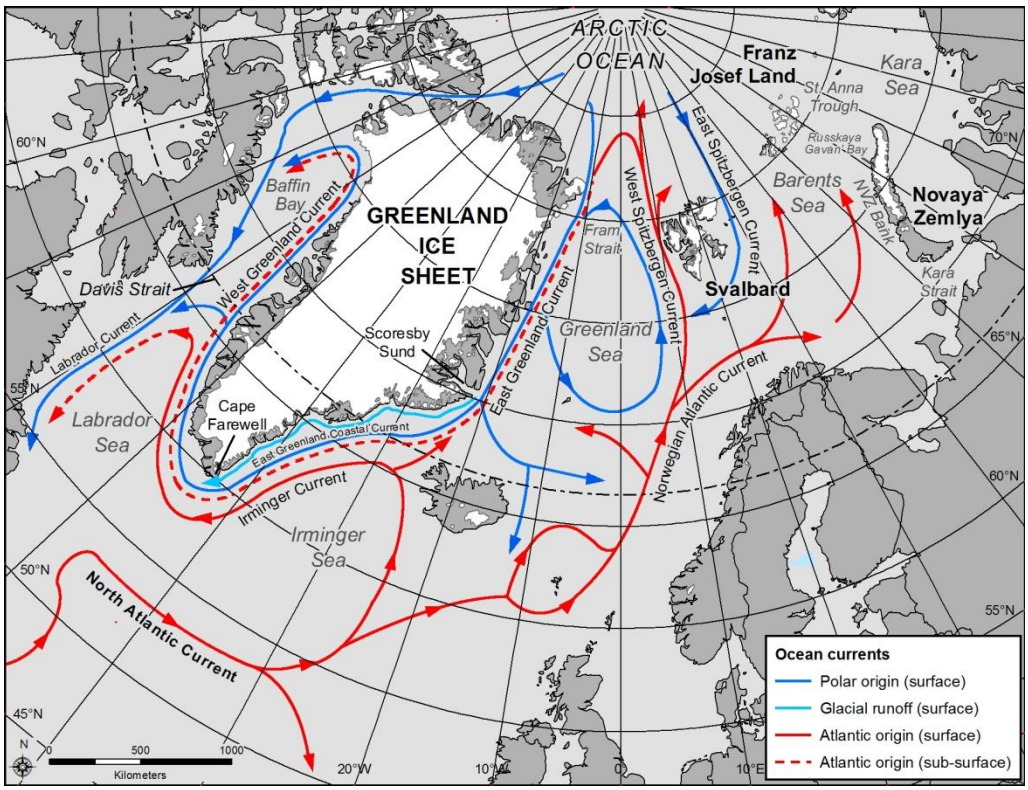

Figure 1.3. *Location of major ocean currents of Arctic and North Atlantic Oceans, in relation to major ice masses. Currents of Atlantic origin are indicated in red, those of polar origin are in dark blue and those fed primarily by glacial runoff are in light blue.*

1.2.2. Svalbard

Svalbard comprises of three main areas, namely Spitzbergen, Austfonna and Vestfonna (Fig. 1.1). The total ice-covered area of Svalbard is 35,000 km^2, which accounts for 6% of global ice cover outside of the polar ice sheets [*Moholdt et al.*, 2010b] and 60% of this area is drained by marine-terminating outlet glaciers [*Blaszczyk et al.*, 2009]. Glacier characteristics show a strong longitudinal gradient across Svalbard [e.g. *Hagen et al.*, 2003; *Moholdt et al.*, 2010b; *Nuth et al.*, 2010]. In the west of the archipelago, Spitzbergen is characterised by a series of ice caps, drained by outlet glaciers that are constrained by the mountainous topography, and by small cirque glaciers [e.g. *Hagen et al.*, 2003; *Moholdt et al.*, 2010b]. In contrast, the large ice caps of Austfonna (8120 km^2) and Vestfonna (2450 km^2) occupy Nordaustlandet in the east and are comparatively low-elevation and low-relief [*Dowdeswell*, 1986; *Hagen et al.*, 2003; *Nuth et al.*, 2010]. A large number of glaciers across Svalbard have been

previously identified as surge type [e.g. *Hamilton and Dowdeswell*, 1996; *Sund et al.*, 2009].

The most recent estimates suggest that, overall, Svalbard lost mass at a rate of -5 ± 2 Gt a^{-1} between 2003 and 2009 [*Gardner et al.*, 2013], and ICESat laser altimetry data has been used to separate recent deficits (2003-2008) according to sub-regions [*Moholdt et al.*, 2010b]. The largest ice volume losses have occurred in north-western (−3.40 ± 0.72 km^3 a^{-1}) and southern (−0.71 ± 0.76 km^3 a^{-1}) Spitzbergen [*Moholdt et al.*, 2010b]. In contrast, north-eastern Spitzbergen (+0.52 ± 0.52 km^3 a^{-1}) and Austfonna ice cap (+0.86 ± 0.32 km^3 a^{-1}) have shown a net gain in volume during this period [*Moholdt et al.*, 2010b]. Previous studies have reported a dichotomous pattern of surface elevation change on Austfonna [*Bamber et al.*, 2004; *Bevan et al.*, 2007], with the interior thickening at rates of up to 0.5 m a^{-1} and the margin thinning at 1-3 m a^{-1} between 2003 and 2008 [*Moholdt et al.*, 2010a]. At longer timescales, Austfonna lost an estimated 11 km^2 a^{-1} of ice between 1973 and 2001, predominantly via retreat of its marine-terminating margins [*Dowdeswell et al.*, 2008a]. Recent changes on Vestfonna have received less scientific attention than those on Austfonna, but the most recent estimates suggest ice volume was lost at a rate of 0.39 ± 0.20 km^3 a^{-1} between 2003 and 2008 [*Moholdt et al.*, 2010b].

The climate of Svalbard is strongly influenced by warm water from the North Atlantic, which flows along the west coast of Spitzbergen in the WSC (Fig. 1.3). The temperature of the surface layer of this current is 1-3 ºC [*Blindheim et al.*, 2000], making the climate of Svalbard comparatively warm for its latitude [*Nuth et al.*, 2010]. Precipitation and air temperatures show large temporal variability, at both seasonal and interannual timescales, as Svalbard is located at the boundary between the warm, moist air masses of Atlantic origin and cool, dry polar air masses from the Arctic [*Moholdt et al.*, 2010b]. There is a substantial climatic gradient across the archipelago, with Austfonna and Vestfonna experiencing comparatively cool conditions and receiving moisture from the Barents Sea [*Hagen et al.*, 2003]. In contrast to the warm

WSC, the East Spitzbergen Current is a cold current that originates in the Arctic and flows southwards along the east coast of Austfonna (Fig. 1.3). The seasonal duration of sea ice-free conditions is much longer in west Spitzbergen (299 days in 2006) than on the eastern (76 days in 2006) or northern (61 days in 2006) coasts of Svalbard [*Rodrigues*, 2008].

1.2.3. Novaya Zemlya

Novaya Zemlya (NVZ) is located in the Russian High Arctic (Fig. 1.1) and contains approximately 22,100 km^2 of ice [*Moholdt et al.*, 2012]. The northern ice cap encompasses 95 % of the total glaciated area and all of NVZ's major marine-terminating outlet glaciers [*Dowdeswell and Williams*, 1997; *Sharov*, 2005]. Between 2003 and 2009, NVZ lost mass at a rate of 7.1 ± 1.2 Gt a^{-1}, which accounted for 80% of the total ice loss from the Russian High Arctic during this period [*Moholdt et al.*, 2012].. There is a marked difference in air temperatures, precipitation, ocean conditions and sea ice regime between the Barents and Kara Sea coasts, which reflects the differing exposure of the two coasts to water masses and weather systems from the Atlantic [*Loeng*, 1991; *Zeeberg and Forman*, 2001]. Modified Atlantic Water is present offshore of the Barents Sea coast of NVZ, within the West Novaya Zemlya Current [*Årthun et al.*, 2011; *Ivanov and Shapiro*, 2005; *Pfirman et al.*, 1994], and warm water (3.5 ºC) of Atlantic origin has been recorded in Russkaya Gavan' Bay, immediately offshore of Shokalskogo glacier (Fig. 1.3) [*Politova et al.*, 2012]. Atlantic-derived water masses enter the Kara Sea via the Kara Strait, St. Anna Trough and the passage between Franz Josef Land and NVZ (Fig. 1.3) [*Karcher et al.*, 2003; *Pavlov and Pfirman*, 1995]. However, it is unclear whether this Atlantic-derived water can reach the glacier termini on the Kara Sea coast.

1.2.4. Franz Josef Land

Franz Josef Land (FJL) is an archipelago located in the Russian High Arctic, between 45-65 ºE and 80-82 ºN (Fig. 1.1). Its total area is 16,100 km^2, of which approximately 85 % is glaciated, and its ice is contained within 44 small ice masses [*Dowdeswell et al.*, 1995; *Dowdeswell et al.*, 1994]. Little is known about the region and it has

undergone limited scientific study [*Dowdeswell et al.*, 1994]. Between 2003 and 2009, FJL's mass budget was only slightly negative at -0.6 ± 0.9 Gt a^{-1} [*Moholdt et al.*, 2012] and recent surface elevation change has been variable across the region, with substantial thickening being recorded on Windy Ice Cap, Graham Bell Island (Fig. 1.1), and a mixture of thinning and thickening occurring elsewhere [*Moholdt et al.*, 2012; *Sharov*, 2005]. Water masses of Atlantic origin enter the Kara Sea to the east of FJL, via the St Anna Trough (Fig. 1.3) [*Karcher et al.*, 2003; *Pavlov and Pfirman*, 1995], where water temperatures of ~1.5 °C have been measured at depths of 300 m [*Hanzlick and Aagaard*, 1980]. However, it is not known whether this water comes into contact with outlet glacier termini on FJL.

1.3. Study glaciers

Within each of the aforementioned regions, the study glaciers are large, marine-terminating outlet glaciers and are located on each of the major ice masses within the Atlantic sector of the Arctic (Fig. 1.1). Glaciers previously identified as surge type [e.g. *Blaszczyk et al.*, 2009; *Grant et al.*, 2009; *Weidick*, 1995] were excluded from the analysis. In order to ensure that the analysis of Arctic-wide retreat rates was not significantly influenced by the choice of study glaciers, we included as many outlets as possible, within the constraints of data availability. This totalled 302 glaciers, of which 143 were located on the GrIS, 24 in Spitzbergen, 7 in Vestfonna, 5 in Austfonna, 22 in NVZ and 17 in FJL (Fig. 1.1). The choice of study glaciers was limited by image availability in certain regions, particularly in east Greenland, northern Greenland and FJL.

1.4. Aim and objectives

The aim of the project is to quantify marine-terminating outlet glacier retreat rates in the Atlantic sector of the Arctic between 1992 and 2010 and to evaluate the spatial variation in the primary factors controlling this retreat. The main objectives are as follows:

1. To quantify retreat rates on large, marine-terminating outlet glaciers on the GrIS, SVB, NVZ and FJL between 1992 and 2010.
2. To map changes in climatic and oceanic conditions in the Atlantic sector of the Arctic between 1992 and 2010.
3. To evaluate observed glacier retreat rates, in relation to changes in oceanic and atmospheric forcing.
4. To investigate the impact of fjord width variation on glacier retreat rates and response to forcing.
5. To assess the influence of basal topography on the contemporary dynamics of large Arctic outlet glaciers.

1.5. Approach

In order to achieve the project aim, a combination of remote sensing, GIS (Geographical Information System) and numerical modelling were used. Remotely sensed and directly measured data on climatic, oceanic, glaciological and topographic conditions were compiled in a GIS. Data were then processed using a range of GIS software and techniques. Similar datasets and methods were employed in each of the specific study areas and for the comparison of retreat rates across the Atlantic sector of the Arctic. The exact methods used are detailed in the 'Methods' sections of Chapters 3 to 6. The primary datasets used in the project and the data source(s) are detailed in Table 1.1. In addition to remotely sensed data, a 1-dimensional flowline model was used to investigate the impact of basal topography on the response of Humboldt Glacier, northern Greenland, to external forcing (Chapter 5). The model has previously been used to simulate the dynamic behaviour of large Greenland outlet glaciers in several studies [e.g. *Nick et al.*, 2012; *Nick et al.*, 2013; *Nick et al.*, 2009; *Vieli and Nick*, 2011] and a detailed description of the model is provided in Chapter 5.

Parameter	Dataset	Data source
Glacier frontal position	Synthetic Aperture Radar Precision Image Mode data & Landsat imagery	European Space Agency & USGS GLOVIS
Sea ice	National/Naval Ice Centre sea ice charts	National/Naval Ice Centre
Air temperature	Meteorological stations	KNMI Climate Explorer, Danish Meteorological Institute, Norwegian Meteorological Institute, National Climate Data and Information Archive, Scientific Research Institute of Hydrometeorological Information
SST	MODIS Aqua monthly SST climatology product & NOAA Optimum Interpolation (OI) SST analysis Version 2	NASA Ocean Color Project & NOAA.
Sub-surface ocean temperature	Previously published data	Previously published data
Fjord width variability	Synthetic Aperture Radar Precision Image Mode data & Landsat imagery	European Space Agency & USGS GLOVIS
Basal topography (GrIS only)	CReSIS Level 2 'Ice Thickness, Ice Surface & Ice Bottom' data & Airbourne laser altimetry data (Humboldt Glacier	Center for Remote Sensing of Ice Sheets (CReSIS) & Greenland Outlet Glacier Geophysics project

	only).	
Bathymetry (NVZ only)	1:200,000 scale Russian topographic map sheets	www.topmap.narod.ru
Ice velocity (GrIS only)	MeASUREs velocity grids	[*Joughin et al.*, 2010b]
Ice surface elevation (GrIS only)	Greenland Mapping Project Digital Elevation Model (GIMP DEM)	[*Howat et al.*, 2012]
Ice surface elevation (NVZ only)	IceSAT laser altimetry data	[*Moholdt et al.*, 2012]

Table 1.1. *Primary project data sources, including glacier frontal position, forcing factors, glacier-specific controls, ice velocities and surface elevation data.*

1.6. Thesis structure

The thesis is presented in the seven following chapters. Chapter 2 provides a review of the key literature relating to marine-terminating outlet glacier dynamics. Chapters 3 to 5 present results from the specific study regions and Chapter 6 details findings at the pan-Arctic scale. Chapters 3 to 6 have either been published in peer-reviewed journals or are in preparation for submission. For each paper, the citation information, an overview of the content, the paper motivation, and the author contributions are detailed at the start of each chapter. Chapter 7 provides an overall discussion of key themes emerging from the thesis and Chapter 8 contains the primary conclusions of the thesis.

1.7. References

Årthun, M., R. B. Ingvaldsen, L. H. Smedsrud, and C. Schrum (2011), Dense water formation and circulation in the Barents Sea, *Deep Sea Research Part I: Oceanographic Research Papers*, *58*(8), 801-817, doi:http://dx.doi.org/10.1016/j.dsr.2011.06.001.

Bacon, S., G. Reverdin, I. G. Rigor, and H. M. Snaith (2002), A freshwater jet on the east Greenland shelf, *Journal of Geophysical Research*, *107*(C7), 3068.

Bamber, J., W. Krabill, V. Raper, and J. Dowdeswell (2004), Anomalous recent growth of part of a large Arctic ice cap: Austfonna, Svalbard, *Geophysical Research Letters*, *31*, L12402, doi:10.1029/2004GL019667.

Bamber, J. L., et al. (2013), A new bed elevation dataset for Greenland, *The Cryosphere*, *7*(2), 499-510, doi:10.5194/tc-7-499-2013.

Bamber, J. L., R. E. M. Riva, B. L. A. Vermeersen, and A. M. LeBrocq (2009), Reassessment of the potential sea-level rise from a collapse of the West Antarctic Ice Sheet, *Science*, *324*, 901–903.

Benn, D. I., and D. J. A. Evans (2010), *Glaciers and Glaciation*, Hodder Education, London.

Bevan, S. L., A. Luckman, T. Murray, H. Sykes, and J. Kohler (2007), Positive mass balance during the late 20th century on Austfonna, Svalbard, revealed using satellite radar interferometry, *Annals of Glaciology*, *46*, 117-122.

Blaszczyk, M., J. A. Jania, and J. M. Hagen (2009), Tidewater glaciers of Svalbard: Recent changes and estimates of calving fluxes, *Polish Polar Resarch*, *30*(2), 85–142.

Blindheim, J., V. Borovkov, B. Hansen, S. A. Malmberg, W. R. Turrell, and S. Osterhaus (2000), Upper layer cooling and freshening in the Norwegian Sea in relation to atmospheric forcing, *Deep Sea Research I*, *46*, 655-680.

Carr, J. R., A. Vieli, and C. R. Stokes (2013), Climatic, oceanic and topographic controls on marine-terminating outlet glacier behavior in north-west Greenland at seasonal to interannual timescales, *Journal of Geophysical Research*, *118*(3), 1210-1226.

Christoffersen, P., and M. J. Hambrey (2006), Is the Greenland Ice Sheet in a state of collapse?, *Geology Today*, *22*, 99-104.

Christoffersen, P., R. Mugford, K. J. Heywood, I. Joughin, J. Dowdeswell, J. P. M. Syvitski, A. Luckman, and T. J. Benham (2011), Warming of waters in an East Greenland fjord prior to glacier retreat: mechanisms and connection to large-scale atmospheric conditions, *The Cryosphere*, *5*, 701-714.

Dowdeswell, J. (1986), Drainage basin characteristics of Nordaustlandet ice caps, Svalbard, *Journal of Glaciology*, *32*(10), 31-38.

Dowdeswell, J., T. J. Benham, T. Strozzi, and J. M. Hagen (2008a), Iceberg calving flux and mass balance of the Austfonna ice cap on Nordaustlandet, Svalbard, *Journal of Geophysical Research*, *113*, F03022.

Dowdeswell, J., A. F. Glazovskii, and Y. Y. Macheret (1995), Ice divides and drainage basins on the ice caps of Franz Josef Land, Russian High Arctic, defined from landsat, KFA-1000, and ERS-1 SAR satellite imagery, *Arctic and Alpine Research*, *27*(3), 264-270.

Dowdeswell, J., M. R. Gorman, A. F. Glazovsky, and Y. Y. Mracheret (1994), Evidence for Floating Ice Shelves in Franz Josef Land, Russian High Arctic, *Arctic and Alpine Research*, *26*(1), 86-92.

Dowdeswell, J., and M. Williams (1997), Surge-type glaciers in the Russian High Arctic identified from digital satellite imagery, *Journal of Glaciology*, *43*(145), 489-494.

Dowdeswell, J. A., D. Ottesen, J. Evans, C. Ó Cofaigh, and J. B. Anderson (2008b), Submarine glacial landforms and rates of ice-stream collapse, *Geology*, *36*, 819-822.

Gardner, A., et al. (2013), A Reconciled Estimate of Glacier Contributions to Sea Level Rise: 2003 to 2009, *Science*, *340*(6134), 852-857, doi:10.1126/science.1234532.

Gardner, A., G. Moholdt, B. Wouters, G. J. Wolken, D. O. Burgess, M. J. Sharp, J. G. Cogley, C. Braun, and C. Labine (2011), Sharply increased mass loss from glaciers and ice caps in the Canadian Arctic Archipelago, *Nature*, *473*, 357-360.

Grant, K. L., C. R. Stokes, and I. S. Evans (2009), Identification and characteristics of surge-type glaciers on Novaya Zemlya, Russian Arctic, *Journal of Glaciology*, *55*(194), 960-972.

Gudmundsson, G. H., J. Krug, G. Durand, L. Favier, and O. Gagliardini (2012), The stability of grounding lines on retrograde slopes, *The Cryosphere Discussions*, *6*, 2597–2619.

Hagen, J. O., J. Kohler, K. Melvold, and J.-G. Winther (2003), Glaciers in Svalbard: mass balance, runoff and freshwater flux, *Polar Research*, *22*(2).

Hamilton, G. S., and J. Dowdeswell (1996), Controls on glacier surging in Svalbard, *Journal of Glaciology*, *42*, 157-168.

Hanna, E., P. Huybrechts, K. Steffen, J. Cappelen, R. Huff, S. C., T. Irvine-Fynn, S. Wise, and M. Griffths (2008), Increased runoff from melt from the Greenland Ice Sheet: A response to global warming, *Journal of Climate*, *21*, 331-341, doi:0.1175/2007JCLI1964.1.

Hanzlick, D., and K. Aagaard (1980), Freshwater and Atlantic water in the Kara Sea, *Journal of Geophysical Research: Oceans*, *85*(C9), 4937-4942, doi:10.1029/JC085iC09p04937.

Heinrich (1988), Origin and consequences of cyclic rafting in the northeast Atlantic Ocean during the past 130,000 years, *Quaternary Research*, *29*, 142-152.

Holland, D. M., R. H. D. Y. Thomas, B., M. H. Ribergaard, and B. Lyberth (2008), Acceleration of Jakobshavn Isbræ triggered by warm subsurface ocean waters, *Nature Geoscience*, *1*, 1-6.

Holliday, N. P., et al. (2008), Reversal of the 1960s to 1990s freshening trend in the northeast North Atlantic and Nordic Seas, *Geophysical Research Letters*, *35*, L03614.

Howat, I. M., I. Joughin, M. Fahnestock, B. E. Smith, and T. Scambos (2008), Synchronous retreat and acceleration of southeast Greenland outlet glaciers 2000-2006; Ice dynamics and coupling to climate, *Journal of Glaciology*, *54*(187), 1-14.

Howat, I. M., A. Negrete, T. Scambos, and T. Haran (2012), A high-resolution elevation model for the Greenland Ice Sheet from combined stereoscopic and photoclinometric data, edited, Byrd Polar Research Centre, Ohio State University.

Hughes (2002), Calving bays, *Quarternary Science Reviews*, *21*(1-3), 267-282.

Hughes, T. (1975), West Antarctic Ice Sheet – instability, disintegration, and initiation of ice ages, *Reviews of Geophysics*, *13*(4), 502 – 526.

Hughes, T. (1986), The Jakobshavns effect, *Geophysical Research Letters*, *13*(1), 46-48.

IPCC (2007), *The Physical Science Basis. Contribution of Working Group I to the Fourth Assessment Report of the Intergovernmental Panel on Climate Change*, Cambridge Univ. Press, Cambridge and New York.

IPCC (2013), Climate Change 2013: The Physical Science Basis. Working Group I Contribution to the IPCC 5th Assessment Report. Online unedited version.

Ivanov, V. V., and G. I. Shapiro (2005), Formation of a dense water cascade in the marginal ice zone in the Barents Sea, *Deep Sea Research Part I: Oceanographic Research Papers*, *52*(9), 1699-1717, doi:http://dx.doi.org/10.1016/j.dsr.2005.04.004.

Jamieson, S. S. R., A. Vieli, S. J. Livingstone, C. Ó Cofaigh, C. R. Stokes, C.-D. Hillenbrand, and J. Dowdeswell (2012), Ice stream stability on a reverse bed slope, *Nature Geoscience*, *5*, 799-802.

Johnson, H. L., A. Münchow, K. K. Falkner, and H. Melling (2011), Ocean circulation and properties in Petermann Fjord, Greenland, *Journal of Geophysical Research*, *116*, C01003.

Joughin, I., and R. B. Alley (2011), Stability of the West Antarctic ice sheet in a warming world, *Nature Geoscience*, *4*, 506-513.

Joughin, I., B. Smith, I. M. Howat, T. Scambos, and T. Moon (2010a), Greenland flow variability from ice-sheet-wide velocity mapping, *Journal of Glaciology*, *56*(197), 415-430.

Joughin, I., B. E. Smith, I. Howat, and T. Scambos (2010b), MEaSUREs Greenland Ice Sheet Velocity Map from InSAR Data, *Boulder, Colorado, USA: National Snow and Ice Data Center. Digital media.*

Karcher, M., M. Kulakov, S. Pivovarov, U. Schauer, F. Kauker, and R. Schlitzer (2003), Atlantic Water flow to the Kara Sea - comparing model results with observations, in *Siberian River Runoff in the Kara Sea: Characterisation, Quantification, Variability and Environmental Significance*, edited by F. Stein, Fütterer, Galimov, Elsevier, Proceedings in Marine Science, pp. 47-69

Kopp, R. E., F. J. Simons, J. X. Mitrovica, A. C. Maloof, and M. Oppenheimer (2009), Probabilistic assessment of sea level during the last interglacial stage, *Nature*, *462*, 863–867.

Loeng, H. (1991), Features of the physical oceanographic conditions of the Barents Sea, *Polar Research*, *10*(1), 5-18.

Mayer, C., N. Reeh, F. Jung-Rothenhäusler, P. Huybrechts, and H. Orter (2000), The subglacial cavity and implied dynamics under Nioghalvfjerdsfjorden Glacier, NE-Greenland, *Geophysical Research Letters*, *27*(15), 2289-2292.

McFadden, E. M., I. M. Howat, I. Joughin, B. Smith, and Y. Ahn (2011), Changes in the dynamics of marine terminating outlet glaciers in west Greenland (2000–2009), *Journal of Geophysical Research*, *116*, F02022.

Meier, M. F., and A. Post (1987), Fast tidewater glaciers, *Journal of Geophysical Research*, *92*, 9051–9058.

Mercer, J. H. (1968), Antarctic ice and Sangamon sea level rise, *IAHS Publ.*, *179*, 217–225

Mercer, J. H. (1978), West Antarctic Ice Sheet and CO2 Greenhouse effect – threat of disaster, *Nature*, *271*(5643), 321-325.

Mernild, S. H., E. Hanna, J. C. Yde, J. Cappelen, and J. K. Malmros (2013), Coastal Greenland air temperature extremes and trends 1890–2010: annual and monthly analysis, *International Journal of Climatology*, n/a-n/a, doi:10.1002/joc.3777.

Moholdt, G., J. M. Hagen, T. Eiken, and T. Schuler (2010a), Geometric changes and mass balance of the Austfonna ice cap, Svalbard, *The Cryosphere*, *4*, 21-34.

Moholdt, G., C. Nuth, J. O. Hagen, and J. Kohler (2010b), Recent elevation changes of Svalbard glaciers derived from ICESat laser altimetry, *Remote Sensing of Environment*, *114*, 2756–2767.

Moholdt, G., B. Wouters, and A. S. Gardner (2012), Recent mass changes of glaciers in the Russian High Arctic, *Geophysical Research Letters*, *39*, L10502.

Moon, T., I. Joughin, B. E. Smith, and I. M. Howat (2012), 21st-Century evolution of Greenland outlet glacier velocities, *Science*, *336*(6081), 576-578.

Morlighem, M., E. Rignot, J. Mouginot, H. Seroussi, and E. Larour (2014), Deeply incised submarine glacial valleys beneath the Greenland ice sheet, *Nature Geosci*, *7*(6), 418-422, doi:10.1038/ngeo2167.

Murray, T., et al. (2010), Ocean regulation hypothesis for glacier dynamics in southeast Greenland and implications for ice sheet mass changes, *Journal of Geophysical Research*, *115*, F03026, doi:10.1029/2009JF001522.

Nick, F. M., A. Luckman, A. Vieli, C. J. van der Veen, D. van As, R. S. W. van de Wal, F. Pattyn, and D. Floricioiu (2012), The response of Petermann Glacier, Greenland, to large calving events, and its future stability in the context of atmospheric and oceanic warming, *Journal of Glaciology*, *58*(208), 229 - 239.

Nick, F. M., C. J. van der Veen, A. Vieli, and D. I. Benn (2010), A physically based calving model applied to marine outlet glaciers and implications for the glacier dynamics, *Journal of Geophysical Research*, *56*(199), 781-794.

Nick, F. M., A. Vieli, M. L. Andersen, I. Joughin, A. J. Payne, T. L. Edwards, F. Pattyn, and R. S. W. van de Wal (2013), Future sea-level rise from Greenland's main outlet glaciers in a warming climate, *Nature*, *497*(7448), 235-238, doi:10.1038/nature12068.

Nick, F. M., A. Vieli, I. M. Howat, and I. Joughin (2009), Large-scale changes in Greenland outlet glacier dynamics triggered at the terminus, *Nature Geoscience*, *2*, 110-114.

Nuth, C., G. Moholdt, J. Kohler, J. O. Hagen, and A. Kääb (2010), Svalbard glacier elevation changes and contribution to sea level rise, *Journal of Geophysical Research*, *115*, F01008, doi:10.1029/2008JF001223.

Pavlov, V. K., and S. L. Pfirman (1995), Hydrographic structure and variability of the Kara Sea: Implications for pollutant distribution, *Deep Sea Research Part II: Topical Studies in Oceanography*, *42*(6), 1369-1390, doi:http://dx.doi.org/10.1016/0967-0645(95)00046-1.

Pfirman, S. L., D. Bauch, and T. Gammelsrød (1994), The Northern Barents Sea: Water Mass Distribution and Modification, *The Polar Oceans and Their Role in Shaping the Global Environment Geophysical Monograph*, *85*, 77-94.

Pickart, R. S., D. J. Torres, and P. S. Fratantoni (2005), The East Greenland Spill Jet, *Journal of Physical Oceanography*, *35*, 1037-1053.

Politova, N. V., V. P. Shevchenko, and V. V. Zernova (2012), Distribution, Composition, and Vertical Fluxes of Particulate Matter in Bays of Novaya Zemlya Archipelago, Vaigach Island at the End of Summer, *Advances in Meteorology*, *2012*, 15, doi:10.1155/2012/259316.

Pritchard, H. D., R. J. Arthern, D. G. Vaughan, and L. A. Edwards (2009), Extensive dynamic thinning on the margins of the Greenland and Antarctic ice sheets, *Nature*, *461*, 971-975.

Ribergaard, M. H., S. M. Olsen, and J. Mortensen (2008), Oceanographic Investigations off West Greenland 2007, *NAFO Science Council Document*, 08/003.

Rignot, E., J. E. Box, E. Burgess, and E. Hanna (2008), Mass balance of the Greenland ice sheet from 1958 to 2007, *Geophysical Research Letters*, *35*, L20502, doi:10.1029/2008GL035417.

Rignot, E., I. Velicogna, M. Van den Broeke, A. Monaghan, and J. Lenaerts (2011), Acceleration of the contribution of the Greenland and Antarctic ice sheets to sea level rise, *Geophysical Research Letters*, *38*, L05503.

Rodrigues, J. (2008), The rapid decline of the sea ice in the Russian Arctic, *Cold Regions Science and Technology*, *54*, 124-142.

Rodrigues, J. (2009), The increase in the length of the ice-free season in the Arctic, *Cold Regions Science and Technology*, *59*, 78–101.

Rudels, B., G. Björk, J. Nilsson, P. Winsord, L. I., and C. Nohr (2005), The interaction between waters from the Arctic Ocean and the Nordic Seas north of Fram Strait and along the East Greenland Current: results from the Arctic Ocean-02 Oden expedition, *Journal of Marine Systems*, *55*, 1-30.

Scherer, R. P., A. Aldahan, S. Tulaczyk, G. Possnert, H. Engelhardt, and B. Kamb (1998), Pleistocene Collapse of the West Antarctic Ice Sheet, *Science*, *281*(5373), 82-85.

Sharov, A. I. (2005), Studying changes of ice coasts in the European Arctic, *Geo-Marine letters*, *25*, 153–166.

Shepherd, A., et al. (2012), A Reconciled Estimate of Ice-Sheet Mass Balance, *Science*, *338*(6111), 1183-1189, doi:10.1126/science.1228102.

Stein, M. (2005), North Atlantic subpolar gyre warming-impacts on Greenland offshore waters, *Journal of Northwest Atlantic Fisheries Science*, *36*, 43-54.

Straneo, F. (2006), Heat and Freshwater Transport through the Central Labrador Sea, *Journal of Physical Oceanography*, *36*, 606-628.

Straneo, F., R. G. Curry, D. A. Sutherland, G. S. Hamltion, C. Cenedese, K. Våge, and L. A. Stearns (2011), Impact of fjord dynamics and glacial runoff on the circulation near Helheim Glacier, *Nature Geoscience*, *4*, 322-327.

Straneo, F., G. S. Hamilton, D. A. Sutherland, L. A. Stearns, F. Davidson, M. O. Hammill, G. B. Stenson, and A. R. Asvid (2010), Rapid circulation of warm subtropical waters in a major glacial fjord in East Greenland, *Nature Geoscience*, *3*, 182-186, doi:10.1038/NGEO764.

Stroeve, J. C., M. C. Serreze, M. M. Holland, J. E. Kay, J. Malanik, and A. P. Barrett (2012), The Arctic's rapidly shrinking sea ice cover: a research synthesis, *Climatic Change*, *110*(3-4), 1005-1027, doi:10.1007/s10584-011-0101-1.

Sund, M., T. Eiken, J. O. Hagen, and A. Kääb (2009), Svalbard surge dynamics derived from geometric changes, *Annals of Glaciology*, *50*, 50-60.

Sutherland, D. A., and R. S. Pickart (2008), The East Greenland Coastal Current: Structure, variability, and forcing, *Progress in Oceanography*, *78*, 58–77.

van den Broeke, M., J. Ettema, W. J. van de Berg, and E. van Meijgaard (2009), Towards a re-assessment of the surface mass balance of the Greenland ice sheet, *European Physical Journal Conferences*, 171-176, doi:10.1140/epjconf/e2009-00918-7.

Vieli, A., and F. M. Nick (2011), Understanding and modelling rapid dynamic changes of tidewater outlet glaciers: issues and implications, *Surveys in Geophysics*, *32*, 437-485.

Warren, C. R., and N. R. J. Hulton (1990), Topographic and glaciological controls on Holocene ice sheet margin dyanmics, central west Greenland, *Annals of Glaciology*, *14*, 307-310.

Weertman, J. (1974), Stability of the junction of an ice sheet and an ice shelf, *Journal of Glaciology*, *13*, 3-11.

Weidick, A. (1995), Satellite Image Atlas of Glaciers of the World, Greenland, *USGS Professional Paper 1386-C, United States Government Printing Office, Washington.*

Yin, J., T. J. Overpeck, S. M. Griffies, A. Hu, J. L. Russell, and R. J. Stouffer (2012), Different magnitudes of projected subsurface ocean warming around Greenland and Antarctica, *Nature Geoscience*, *4*, 524-528.

Zeeberg, J., and S. L. Forman (2001), Changes in glacier extent on north Novaya Zemlya in the Twentieth Century, *The Holocene*, *11*(2), 161-175.

Zwally, H. J., et al. (2011), Greenland ice sheet mass balance: distribution of increased mass loss with climate warming; 2003–07 versus 1992–2002, *Journal of Glaciology*, *57*(201), 88-102.

Chapter 2: Recent progress in understanding marine-terminating Arctic outlet glacier response to climatic and oceanic forcing: Twenty years of rapid change

Carr, J.R., Stokes, C.R. and Vieli, A., 2013a. *Progress in Physical Geography*, 37 (4) 435 – 466.

Overview: This paper reviews the progress made during the past twenty years in our understanding of marine-terminating outlet glacier dynamics and their response to forcing. Specifically, it focuses on the three primary external controls: air temperatures, sea ice and ocean temperatures. It then highlights key outstanding uncertainties and directions for future research, namely: assessing the spatial variation in the relative importance of forcing factors; the role of glacier-specific factors and; quantitative assessment of glacier response to forcing, using numerical modelling.

Motivation: The paper introduces the key theories relating to marine-terminating outlet glacier dynamics and highlights the main limitations in our understanding of this behaviour. Thus, it provides important background information and context for the thesis and sets out the primary areas of uncertainty that are then explored within the project, specifically the spatial variation in glacier response to forcing and the role of glacier-specific factors.

Author contributions: In this paper, I wrote the text, created the figures and led the paper development. My co-authors provided editorial input and guidance on the development of the paper.

Abstract

Until relatively recently, it was assumed that Arctic ice masses would respond to climatic/oceanic forcing over millennia, but observations made during the past two decades have radically altered this viewpoint and have demonstrated that marine-terminating outlet glaciers can undergo dramatic dynamic change at annual timescales. This paper reviews the substantial progress made in our understanding of the links

between marine-terminating Arctic outlet glacier behaviour and the ocean-climate system during the past twenty years, when many ice masses have rapidly lost mass. Specifically, we assess three primary climatic/oceanic controls on outlet glacier dynamics, namely air temperature, ocean temperature and sea ice concentrations, and discuss key linkages between them. Despite recent progress, significant uncertainty remains over the response of marine-terminating outlet glaciers to these forcings, most notably (i), the spatial variation in the relative importance of each factor; (ii), the contribution of glacier-specific factors to glacier dynamics; and iii) the limitations in our ability to accurately model marine-terminating outlet glacier behaviour. Our present understanding precludes us from identifying patterns of outlet glacier response to forcing that are applicable across the Arctic and we underscore the potential danger of extrapolating rates of mass loss from a small sample of study glaciers.

2.1. Introduction

Arctic warming is expected to far exceed the global average and is forecast to reach 4 to 7°C by 2100 [*IPCC*, 2007; *Meier et al.*, 2007]. Consequently, Arctic ice masses are expected to undergo rapid change during the 21st century and to contribute significantly to global sea level rise [e.g. *Bamber et al.*, 2007]. Indeed, estimates suggest that the Greenland Ice Sheet (GrIS) contributed 0.46 mm a^{-1} to sea level rise between 2000 and 2008 [*van den Broeke et al.*, 2009]. Assessing the potential response of Arctic ice masses to climate change is therefore crucial for the accurate prediction of near-future sea level rise [*IPCC*, 2007]. For the purposes of this paper, we define 'Arctic ice masses' as the major glaciated archipelagos within the Arctic Circle, namely the Greenland Ice Sheet (GrIS), Svalbard, Novaya Zemlya (NZ), Severnaya Zemlya (SZ), Franz Josef Land (FJL) and the Canadian Arctic (Fig. 2.1). Alaska is also included as results from the region have contributed significantly to our knowledge of marine-terminating outlet glacier dynamics. Here we define a marine-terminating outlet glacier

as a channel of fast-moving ice that drains an ice cap or ice sheet and terminates in the ocean, at either a floating or grounded margin (Benn and Evans, 2010) (Fig 2.2).

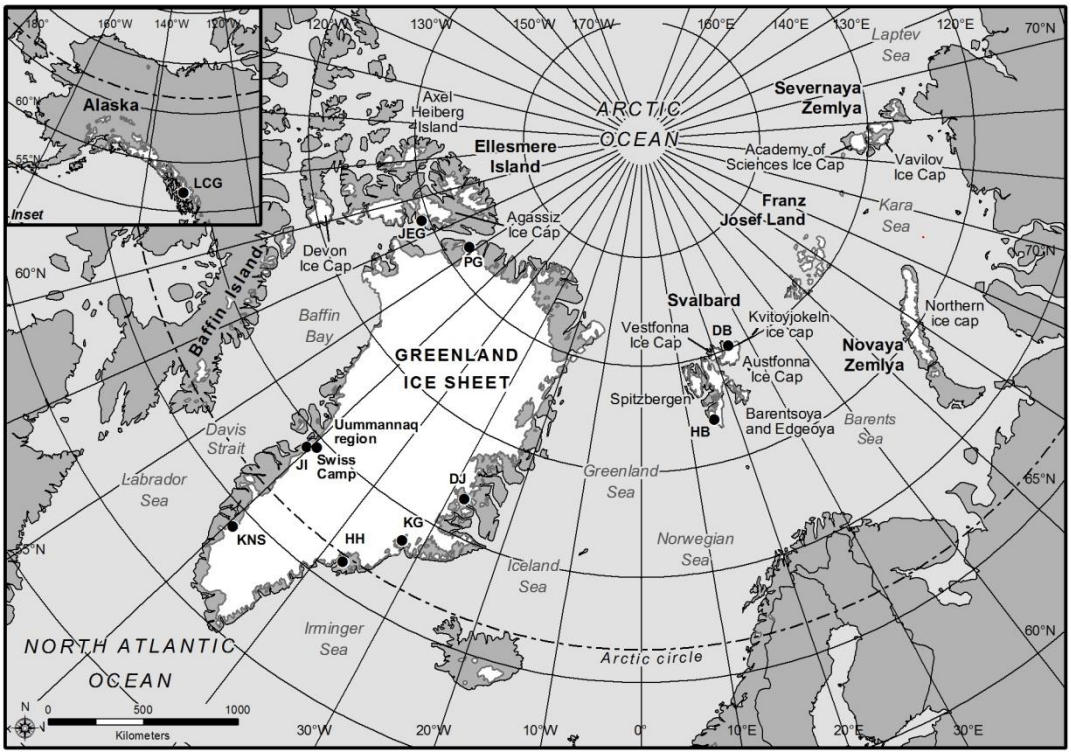

Figure 2.1. *Regional overview map showing the location of major ice masses, outlet glaciers and other sites discussed in the text. Major water masses are also labelled. Glacier abbreviations are as follows: Helheim Glacier (HH), Kangerdlugssuaq Glacier (KG), Daugaard Jensen Gletscher (DJ), Kangiata Nunata Sermia (KNS), Jakobshavn Isbrae (JI), Petermann Glacier (PG), Hansbreen (HB), Duvebreen (DB) and John Evans Glacier (JEG). Inset: Overview map of Alaska, showing the location of LeConte Glacier (LCG).*

Our understanding of Arctic ice mass behaviour has advanced dramatically during the last twenty years, particularly during the last decade. Previously, it was generally assumed that large Arctic ice masses would respond to climatic warming at millennial timescales, primarily through increased surface melting, and that changes in ice flow would occur only at centennial timescales or longer [*Greve*, 2000; *Huybrechts et al.*, 1991; *IPCC*, 2001]. However, studies published during the past two decades have dramatically altered this viewpoint [e.g. *Joughin et al.*, 2010; *Rignot et al.*, 2008; *van den Broeke et al.*, 2009] and have shown that most Arctic ice masses have rapidly lost

mass since the 1990s. Crucially, losses have been concentrated at the coastal margins, particularly on marine-terminating outlet glaciers [e.g. *Joughin et al.*, 2010; *Meier et al.*, 2007; *Thomas et al.*, 2009]. Indeed, recent studies have demonstrated that marine-terminating Arctic outlet glaciers can respond rapidly to climatic/oceanic forcing [e.g. *Andresen et al.*, 2012; *Howat et al.*, 2011; *Howat et al.*, 2008a; *Howat et al.*, 2007; *Joughin et al.*, 2008b; *Joughin et al.*, 2010; *Kjær et al.*, 2012] and can significantly influence the mass budget of their parent ice masses over annual to decadal timescales [e.g. *Pritchard et al.*, 2009; *Rignot et al.*, 2008; *Stearns and Hamilton*, 2007].

Results from the Antarctic, particularly Pine Island Glacier [*Payne et al.*, 2004], have also highlighted the role of outlet glaciers and ice streams in enabling rapid coupling between forcing at the margins and the ice sheet interior and have raised concerns over the vulnerability of some regions to rapid mass loss [*Joughin and Alley*, 2011]. Furthermore, iceberg-rafted debris from palaeo-ice sheets attest to major episodes of ice sheet collapse [e.g. *Bond et al.*, 1992] and reconstructions of marine-based palaeo-ice sheets have highlighted the potential for rapid ice stream/outlet glacier retreat [*Briner et al.*, 2009; e.g. *Winsborrow et al.*, 2010]. Theoretical considerations also suggest that glaciers resting on reverse bed slopes may potentially be unstable [*Thomas*, 1979; *Weertman*, 1974]. Although this review focuses on the Arctic, these findings have demonstrated that marine-terminating outlet glaciers can respond rapidly to climatic/oceanic forcing and play a key role in regulating the mass balance of marine-based ice sheets. As a result, the factors controlling marine-terminating outlet glacier dynamics have emerged as a primary area of research.

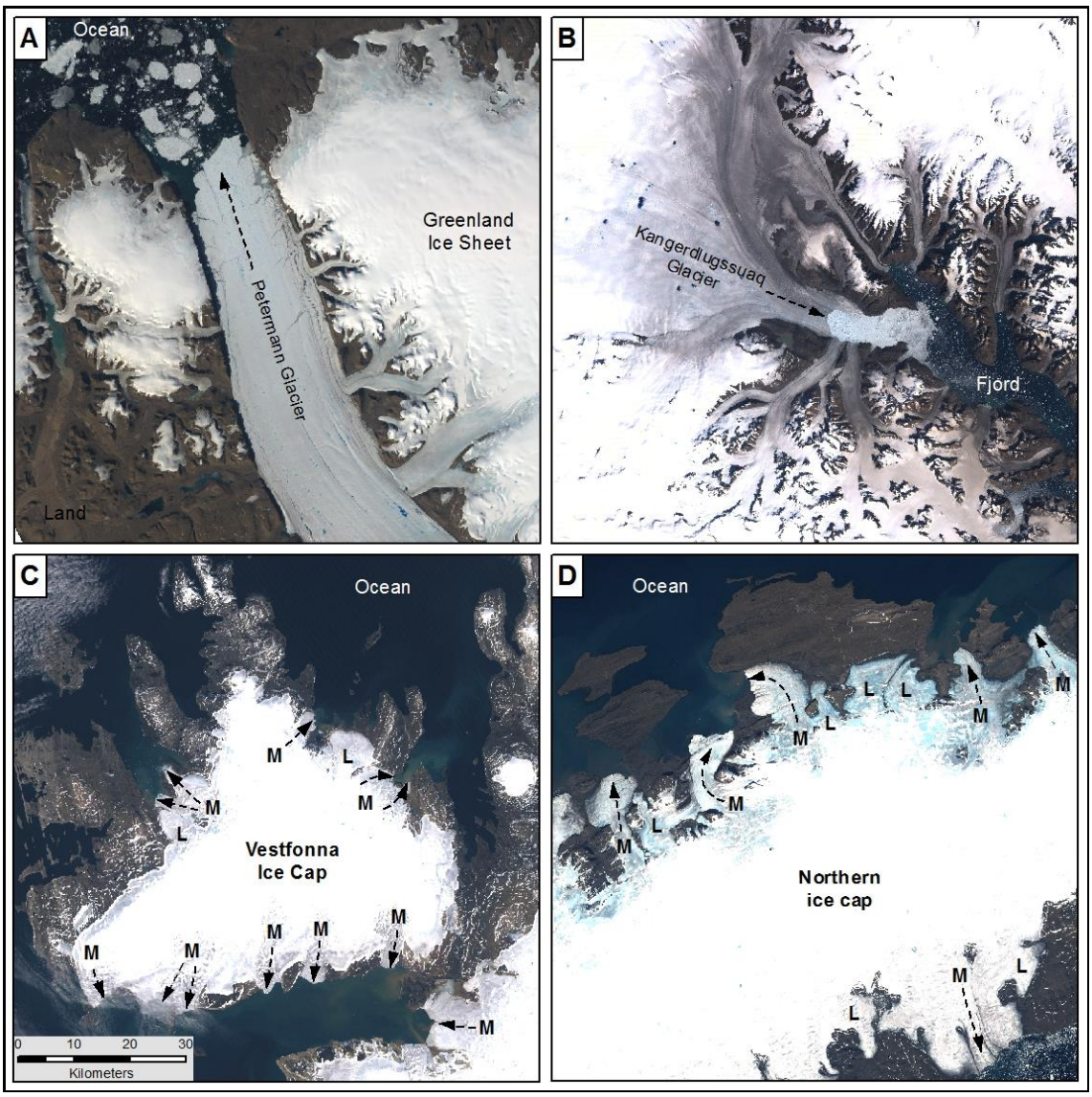

Figure 2.2. *Visible satellite imagery of selected marine-terminating Arctic outlet glaciers and Arctic ice masses at 1:1,000,000 scale. Images are ordered by glacier location, from west to east, and show (A) Petermann Glacier, northwest Greenland; (B) Kangerdlugssuaq Glacier, east Greenland; (C) Vestfonna Ice Cap, Svalbard; (D) northern ice cap, Novaya Zemlya. Outlet glacier and ice mass locations are shown in Figure 2.1. Major outlet glaciers are labelled according to terminus type (M=marine; L = land) and approximate near-terminus flow direction is marked (dashed lines). Imagery source: Global Land Cover Facility (www.landcover.org).*

Recent mass deficits have been attributed to both increased marine-terminating outlet glacier discharge and to a more negative surface mass balance (SMB), primarily resulting from increased surface melting relative to accumulation [*Rignot et al.*, 2008; *Rignot et al.*, 2011; *van den Broeke et al.*, 2009; *Zwally et al.*, 2011]. The relative

contribution of each of these two components varies across the Arctic, but is presently approximately equal on the GrIS [*van den Broeke et al.*, 2009]. A number of potential controls on marine-terminating outlet glacier behaviour have been identified (Fig. 2.3), which we broadly classify as (i), glacier-specific factors, which relate to the glaciological, topographic and geological setting of the glacier; and (ii), climatic/oceanic forcing, including air and ocean temperatures, sea ice and precipitation. Important glacier-specific factors include subglacial topography and geology, fjord bathymetry and topography, sedimentation at the grounding line and glacier velocity, size, surface slope and catchment area (Fig. 2.3) [*Alley*, 1991; *Joughin et al.*, 2008b; *Meier and Post*, 1987]. Theory suggests that changes in marine-terminating outlet glacier dynamics can occur independently of climatic/oceanic forcing [e.g. *Alley*, 1991; *Meier and Post*, 1987] and the importance of glacier-specific factors, particularly subglacial topography, has been highlighted by recent studies [*Joughin et al.*, 2010; *Joughin et al.*, 2012; *Thomas et al.*, 2009]. Despite their apparent significance, however, the influence of glacier-specific factors on Arctic marine-terminating glacier behaviour is poorly understood.

In contrast, concerns over anthropogenic climate change in the 1990s resulted in an increasing focus on climatic/oceanic forcing factors and recent work has emphasised the widespread and synchronous nature of dynamic changes in many regions, particularly south-eastern Greenland [e.g. *Howat et al.*, 2008a; *Murray et al.*, 2010]. Consequently, this paper focuses on the climatic/oceanic drivers of marine-terminating Arctic outlet glacier dynamics and discusses three primary controls: air temperatures, ocean temperatures and sea ice concentrations (Fig. 2.3). It should be noted, however, that these forcing factors are not independent (Fig. 2.3) and that interconnections between them may significantly influence outlet glacier behaviour, yet many of these relationships are poorly understood. We aim to: i), review and summarise recent developments relating to each of these climatic/oceanic forcing factors; ii), highlight key

uncertainties surrounding marine-terminating Arctic outlet glacier response to climatic/oceanic forcing; and iii), recommend directions for future research.

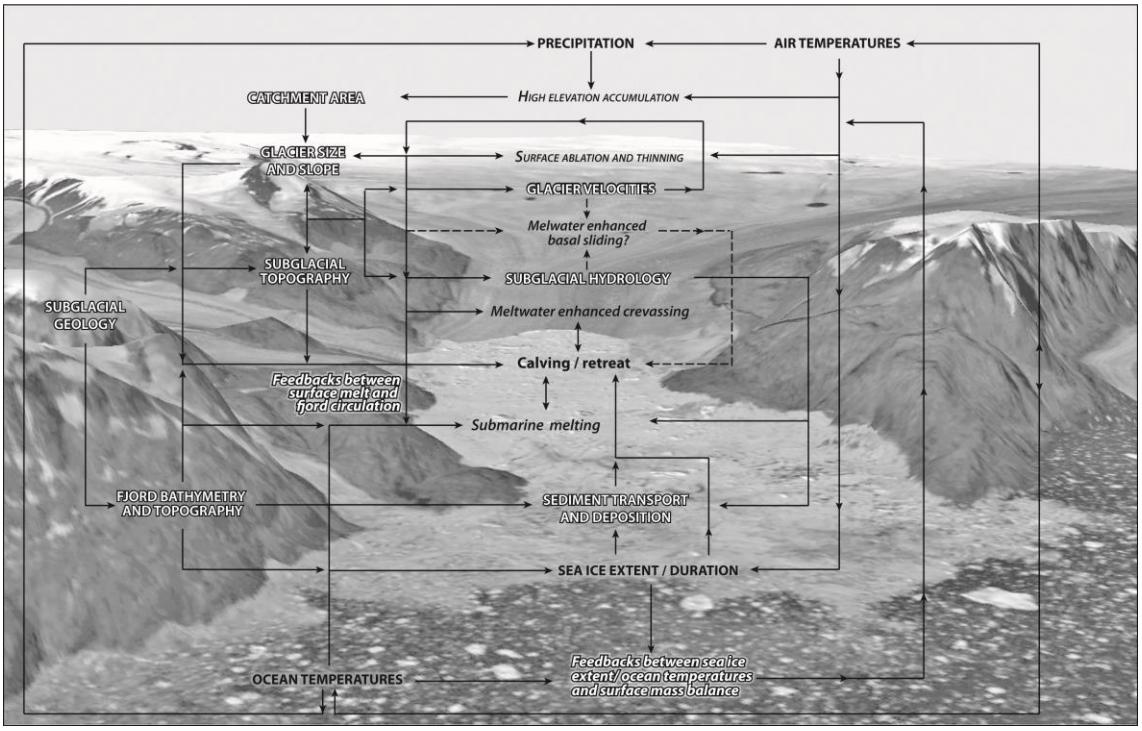

Figure 2.3. *Illustration of the primary climatic/oceanic forcing factors (black CAPS) and glacier-specific controls (white CAPS) thought to influence marine-terminating Arctic outlet glacier behaviour and mass balance. The major processes (black italics) and potential feedback mechanisms (white italics) are included. The role of meltwater enhanced basal sliding is represented with a dashed line as its influence on multi-year glacier behaviour remains equivocal. Imagery source: Global Land Cover Facility (www.landcover.org).*

2.2. Arctic mass balance trends: 1990 to 2010

Rapid mass loss from Arctic masses has been documented since the early 1990s by numerous independent studies (Table 1) [e.g. *Gardner et al.*, 2011; *Krabill et al.*, 2004; *Moholdt et al.*, 2010b; *Rignot and Kanagaratnam*, 2006; *Velicogna and Wahr*, 2006]. Due to their remote location and considerable size, mass balance is usually determined indirectly using remotely sensed data and/or SMB modelling. Considerable advances have been made in these techniques during the past twenty years, which have substantially improved our ability to quantify mass budgets and to assess the relative

contribution of ice dynamics to mass loss [*Krabill et al.*, 2004; *Rignot and Kanagaratnam*, 2006; *van den Broeke et al.*, 2009; *Velicogna and Wahr*, 2006]. At present, the primary techniques include Gravity Recovery and Climate Experiment (GRACE) data [e.g. *Arendt et al.*, 2008; *Bergmann et al.*, 2012; *Jacob et al.*, 2012; *Khan et al.*, 2010; *Luthcke et al.*, 2006; *Mémin et al.*, 2011; *Velicogna*, 2009; *Velicogna and Wahr*, 2006; *Wouters et al.*, 2008], comparison of SMB with outlet glacier discharge [*Rignot et al.*, 2008; *Rignot and Kanagaratnam*, 2006; *Rignot et al.*, 2011; *van den Broeke et al.*, 2009] and repeat laser or radar altimetry measurements [*Abdalati et al.*, 2001; *Krabill et al.*, 2004; *Pritchard et al.*, 2009; *Thomas et al.*, 2006; 2009].

The negative mass balance of the GrIS has received particular attention and has been estimated via a number of techniques and for a range of time periods. The most recent values from GRACE [*Jacob et al.*, 2012] and from the comparison of SMB/outlet glacier discharge [*Rignot et al.*, 2011] are presented in Table 1. An important new trend is the rapid mass loss from the Canadian Arctic between 2007 and 2009, which made the archipelago the primary cryospheric contributor to eustatic sea level rise outside of the Greenland and Antarctic ice sheets (Table 1) [*Gardner et al.*, 2011]. Furthermore, the area has been highlighted as the largest potential contributor to ice loss and sea level rise of any glaciated region during the 21st century [*Radić and Hock*, 2011]. Negative mass balance trends have also been documented in Svalbard [*Hagen et al.*, 2009; *Moholdt et al.*, 2010b; *Nuth et al.*, 2010] and the Russian Arctic (Table 1) [*Kotlyakov et al.*, 2010; *Sharov et al.*, 2009]. However, the mass balance of the Russian Arctic archipelagos have been comparatively poorly documented [*Bassford et al.*, 2006]. This represents a significant limitation to our understanding of the Arctic cryosphere and highlights the need for further research in the region, as NZ, SZ and FJL account for approximately 20% of the glaciated area of the Arctic, excluding the GrIS [*Dowdeswell et al.*, 1997].

2.2.1. Spatial trends in Arctic mass balance

Arctic mass balance trends have been spatially non-uniform, with many areas exhibiting slight growth at high elevations and rapid marginal thinning [e.g. *Hagen et al.*, 2009; *Pritchard et al.*, 2009; *Sharov*, 2010; *Sharov et al.*, 2009; *Thomas et al.*, 2008; *Thomas et al.*, 2006; *Zwally et al.*, 2011]. Substantial thickening has been observed at high elevations on the GrIS [*Ettema et al.*, 2009; *Johannessen et al.*, 2005; *Thomas et al.*, 2006; *Zwally et al.*, 2005]; Austfonna ice cap, Svalbard [*Bamber et al.*, 2004; *Moholdt et al.*, 2010a; *Moholdt et al.*, 2010b; *Raper et al.*, 2005]; the northern ice cap, NZ [*Sharov et al.*, 2009]; Tyndall and Windy ice domes in FJL; Schmidt and Vavilov ice caps in SZ [*Sharov*, 2010]; and some Canadian Arctic ice caps [*Abdalati et al.*, 2004; *Mair et al.*, 2009]. A number of potential explanations have been proposed for this interior thickening, including increased precipitation [*Thomas et al.*, 2006; *Zwally et al.*, 2005], possibly related to changes in sea ice extent [*Bamber et al.*, 2004; *Mair et al.*, 2009; *Raper et al.*, 2005], long-term accumulation trends [*Koerner*, 2005; *Moholdt et al.*, 2010a] and/or surge dynamics [*Bevan et al.*, 2007]. However, interior gains have been far outweighed by low-elevation thinning and marginal retreat [e.g. *van den Broeke et al.*, 2009; *Zwally et al.*, 2011], resulting in an overall negative mass balance in many regions (Table 1).

Region	Sub-region	Rate of mass loss ($km^3\ a^{-1}$)	Measurement period	Measurement method	Source
Greenland	Greenland Ice Sheet	224.76 ± 19*	1992-2009	SMB /D	Rignot et al., 2011
Greenland	Greenland Ice Sheet	203.57± 8.25*#	2003-2010	GRACE	Jacob et al., 2012
Canadian Arctic	Ellesmere, Devon, Axel Heiberg and Baffin islands	56.24 ± 6.42*	2004-2009	SMB/D, ICESat laser altimetry and GRACE	Gardner et al., 2011
Canadian Arctic	Ellesmere, Devon, Axel Heiberg islands	34.23 ± 4.56*	2004-2009	SMB/D, ICESat laser altimetry and GRACE	Gardner et al., 2011
Canadian Arctic	Baffin Island	22.0 ± 4.28*	2004-2009	SMB/D, ICESat laser altimetry and GRACE	Gardner et al., 2011
Russian Arctic	Novaya Zemlya	3.67 ± 2	2003 - 2010	GRACE	Jacob et al., 2012
Russian Arctic	Severnaya Zemlya	0.92 ± 2	2003 - 2010	GRACE	Jacob et al., 2012
Russian Arctic	Franz Josef Land	0 ± 2	2003 - 2010	GRACE	Jacob et al., 2012
Svalbard	Spitzbergen	3.59 ± 1.17	2003-2008	ICESat laser altimetry and SPOT HRS 5 stereoscopic images	Moholdt et al., 2010b
Svalbard	Austfonna Ice Cap	1.3 ± 0.5	2002-2008	ICESat laser altimetry, airborne laser altimetry, GNSS surface profiles and RES	Moholdt et al., 2010a
Svalbard	Barentsoya and Edgeoya	0.46 ± 0.30	2003-2008	ICESat laser altimetry and topographic maps	Moholdt et al., 2010b
Svalbard	Vestfonna Ice Cap	0.39 ± 0.20	2003-2008	ICESat laser altimetry and topographic maps	Moholdt et al., 2010b
Svalbard	Kvitoyjokeln ice cap	0.32 ± 0.08	2003-2008	ICESat laser altimetry and topographic maps	Moholdt et al., 2010b

Table 2.1. *Recent mass losses from the major glaciated regions and sub-regions of the Arctic. Data are first ordered according to regional mass loss rates and then according to mass loss rates from each sub-region. The most recent estimates of total mass loss were used for each region and the latest values obtained from GRACE and SMB/D are presented for the GrIS. Abbreviations are as follows: (SMB) Surface mass balance, (D) Discharge, (GRACE) Gravity Recovery and Climate Experiment, (SPOT) Système Pour l'Observation de la Terre, (GNSS) Global Navigation Satellite System and (RES) Radio Echo Sounding.* Mass loss rates converted from Gt a^{-1} to $km^3\ a^{-1}$, assuming an ice density of 0.917 kg km^3 [IPCC, 2007]. #This value includes peripheral ice caps and glaciers [Jacob et al., 2012].*

2.2.2. Dynamic contribution of marine-terminating outlet glaciers to mass loss

In addition to rapid marginal thinning, peak losses have occurred on marine-terminating outlet glaciers [*Moon and Joughin*, 2008; *Pritchard et al.*, 2009; *Sole et al.*, 2008]. On many of these glaciers, thinning rates of 10s of m a^{-1} have far exceeded surface melt rates, suggesting that thinning is largely 'dynamic' (i.e. resulting from changes in ice flow, rather than increased surface melting) [e.g. *Abdalati et al.*, 2001; *Burgess and Sharp*, 2008; *Krabill et al.*, 2004; *Thomas et al.*, 2009]. The contribution of glacier dynamics to recent mass deficits has been further emphasised by rapid retreat rates, which have reached kilometres per year on the GrIS [e.g. *Howat et al.*, 2008a; *Joughin et al.*, 2008b; *Joughin et al.*, 2010; *Moon and Joughin*, 2008] and hundreds of metres per year elsewhere [e.g. *Blaszczyk et al.*, 2009; *Burgess and Sharp*, 2004; *Nuth et al.*, 2010; *Sharov*, 2005]. Furthermore, recent research has underscored the contribution of dynamic changes to decadal-scale losses, as initial perturbations at the glacier terminus may be rapidly transmitted to inland areas, producing widespread, substantial thinning [*Howat et al.*, 2005; *Howat et al.*, 2008b; *Pritchard et al.*, 2009; *Thomas et al.*, 2011; *Zwally et al.*, 2011]. This longer-term component of dynamic loss is an important emerging area of research and has the potential to be the primary component of the GrIS contribution to 21st century sea level rise [*Price et al.*, 2011; *Vieli and Nick*, 2011].

Although the dynamics of marine-terminating outlet glaciers are now recognised as a key component of Arctic ice mass loss, they have also been highlighted as a principle area of uncertainty [*IPCC*, 2007]. Specifically, the primary climatic/oceanic controls and the mechanisms by which they induce a dynamic response are yet to be fully understood [*Howat et al.*, 2010; *Sole et al.*, 2008; *Vieli and Nick*, 2011]. The following sections review the three main climatic/oceanic controls identified to date, namely surface air temperatures, ocean temperatures and sea ice concentrations, and discuss the primary linkages between these factors (Fig. 2.3). All three forcing factors have undergone marked changes in recent years, which have been linked to both recent

climatic warming [*ACIA*, 2004; *IPCC*, 2007] and to the onset of a negative phase of the North Atlantic Oscillation (NAO) in the mid-1990s [*Gerdes et al.*, 2003; e.g. *Holliday et al.*, 2008; *Hurrell et al.*, 2003; *Stern and Heide-Jørgensen*, 2003].

2.3. Air temperature forcing

Arctic air temperatures have risen substantially since the mid-1990s [*ACIA*, 2004; *Hanna et al.*, 2008; *IPCC*, 2007], although they are not unprecedented at decadal timescales [*Box et al.*, 2009; *Chylek et al.*, 2006]. We present a new synthesis of air temperature data to investigate the spatial distribution of Arctic warming between 1990 and 2010 and to visualise this trend both in terms of magnitude and statistical significance (Fig. 2.4). Linear trends were calculated from annual air temperature series, which were compiled from meteorological station data of varying temporal resolution (three-hourly to monthly). In order to account for missing values, three-hourly data were used only if: i), no more than two consecutive records were missing in a day and; ii), no more than three records in total were missing in a day. Daily data were only used if values were available for 22 or more days per month and monthly values were used only if data were available for all months of the year [*Cappelen*, 2011].

Results suggest that warming has been greatest at coastal stations surrounding Baffin Bay and the Davis Strait (Fig. 2.4), which is consistent with dramatic mass loss from the Canadian Arctic between 2004 and 2009 [*Gardner et al.*, 2011]. Significant warming has also occurred in the Kara Sea region, particularly on FJL (Fig. 2.4), although data coverage is comparatively sparse. Warming from the mid-1990s has been linked to negative SMB on a number of Arctic ice masses, particularly the GrIS [e.g. *Abdalati and Steffen*, 2001; *Bhattacharya et al.*, 2009; *Box et al.*, 2006; *Ettema et al.*, 2009; *Hanna et al.*, 2008; *Mote*, 2007]. However, whilst warming directly affects SMB, a key recent development has been to consider the potential impact of meltwater on outlet glacier dynamics.

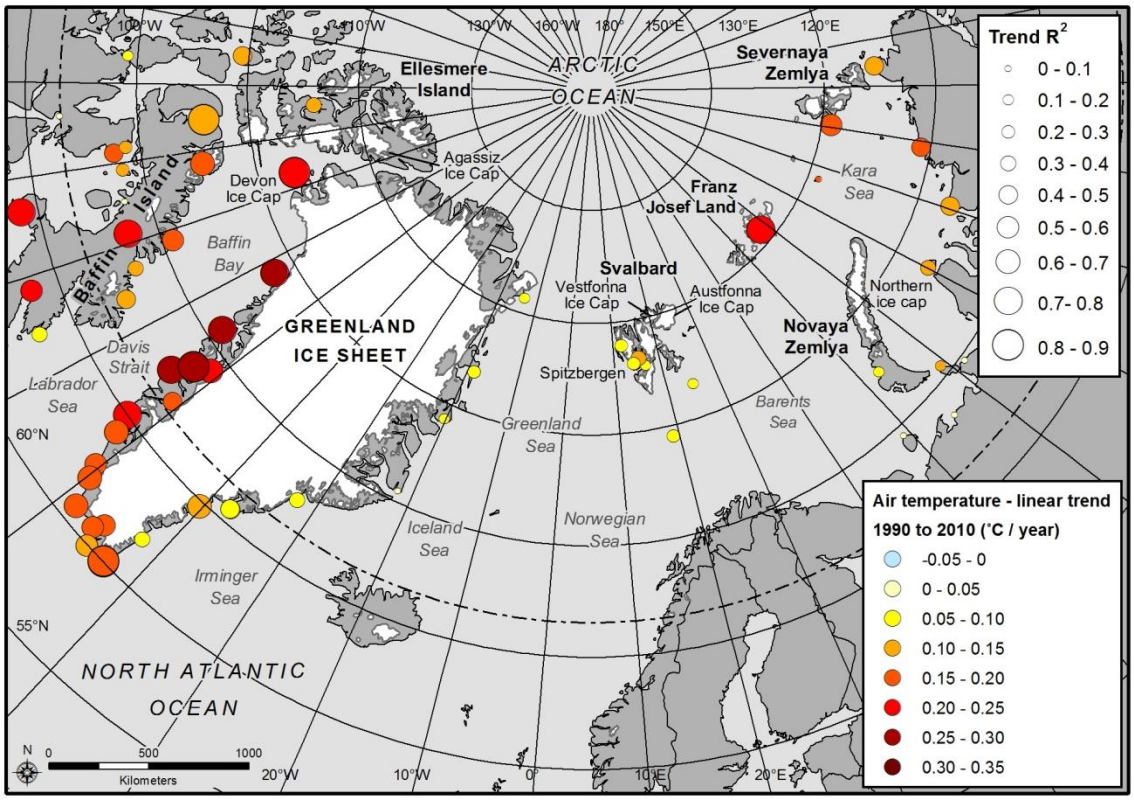

Figure 2.4. *Linear trend in mean annual air temperatures between 1990 and 2010 for selected Arctic meteorological stations. Symbol colour shows the magnitude of the linear trend in °C per year between 1990 and 2010. Symbol size shows the R^2 value of the relationship: a larger symbol represents a larger R^2 value and therefore the trend line better fits the data. Meteorological stations were selected according to data availability for the study period. Meteorological data sources: Danish Meteorological Institute, weather and climate data from Greenland 1958– 2010; Norwegian Meteorological Institute, Eklima climate database; Royal Netherlands Meteorological Institute, Climate Explorer; Scientific Research Institute of Hydrometeorological Information, World Data Center – Baseline Climatological Data Sets; and National Climate Data and Information Archive, Canadian Daily Climate Data.*

2.3.1. Air temperatures, meltwater production and ice velocities on temperate and polythermal glaciers

The relationship between air temperatures, meltwater supply and ice velocities has been well-documented on temperate glaciers [e.g. *Fountain and Walder*, 1998; *Iken and Bindschadler*, 1986; *Willis*, 1995], but had not been extensively considered on large Arctic ice masses until relatively recently. On temperate glaciers, surface

meltwater is thought to access large portions of the glacier bed during the melt season, resulting in elevated basal water pressures, reduced basal drag and enhanced ice motion [e.g. *Fountain and Walder*, 1998; *Iken and Bindschadler*, 1986; *Kamb*, 1987; *Nienow et al.*, 1998; *Willis*, 1995]. As the melt season progresses, continued meltwater input promotes the development of a more efficient subglacial drainage system, which lowers basal water pressures and reduces the sensitivity of glacier velocities to additional melt (Fig. 2.5) [e.g. *Nienow et al.*, 1998; *Willis*, 1995]. Recent studies have demonstrated a similar relationship on polythermal glaciers in the Canadian Arctic [e.g. *Bingham et al.*, 2008; *Bingham et al.*, 2003; *Boon and Sharp*, 2003; *Copland et al.*, 2003] and in Svalbard [*Nuttall and Hodgkins*, 2005; *Rippin et al.*, 2005; *Vieli et al.*, 2004]. In particular, extensive investigations on John Evans Glacier (JEG), Ellesmere Island, Canada, showed that surface meltwater could rapidly access the bed through predominantly cold ice and cause substantial seasonal acceleration [*Bingham et al.*, 2008; *Bingham et al.*, 2003; *Bingham et al.*, 2005; *Copland et al.*, 2003].

2.3.2. Surface meltwater and ice velocities in the GrIS ablation zone

Until a decade ago, it was largely assumed that penetration of surface meltwater to the bed of large Arctic ice masses would be minimal and that its effect on ice velocities would be limited, especially on the GrIS [*Copland et al.*, 2003; *Hodgkins*, 1997; *Zwally et al.*, 2002]. This viewpoint was radically altered by GPS measurements from Swiss Camp in the West Greenland ablation zone, which first demonstrated a close correspondence between surface meltwater inputs and ice velocities [*Zwally et al.*, 2002]. Here we define the ablation zone as areas that experience melt, with the exception of fast-flowing, marine terminating outlet glaciers, which are discussed separately (Section 2.2.3), due to their differing response to meltwater inputs. Results from Swiss Camp showed that velocities closely followed seasonal and interannual variations in surface melwater production, as previously observed on temperate glaciers, and this was attributed to meltwater-enhanced basal sliding [*Zwally et al.*,

2002]. Most importantly, the study highlighted meltwater-enhanced basal lubrication as a potential mechanism for rapid, dynamic and widespread response of the GrIS to atmospheric warming [*Zwally et al.*, 2002].

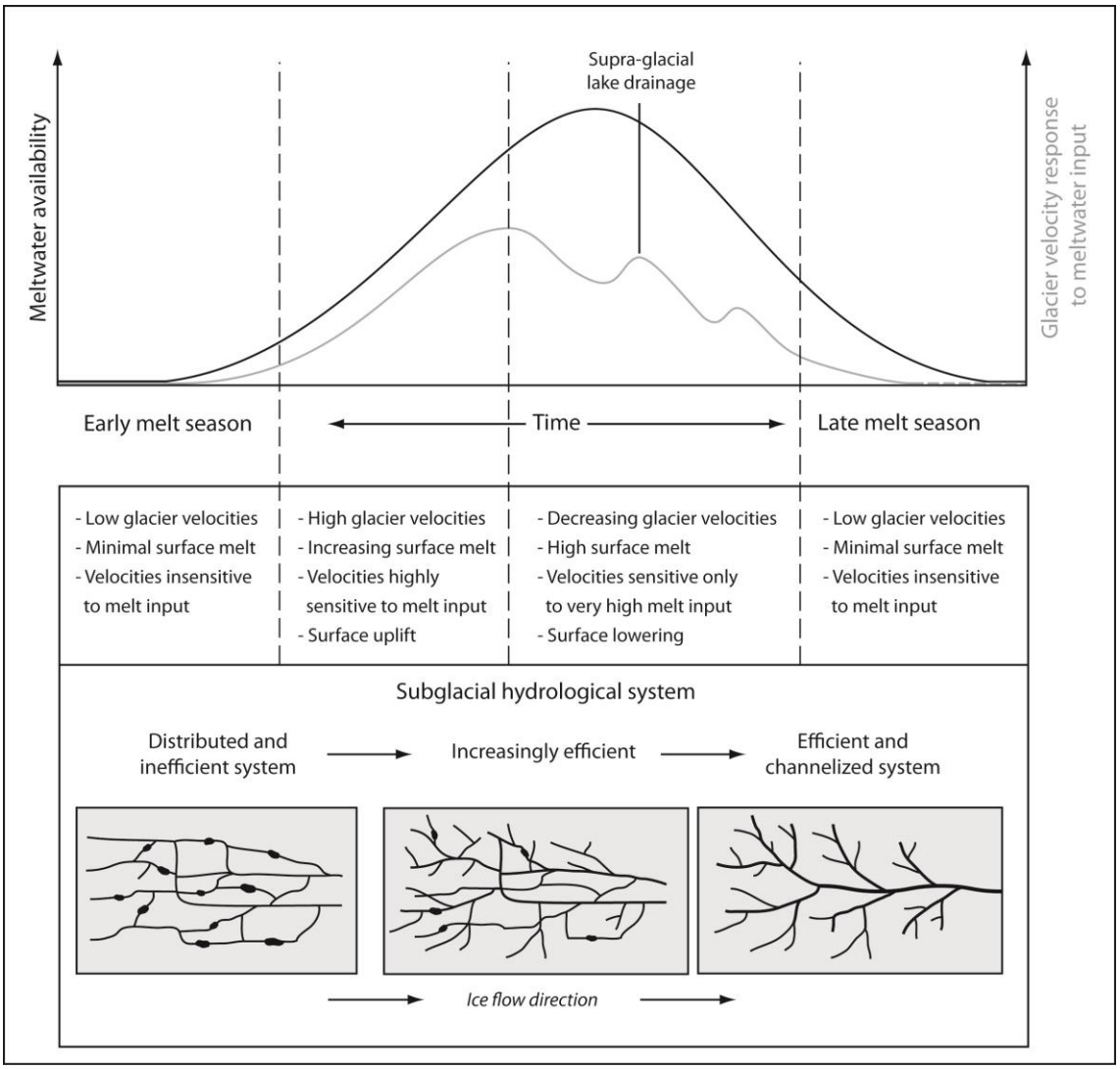

Figure 2.5. *Idealized seasonal evolution of glacier response to meltwater inputs. The graph illustrates the theoretical response of outlet glacier velocities to meltwater inputs during the melt season. The bottom panels illustrate an idealized plan view of the subglacial hydrological system at different stages of the melt season (bottom panels modified from Fountain and Walder, 1998). Individual glacier response to meltwater forcing may vary significantly from this idealized situation.*

The work of Zwally *et al.* (2002) was supported by subsequent results from the West Greenland ablation zone, which provided further evidence of rapid coupling between

seasonal meltwater inputs and ice velocities [e.g. *Bartholomew et al.*, 2010; *Bartholomew et al.*, 2011; *Catania and Neumann*, 2010; *Das et al.*, 2008; *Joughin et al.*, 2008a; *van de Wal et al.*, 2008]. Studies also identified supraglacial lake drainage events as a potential mechanism for rapid transfer of meltwater to the bed [e.g. *Das et al.*, 2008; *Krawczynski et al.*, 2009]. Large volumes of water released during drainage events may promote crevasse propagation through the full ice thickness by offsetting rapid refreezing and maintaining high water pressures at the crevasse tip [*Alley et al.*, 2005; *Krawczynski et al.*, 2009; *van der Veen*, 1998; 2007]. Drainage events have immediately preceded velocity increases in the West Greenland ablation zone (Das *et al.*, 2008; Box and Ski, 2007; McMillan *et al.*, 2007), on land-terminating West Greenland outlet glaciers [*Shepherd et al.*, 2009; *Sneed and Hamilton*, 2007] and on JEG [*Bingham et al.*, 2003; *Boon and Sharp*, 2003; *Copland et al.*, 2003], providing empirical support for their role in meltwater delivery to the bed.

The potential impact of surface meltwater inputs on the GrIS was also explored using numerical modelling, which predicted far greater losses with enhanced basal sliding [*Huybrechts and de Wolde*, 1999; *Parizek and Alley*, 2004; *van de Wal and Oerlemans*, 1997]. This occurred via a number of proposed feedback mechanisms, which are illustrated for an idealised section of the GrIS (Fig. 2.6). Specifically, feedbacks could develop between glacier acceleration, dynamic thinning and surface melting: increased basal sliding would promote dynamic thinning and bring a greater portion of the ice sheet into the ablation zone, thus exposing a greater area to melting and enhanced lubrication (Fig. 2.6) [*Parizek and Alley*, 2004].

2.3.3. Surface meltwater and marine-terminating Arctic outlet glacier dynamics

The close coupling between surface meltwater and ice velocities observed in the GrIS ablation zone led to increased consideration of the influence of meltwater on marine-terminating outlet glacier dynamics (e.g. Hall et al., 2008; Krabill et al., 2004). This was further motivated by the concurrence of the onset of marine-terminating Arctic glacier

retreat from the mid-1990s with atmospheric warming [e.g. *Bevan et al.*, 2012a; *Dyurgerov and McCabe*, 2006; *Howat and Eddy*, 2011] and the coincidence of substantial changes in glacier dynamics with elevated air temperatures [e.g. *Howat et al.*, 2008a; *Moon and Joughin*, 2008; *Rignot and Kanagaratnam*, 2006].

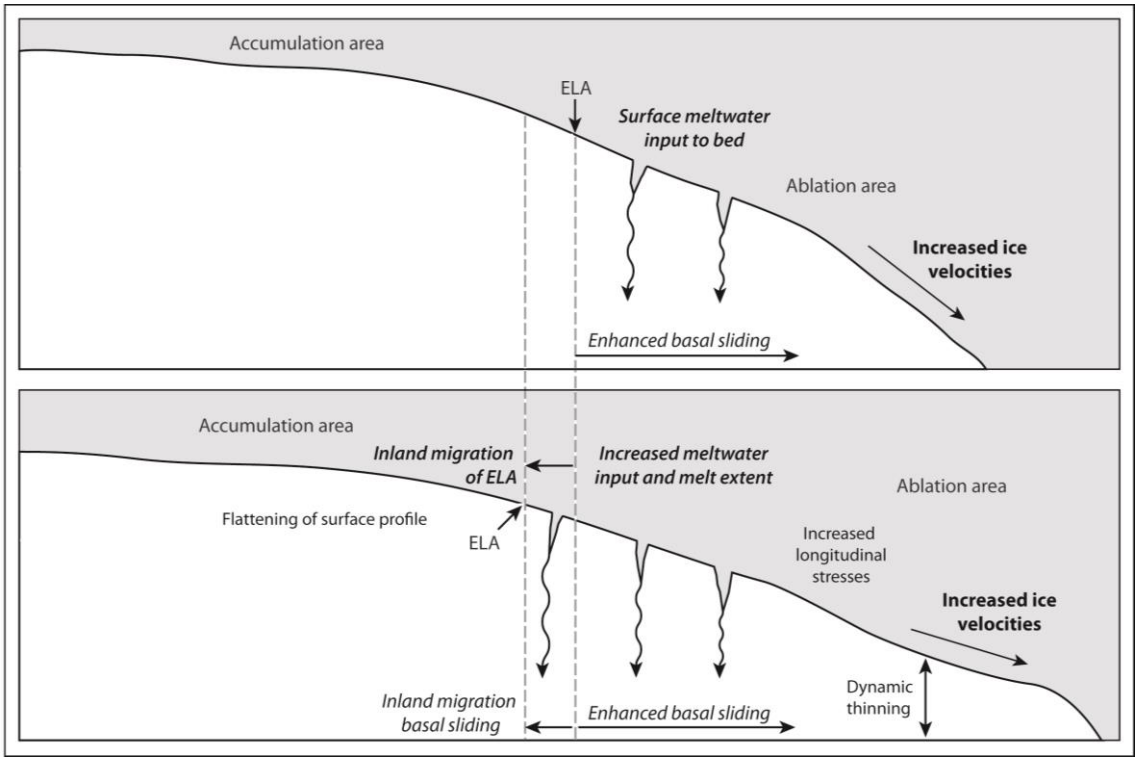

Figure 2.6. *Proposed feedback mechanisms between surface meltwater availability, basal sliding and ice sheet geometry for an idealized section of the GrIS. Atmospheric warming may increase surface meltwater input to the bed, resulting in enhanced basal sliding and transfer of a greater portion of the outlet glacier to the ablation zone. Further feedbacks may then develop between dynamic thinning, inland migration of basal sliding and ice acceleration. The response of individual sections of the ice sheet may vary significantly from these idealized theoretical responses.*

Recent results from marine-terminating Arctic outlet glaciers appear to support meltwater-enhanced basal lubrication as a mechanism for ice acceleration at sub-annual timescales: glacier velocities in the Uummannaq region of West Greenland [*Howat et al.*, 2010] and on Duvebreen, Austfonna [*Dunse et al.*, 2012] (Fig. 2.1), closely corresponded to the seasonal melt cycle. Similarly, results from Petermann

Glacier (Figures 1 & 2) [*Nick et al.*, 2012] and Daugaard Jensen Gletscher (Fig. 2.1) [*Bevan et al.*, 2012b] suggest that seasonal velocities primarily reflect variations in surface meltwater availability and data from Helheim Glacier (HH) (Fig. 2.1) indicate that surface meltwater can be transmitted to the bed within 12 to 36 hours [*Andersen et al.*, 2010a].

Despite an apparent relationship at seasonal or shorter timescales, however, the influence of meltwater-enhanced basal lubrication on interannual marine-terminating outlet glacier behaviour remains equivocal [e.g. *Bingham et al.*, 2003; *McFadden et al.*, 2011; *Seale et al.*, 2011; *van de Wal et al.*, 2008; *Vieli et al.*, 2004]. Evidence from the GrIS suggests that meltwater input to the bed may have a limited impact on interannual velocity changes on fast-flowing marine-terminating outlet glaciers and that ice flow may be more responsive to conditions at the ice-ocean interface [*Joughin et al.*, 2008a; *Nick et al.*, 2009]. A similar pattern has been observed on JEG [*Bingham et al.*, 2003] and Hansbreen, Spitzbergen (Fig. 2.1) [*Vieli et al.*, 2004], where periods of high melt coincided with reduced seasonal acceleration or even deceleration. Furthermore, numerical modelling results from HH [*Nick et al.*, 2009] suggest that changes in frontal position, as opposed to meltwater-enhanced basal lubrication, are the dominant control on interannual behaviour. Thus, evidence suggests that meltwater-enhanced basal lubrication may significantly influence marine-terminating outlet glacier dynamics at subannual timescales, but its role in driving interannual retreat remains uncertain.

To date, research into the influence of meltwater on marine-terminating outlet glacier dynamics has predominantly focused on enhanced basal lubrication. However, meltwater may also influence dynamics by promoting crevasse propagation at the terminus and/or lateral margins (Fig. 2.3), which together could reduce resistive stresses and promote glacier retreat [*Andersen et al.*, 2010b; *Sohn et al.*, 1998; *van der Veen*, 1998; *van der Veen et al.*, 2011; *Vieli et al.*, 2007]. This partly agrees with model results from JI, which suggest that increased crevasse water levels can partially

reproduce observed patterns of retreat and acceleration, but this may also reflect the choice of calving model [*Vieli and Nick*, 2011]. Numerical modeling studies also suggest that acceleration at Jakobshavn Isbrae (JI), West Greenland, may have resulted from weakening at its lateral margins, potentially due to hydrofracturing and/or meltwater induced warming of the ice [*van der Veen et al.*, 2011]. Thus, whilst the role of meltwater-enhanced fracture as a primary trigger of retreat remains equivocal, this mechanism warrants further consideration given the sensitivity of marine-terminating glaciers to changes at the terminus [*Nick et al.*, 2009; *Vieli and Nick*, 2011].

2.3.4. Subglacial drainage systems of large Arctic ice masses

Research into the subglacial hydrology of Arctic ice masses has predominantly focused on land-terminating sections, but recent advances, particularly from the GrIS, may provide insight into the comparative insensitivity of marine-terminating outlet glaciers to meltwater-enhanced basal lubrication at interannual timescales. Although the subglacial hydrology of marine-terminating outlet glaciers is comparatively poorly understood and the response of individual glaciers may vary significantly, observations suggest that the seasonal evolution of the subglacial drainage system is very similar to that observed on temperate, polythermal and land-terminating outlet glaciers and sections of the GrIS ablation zone: the subglacial drainage system is thought to evolve during the melt season, causing variation in the sensitivity of ice velocities to meltwater inputs (Fig. 2.5) [e.g. *Bartholomew et al.*, 2010; *Bartholomew et al.*, 2011; *Copland et al.*, 2003; *Dunse et al.*, 2012; *Howat et al.*, 2010; *Shepherd et al.*, 2009; *Sole et al.*, 2011; *Vieli et al.*, 2004]. Early in the melt season, the drainage system may be relatively inefficient (Fig. 2.5) [*Bartholomew et al.*, 2010; *Bingham et al.*, 2003; *Kamb*, 1987; *Price et al.*, 2008]. Consequently, meltwater can rapidly increase basal water pressures, causing rapid ice acceleration and surface uplift [*Bartholomew et al.*, 2010; *Bingham et al.*, 2005; *Copland et al.*, 2003]. As the melt season progresses, continued inflow of surface meltwater may promote the development of a more efficient,

chanellized drainage system which operates at lower basal water pressures (Fig. 2.5) [*Bingham et al.*, 2003; *Bingham et al.*, 2006; *Kamb*, 1987; *Palmer et al.*, 2011; *Shepherd et al.*, 2009; *Sole et al.*, 2011]. Thus, the sensitivity of ice velocities to surface melt may decline and only large meltwater inputs may induce substantial velocity change (Fig. 2.5) [*Bartholomew et al.*, 2010; *Dunse et al.*, 2012; *Schoof*, 2010; *Shepherd et al.*, 2009]. The primary implication of these results is that ice velocities depend not only on surface meltwater inputs, but also on the subglacial hydrological system.

The evolution of the subglacial drainage system has important implications for the response of marine-terminating outlet glaciers to interannual variations in meltwater availability and atmospheric warming [*Price et al.*, 2008; *Schoof*, 2010; *Sundal et al.*, 2011; *van de Wal et al.*, 2008]. As observed at seasonal timescales, continually high meltwater inputs are likely to promote the formation of an efficient basal drainage system, operating at low water pressures (Fig. 2.5). Consequently, increased meltwater input at interannual timescales may not necessarily equate to increased ice velocities, and may even cause deceleration above critical thresholds of water supply [*Schoof*, 2010; *Sundal et al.*, 2011; *Vieli et al.*, 2004]. This is consistent with empirical results from Kangiata Nunata Sermia, south-western Greenland, where meltwater-induced summer speed-up events are thought to contribute little to annual ice velocities, partly because they are offset by the deceleration associated with the formation of an efficient subglacial system [*Sole et al.*, 2011]. The key conclusion of these findings is that the evolution of the hydrological system may act as a buffer against accelerated ice loss through meltwater-enhanced basal sliding in response to increased melt and atmospheric warming [*Price et al.*, 2008; *Schoof*, 2010; *Vieli et al.*, 2004].

2.4. Oceanic forcing

Whilst atmospheric warming has received substantial scientific attention, oceanic forcing has been recently recognised as a key control on marine-terminating outlet

glacier dynamics. This was partly instigated by results from the GrIS [e.g. *Moon and Joughin*, 2008; *Pritchard et al.*, 2009; *Sole et al.*, 2008], where retreat rates were approximately two orders of magnitude greater on marine-terminating glaciers (10s to 1000s of m a^{-1}) than on their land-terminating counterparts (0.1 to 1 m a^{-1}) (Fig. 2.7). A similar pattern has been observed elsewhere in the Arctic, including Austfonna ice cap [*Dowdeswell et al.*, 2008], Devon Ice Cap [*Burgess and Sharp*, 2004; 2008; *Dowdeswell et al.*, 2004; *Shepherd et al.*, 2007] and in Arctic Alaska [*Arendt et al.*, 2006]. Furthermore, thinning rates have been greatest on glaciers occupying deep bedrock troughs [*Thomas et al.*, 2009], which may allow warm, sub-surface Atlantic Water (AW) from the continental shelf to access the glacier termini [e.g. *Rignot et al.*, 2010; *Straneo et al.*, 2011; *Straneo et al.*, 2010]. Oceanic forcing may be of particular concern in the near-future, as model predictions suggest that ocean temperatures around the GrIS may warm by 1.7 to 2°C by 2100 [*Yin et al.*, 2012].

2.4.1. Submarine melting at marine-terminating outlet glacier termini

Measurements of submarine melt rates at the termini of marine-terminating glaciers are rare, but estimates suggest that rates range between 0.7± 0.2 and 3.9 ± 0.8 m per day in central West Greenland [*Rignot et al.*, 2010] and 4.34 ± 0.94 m per day at JI [*Motyka et al.*, 2011]. Substantially higher melt rates of 6.9 to 12.4 m per day have been estimated at LeConte Glacier, Alaska (Fig. 2.1) [*Motyka et al.*, 2003], probably reflecting its comparatively southerly location. These results highlight the potential sensitivity of marine-terminating glaciers to oceanic warming, which could influence outlet glacier dynamics via a number of mechanisms (Fig. 2.8). First, enhanced submarine melting may cause grounding-line retreat at floating and grounded margins, potentially resulting in further un-grounding and the development of positive feedbacks if retreat occurs into deeper water [*Howat et al.*, 2008a; *Joughin et al.*, 2008b; *Meier and Post*, 1987; *Nick et al.*, 2012; *Vieli et al.*, 2001; *Vieli and Nick*, 2011]. Second, oceanic warming may cause rapid thinning of floating termini [e.g. *Motyka et al.*, 2011;

Nick et al., 2012; *Thomas*, 2004] and the formation of deeply incised basal channels [*Rignot and Steffen*, 2008], which together make the termini more vulnerable to full thickness fracture and eventual disintegration (Fig. 2.8). Third, submarine melting may influence the terminus geometry and calving rates by undercutting at the grounding line and/or waterline (Fig. 2.8) [*Benn et al.*, 2007; *Vieli et al.*, 2002].

2.4.2. Oceanic controls on marine-terminating glacier dynamics

Our understanding of oceanic forcing has been largely developed from observations from the GrIS, where warming has immediately preceded the retreat and acceleration of a number of marine-terminating outlet glaciers [e.g. *Bevan et al.*, 2012a; *Hanna et al.*, 2009; *Holland et al.*, 2008; *Motyka et al.*, 2011; *Murray et al.*, 2010; *Rignot et al.*, 2012]. This was first investigated in detail at JI, which was one of the earliest and most significant contributors to recent GrIS mass losses [*Joughin et al.*, 2004; *Joughin et al.*, 2008c; *Motyka et al.*, 2010; *Motyka et al.*, 2011; *Rignot and Kanagaratnam*, 2006; *Thomas et al.*, 2003]. Following 50 years of comparative stability [*Csatho et al.*, 2008; *Sohn et al.*, 1998], JI's floating terminus began to retreat in October 1998 [*Luckman and Murray*, 2005] and subsequent periods of acceleration often coincided with the loss of sections of its tongue [*Joughin et al.*, 2004; *Joughin et al.*, 2008c]. Initial retreat was accompanied by rapid thinning, which may have ungrounded the tongue from its underlying pinning points, and caused a substantial reduction in resistive stresses [*Joughin et al.*, 2004; *Thomas*, 2004; *Thomas et al.*, 2003]. This may have initiated feedbacks between retreat, dynamic thinning and acceleration, which led to the disintegration of the ice tongue by spring 2003 [*Joughin et al.*, 2004; *Joughin et al.*, 2008c; *Thomas*, 2004].

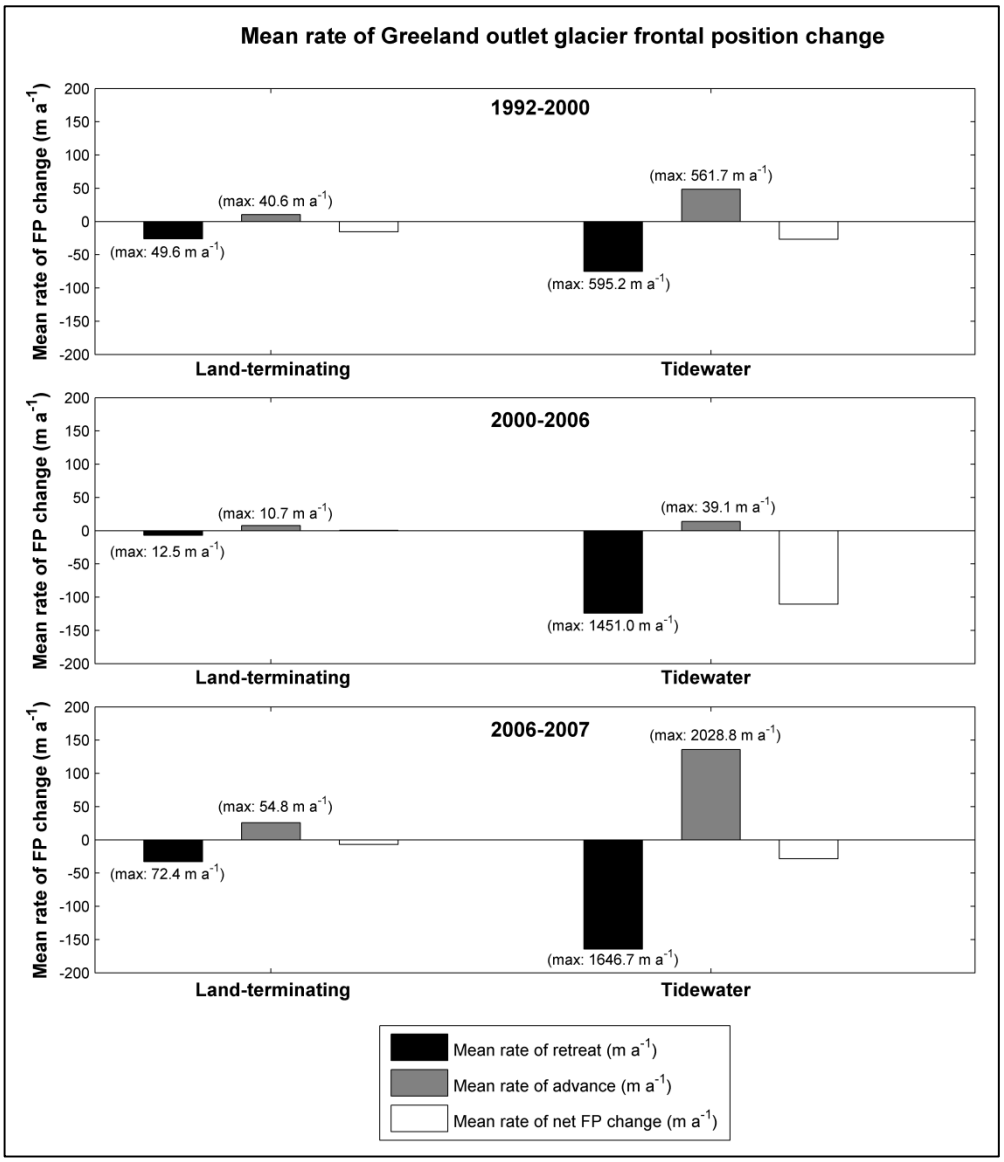

Figure 2.7. *Mean rate of Greenland outlet glacier frontal position change (m a^{-1}) grouped according to terminus type. The mean rate of retreat, advance and net frontal position change were calculated for land-terminating and tidewater glacier termini and are shown in the bars above. Values were calculated for three time periods (1992– 2000, 2000–2006 and 2006–2007) and maximum rates of retreat/advance are given in brackets above the corresponding bar. Mean values are calculated from a sample of 139 (1992–2000), 169 (2000–2006) and 154 (2006–2007) tidewater glaciers, and 10 (1992–2000), 14 (2000–2006) and 13 (2006–2007) land-terminating glaciers. Glaciers terminating in ice shelves were excluded from the analysis, as data were only available from three glaciers for 1992–2000 and 2000–2006 and no data were available for 2006–2007. Source: Data provided by T. Moon, 2011 (Moon and Joughin, 2008).*

The underlying driver(s) of mass losses at JI remain subject to debate, but evidence suggests that oceanic warming, rather than increased air temperatures, was the primary cause [*Holland et al.*, 2008; *Motyka et al.*, 2010; *Motyka et al.*, 2011; *Thomas*, 2004]. Thinning rates on JI's floating tongue far exceeded estimated surface melt rates and closely followed substantial sub-surface ocean warming, which is thought to have increased basal melt rates by 25% [*Holland et al.*, 2008; *Motyka et al.*, 2011; *Thomas et al.*, 2003]. Estimates suggest that the resultant thinning was sufficient to destabilise the ice tongue and to initiate rapid mass loss [*Motyka et al.*, 2011]. Numerical modelling results agree with these findings and suggest that increased submarine melting is capable of triggering the behaviour observed at JI, but that dynamic feedbacks are also required [*Vieli and Nick*, 2011].

Subsequent to retreat at JI, marine-terminating outlet glaciers in south-eastern Greenland followed a similar progression of dynamic change [e.g. *Howat et al.*, 2008a; *Howat et al.*, 2007; *Joughin et al.*, 2008b; *Luckman et al.*, 2006]. Losses began with retreat, thinning and acceleration proportional to retreat, which suggests that changes also resulted from a loss of resistive stresses at the terminus [*Howat et al.*, 2008a; *Howat et al.*, 2007; *Howat et al.*, 2005]. The trigger for these changes remains equivocal, with both air temperatures [*Box et al.*, 2009; *Hanna et al.*, 2008] and ocean temperatures [*Hanna et al.*, 2009; *Murray et al.*, 2010; *Seale et al.*, 2011] increasing substantially prior to retreat. However, the initiation of glacier response at the terminus [*Howat et al.*, 2008a; *Howat et al.*, 2007; *Howat et al.*, 2005] suggests that meltwater-enhanced basal lubrication was unlikely to be the primary trigger and that forcing factors operating at the calving front, such as oceanic warming, were the more likely cause. This is consistent with numerical modelling results from HH, which suggested that interannual glacier dynamics are comparatively insensitive to enhanced basal lubrication, but are acutely sensitive to calving front perturbations [*Nick et al.*, 2009].

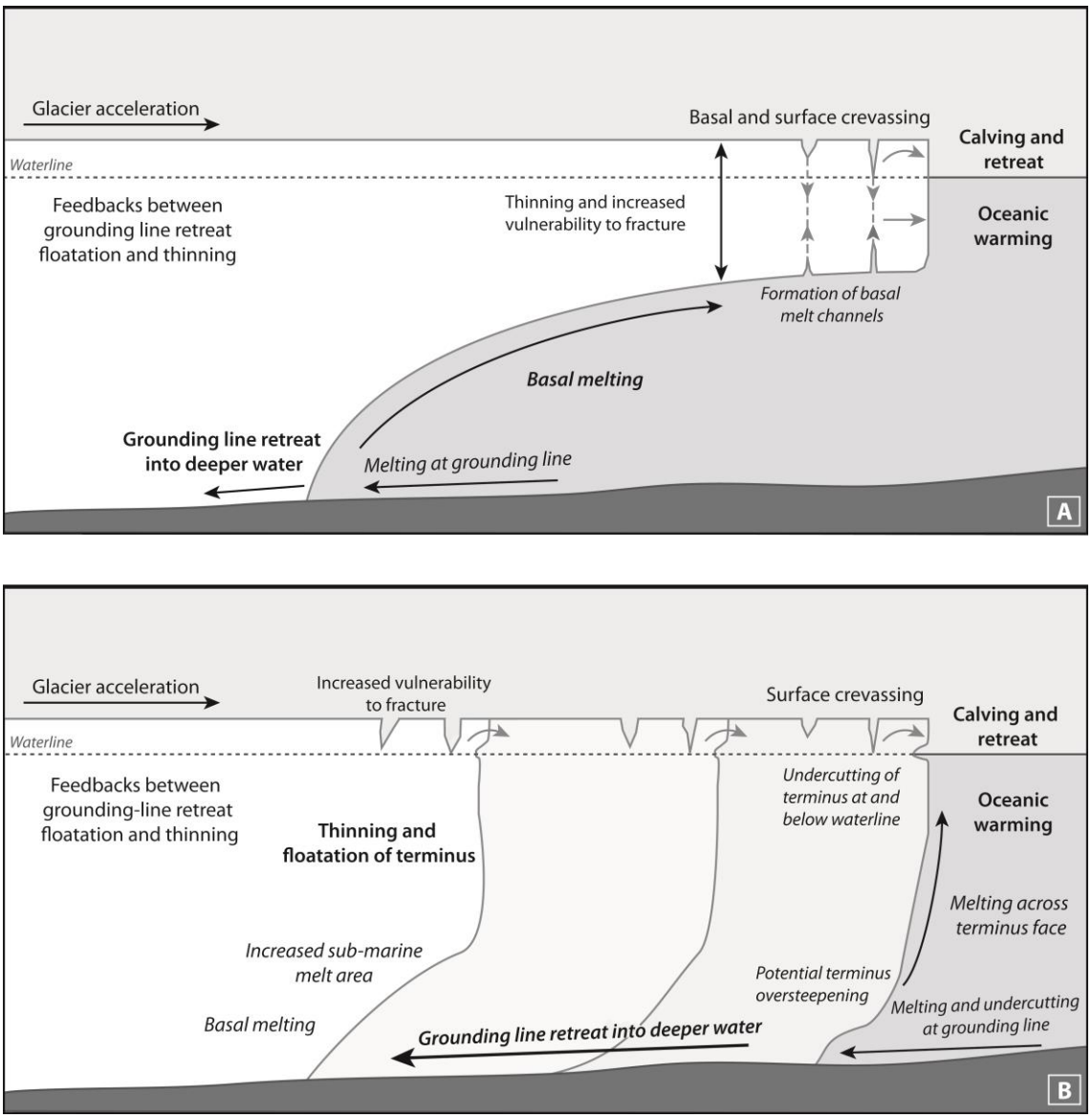

Figure 2.8. *Illustration of the influence of oceanic warming and submarine melting on outlet glacier dynamics and geometry for (A) an initially floating terminus and (B) an initially grounded terminus. In (A), feedbacks may develop between submarine melting, grounding-line retreat, thinning and calving front retreat. In (B), changes in terminus geometry may initiate feedbacks between grounding-line/terminus retreat, thinning and floatation.*

2.4.3. Marine-terminating outlet glacier dynamics and Atlantic Water distribution

An important emerging theme has been the relationship between marine-terminating outlet glacier dynamics and variations in the distribution and properties of warm Atlantic Water (AW) [*Andresen et al.*, 2012; *Holland et al.*, 2008; *Murray et al.*, 2010; *Straneo et al.*, 2011; *Straneo et al.*, 2010]. Until recently, it was assumed that oceanic changes at

the continental shelf could be transmitted into outlet glacier fjords, but this was largely untested [*Mortensen et al.*, 2011; *Straneo et al.*, 2010]. However, recent studies have shown that AW can access the fjords of a number of large outlet glaciers in Greenland [*Christoffersen et al.*, 2011; *Holland et al.*, 2008; *Johnson et al.*, 2011; *Mayer et al.*, 2000; *Straneo et al.*, 2011; *Straneo et al.*, 2010] and Svalbard [*Nilsen et al.*, 2008]. These results marked a significant advance in our understanding, as they demonstrated that rapid connections could exist between marine-terminating outlet glaciers and oceanic variability in the northern North Atlantic, particularly via deep fjords [*Straneo et al.*, 2010]. This conclusion was supported by the coincidence of glacier retreat in south-eastern Greenland in the early 2000s with AW incursion onto the coast [*Christoffersen et al.*, 2011; *Murray et al.*, 2010; *Seale et al.*, 2011] and provides a plausible mechanism for widespread and synchronous retreat.

2.4.4. Marine-terminating outlet glacier dynamics and fjord circulation

Recent research into the role of AW has led to increased consideration of the factors controlling its distribution within glacial fjords. A number of possible controls have been identified (Fig. 2.9), including: the temperature, salinity and volume of subtropical waters at the continental shelf; along-shore wind patterns; storm tracks; and fjord stratification [*Christoffersen et al.*, 2011; *Nilsen et al.*, 2008; *Straneo et al.*, 2011; *Straneo et al.*, 2010]. Fjord circulation can also be influenced by subglacial meltwater, which forms a rising plume of cool, buoyant water at the calving front and promotes a compensatory inflow of warmer water at depth (Fig. 2.9) [*Motyka et al.*, 2003; *Motyka et al.*, 2011; *Straneo et al.*, 2011]. Thus, plumes may substantially increase submarine melt rates [*Jenkins*, 2011; *Motyka et al.*, 2003; *Seale et al.*, 2011] and model results suggest that melt increases linearly with oceanic warming and to the power of one-third with subglacial discharge [*Jenkins*, 2011; *Xu et al.*, 2012]. A key implication of this relationship is that positive feedbacks could develop, whereby atmospheric warming increases subglacial discharge and ice sheet runoff, which strengthens the plume and

enhances submarine melt rates [*Seale et al.*, 2011]. Feedbacks between glacier runoff and ocean properties have been identified as a potential trigger for recent retreat in south-eastern Greenland [*Murray et al.*, 2010; *Seale et al.*, 2011] and variations in meltwater production may be an important control on AW distribution in the region [*Murray et al.*, 2010].

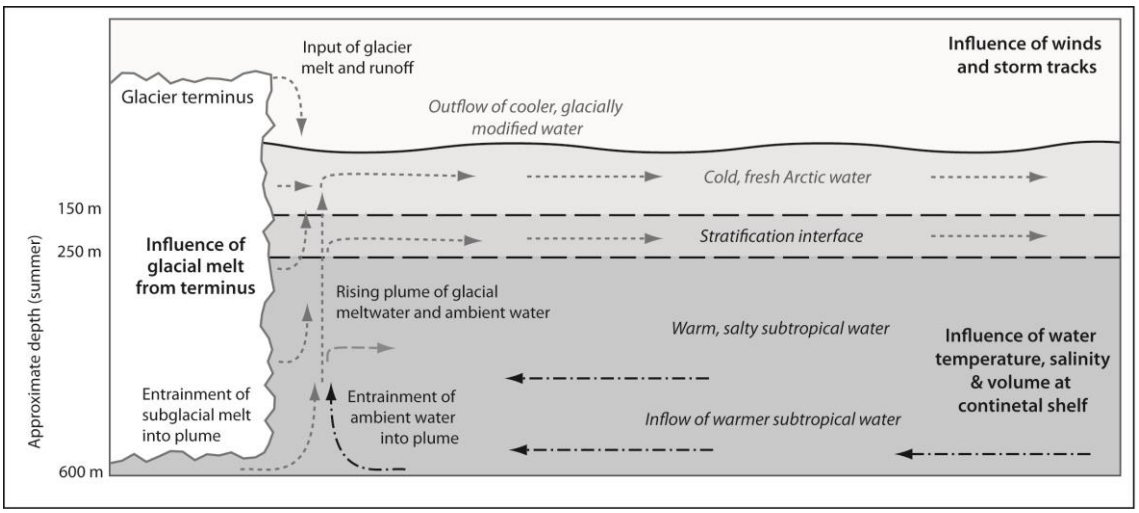

Figure 2.9. *Schematic illustrating the circulation pattern and water properties within a large Arctic outlet glacier fjord. Fjord circulation and water mass depths are based on conditions within Helheim Glacier fjord [Straneo et al., 2011]. The primary controls on fjord circulation are thought to be water properties at the continental shelf, wind/storm tracks and glacial meltwater input.*

2.5. Sea ice forcing

The increasing focus on oceanic forcing has led to further consideration of the influence of sea ice on marine-terminating Arctic outlet glacier behaviour (Fig. 2.3). Although sea ice is discussed separately, it should be noted that it is influenced by both air and ocean temperatures (Fig. 2.3) and that these factors are not independent. It should also be noted that sea ice concentrations may significantly affect SMB, through their influence on accumulation and ablation patterns (Fig. 2.3) [e.g. *Bamber et al.*, 2004; *Rennermalm et al.*, 2009]. The influence of sea ice on marine-terminating Arctic outlet glacier dynamics was first documented in northern Greenland, where semi-

permanent fast ice contributed significantly to the stability of several marine-terminating outlet glaciers [*Higgins*, 1989; 1990; *Mayer et al.*, 2000; *Reeh et al.*, 2001; *Weidick*, 1975]. Fast-ice was thought to promote glacier stability by suppressing calving and by preventing calved material from moving away from the terminus [*Higgins*, 1990; *Reeh et al.*, 2001]. In contrast, periods of fast-ice disintegration were accompanied by rapid calving and release of trapped ice. Early investigations suggested that fast-ice break-up occurred at decadal intervals, when summer temperatures were exceptionally warm [*Higgins*, 1989; 1990; *Reeh et al.*, 2001], but this pattern has changed substantially in recent years, with disintegration now occurring several times per decade [*Hughes et al.*, 2011].

2.5.1. Sea ice influence on the seasonal calving cycle

Recent studies have investigated the influence of sea ice on calving rates at more southerly Greenland glaciers [*Ahn and Box*, 2010; *Howat et al.*, 2010], particularly on JI [*Amundson et al.*, 2010; *Joughin et al.*, 2008c; *Sohn et al.*, 1998]. As in northern Greenland, sea ice concentrations at JI appear to influence the timing and nature of calving events, but this occurs on seasonal, as opposed to decadal, timescales [*Amundson et al.*, 2010; *Joughin et al.*, 2008c]. In winter, sea ice binds together icebergs to form a semi-rigid, seasonal ice shelf, or mélange, which is pushed along the fjord as a coherent mass by the advancing calving front (Fig. 2.10) [*Amundson et al.*, 2010]. The mélange suppresses calving rates by up to a factor of six and alters the terminus geometry and near-front stress fields, causing seasonal terminus advance and deceleration [*Amundson et al.*, 2010; *Joughin et al.*, 2008c; *Sohn et al.*, 1998]. Conversely, spring-time mélange disintegration allows high rates of summer calving to commence, which initiates seasonal retreat and acceleration (Fig. 2.10) [*Ahn and Box*, 2010; *Amundson et al.*, 2010; *Howat et al.*, 2010; *Joughin et al.*, 2008c]. A similar relationship has been documented on the Agassiz Ice Cap, Ellesmere Island, Arctic Canada, where peak glacier velocities have coincided with seasonal sea ice

disintegration [*Williamson et al.*, 2008]. However, observations also indicated that sea ice weakening and/or thinning, as opposed to complete disintegration, may be sufficient to initiate seasonal acceleration [*Williamson et al.*, 2008].

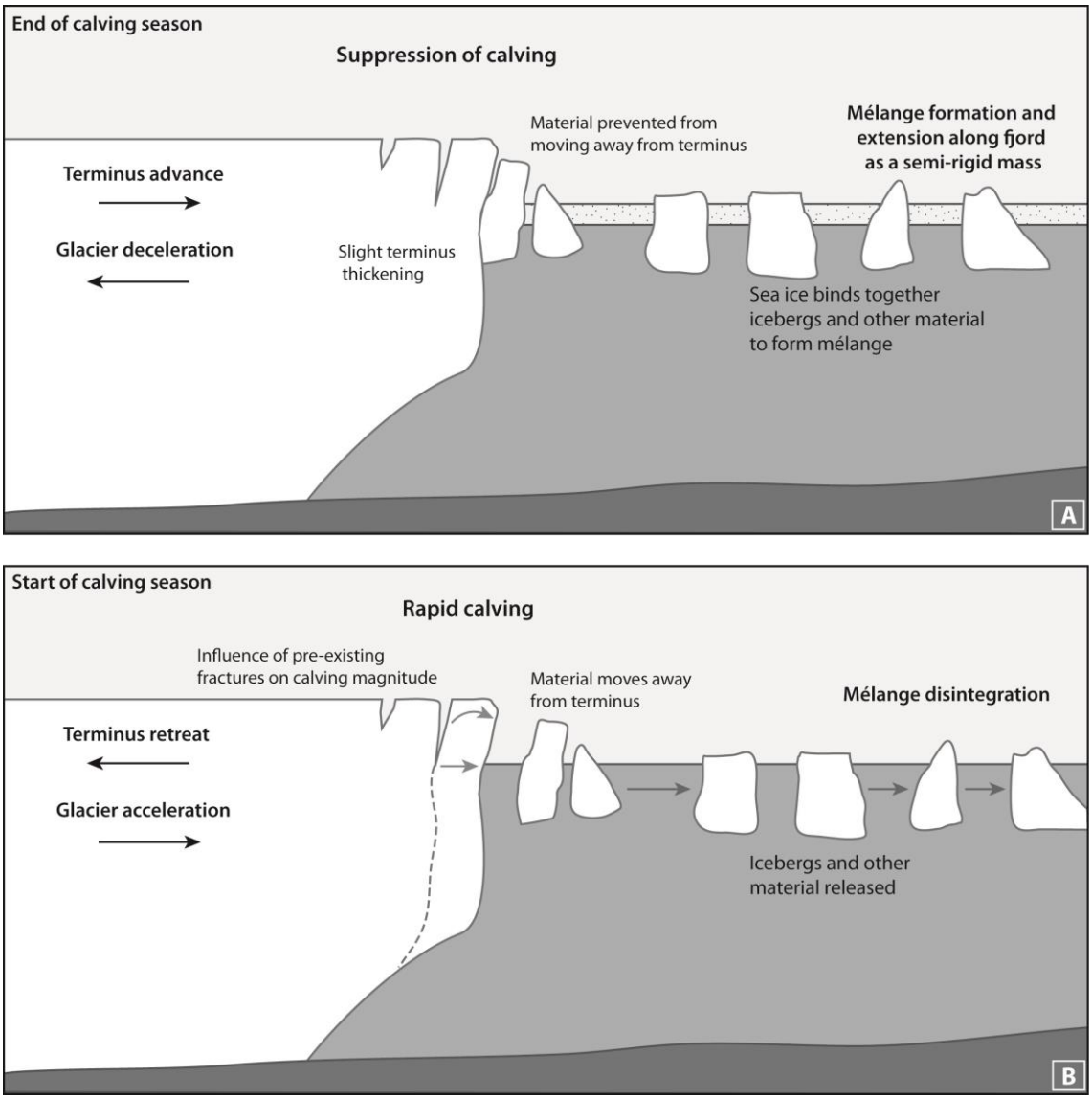

Figure 2.10. *Illustration of the influence of sea ice and mélange formation on Arctic outlet glacier dynamics during (A) mélange formation at the end of the calving season and (B) mélange disintegration at the start of the calving season. In (A) the mélange binds together material within the fjord, thus suppressing calving and promoting seasonal advance. In (B) mélange disintegration allows seasonally high calving rates to commence and promotes glacier retreat.*

2.5.2. Sea ice influence on interannual marine-terminating outlet glacier behaviour

Observations from JI have contributed substantially to our understanding of sea ice forcing at seasonal timescales, but have also highlighted its potential influence on interannual behaviour of marine-terminating outlet glaciers [*Joughin et al.*, 2008c]. Initial retreat at JI began within one year of the onset of sea ice decline in the surrounding Disko Bay [*Joughin et al.*, 2008c]. Estimates suggest that the extension of ice free conditions by one or two months may have been sufficient to trigger the initial retreat by extending the duration of seasonally high calving rates [*Joughin et al.*, 2008c]. This is consistent with numerical modelling results which demonstrated that reduced mélange duration could trigger rapid retreat at JI, although it could not replicate the magnitude of subsequent seasonal variations in terminus position [*Vieli and Nick*, 2011]. A similar response has been observed in the Uummannaq region [*Howat et al.*, 2010] and at KG [*Christoffersen et al.*, 2011; *Seale et al.*, 2011], where interannual retreats also followed sea ice decline. It is thought that delayed winter sea ice formation at KG [*Christoffersen et al.*, 2011; *Seale et al.*, 2011] and early mélange clearance in the Uummannaq region [*Howat et al.*, 2010] may have initiated glacier retreat by extending the calving season.

Although the influence of sea ice on marine-terminating outlet glacier behaviour has been little-studied outside of the GrIS, Arctic sea ice has declined markedly in recent years [e.g. *Kwok and Rothcock*, 2009; *Rodrigues*, 2009; *Serreze et al.*, 2009] and its influence may become increasingly widespread if current losses continue. On the basis of the relationships observed in Greenland, we suggest that sea ice decline may affect glacier dynamics via two potential mechanisms: i), seasonal calving may be extended in areas which currently experience seasonally ice-free conditions; and ii), areas currently characterised by interannual fast-ice may transition to a seasonal sea-ice loss. We suggest that the former process may become increasingly significant on the

eastern and central-western Greenland coast, on the western coasts of NZ and Svalbard and in the southern Canadian Arctic, where the ice-free season has extended markedly during the past thirty years [*Rodrigues*, 2008] and losses are predicted to continue during the 21st century (Fig. 2.11) [*ACIA*, 2004; *IPCC*, 2007]. This mechanism may eventually cease, however, if areas become perennially ice-free. The latter process may become increasingly important on the coasts of north-eastern Greenland, north-eastern Svalbard, eastern NZ, southern FJL and the northern Canadian Arctic, where sea ice concentrations are predicted to decline markedly by 2100 (Fig. 2.11) [*ACIA*, 2004; *IPCC*, 2007]. Observations suggest that this may already be occurring in north-eastern Greenland, where fast-ice break up has occurred several times in the past decade [*Hughes et al.*, 2011], in comparison to the decadal intervals recorded by earlier work [*Higgins*, 1989; 1990; *Reeh et al.*, 2001].

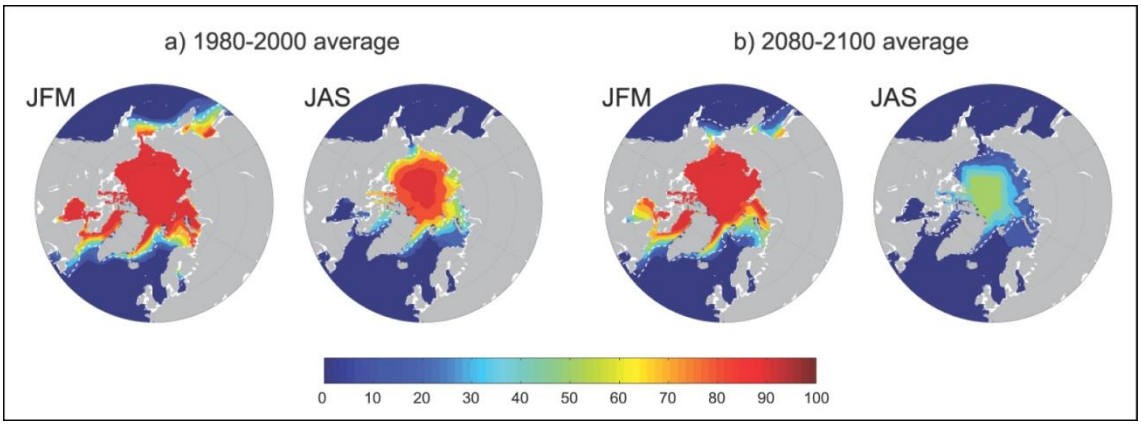

Figure 2.11. *Multi-model mean sea ice concentration (%) for January to March (JFM) and June to September (JAS) in the Arctic for the periods (a) 1980–2000 and (b) 2080–2100 for the SRES A1B scenario. The dashed white line indicates the present-day 15% average sea ice concentration limit. Note the substantial reduction in summer sea ice concentrations predicted across the Arctic by 2100, which may extend seasonally ice-free conditions in southerly areas and may result in a transition from multi-year fast-ice to seasonal sea ice disintegration in northern regions. Source: Modified from IPCC (2007) and Flato et al. (2004).*

2.6. Key uncertainties and future directions for research

Despite recent advances, the response of marine-terminating outlet glaciers to climatic/oceanic forcing continues to be an area of rapidly developing research and significant uncertainties remain over the relative importance of each forcing factor and the mechanisms by which these factors influence glacier dynamics [*Howat et al.*, 2010; *Sole et al.*, 2008; *Vieli and Nick*, 2011]. The following subsections outline the primary uncertainties surrounding marine-terminating Arctic outlet glacier behaviour and highlight key areas for future research.

2.6.1. Spatial variation in the relative importance of climatic/oceanic forcing factors

Our understanding of marine-terminating Arctic outlet glacier response to climatic/oceanic forcing has been primarily based on observations from a small number of Greenland outlet glaciers, with the majority of research focusing on JI and south-eastern Greenland, particularly HH and KG. Consequently, it is uncertain whether the relationships observed at these locations can be extrapolated to other Arctic regions and/or whether recent changes represent a longer-term trend or shorter-term variability [*Price et al.*, 2011; *Vieli and Nick*, 2011]. Although glaciers within certain regions have shown some common response to climatic/oceanic forcing, most notably south-eastern Greenland [*Bjørk et al.*, 2012; *Howat et al.*, 2008a; *Murray et al.*, 2010], this pattern is far from ubiquitous. Results from West Greenland found no correlation between retreat and climatic/oceanic forcing for a sample of 59 marine-terminating outlet glaciers [*McFadden et al.*, 2011] and comparison of 15 major Greenland outlet glaciers between 1985 and 2011 showed some common response to forcing, but also highlighted several notable differences [*Bevan et al.*, 2012a]. Furthermore, assessment of decadal and interannual velocity changes on >200 major Greenland outlet glaciers demonstrated substantial variations in glacier behaviour at both regional and local scales and highlighted the importance of glacier-specific factors [*Moon et al.*, 2012]. In

contrast to the GrIS, observations in the Canadian Arctic [*Gardner et al.*, 2011] and Novaya Zemlya [*Moholdt et al.*, 2012] have found no difference between area-averaged thinning rates in land- and marine-terminating basins [*Gardner et al.*, 2011]. Moreover, the longer-term evolution of HH, KG and JI has differed markedly following their earlier mass losses [*Howat et al.*, 2011; *Thomas et al.*, 2011] and numerical modelling studies indicate that marine-terminating outlet glaciers can rapidly adjust to short-term calving front perturbations [*Vieli and Nick*, 2011]. Together, this evidence suggests that the relative importance of climatic/oceanic controls varies across the Arctic and that present theories of outlet glacier response to forcing cannot be universally applied to all glaciers, regions or ice masses. We therefore draw attention to the danger of extrapolating recent rapid mass losses from a small number of glaciers and highlight the need for continued research into the climatic/oceanic drivers of marine-terminating outlet glacier behaviour on each of the major Arctic ice masses.

2.6.2. Glacier-specific factors

Results from the GrIS have highlighted the substantial variation in marine-terminating outlet glacier response to climatic/oceanic forcing, [*McFadden et al.*, 2011; *Moon et al.*, 2012] and the role of glacier-specific controls, particularly fjord geometry and basal topography, is being increasingly recognised [*Bevan et al.*, 2012a; *Howat and Eddy*, 2011; *Joughin et al.*, 2010; *Joughin et al.*, 2012; *Nick et al.*, 2009; *Thomas et al.*, 2009]. Traditional theories of tidewater glacier dynamics and ice sheet instability suggest that a reverse basal slope may initiate rapid retreat via a series of positive feedbacks, as the glacier terminus retreats into progressively deeper water (Fig. 2.12) [e.g. *Hughes*, 1986; *Joughin et al.*, 2008b; *Meier and Post*, 1987; *Vieli et al.*, 2001; *Vieli et al.*, 2002; *Weertman*, 1974]. This behaviour may occur independently of climatic/oceanic forcing [e.g. *Alley*, 1991; *Pfeffer*, 2003], but may also be initiated by perturbations at the calving front [e.g. *Howat et al.*, 2008a; *Joughin et al.*, 2008b; *Meier and Post*, 1987; *Nick et al.*, 2009; *Pfeffer*, 2007]. However, the influence of overdeepenings on glacier

dynamics remains subject to debate and recent modelling results suggest that stable grounding-line positions can be achieved on a reverse bedrock slope [*Gudmundsson et al.*, 2012; *Nick et al.*, 2010]. Furthermore, the importance of other glacier-specific factors, such as variations in fjord width, is being increasingly acknowledged [*Jamieson et al.*, 2012]. Assessing the role of glacier-specific controls is a key area for future study, as inadequate consideration of these factors may lead to substantial errors in estimates of glacier response to climatic/oceanic forcing and their contribution to sea level rise. A full analysis is, however, currently constrained by limited data availability.

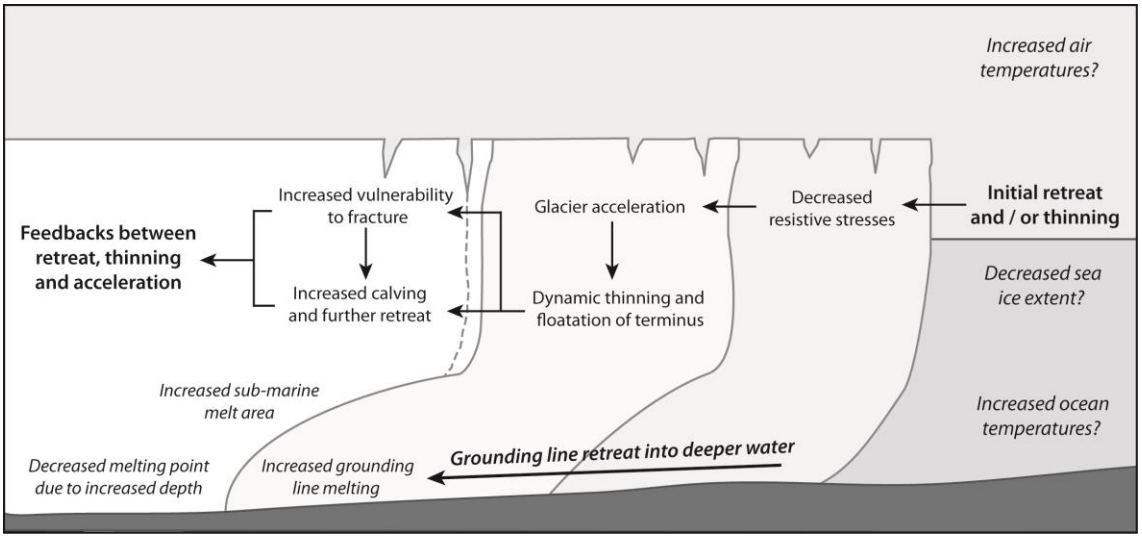

Figure 2.12. *Illustration of feedbacks between glacier retreat, dynamic thinning and ice acceleration during retreat into progressively deeper water. Initial retreat reduces resistive stresses acting on the outlet glacier, promoting dynamic thinning and terminus floatation, which in turn makes the terminus increasingly vulnerable to fracture and further retreat. Positive feedbacks may also develop between grounding-line retreat and submarine melt rates. These feedbacks may occur independently of climatic/oceanic forcing, but may also be triggered by forcing.*

2.6.3. Quantitative assessment of marine-terminating outlet glacier response to climatic/oceanic forcing

Even on comparatively well-studied sections of the GrIS, previous studies have tended to infer causality from the coincidence of climatic/oceanic change and marine-terminating outlet glacier response [e.g. *Luckman et al.*, 2006; *Moon and Joughin*,

2008]. As a consequence, the mechanisms linking climatic/oceanic forcing and glacier dynamics are often poorly understood [*Nick et al.*, 2009; *Vieli and Nick*, 2011] and the extent to which forcing can explain glacier behaviour has not been extensively assessed. This has been improved in recent years through the development of numerical models focusing on the response of individual outlet glaciers to forcing [*Nick et al.*, 2009; *Vieli and Nick*, 2011]. However, marine-terminating outlet glacier dynamics are not yet adequately represented in ice sheet-scale models [*Price et al.*, 2011; *Vieli and Nick*, 2011; *Zwally et al.*, 2011] and this is recognised as a significant limitation in our capacity to accurately predict near-future sea level rise [*IPCC*, 2007]. We therefore highlight numerical modelling as an important area for future development and emphasise the need to combine results with remotely sensed and observational data, in order to improve our understanding of recent changes in Arctic marine-terminating outlet glacier dynamics.

2.7. Conclusions

Arctic ice masses have rapidly lost mass since the mid-1990s due to a combination of negative SMB and accelerated discharge from marine-terminating glaciers [*van den Broeke et al.*, 2009]. Studies conducted during the past twenty years have fundamentally altered our understanding of ice mass response to climatic/oceanic forcing and have demonstrated that changes in marine-terminating glacier dynamics can result in dramatic mass losses at annual timescales [e.g. *Howat et al.*, 2008b; *Rignot and Kanagaratnam*, 2006; *Stearns and Hamilton*, 2007]. In this paper, we identify and review three primary climatic/oceanic drivers of marine-terminating Arctic outlet glacier behaviour: air temperatures, ocean temperatures and sea ice. Although discussed separately, these factors are interconnected and we highlight a number of potentially important linkages which may significantly influence glacier dynamics. We suggest that meltwater-enhanced basal sliding may contribute to marine-terminating outlet glacier velocities at seasonal timescales [*Howat et al.*, 2010; *Nick et al.*, 2012],

but its net effect on interannual behaviour may be limited, potentially due to the capacity of the subglacial hydrological system to evolve in response to meltwater inputs [*Price et al.*, 2008; *Sundal et al.*, 2011]. Instead, marine-terminating outlet glaciers may respond to atmospheric warming via a number of alternative mechanisms, including: i) hydrofracture of crevasses at the terminus/lateral margins; ii) meltwater-enhanced submarine melting, via plume circulation and; iii) sea ice loss due to atmospheric warming. Marine-terminating outlet glaciers are potentially highly sensitive to oceanic warming [*Rignot et al.*, 2010], which may cause retreat through: i) submarine melting and rapid thinning across floating sections; ii) grounding-line retreat; iii) alteration of the calving front geometry at the grounding line and/or waterline and; iv) sea ice loss due to oceanic warming. We emphasise the need to further investigate controls on Atlantic Water distribution within glacier fjords and feedbacks between fjord circulation, subglacial meltwater and submarine melting. We also underscore the influence of sea ice on seasonal and interannual outlet glacier dynamics, via its influence on calving rates [*Amundson et al.*, 2010; *Joughin et al.*, 2008c], and suggest that sea ice forcing may become increasingly important during the 21st century if current negative trends continue.

We suggest that the respective role of each climatic/oceanic factor varies across the Arctic and that outlet glacier response to forcing within one region cannot be assumed to apply elsewhere. Moreover, glacier-specific factors may substantially modulate the response of individual glaciers to climatic/oceanic forcing and we highlight this as priority area for future research. Numerical modelling results have improved our understanding of marine-terminating outlet glacier behaviour, but remain a key area for future development. Notwithstanding recent advances, substantial uncertainties remain over the respective roles of the various climatic/oceanic and glacier-specific forcing factors and we highlight the potential danger of extrapolating mass loss rates from a small number of study glaciers. Consequently, the response of marine-terminating

Arctic outlet glaciers to climatic/oceanic forcing remains a key area for future research and is crucial for accurate prediction of near-future sea level rise and Arctic ice mass response to climate warming.

Acknowledgements

This work was supported by a Durham Doctoral Studentship granted to J.R. Carr. We thank T. Moon for the provision of Greenland frontal position data and G. Moholdt for helpful comments on Svalbard mass balance data. We thank E. Hanna and N.J. Cox for their assistance with the air temperature data. Two anonymous reviewers are thanked for their constructive comments on the manuscript.

2.8. References

Abdalati, W., W. Krabill, E. Frederick, S. Manizade, C. Martin, J. Sonntag, R. Swift, R. H. Thomas, W. Wright, and J. Yungel (2001), Outlet glacier and margin elevation changes: Near-coastal thinning of the Greenland ice sheet, *Journal of Geophysical Research*, *106*(D24), 33,729 –733,741.

Abdalati, W., W. Krabill, E. Frederick, S. Manizade, C. Martin, J. Sonntag, R. Swift, R. H. Thomas, J. Yungel, and R. Koerner (2004), Elevation changes of ice caps in the Canadian Arctic Archipelago, *Journal of Geophysical Research*, *109*, F04007.

Abdalati, W., and K. Steffen (2001), Greenland ice sheet melt extent: 1979–1999, *Journal of Geophysical Research*, *106*(D24), 33983-33988.

ACIA (2004), *Impacts of a Warming Arctic: Arctic Climate Impact Assessment*, Cambridge University Press, Cambridge.

Ahn, Y., and J. E. Box (2010), Glacier velocities from time-lapse photos: technique development and first results from the Extreme Ice Survey (EIS) in Greenland, *Journal of Glaciology*, *198*, 723-734.

Alley, R. B. (1991), Sedimentary processes may cause fluctuations of tidewater glaciers, *Annals of Glaciology*, *15*, 119-124.

Alley, R. B., T. K. Dupont, B. R. Parizek, and S. Anandakrishnan (2005), Access of surface meltwater to beds of sub-freezing glaciers: preliminary insights, *Annals of Glaciology*, *40*, 8-14.

Amundson, J. M., M. Fahnestock, M. Truffer, J. Brown, M. P. Lüthi, and R. J. Motyka (2010), Ice mélange dynamics and implications for terminus stability, Jakobshavn Isbræ, Greenland, *Journal of Geophysical Research*, *115*, F01005, doi:10.1029/2009JF001405.

Andersen, C. S., et al. (2010a), Spatial and temporal melt variability at Helheim Glacier, East Greenland, and its effect on ice dynamics, *Journal of Geophysical Research*, *115*, F04041.

Andersen, M. L., et al. (2010b), Spatial and temporal melt variability at Helheim Glacier, East Greenland, and its effect on ice dynamics, *Journal of Geophysical Research*, *115*, F04041.

Andresen, C. S., et al. (2012), Rapid response of Helheim Glacier in Greenland to climate variability over the past century, *Nature Geoscience*, *5*, 37-41.

Arendt, A., K. Echelmeyer, W. Harrison, C. Lingle, S. Zirnheld, V. Valentine, B. Ritchie, and M. Druckenmiller (2006), Updated estimates of glacier volume changes in the western Chugach Mountains, Alaska, and a comparison of regional extrapolation methods, *Journal of Geophysical Research*, *111*, F03019.

Arendt, A., S. B. Luthcke, C. F. Larsen, W. Abdalati, W. Krabill, and M. J. Beedle (2008), Validation of high-resolution GRACE mascon estimates of glacier mass changes in the St Elias Mountains, Alaska, USA, using aircraft laser altimetry, *Journal of Glaciology*, *54*(188), 778-787.

Bamber, J., R. B. Alley, and I. Joughin (2007), Rapid response of modern day ice sheets to external forcing, *Earth and Planetary Science Letters*, *257*, 1-13.

Bamber, J., W. Krabill, V. Raper, and J. Dowdeswell (2004), Anomalous recent growth of part of a large Arctic ice cap: Austfonna, Svalbard, *Geophysical Research Letters*, *31*, L12402, doi:10.1029/2004GL019667.

Bartholomew, I., P. Nienow, D. Mair, A. Hubbard, M. A. King, and A. Sole (2010), Seasonal evolution of subglacial drainage and acceleration in a Greenland outlet glacier, *Nature Geoscience*, *3*, 408-411.

Bartholomew, I., A. Sole, D. Mair, T. Cowton, S. Palmer, and J. Wadham (2011), Supraglacial forcing of subglacial drainage in the ablation zone of the Greenland ice sheet, *Geophysical Research Letters*, *38*, L08502.

Bassford, R. P., M. J. Siegert, J. Dowdeswell, J. Oerlemans, A. F. Glazovsky, and Y. Y. Macheret (2006), Quantifying the Mass Balance of Ice Caps on Severnaya Zemlya, Russian High Arctic. I: Climate and Mass Balance of the Vavilov Ice Cap, *Arctic, Antarctic and Alpine Research*, *38*(1), 1-12.

Benn, D. I., C. R. Warren, and R. H. Mottram (2007), Calving processes and the dynamics of calving glaciers, *Earth Science Reviews*, *82*, 143-179.

Bergmann, I., G. Ramillien, and F. Frappart (2012), Climate-driven interannual ice mass evolution in Greenland, *Global and Planetary Change*, *82-83*, 1-11.

Bevan, S. L., A. Luckman, T. Murray, H. Sykes, and J. Kohler (2007), Positive mass balance during the late 20th century on Austfonna, Svalbard, revealed using satellite radar interferometry, *Annals of Glaciology*, *46*, 117-122.

Bevan, S. L., A. J. Luckman, and T. Murray (2012a), Glacier dynamics over the last quarter of a century at Helheim, Kangerdlugssuaq and 14 other major Greenland outlet glaciers, *The Cryosphere*, *6*, 923–937.

Bevan, S. L., T. Murray, A. Luckman, E. Hanna, and P. Huybrechts (2012b), Stable dynamics in a Greenland tidewater glacier over 26 years despite reported thinning, *Annals of Glaciology*, *53*(60), 241-248.

Bhattacharya, I., K. C. Jezek, L. Wang, and H. Liu (2009), Surface melt area variability of the Greenland ice sheet: 1979–2008, *Geophysical Research Letters*, *36*, L20502.

Bingham, R. G., A. Hubbard, P. Nienow, and M. J. Sharp (2008), An investigation into the mechanisms controlling seasonal speedup events at a High Arctic glacier, *Journal of Geophysical Research*, *113*, F02006.

Bingham, R. G., P. Nienow, and M. J. Sharp (2003), Intra-annual and intra-seasonal flow dynamics of a High Arctic polythermal valley glacier, *Annals of Glaciology*, *37*, 181-188.

Bingham, R. G., P. Nienow, M. J. Sharp, and S. Boon (2005), Subglacial drainage processes at a High Arctic polythermal valley glacier, *Journal of Glaciology*, *51*(172), 15-24.

Bingham, R. G., P. Nienow, M. J. Sharp, and L. Copland (2006), Hydrology and dynamics of a polythermal (mostly cold) High Arctic glacier, *Earth Surface Processes and Landforms*, *31*, 1463–1479.

Bjørk, A. A., K. H. Kjær, N. J. Korsgaard, S. A. Khan, K. K. Kjeldsen, C. S. Andresen, J. E. Box, N. J. Larsen, and S. Funder (2012), An aerial view of 80 years of climate-related glacier fluctuations in southeast Greenland, *Nature Geoscience*, *Advacned online publication*.

Blaszczyk, M., J. A. Jania, and J. M. Hagen (2009), Tidewater glaciers of Svalbard: Recent changes and estimates of calving fluxes, *Polish Polar Resarch*, *30*(2), 85–142.

Bond, G., et al. (1992), Evidence for massive discharges of icebergs into the North Atlantic ocean during the last glacial period, *Nature*, *360*, 245-249.

Boon, S., and M. J. Sharp (2003), The role of hydrologically-driven ice fracture in drainage system evolution on an Arctic glacier, *Geophysical Research Letters*, *30*(18), 1916.

Box, J. E., D. H. Bromwich, B. A. Veenhuis, L.-S. Bai, J. C. Stroeve, J. C. Rogers, K. Steffen, T. Haran, and S.-H. Wang (2006), Greenland Ice Sheet Surface Mass Balance Variability (1988–2004) from calibrated Polar MM5 Output, *Journal of Climate*, *19*, 2783-2800.

Box, J. E., L. Yang, D. H. Bromwich, and L. S. Bai (2009), Greenland Ice Sheet Surface Air Temperature Variability: 1840–2007, *Journal of Climate*, *22*, 4029-4049.

Briner, J. P., A. C. Bini, and R. S. Anderson (2009), Rapid early Holocene retreat of a Laurentide outlet glacier through an Arctic fjord, *Nature Geoscience*, *2*(7), 496-499.

Burgess, D. O., and M. J. Sharp (2004), Recent Changes in Areal Extent of the Devon Ice Cap, Nunavut, Canada, *Arctic, Antarctic, and Alpine Research*, *36*(2), 261-271.

Burgess, D. O., and M. J. Sharp (2008), Recent changes in thickness of the Devon Island ice cap, Canada, *Journal of Geophysical Research*, *113*, B07204.

Cappelen, J. (2011), Technical Report 11-05: DMI Monthly Climate Data Collection 1768-2010, Denmark, The Faroe Islands and Greenland *Rep.*, Danish Meteorological Institute, Copenhagen.

Catania, G. A., and T. A. Neumann (2010), Persistent englacial drainage features in the Greenland Ice Sheet, *Geophysical Research Letters*, *37*, L02501.

Christoffersen, P., R. Mugford, K. J. Heywood, I. Joughin, J. Dowdeswell, J. P. M. Syvitski, A. Luckman, and T. J. Benham (2011), Warming of waters in an East Greenland fjord prior to glacier retreat: mechanisms and connection to large-scale atmospheric conditions, *The Cryosphere*, *5*, 701-714.

Chylek, P., M. K. Dubey, and G. Lesins (2006), Greenland warming of 1920–1930 and 1995–2005, *Geophysical Research Letters*, *33*, L11707.

Copland, L., M. J. Sharp, and P. Nienow (2003), Links between short-term velocity variations and the subglacial hydrology of a predominantly cold polythermal glacier, *Journal of Glaciology*, *49*(166), 337-348.

Csatho, B., T. Schenk, C. J. van der Veen, and W. Krabill (2008), Intermittent thinning of Jakobshavn Isbræ, West Greenland, since the Little Ice Age, *Journal of Glaciology*, *54*(184), 131-144.

Das, S. B., I. Joughin, M. D. Behn, I. M. Howat, M. A. King, D. Lizarralde, and M. P. Bhatia (2008), Fracture propagation to the base of the Greenland Ice Sheet during supraglacial lake drainage, *Science*, *320*, 778 – 781.

Dowdeswell, J., T. J. Benham, M. R. Gorman, D. O. Burgess, and M. J. Sharp (2004), Form and flow of the Devon Island Ice Cap, Canadian Arctic, *Journal of Geophysical Research*, *109*, F02002.

Dowdeswell, J., T. J. Benham, T. Strozzi, and J. M. Hagen (2008), Iceberg calving flux and mass balance of the Austfonna ice cap on Nordaustlandet, Svalbard, *Journal of Geophysical Research*, *113*, F03022.

Dowdeswell, J., et al. (1997), The Mass Balance of Circum-Arctic Glaciers and Recent Climate Change, *Quaternary Research*, *48*, 1-14.

Dunse, T., T. V. Schuler, J. O. Hagen, and C. H. Reijmer (2012), Seasonal speed-up of two outlet glaciers of Austfonna, Svalbard, inferred from continuous GPS measurements, *The Cryosphere*, *6*, 453-466.

Dyurgerov, M. B., and G. J. McCabe (2006), Associations between Accelerated Glacier Mass Wastage and Increased Summer Temperature in Coastal Regions, *Arctic, Antarctic and Alpine Research*, *38*(2), 190-197.

Ettema, J., M. Van den Broeke, E. van Meijgaard, W. J. van de Berg, J. Bamber, J. E. Box, and R. C. Bales (2009), Higher surface mass balance of the Greenland Ice Sheet revealed by high-resolution climate modeling, *Geophysical Research Letters*, *36*, L12501.

Fountain, A. G., and J. S. Walder (1998), Water flow through temperate glaciers, *Reviews of Geophysics*, *36*(3), 299-328.

Gardner, A., G. Moholdt, B. Wouters, G. J. Wolken, D. O. Burgess, M. J. Sharp, J. G. Cogley, C. Braun, and C. Labine (2011), Sharply increased mass loss from glaciers and ice caps in the Canadian Arctic Archipelago, *Nature*, *473*, 357-360.

Gerdes, R., M. J. Larcher, F. Kauker, and U. Schauer (2003), Causes and development of repeated Arctic Ocean warming events, *Geophysical Research Letters*, *30*(19), OCE2.1-OCE2.4 doi:10.1029/2003GL018080.

Greve, R. (2000), On the response of the Greenland Ice Sheet to greenhouse climate change, *Climatic Change*, *46*, 289-303.

Gudmundsson, G. H., J. Krug, G. Durand, L. Favier, and O. Gagliardini (2012), The stability of grounding lines on retrograde slopes, *The Cryosphere Discussions*, *6*, 2597–2619.

Hagen, J. M., T. Dunse, T. Eiken, J. Kohler, G. Moholdt, C. Nuth, T. Schuler, and M. Sund (2009), GLACIODYN - The dynamic response of Arctic glaciers to global warming, *American Geophysical Union, Fall Meeting*, Abstract #C53B-06.

Hanna, E., J. Cappelen, X. Fettweis, P. Huybrechts, A. Luckman, and M. H. Ribergaard (2009), Hydrologic response of the Greenland Ice Sheet: the role of oceanographic warming, *Hydrological processes*, *23*, 7-30, doi:10.1002/hyp.7090.

Hanna, E., P. Huybrechts, K. Steffen, J. Cappelen, R. Huff, S. C., T. Irvine-Fynn, S. Wise, and M. Griffths (2008), Increased runoff from melt from the Greenland Ice Sheet: A response to global warming, *Journal of Climate*, *21*, 331-341, doi:0.1175/2007JCLI1964.1.

Higgins, A. K. (1989), North Greenland ice islands, *Polar Record*, *25*(154), 209-212.

Higgins, A. K. (1990), North Greenland glacier velocities and calf ice production, *Polarforschung*, *60*(1), 1-23.

Hodgkins, R. (1997), Glacier hydrology in Svalbard,NorwegianHigh Arctic, *Quaternary Science Reviews*, *16*(9), 957-973.

Holland, D. M., R. H. D. Y. Thomas, B., M. H. Ribergaard, and B. Lyberth (2008), Acceleration of Jakobshavn Isbræ triggered by warm subsurface ocean waters, *Nature Geoscience*, *1*, 1-6.

Holliday, N. P., et al. (2008), Reversal of the 1960s to 1990s freshening trend in the northeast North Atlantic and Nordic Seas, *Geophysical Research Letters*, *35*, L03614.

Howat, I. M., Y. Ahn, I. Joughin, M. van den Broeke, J. Lenaerts, and B. Smith (2011), Mass balance of Greenland's three largest outlet glaciers, 2000–2010, *Geophysical Research Letters*, *38*, L12501.

Howat, I. M., J. E. Box, Y. Ahn, A. Herrington, and E. M. McFadden (2010), Seasonal variability in the dynamics of marine-terminating outlet glaciers in Greenland, *Journal of Glaciology*, *56*(198), 601-613.

Howat, I. M., and A. Eddy (2011), Multi-decadal retreat of Greenland's marine-terminating glaciers, *Journal of Glaciology*, *57*(203), 389-396.

Howat, I. M., I. Joughin, M. Fahnestock, B. E. Smith, and T. Scambos (2008a), Synchronous retreat and acceleration of southeast Greenland outlet glaciers 2000-2006; Ice dynamics and coupling to climate, *Journal of Glaciology*, *54*(187), 1-14.

Howat, I. M., I. Joughin, and T. A. Scambos (2007), Rapid changes in ice discharge from Greenland outlet glaciers, *Science*, *315*(5818), 1559-1561.

Howat, I. M., I. Joughin, S. Tulaczyk, and S. P. Gogineni (2005), Rapid retreat and acceleration of Helheim Glacier, east Greenland, *Geophysical Research Letters*, *32*, L22502.

Howat, I. M., B. E. Smith, I. Joughin, and T. Scambos (2008b), Rates of southeast Greenland ice volume loss from combined ICESat and ASTER observations, *Geophysical Research Letters*, *35*, L17505.

Hughes, N. E., J. P. Wilkinson, and P. Wadhams (2011), Multi-satellite sensor analysis of fast-ice development in the Norske Øer Ice Barrier, northeast Greenland, *Annals of Glaciology*, *52*(57), 151-160.

Hughes, T. (1986), The Jakobshavns effect, *Geophysical Research Letters*, *13*(1), 46-48.

Hurrell, J. W., Y. Kushnir, M. M. Visbeck, and G. G. Ottersen (2003), An Overview of the North Atlantic Oscillation., in *The North Atlantic Oscillation: Climate Significance and Environmental Impact, Geophysical Monograph Series*, edited by J. W. Hurrell, Y. Kushnir, G. G. Ottersen and M. M. Visbeck, pp. 1-35.

Huybrechts, P., and J. de Wolde (1999), The dynamic response of the Greenland and Antarctic ice sheets to multiple-century warming, *Journal of Climate*, *21*, 2169–2188.

Huybrechts, P., A. Letreuilly, and N. Reeh (1991), The Greenland ice sheet and greenhouse warming, *Palaeogeography, Palaeoclimatolagy, Palaeoecology*, *89*, 399-412.

Iken, A., and R. A. Bindschadler (1986), Combined measurements of subglacial water pressure and surface velocity of Findelengletscher, Switzerland: Conclusions about drainage system and sliding mechanism, *Journal of Glaciology*, *32*, 101-119.

IPCC (2001), *The Physical Science Basis. Contribution of Working Group I to the Fourth Assessment Report of the Intergovernmental Panel on Climate Change*, Cambridge Univ. Press, Cambridge and New York.

IPCC (2007), *The Physical Science Basis. Contribution of Working Group I to the Fourth Assessment Report of the Intergovernmental Panel on Climate Change*, Cambridge Univ. Press, Cambridge and New York.

Jacob, T., J. Wahr, W. T. Pfeffer, and S. Swenson (2012), Recent contributions of glaciers and ice caps to sea level rise, *Nature*, *428*, 514–518.

Jamieson, S. S. R., A. Vieli, S. J. Livingstone, C. Ó Cofaigh, C. R. Stokes, C.-D. Hillenbrand, and J. Dowdeswell (2012), Ice stream stability on a reverse bed slope, *Nature Geoscience*, *5*, 799-802.

Jenkins, A. (2011), Convection-Driven Melting near the Grounding Lines of Ice Shelves and Tidewater Glaciers, *Journal of Physical Oceanography*, *41*, 2279–2294.

Johannessen, O. M., K. Khvorostovsky, M. W. Miles, and L. P. Bobylev (2005), Recent ice-sheet growth in the interior of Greenland, *Science*, *310*(5750), 1013 – 1016.

Johnson, H. L., A. Münchow, K. K. Falkner, and H. Melling (2011), Ocean circulation and properties in Petermann Fjord, Greenland, *Journal of Geophysical Research*, *116*, C01003.

Joughin, I., W. Abdalati, and M. Fahnestock (2004), Large fluctuations in speed on Greenland's Jakobshavn Isbræ glacier, *Nature*, *432*(2), 608-610.

Joughin, I., and R. B. Alley (2011), Stability of the West Antarctic ice sheet in a warming world, *Nature Geoscience*, *4*, 506-513.

Joughin, I., S. B. Das, M. A. King, B. E. Smith, I. M. Howat, and T. Moon (2008a), Seasonal Speedup Along the Western Flank of the Greenland Ice Sheet, *Science*, *320*, 781-783, doi:10.1126/science.1153288.

Joughin, I., I. M. Howat, R. B. Alley, G. Ekström, M. Fahnestock, T. Moon, NettlesM., M. Truffer, and V. C. Tsai (2008b), Ice-front variation and tidewater behaviour on Helheim and

Kangerdlugssuaq Glaciers, Greenland, *Journal of Geophysical Research*, *113*, F01004, doi:10.1029/2007JF000837.

Joughin, I., I. M. Howat, M. Fahnestock, B. Smith, W. Krabill, R. B. Alley, H. Stern, and M. Truffer. (2008c), Continued evolution of Jakobshavn Isbrae following its rapid speedup, *Journal of Geophysical Research*, *113*, F04006, doi:10.1029/2008JF001023.

Joughin, I., B. Smith, I. M. Howat, T. Scambos, and T. Moon (2010), Greenland flow variability from ice-sheet-wide velocity mapping, *Journal of Glaciology*, *56*(197), 415-430.

Joughin, I., B. E. Smith, I. Howat, D. Floricioiu, R. B. Alley, M. Truffer, and M. Fahnestock (2012), Seasonal to decadal scale variations in the surface velocity of Jakobshavn Isbrae, Greenland: Observation and model-based analysis, *Journal of Geophysical Research*, *117*, F02030.

Kamb, B. (1987), Glacier surge mechanism based on linked cavity configuration of the basal water conduit system, *Journal of Geophysical Research*, *92*(B9), 9083-9100.

Khan, S. A., J. Wahr, M. Bevis, I. Velicogna, and K. E. (2010), Spread of ice mass loss into northwest Greenland observed by GRACE and GPS, *Geophysical Research Letters*, *37*, L06501, doi:10.1029/2010GL042460.

Kjær, K. H., et al. (2012), Aerial photographs reveal late–20th-Century dynamic ice loss in northwestern Greenland, *Science*, *337*, 596-573.

Koerner, R. (2005), Mass balance of glaciers in the Queen Elizabeth Islands, Nunavut, Canada, *Annals of Glaciology*, *42*, 417-423.

Kotlyakov, V. M., A. F. Glazovskii, and I. E. Frolov (2010), Glaciation in the Arctic, *Herald of the Russian Academy of Sciences*, *80*(2), 155–164.

Krabill, W., et al. (2004), Greenland Ice Sheet: Increased coastal thinning, *Geophysical Research Letters*, *31*, L24402.

Krawczynski, M. J., M. D. Behn, S. B. Das, and I. Joughin (2009), Constraints on the lake volume required for hydro-fracture through ice sheets, *Geophysical Research Letters*, *36*, L10501.

Kwok, R., and D. A. Rothcock (2009), Decline in Arctic sea ice thickness from submarine and ICESat records: 1958–2008, *Geophysical Research Letters*, *36*, L15501.

Luckman, A., and T. Murray (2005), Seasonal variation in velocity before retreat of Jakobshavn Isbrae, Greenland, *Geophysical Research Letters*, *32*, L08501, doi:10.1029/2005GL022519.

Luckman, A., T. Murray, R. de Lange, and E. Hanna (2006), Rapid and synchronous ice-dynamic changes in East Greenland, *Geophysical Research Letters*, *33*(3), L03503.

Luthcke, S. B., H. J. Zwally, W. Abdalati, D. D. Rowlands, R. D. Ray, R. S. Nerem, F. G. Lemoine, J. J. McCarthy, and D. S. Chinn (2006), Recent Greenland ice mass loss by drainage system from satellite gravity observations, *Science*, *314*, 1286–1289.

Mair, D., D. O. Burgess, M. J. Sharp, J. Dowdeswell, T. J. Benham, S. Marshall, and F. Cawkwell (2009), Mass balance of the Prince of Wales Icefield, Ellesmere Island, Nunavut, Canada, *Journal of Geophysical Research*, *114*, F02011.

Mayer, C., N. Reeh, F. Jung-Rothenhäusler, P. Huybrechts, and H. Orter (2000), The subglacial cavity and implied dynamics under Nioghalvfjerdsfjorden Glacier, NE-Greenland, *Geophysical Research Letters*, *27*(15), 2289-2292.

McFadden, E. M., I. M. Howat, I. Joughin, B. Smith, and Y. Ahn (2011), Changes in the dynamics of marine terminating outlet glaciers in west Greenland (2000–2009), *Journal of Geophysical Research*, *116*, F02022.

Meier, M. F., M. B. Dyurgerov, U. K. Rick, S. O'Neel, W. T. Pfeffer, R. S. Anderson, S. P. Anderson, and A. F. Glazovsky (2007), Glaciers Dominate Eustatic Sea-Level Rise in the 21st Century. , *Science*, *317*, 1064-1067.

Meier, M. F., and A. Post (1987), Fast tidewater glaciers, *Journal of Geophysical Research*, *92*, 9051–9058.

Mémin, A., Y. Rogister, J. Hinderer, O. C. Omang, and B. Luck (2011), Secular gravity variation at Svalbard (Norway) from ground observations and GRACE satellite data, *Geophysical Journal International*, *184*, 1119-1130.

Moholdt, G., J. M. Hagen, T. Eiken, and T. Schuler (2010a), Geometric changes and mass balance of the Austfonna ice cap, Svalbard, *The Cryosphere*, *4*, 21-34.

Moholdt, G., C. Nuth, J. O. Hagen, and J. Kohler (2010b), Recent elevation changes of Svalbard glaciers derived from ICESat laser altimetry, *Remote Sensing of Environment*, *114*, 2756–2767.

Moholdt, G., B. Wouters, and A. S. Gardner (2012), Recent mass changes of glaciers in the Russian High Arctic, *Geophysical Research Letters*, *39*, L10502.

Moon, T., and I. Joughin (2008), Changes in ice-front position on Greenland's outlet glaciers from 1992 to 2007, *Journal of Geophysical Research*, *113*, F02022, doi:10.1029/2007JF000927.

Moon, T., I. Joughin, B. E. Smith, and I. M. Howat (2012), 21st-Century evolution of Greenland outlet glacier velocities, *Science*, *336*(6081), 576-578.

Mortensen, J., K. Lennert, J. Bendtsen, and S. Rusgaard (2011), Heat sources for glacial melt in a sub-Arctic fjord (Godthåbsfjord) in contact with the Greenland Ice Sheet, *Journal of Geophysical Research*, *116*, C01013.

Mote, T. L. (2007), Greenland surface melt trends 1973–2007: Evidence of a large increase in 2007, *Geophysical Research Letters*, *34*, L22507.

Motyka, R. J., M. Fahnestock, and M. Truffer (2010), Volume change of Jakobshavn Isbræ, West Greenland: 1985–1997–2007, *Journal of Glaciology*, *56*(198), 635-645.

Motyka, R. J., L. Hunter, K. Echelmeyer, and C. Connor (2003), Submarine melting at the terminus of a temperate tidewater glacier, LeConte Glacier, Alaska, U.S.A., *Annals of Glaciology*, *36*, 57-65.

Motyka, R. J., M. Truffer, M. Fahnestock, J. Mortensen, S. Rysgaar, and I. M. Howat (2011), Submarine melting of the 1985 Jakobshavn Isbræ floating tongue and the triggering of the current retreat, *Journal of Geophysical Research*, *166*, F01007.

Murray, T., et al. (2010), Ocean regulation hypothesis for glacier dynamics in southeast Greenland and implications for ice sheet mass changes, *Journal of Geophysical Research*, *115*, F03026, doi:10.1029/2009JF001522.

Nick, F. M., A. Luckman, A. Vieli, C. J. van der Veen, D. van As, R. S. W. van de Wal, F. Pattyn, and D. Floricioiu (2012), The response of Petermann Glacier, Greenland, to large calving events, and its future stability in the context of atmospheric and oceanic warming, *Journal of Glaciology*, *58*(208), 229 - 239.

Nick, F. M., C. J. van der Veen, A. Vieli, and D. I. Benn (2010), A physically based calving model applied to marine outlet glaciers and implications for the glacier dynamics, *Journal of Geophysical Research*, *56*(199), 781-794.

Nick, F. M., A. Vieli, I. M. Howat, and I. Joughin (2009), Large-scale changes in Greenland outlet glacier dynamics triggered at the terminus, *Nature Geoscience*, *2*, 110-114.

Nienow, P., M. J. Sharp, and I. C. Willis (1998), Seasonal changes in the morphology of the subglacial drainage system, Haut Glacier d'Arolla, Switzerland, *Earth Surface Processes and Landforms*, *23*(9), 825-843.

Nilsen, F., F. Cottier, R. Skogseth, and S. Mattsson (2008), Fjord– shelf exchanges controlled by ice and brine production: The interannual variation of Atlantic Water in Isfjorden, Svalbard, *Continental Self Research*, *28*, 1838– 1853.

Nuth, C., G. Moholdt, J. Kohler, J. O. Hagen, and A. Kääb (2010), Svalbard glacier elevation changes and contribution to sea level rise, *Journal of Geophysical Research*, *115*, F01008, doi:10.1029/2008JF001223.

Nuttall, A.-M., and R. Hodgkins (2005), Temporal variations in flow velocity at Finsterwalderbreen, a Svalbard surge-type glacier, *Annals of Glaciology*, *42*, 71-76.

Palmer, S., A. Shepherd, P. Nienow, and I. Joughin (2011), Seasonal speedup of the Greenland Ice Sheet linked to routing of surface water, *Earth and Planetary Science Letters*, *302*, 423-428.

Parizek, B. R., and R. B. Alley (2004), Implications of increased Greenland surface melt under global-warming scenarios: Ice-sheet simulations, *Quaternary Science Reviews*, *23*, 1013– 1027.

Payne, A. J., A. Vieli, A. P. Shepherd, D. J. Wingham, and E. Rignot (2004), Recent dramatic thinning of largest West Antarctic ice stream triggered by oceans, *Geophysical Research Letters*, *31*, L23401.

Pfeffer, W. T. (2003), Tidewater glaciers move at their own pace, *Nature*, *426*, 602.

Pfeffer, W. T. (2007), A simple mechanism for irreversible tidewater glacier retreat, *Journal of Geophysical Research*, *112*, F03S25.

Price, S., H. Conway, E. D. Waddington, and R. A. Bindschadler (2008), Model investigations of inland migration of fast-flowing outlet glaciers and ice streams, *Journal of Glaciology*, *54*(184), 49-60.

Price, S., A. J. Payne, I. M. Howat, and B. Smith (2011), Committed sea-level rise for the next century from Greenland ice sheet dynamics during the past decade, *Proceedings of the National Academy of Sciences*, *108*(22), 8978-8983.

Pritchard, H. D., R. J. Arthern, D. G. Vaughan, and L. A. Edwards (2009), Extensive dynamic thinning on the margins of the Greenland and Antarctic ice sheets, *Nature*, *461*, 971-975.

Radić, V., and R. Hock (2011), Regionally differentiated contribution of mountain glaciers and ice caps to future sea-level rise, *Nature Geoscience*, *4*, 91-94.

Raper, V., J. Bamber, and W. Krabill (2005), Interpretation of the anomalous growth of Austfonna, Svalbard, a large Arctic ice cap, *Annals of Glaciology*, *42*, 373-379.

Reeh, N., H. H. Thomsen, A. K. Higgins, and A. Weidick (2001), Sea ice and the stability of north and northeast Greenland floating glaciers, *Annals of Glaciology*, *33*, 474-480.

Rennermalm, A. K., L. C. Smith, J. C. Stroeve, and V. W. Chu (2009), Does sea ice influence Greenland ice sheet surface-melt?, *Environmental Research Letters*, *4*, 024011, doi:doi:10.1088/1748-9326/4/2/024011.

Rignot, E., J. E. Box, E. Burgess, and E. Hanna (2008), Mass balance of the Greenland ice sheet from 1958 to 2007, *Geophysical Research Letters*, *35*, L20502, doi:10.1029/2008GL035417.

Rignot, E., I. Fenty, D. Menemenlis, and Y. Xu (2012), Spreading of warm ocean waters around Greenland as a possible cause for glacier acceleration, *Annals of Glaciology*, *53*(60), 257-266.

Rignot, E., and P. Kanagaratnam (2006), Changes in the velocity structure of the Greenland Ice Sheet, *Science*, *311*(5763), 986–990.

Rignot, E., M. Koppes, and I. Velicogna (2010), Rapid submarine melting of the calving faces of West Greenland glaciers, *Nature Geoscience*, *3*, 187-191, doi:10.1038/NGEO765.

Rignot, E., and K. Steffen (2008), Channelized bottom melting and stability of floating ice shelves, *Geophysical Research Letters*, *35*, L02503.

Rignot, E., I. Velicogna, M. Van den Broeke, A. Monaghan, and J. Lenaerts (2011), Acceleration of the contribution of the Greenland and Antarctic ice sheets to sea level rise, *Geophysical Research Letters*, *38*, L05503.

Rippin, D. M., I. C. Willis, N. S. Arnold, A. J. Hodson, and M. Brinkhaus (2005), Spatial and temporal variations in surface velocity and basal drag across the tongue of the

polythermal glacier midre Lovénbreen, Svalbard, *Journal of Glaciology*, *51*(175), 588-600.

Rodrigues, J. (2008), The rapid decline of the sea ice in the Russian Arctic, *Cold Regions Science and Technology*, *54*, 124-142.

Rodrigues, J. (2009), The increase in the length of the ice-free season in the Arctic, *Cold Regions Science and Technology*, *59*, 78–101.

Schoof, C. (2010), Ice-sheet acceleration driven by melt supply variability, *Nature*, *468*, 803-806.

Seale, A., P. Christoffersen, R. Mugford, and M. O'Leary (2011), Ocean forcing of the Greenland Ice Sheet: Calving fronts and patterns of retreat identified by automatic satellite monitoring of eastern outlet glaciers, *Journal of Geophysical Research*, *116*(F3), F03013.

Serreze, M. C., A. P. Barrett, J. C. Stroeve, D. N. Kindig, and M. M. Holland (2009), The emergence of surface-based Arctic amplification, *The Cryosphere*, *3*, 11-19.

Sharov, A. I. (2005), Studying changes of ice coasts in the European Arctic, *Geo-Marine letters*, *25*, 153–166.

Sharov, A. I. (2010), *Satellite Monitoring and Regional Analysis of Glacier Dynamics in the Barents-Kara Region*, JOANNEUM RESEARCH Forschungsgesellschaft mbH, Institute of Digital Image Processing, Graz, Austria.

Sharov, A. I., W. Schöner, and P. R. (2009), Spatial features of glacier changes in the Barents-Kara Sector, *EGU General Assembly*, *11*, EGU2009-3046.

Shepherd, A., Z. Du, T. J. Benham, J. Dowdeswell, and E. M. Morris (2007), Mass balance of Devon Ice Cap, Canadian Arctic, *Annals of Glaciology*, *46*, 249-254.

Shepherd, A., A. Hubbard, P. Nienow, M. King, M. McMillan, and I. Joughin (2009), Greenland ice sheet motion coupled with daily melting in late summer, *Geophysical Research Letters*, *36*, L01501, doi:10.1029/2008GL035758.

Sneed, W. A., and G. S. Hamilton (2007), Evolution of melt pond volume on the surface of the Greenland Ice Sheet, *Geophysical Research Letters*, *34*, L03501.

Sohn, H. G., K. C. Jezek, and C. J. van der Veen (1998), Jakobshavn Glacier, West Greenland: 30 years of Spacebourne observations, *Geophysical Research Letters*, *25*(14), 2699-2702.

Sole, A., D. W. Mair, P. W. Nienow, I. D. Bartholomew, M. A. King, M. J. Burke, and I. Joughin (2011), Seasonal speedup of a Greenland marine-terminating outlet glacier forced by surface melt–induced changes in subglacial hydrology, *Journal of Geophysical Research*, *116*, F03014.

Sole, A., T. Payne, J. Bamber, P. Nienow, and W. Krabill (2008), Testing hypotheses of the cause of peripheral thinning of the Greenland Ice Sheet: is land-terminating ice thinning at anomalously high rates?, *The Cryosphere Discussions*, *2*, 673–710.

Stearns, A., and G. S. Hamilton (2007), Rapid volume loss from two East Greenland outlet glaciers quantified using repeat stereo satellite imagery, *Geophysical Research Letters*, *34*, L05503.

Stern, H., and M. P. Heide-Jørgensen (2003), Trends and variability of sea ice in Baffin Bay and Davis Strait, 1953–2001, *Polar Research*, *22*(1), 11-18.

Straneo, F., R. G. Curry, D. A. Sutherland, G. S. Hamltion, C. Cenedese, K. Våge, and L. A. Stearns (2011), Impact of fjord dynamics and glacial runoff on the circulation near Helheim Glacier, *Nature Geoscience*, *4*, 322-327.

Straneo, F., G. S. Hamilton, D. A. Sutherland, L. A. Stearns, F. Davidson, M. O. Hammill, G. B. Stenson, and A. R. Asvid (2010), Rapid circulation of warm subtropical waters in a major glacial fjord in East Greenland, *Nature Geoscience*, *3*, 182-186, doi:10.1038/NGEO764.

Sundal, A. V., A. Shepherd, P. Nienow, E. Hanna, S. Palmer, and P. Huybrechts (2011), Melt-induced speed-up of Greenland ice sheet offset by efficient subglacial drainage, *Nature*, *469*, 521-524.

Thomas, R. H. (1979), The dynamics of marine ice sheets., *Journal of Glaciology*, *24*, 167-177.

Thomas, R. H. (2004), Force-perturbation analysis of recent thinning and acceleration of Jakobshavn Isbrae, Greenland, *Journal of Glaciology*, *50*(168), 57-66.

Thomas, R. H., W. Abdalati, E. Frederick, W. Krabill, S. Manizade, and K. Steffen (2003), Investigation of surface melting and dynamic thinning on Jakobshavn Isbrae, Greenland, *Journal of Glaciology*, *49*(165), 231-239.

Thomas, R. H., E. Frederick, W. Krabill, Y. Li, S. Manizade, and C. Martin (2008), A comparison of Greenland ice-sheet volume changes derived from altimetry measurements, *Journal of Glaciology*, *54*(185), 203-212.

Thomas, R. H., E. Frederick, W. Krabill, S. Manizade, and C. Martin (2006), Progressive increase in ice loss from Greenland, *Geophysical Research Letters*, *33*, L10503, doi:10.1029/2006GL026075.

Thomas, R. H., E. Frederick, W. Krabill, S. Manizade, and C. Martin (2009), Recent changes on Greenland outlet glaciers, *Journal of Glaciology*, *55*(189), 147-162.

Thomas, R. H., E. Frederick, J. Li, W. Krabill, S. Manizade, J. Paden, J. Sonntag, R. Swift, and J. Yungel (2011), Accelerating ice loss from the fastest Greenland and Antarctic glaciers, *Geophysical Research Letters*, *38*, L10502.

van de Wal, R. S. W., W. Boot, M. R. van den Broeke, C. J. P. P. Smeets, C. H. Reijmer, J. J. A. Donker, and J. Oerlemans (2008), Large and Rapid Melt-Induced Velocity Changes in the Ablation Zone of the Greenland Ice Sheet, *Science*, *321*(5885), 111 - 113.

van de Wal, R. S. W., and J. Oerlemans (1997), Modelling the short-term response of the Greenland ice-sheet to global warming, *Climate Dynamics*, *13*, 733-744.

van den Broeke, M., J. Bamber, J. Ettema, E. Rignot, E. Schrama, W. J. van de Berg, E. van Meijgaard, I. Velicogna, and B. Wouters (2009), Partitioning Recent Greenland Mass Loss, *Science*, *326*, 984-986.

van der Veen, C. J. (1998), Fracture mechanics approach to penetration of surface crevasses on glaciers *Cold Regions Science and Technology*, *27*(1), 31-47.

van der Veen, C. J. (2007), Fracture propagation as means of rapidly transferring surface meltwater to the base of glaciers, *Geophysical Research Letters*, *34*, L01501.

van der Veen, C. J., J. C. Plummer, and L. A. Stearns (2011), Controls on the recent speed-up of Jakobshavn Isbræ, West Greenland, *Journal of Glaciology*, *57*(204), 770–782.

Velicogna, I. (2009), Increasing rates of ice mass loss from the Greenland and Antarctic ice sheets revealed by GRACE, *Geophysical Research Letters*, *36*, L19503, doi:10.1029/2009GL040222.

Velicogna, I., and J. Wahr (2006), Acceleration of Greenland ice mass loss in spring 2004, *Nature*, *443*, 329- 331.

Vieli, A., M. Funk, and H. Blatter (2001), Flow dynamics of tidewater glaciers: a numerical modelling approach, *Journal of Glaciology*, *47*(159), 595-606.

Vieli, A., J. A. Jania, H. Blatter, and M. Funk (2004), Short-term velocity variations on Hansbreen, a tidewater glacier in Spitsbergen, *Journal of Glaciology*, *50*(170), 389-398.

Vieli, A., J. A. Jania, and K. Lezek (2002), The retreat of a tidewater glacier: observations and model calculations on Hansbreen, Spitsbergen, *Journal of Glaciology*, *48*(163), 592-600.

Vieli, A., and F. M. Nick (2011), Understanding and modelling rapid dynamic changes of tidewater outlet glaciers: issues and implications, *Surveys in Geophysics*, *32*, 437-485.

Vieli, A., A. J. Payne, A. Shepherd, and Z. Du (2007), Causes of pre-collapse changes of the Larsen B ice shelf: Numerical modelling and assimilation of satellite observations, *Earth and Planetary Science Letters*, *259*, 297-306.

Weertman, J. (1974), Stability of the junction of an ice sheet and an ice shelf, *Journal of Glaciology*, *13*, 3-11.

Weidick, A. (1975), A review of Quaternary investigations in Greenland, *Institute of Polar Studies Report*, *55*, 161.

Williamson, S., M. J. Sharp, J. Dowdeswell, and T. J. Benham (2008), Iceberg calving rates from northern Ellesmere Island ice caps, Canadian Arctic, 1999–2003, *Journal of Glaciology*, *54*(186), 391-400.

Willis, I. C. (1995), Intra-annual variations in glacier motion: a review, *Progress in Physcical Geography*, *19*(1), 61-106.

Winsborrow, M. C. M., K. Andreassen, G. D. Corner, and J. S. Laberg (2010), Deglaciation of a marine-based ice sheet: Late Weichselian palaeo-ice dynamics and retreat in the southern Barents Sea reconstructed from onshore and offshore glacial geomorphology, *Quaternary Science Reviews*, *29*(3-4), 424-442.

Wouters, B., D. Chambers, and E. J. O. Schrama (2008), GRACE observes small-scale mass loss in Greenland, *Geophysical Research Letters*, *35*, L20501.

Xu, Y., E. Rignot, D. Menemenlis, and M. N. Koppes (2012), Numerical experiments on subaqueous melting of Greenland tidewater glaciers in response to ocean warming and enhanced subglacial discharge, *Annals of Glaciology*, *53*(60), 229–234.

Yin, J., T. J. Overpeck, S. M. Griffies, A. Hu, J. L. Russell, and R. J. Stouffer (2012), Different magnitudes of projected subsurface ocean warming around Greenland and Antarctica, *Nature Geoscience*, *4*, 524-528.

Zwally, H. J., W. Abdalati, T. Herring, K. Larson, J. Saba, and K. Steffen (2002), Surface melt-induced acceleration of Greenland ice-sheet flow, *Science*, *297*(5579), 218–222.

Zwally, H. J., M. B. Giovinetto, L. Jun, H. G. Cornejo, M. A. Beckley, A. C. Brenner, J. L. Saba, and Y. Donghui (2005), Mass changes of the Greenland and Antarctic ice sheets and shelves and contributions to sea level rise: 1992-2002, *Journal of Glaciology*, *51*(175), 509-527.

Zwally, H. J., et al. (2011), Greenland ice sheet mass balance: distribution of increased mass loss with climate warming; 2003–07 versus 1992–2002, *Journal of Glaciology*, *57*(201), 88-102.

Chapter 3: Influence of sea ice decline, atmospheric warming and glacier width on marine-terminating outlet glacier behavior in north-west Greenland at seasonal to interannual timescales

Carr, J.R**.**, Vieli, A. and Stokes, C.R., 2013. *Journal of Geophysical Research*, 118 (3), 1210-1226

Overview: Remotely sensed data were used to investigate the factors controlling the frontal position of Alison Glacier, north-west Greenland, and the nine neighbouring marine-terminating outlet glaciers. The paper documents rapid retreat on Alison Glacier, which totalled almost 10 km in four years, and followed at least 25 years of minimal change. Retreat coincided with strong atmospheric warming and marked sea ice decline. However, there was large variation in retreat rates across the study region. This was attributed to fjord width variation, basal topography and terminus type, which modulated the response of individual glaciers to forcing.

Motivation: The study area was selected as north-west Greenland has recently undergone rapid ice loss [*Khan et al.*, 2010], glacier acceleration [*Moon et al.*, 2012] and retreat [*Howat and Eddy*, 2011], but has been comparatively little-studied. Results suggested that sea ice and air temperatures were key external controls, but also highlighted the capacity for glacier-specific factors to strongly modulate the response of individual glaciers. As the region contained only a small number of study glaciers, these results provided the motivation to investigate glacier-specific controls elsewhere, in order to assess whether their influence was significant in other regions.

Contribution: My contribution to this paper was to carry out the GIS and data analysis tasks (e.g. image processing, data acquisition and data processing). I

wrote the text, created the figures and lead the paper development. My co-authors provided editorial input and guidance on research development.

Abstract

Discharge from marine-terminating outlet glaciers represents a key component of the Greenland Ice Sheet mass budget and observations suggest that mass loss from north-west Greenland has recently accelerated. Despite this, the factors controlling outlet glacier dynamics within this region have been comparatively poorly studied. Here, we use remotely sensed data to investigate the influence of atmospheric, oceanic and glacier-specific controls on the frontal position of Alison Glacier (AG), north-west Greenland and nine surrounding outlet glaciers. AG retreated by 9.7 km between 2001 and 2005, following at least 25 years of minimal change. Results suggest that sea ice and air temperatures influence glacier frontal position at seasonal and interannual timescales. However, the response of individual outlet glaciers to forcing was strongly modified by factors specific to each glacier, specifically variations in fjord width and terminus type. Overall, our results underscore the need to consider these factors in order to interpret recent rapid changes and predict the dynamic response of marine-terminating outlet glaciers to atmospheric and oceanic forcing.

3.1. Introduction

Numerous studies have documented rapid mass loss from the Greenland Ice Sheet (GrIS) during the past twenty years [e.g. *Jacob et al.*, 2012; *Rignot and Kanagaratnam*, 2006; *Sasgen et al.*, 2012; *van den Broeke et al.*, 2009], with deficits accelerating by 20.1 ± 1 km^3 a^{-2} between 1992 and 2010 [*Rignot et al.*, 2011]. This loss was attributed approximately equally to negative surface mass balance (SMB), primarily resulting from an increase in surface melting relative to accumulation, and increased ice discharge from marine-terminating outlet glaciers [*Rignot et al.*, 2008; *Rignot et al.*, 2011; *van den Broeke et al.*, 2009]. Indeed, observations have demonstrated that outlet glaciers can undergo rapid dynamic change and produce substantial mass loss at annual to decadal timescales [*Bevan et al.*, 2012; *Howat et al.*, 2008; *Joughin et al.*, 2012; *Pritchard et al.*,

2009; *Rignot et al.*, 2008]. Consequently, understanding the factors controlling Greenland outlet glacier dynamics is crucial for accurate prediction of near-future sea-level rise and GrIS response to climate change [*IPCC*, 2007].

At present, considerable uncertainty remains over the primary drivers of Greenland outlet glacier behavior, with potential controls including air temperatures, ocean temperatures, sea ice, and factors specific to individual glaciers, such as basal topography, fjord geometry, glacier velocity, width and catchment area [*Carr et al.*, 2013]. Here we use the term 'oceanic' to refer to forcing associated with sea ice, sea surface temperatures and subsurface ocean temperatures. Increasing concern over climate warming from the 1990s together with the synchronous nature of Greenland outlet glacier retreat in the early 2000s, particularly in south-eastern Greenland [e.g. *Howat et al.*, 2008; *Murray et al.*, 2010], led researchers to focus on the role of atmospheric and oceanic forcing in driving outlet glacier dynamics. However, recent studies have demonstrated that the response of individual glaciers to these factors can vary substantially at regional scales [*McFadden et al.*, 2011] and that glacier-specific factors, particularly bed topography, may significantly influence Greenland outlet glacier behavior [*Howat et al.*, 2011; *Joughin et al.*, 2010a; *Nick et al.*, 2009; *Thomas et al.*, 2009]. Here we focus specifically on the role of fjord width, terminus type and, to a lesser extent, basal topography in modulating the response of outlet glaciers to external forcing. Although the potential influence of basal topography on glacier dynamics has been recognized for some time [*Alley*, 1991; *Meier and Post*, 1987; *Weertman*, 1974], it has yet to be widely investigated on the GrIS, due to limited data availability, and other glacier-specific controls, such as fjord width variations, remain poorly studied [*Carr et al.*, 2013]. Understanding the role of these controls is crucial for accurate sea level rise prediction, as mass loss rates are frequently extrapolated from a small number of study glaciers and so inadequate consideration of glacier-specific factors could lead to substantial over- or under-estimates.

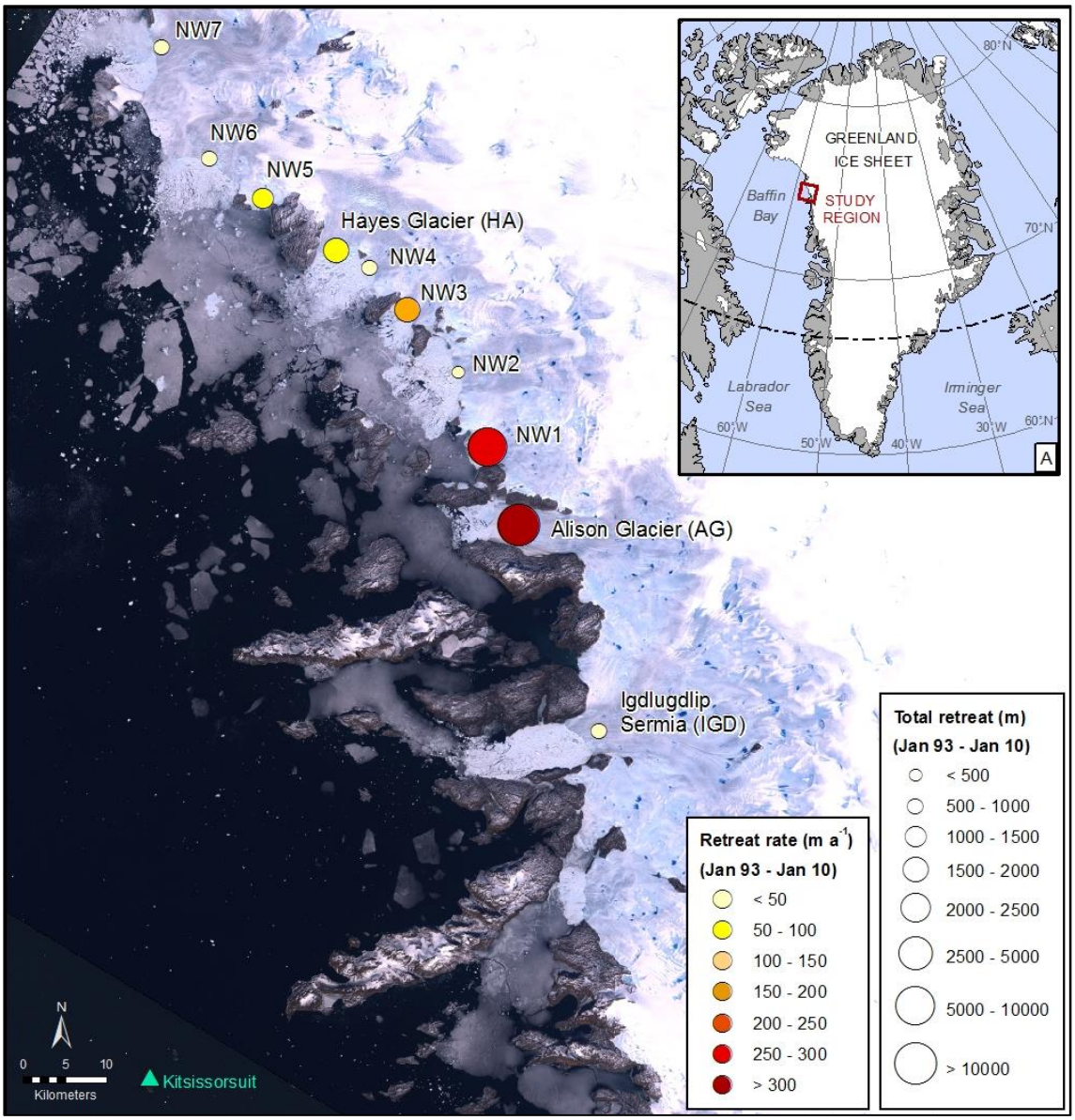

Figure 3.1. *Location of study glaciers, Kitsissorsuit meteorological station (green triangle) and average outlet glacier retreat rate (symbol color) and total retreat (symbol size) between 2nd January 1993 and 26th January 2010. Base image: Landsat scene acquired 27th June 2001 and provided by Global Land Cover Facility.*

Here we investigate the influence of atmospheric, oceanic and glacier-specific controls on the frontal position of Alison Glacier (AG), north-west Greenland, and its nine neighboring marine-terminating outlet glaciers (Fig. 3.1). North-west Greenland has undergone rapid mass loss [*Khan et al.*, 2010] and significant changes in glacier dynamics in the past decade [*Kjær et al.*, 2012], including widespread retreat [*Howat and Eddy*, 2011], substantial acceleration [*Moon et al.*, 2012] and an increased

frequency of glacial earthquakes [*Veitch and Nettles*, 2012]. We focus particularly on AG as it has recently exhibited exceptionally high retreat rates [*Joughin et al.*, 2010a; *McFadden et al.*, 2011] in comparison to both regional and ice-sheet wide values, yet it has been relatively poorly studied. We first investigate the influence of atmospheric and oceanic forcing on seasonal changes in frontal position between 2004 and 2010. We then assess the relative importance of these controls at interannual timescales for the period 1993 to 2010 and evaluate longer-term glacier behavior from 1976 to present. Finally, we investigate the role of fjord width, terminus type and basal topography in modulating glacier response to atmospheric and oceanic forcing.

3.2. Methods

3.2.1. Glacier frontal position

Outlet glacier frontal positions were obtained from a combination of radar and visible satellite imagery from 1976 to 2012. The primary source was Synthetic Aperture Radar (SAR) Image Mode Precision imagery, acquired as part of the ERS1, ERS2 and Envisat missions and provided by the European Space Agency (ESA). Scenes were selected as close to the end of the calendar month as possible to allow for comparison with monthly climatic and oceanic data. The images were processed by applying precise orbital state vectors, provided by the ESA, and radiometric calibration was applied. Images were then multi-looked to reduce speckle and were terrain corrected using Version 2 of the 30 m resolution Advanced Spaceborne Thermal Emission and Reflection Radiometer (ASTER) Global Digital Elevation Model (GDEM). ERS images were coregistered with corresponding Envisat scenes, which have a higher geolocation accuracy. Processed scenes were output at a spatial resolution of 37.5 m. Where possible, periods of limited SAR Image Mode data availability were supplemented with Landsat data obtained from the Global Land Cover Facility (http://glcf.umiacs.umd.edu/), the USGS Global Visualization Viewer (http://glovis.usgs.gov/) and USGS Earth Explorer (http://earthexplorer.usgs.gov/). Frontal positions from 1976 were obtained from Landsat MSS images acquired on 22nd

Mar (IGD) and 9th April (other glaciers) 1976. Frontal positions for 1986 were identified from a SPOT-1 panchromatic image, acquired on 9th Aug 1986).

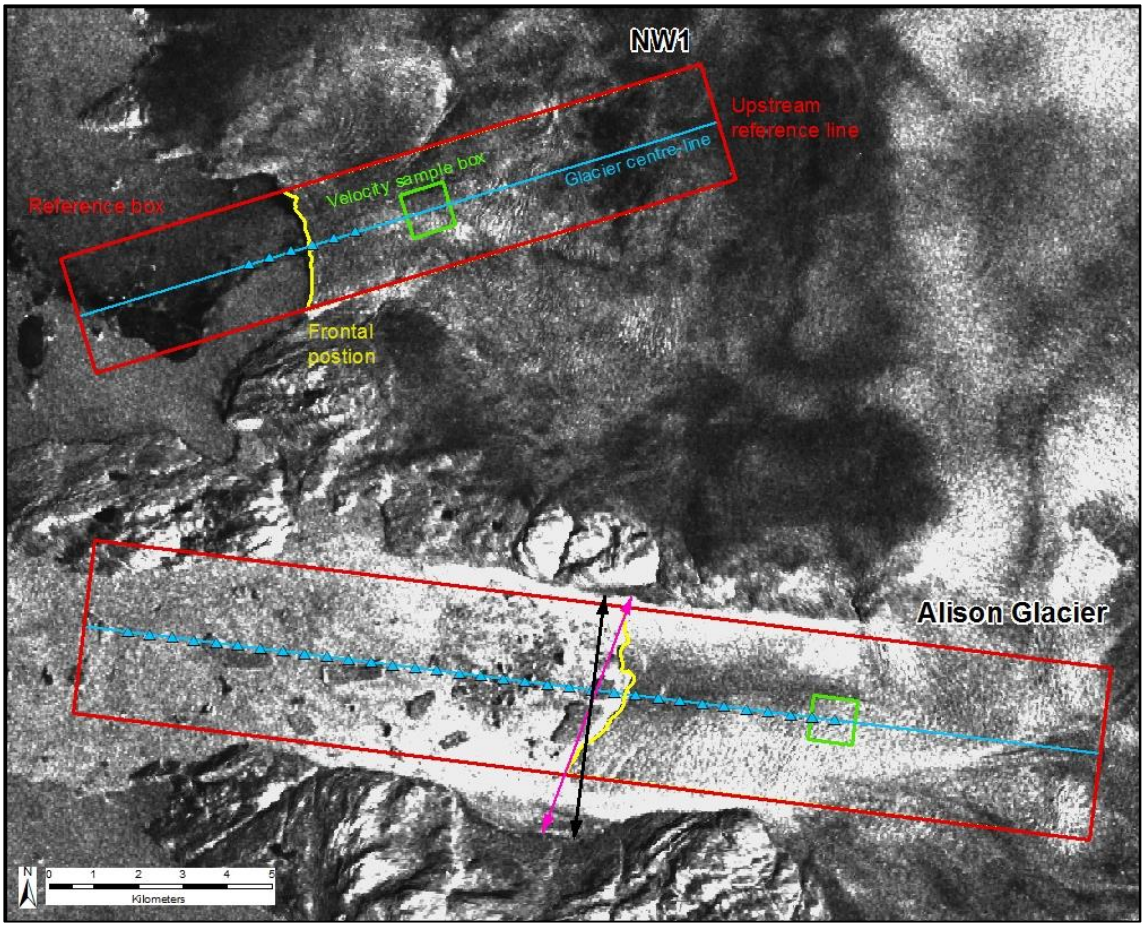

Figure 3.1. *Illustration of the method used for measuring outlet glacier frontal positions, ice velocities and fjord width. A reference box was defined which extends parallel to the main ice flow direction from an arbitrary upstream reference line (red box) and the glacier terminus was repeatedly digitized from successive images (yellow line). Mean ice velocities were sampled within a 1 km² box (green box), orientated parallel to and centered on the glacier centre-line (blue line). Blue triangles indicate sampling locations for fjord width perpendicular to the centerline. Fjord width was measured i) perpendicular to the glacier centerline (black line) at 500 m intervals from the upstream reference line (blue triangles) and; ii) approximately parallel to the glacier terminus for each available terminus position (pink line). The base image provides a typical example of an ENVISAT scene used for terminus mapping and shows the ice mélange and calving of large, tabular icebergs from the terminus of Alison Glacier during its rapid retreat phase. Base image: ENVISAT ASAR image, acquired 2nd October 2004, courtesy of ESA (European Space Agency).*

Adopting previous methods [*Howat et al.*, 2010; *Howat et al.*, 2008; *McFadden et al.*, 2011; *Moon and Joughin*, 2008], changes in terminus position were calculated by repeatedly digitizing the ice front within a reference box of fixed width (Fig. 3.2). The edges of the reference box were orientated approximately parallel to the main ice flow direction and were joined by a reference line at an arbitrary distance up-glacier (Fig. 3.2). The glacier terminus was digitized from sequential images and the mean change in frontal position was calculated by dividing the change in the area of the reference box by its width. This method improves upon using a single centerline reference point, as it accounts for uneven changes in the ice front and provides a more representative measure of frontal position change [*Howat et al.*, 2008; *Moon and Joughin*, 2008]. Total retreat and retreat rates were calculated relative to 2nd January 1993, which was the earliest image available for all of the study glaciers. Due to data availability, the temporal resolution of the frontal positions varied during the study period: data were available at a decadal resolution between 1976 and 1992, at sub-annual to annual resolution between 1993 and 2003 and at approximately monthly intervals between 2004 and 2010.

Potential sources of error in frontal position are: 1) coregistration of ERS and Envisat images; 2) geolocation accuracy of Envisat data; 3) relative geolocation accuracy of ERS/Envisat and visible imagery and; 4) manual digitzing errors. The error associated with coregistration was assessed by manually checking the coregistration of each ERS scene against its partner Envisat image: ERS scenes that did not coregister at the imagery resolution were rejected. On the basis of previous geolocation accuracy assessments, errors in Envisat geolocation are likely to be substantially less than the image resolution [*Small et al.*, 2004]. The relative geolocation of the radar and visible imagery, and manual digitizing errors, were evaluated by repeatedly digitizing 22 sections of rock coastline from a sub-sample of five ERS, five Envisat and five Landsat images, where there should be no discernible change in coastline position between scenes. The resultant total mean error in frontal position was 28.9 m, which is below

the image resolution and can be primarily attributed to manual digitizing. Due to their comparatively poor original georeferencing, the two Landsat MSS images were georeferenced to a later Landsat image (acquired on 27th Jun 2001) using distinctive features on the rock coastline. The resultant root mean square error was 62 m for the image acquired on the 22nd March 1976 and 78 m for the image from 9th April 1976.

3.2.2. Glacier and fjord width

The initial terminus width of each study glacier was measured from the earliest common image from 2nd Jan 1993. Terminus width was measured by drawing a line approximately parallel to each calving front and measuring the distance between the two points where the line intersected with the lateral margins of the terminus at sea level. Fjord width was measured in two ways. First, lines were drawn perpendicular to the glacier centerline at intervals of 500 m from the upstream reference line, and fjord width was measured between the two points where the lines intersected with the fjord walls at sea level (Fig. 3.2). Second, lines were drawn approximately parallel to the calving front using each available frontal position and fjord width was measured between the points where the lines intersected with the fjord walls at sea level (Fig. 3.2). NW1 retreated inland of its fjord during the study period and fjord width was therefore only measured in the section where the terminus was between the fjord walls. Furthermore, width was not measured perpendicular to the calving front, as it became highly concave toward the end of the study period which precluded accurate width measurements using this approach.

3.2.3. Outlet glacier velocities

Ice velocity data were extracted at two time steps (winter 2000-01 and winter 2005-06) from the annual ice-sheet-wide velocity maps for the GrIS, developed as part of the NASA Making Earth Science Data Records for Use in Research Environments (MEaSUREs) program [*Joughin et al.*, 2010b]. The velocity data were derived using Interferometric Synthetic Aperture Radar (InSAR) data from the RADARSAT-1 satellite. Mean ice velocities were sampled within a 1 km^2 box, which was centered on and

orientated parallel to the glacier centre-lines and located 1 km from the glacier terminus, as identified from the winter 2005-06 velocity map (Fig. 3.2).

3.2.4. Subglacial topography

Subglacial topographic data were supplied by CReSIS (Center for Remote Sensing of Ice Sheets) (ftp://data.cresis.ku.edu/data). The Level 2 'Ice Thickness', 'Ice Surface', and 'Ice Bottom' elevations products were used, which provides measurements of ice-bottom elevations along a series of flightlines across the GIS. Here we used the 2010 Greenland P-3 dataset, which was collected between 19th and 21st May 2010 as part of Operation IceBridge aircraft surveys, using the Multichannel Coherent Radar Depth Sounder (MCoRDS) sensor on the NASA P-3B platform. This dataset was selected as it provided the best spatial coverage and data quality within the study region. Data were available for one flightline perpendicular to the coastline and six parallel to the coastline, which were spaced between 2 and 5 km apart. The along-track sample spacing was approximately 14.5 m and the along-track horizontal resolution was approximately 25 m (http://nsidc.org/data/docs/daac/icebridge/irmcr2/index.html). The depth resolution of the data was 4.5 m. In-built quality flags identify data points as a high, medium and low confidence pick: this information was used to exclude all data points that were medium or low confidence. Landsat imagery was then used to remove any data points acquired over ocean or land. Further information on data processing, error sources and specific errors associated with the 2010 Greenland P-3 data are available from http://nsidc.org/data/docs/daac/icebridge/irmcr2/index.html.

3.2.5. Atmospheric and oceanic data

Atmospheric and oceanic data were compiled from a variety of sources and seasonal and monthly means were calculated for comparison with glacier frontal position data. Surface air temperature (SAT) data were obtained from Kitsissorsuit meteorological station (57°49'36"W 74°1'58"N; Fig. 3.1) and were provided by the Danish Meteorological Institute (DMI) at a three-hourly temporal resolution [*Carstensen and Jørgensen*, 2011]. Data were filtered to account for missing values and were only used

in the calculation of monthly/annual averages if the following criteria were met [*Cappelen*, 2011]: i) no more than two consecutive records were missing in a day; ii) no more than three records in total were missing in a day; iii) daily averages were available for 22 or more days per month and; iv) monthly averages were available for all months of the year. The filtered data were then used to calculate mean monthly, summer (JJA) and annual air temperatures and the number of positive degree days per year.

In order to assess the extent to which temperature data at Kitsissosuit are representative across the study region, a latitudinal lapse rate was calculated using mean monthly data from DMI meteorological stations at Nuusuaq (located 386 km south of Kitsissosuit) and Kitsussut (located 512 km north of Kitsissosuit). The estimated lapse rate was 0.004 °C/km, which equates to a mean temperature difference of 0.43 °C between Kitsissosuit and the most northerly glacier, NW7. This value is substantially smaller than the magnitude of interannual warming and we focus primarily on air temperature trends, rather than absolute values. At seasonal timescales, we focus on IGD, AG and NW1, which are the closest to Kitsissosuit, and the mean air temperature difference between these glaciers was minimal (0.14 °C). Furthermore, our frontal position data are at a monthly temporal resolution, so potential differences in seasonal retreat due to a later onset of melt towards the north of the transect are unlikely to be detectable within the data resolution.

Sea ice data were extracted from charts provided by the National Ice Centre (NIC), which were compiled from a range of directly measured and remotely sensed data sources (http://www.natice.noaa.gov/). Various imagery sources are incorporated into the charts, including Envisat, Defense Meteorological Satellite Program (DMSP) Operational Linescan System (OLS), AVHRR (Advanced Very High Resolution Radiometer), and RADARSAT, which have a spatial resolution down to 50 m. Data are provided at a weekly to bi-weekly temporal resolution and the accuracy of sea ice concentrations is estimated to be ± 10 % [*Partington*, 2003]. The dataset uses

information from multiple sensors and manual interpretation, which generally provides more accurate sea ice information than a single data source.

Data were sampled at each study glacier from a polygon extending the full width of the terminus and 50 m perpendicular to it, in order to extract sea ice concentrations from as close to the terminus as possible. For the seasonal analysis, monthly means were calculated for each study glacier. Sea ice data from all study glaciers were then used to calculate monthly and seasonal means for the study region. On average, monthly and seasonal means for individual glaciers varied from the regional average by 3.2 % and 3.8 %, respectively, suggesting that sea ice concentrations do not vary substantially across the region and that regional means are representative of conditions at each study glacier. Regional averages were also used to calculate the number of ice-free months per year, which are defined as months when mean monthly sea ice concentrations are equal to zero.

Monthly Sea Surface Temperature (SST) data were obtained from the Moderate Resolution Imaging Spectrometer (MODIS), provided by the NASA Ocean Color Project (http://oceancolor.gsfc.nasa.gov/), and from Version 2 of the Reynolds SST analysis dataset [*Reynolds et al.*, 2007]. SST data were used to investigate surface ocean temperatures only and are not necessarily representative of conditions at depth. MODIS data were used for the period 2000 to 2010 and have a spatial resolution of 5 km. The in-built data quality mask was used to remove pixels flagged as low quality and a combination of Landsat imagery and the in-built land mask were used to remove land pixels. SSTs were then sampled from all grid squares located within 25 km of each study glacier terminus.

As MODIS data were only available from 2000 onwards, Reynolds SST analysis data were also used to assess interannual changes in SSTs. However, the Reynolds data have a comparatively coarse spatial resolution (0.25°) and MODIS data were therefore used for the more detailed seasonal analysis between 2004 and 2010. The in-built

mask was used to remove pixels identified as land and sea ice and values were sampled from the grid squares closest to the glacier termini. Both datasets were sampled as close to the termini as possible, as SSTs proximal to the glaciers are likely to be strongly affected by local factors such as sea ice, glacial meltwater discharge and icebergs. Monthly values from each dataset were then used to calculate mean Jul-Sep SSTs for the study region, as these months were identified as ice free in the data quality masks for both datasets for all years.

In addition to the SST data, sub-surface ocean temperatures were obtained from the Hadley Centre EN3 quality controlled sub-surface ocean temperature and salinity dataset [*Ingleby and Huddleston*, 2007], which is available at a monthly temporal resolution. Data were sampled from the 1˚ by 1˚ model grid square that was located closest to the study glaciers, situated at a distance of 37 to 71 km from the glacier termini. The data provide information on ocean temperatures on the continental shelf and do not account for the complex processes within the glacier fjords or at the calving front. The data are therefore unsuitable for assessing oceanic conditions at the glacier front and instead are used to give a general indication of temperature change with depth in the water column at the continental shelf.

3.3. Results

3.3.1. Outlet glacier frontal position

3.3.1.1. Seasonal variation

The temporal resolution of the data allows for analysis of seasonal frontal position variations from 2004 onwards. Data are presented for AG, NW1 and IGD (Fig. 3.3), which encompass the range of the different types of seasonal frontal position variation and response to forcing within the study region (seasonal data for the other study glaciers are provided in the auxiliary material). The onset of seasonal retreat within the study region usually begins between April and July and seasonal advance generally commences between the end of August and the end of November (Fig. 3.3). However, there is substantial variation in the timing of seasonal advance/retreat, both on

individual glaciers and across the study region (Fig. 3.3). With the exception of AG and NW1, seasonal frontal position variation within the study area averaged approximately ±400 m and ranged between ± 660 m at Hayes Glacier and ±210 m at NW6. Aside from AG and NW1, the magnitude of seasonal retreat varied little from year-to-year and seasonal variations were significantly greater than the interannual trend, despite an overall pattern of retreat (Figs. 3.1 & 3.3). In contrast, the amount of seasonal retreat at AG fluctuated substantially over the study period: during the summers of 2004 and 2005 the glacier retreated by 3.61 km and 2.29 km, respectively, and underwent little seasonal advance (Fig. 3.3A). In contrast, seasonal retreat in 2008 and 2009 amounted to only 0.89 km and 0.50 km, respectively (Fig. 3.3A). The magnitude of seasonal retreat at NW1 also showed substantial interannual variation and reached a maximum of 1.7 km in summer 2005. Subsequent to winter 2004, seasonal retreat at NW1 was generally far greater than seasonal advance (Fig. 3.3D). To obtain an approximate estimate of winter calving, we compared seasonal advance rates and ice velocities in winter 2005-06. AG, NW1 and a number of the other study glaciers advanced at a rate which was very similar to their flow speed (Table 3.1), suggesting that winter calving was minimal. However, the rate of winter advance was considerably less than the terminus velocity on other glaciers, including IGD, NW2 and NW7 (Table 3.1), indicating that calving may have persisted during the winter.

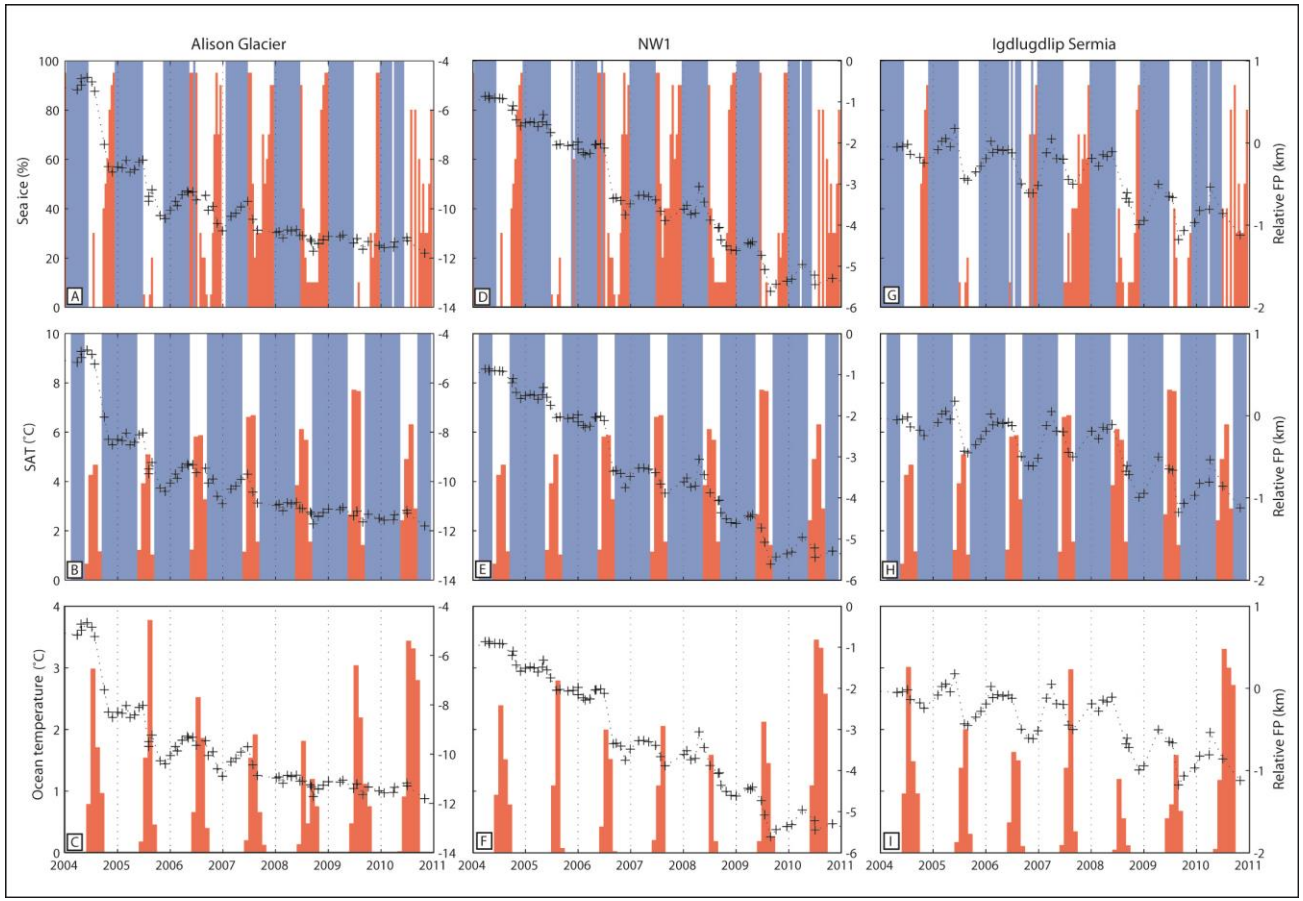

Figure 3.2. *Outlet glacier frontal position (black crosses) and seasonal atmospheric and oceanic forcing factors at Alison Glacier (left-hand panels), NW1 (middle panels) and IGD (right-hand panels). Panels A, D & G: mean monthly sea ice concentrations plotted in percent, with fast ice (i.e. 100 %) in blue and all other values in red. Panels B, E & H: mean monthly air temperatures for Kitsissorsuit meteorological station, plotted in red for temperatures above 0˚C and blue for temperatures below 0˚C. Panels C, F & I: mean monthly sea surface temperatures (SST) from MODIS data.*

3.3.1.2. Interannual variation

Due to data availability, interannual glacier retreat was compared to atmospheric and oceanic forcing data between 1993 and 2010, and the limited number of frontal positions available prior to 1992 were used to provide a longer-term context. Between 1993 and 2010, all study glaciers underwent net retreat, which predominantly occurred during the past decade, and the magnitude of retreat varied dramatically between glaciers (Table 3.1 and Figs. 3.1 & 3.4A). At AG, both the rate and magnitude of retreat far exceeded the regional average, with retreat totaling 11.6 km between 1993 and 2010. Approximately 10 km (84 %) of the total retreat at AG occurred between July 2001 and October 2005, and retreat rates peaked between July and October 2004, when the glacier retreated over 3 km (Figs. 3.1 & 3.4A). Retreat was accompanied by a 63% increase in ice velocities at AG's terminus between winter 2000-01 and 2005-06 (Table 3.1). At NW1, frontal position varied little between 1992 and 2001 and retreat rates were low (24.8 m a^{-1}) (Fig. 3.4A). Retreat rates then increased in two phases: retreat averaged 221.2 m a^{-1} between June 2001 and July 2006 and increased to 352.5 m a^{-1} thereafter (Fig. 3.4A). The most rapid retreat at NW1 occurred between July 2006 and September 2006, when the glacier retreated by 1.2 km, and rapid retreat phases also occurred during the summers of 2008 and 2009.

The other study glaciers began to retreat from 2001 onwards (Figs. 3.1 & 3.4A), but the magnitude of total retreat was smaller (200 m to 2 km) and average retreat rates were slower (10 to 100 m a^{-1}) than at AG or NW1 (Table 3.1 and Figs. 3.1 & 3.4A). Although the overall trend was one of retreat, it was comparatively gradual on these glaciers and interannual retreat rates were significantly less than the seasonal variability in frontal position. Between 2000/01 and 2005/06, the glaciers underwent minimal acceleration near to the terminus and a number of glaciers underwent slight deceleration (Table 3.1). Two patterns of interannual retreat are therefore apparent within the study region between 1993 and 2010: i) rapid, non-linear, step-wise recession, which results in high-magnitude retreat at interannual timescales and occurred at AG and NW1; and ii)

slower, more gradual retreat, which produces far lower total retreat rates and occurred on the remaining study glaciers.

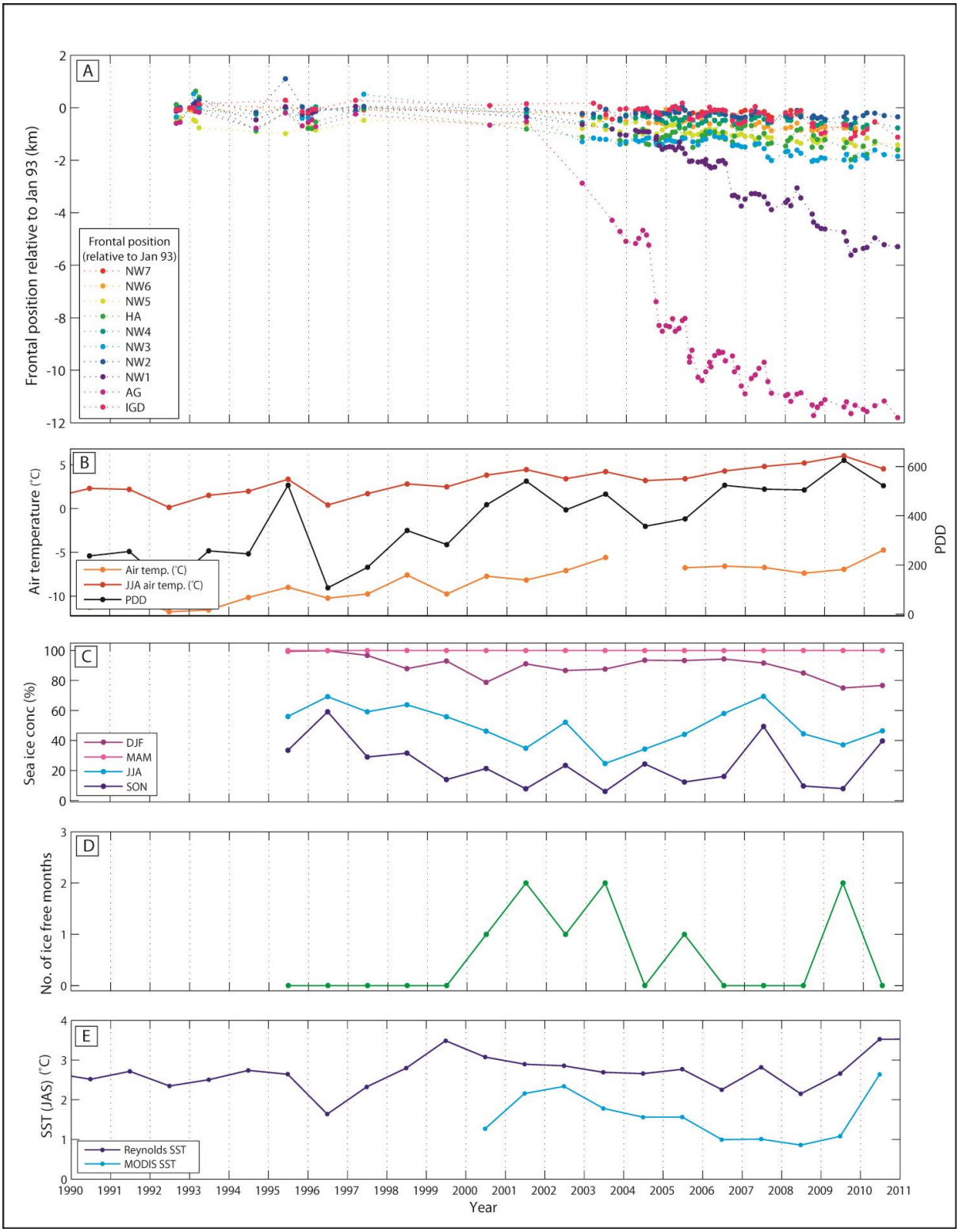

Figure 3.4. *Relative glacier frontal position and climatic/oceanic forcing factors. (A) Frontal position for all glaciers, relative to January 1993, color-coded according to glacier. (B) Mean annual and mean summer (JJA) air temperatures and number of positive degree days (PDD) at Kitsissorsuit meteorological station. (C) Mean seasonal sea ice concentrations for all study*

glaciers for the periods Dec–Feb (DJF), Mar-May (MAM), Jun-Aug (JJA) and Sep-Nov (SON). (D) Number of months of ice-free conditions for all study glaciers. (E) Mean sea surface temperatures for Jul-Sep (JAS) from MODIS (light blue) and Reynolds (dark blue) SST data.

Frontal positions on the majority of the study glaciers showed little net change between 1976 and 2001 (Figs. 3.5 & 3.6) and their retreat rates were substantially lower than between 2001 and 2010 (Table 3.1). Exceptions to this were NW1 and NW2 (Fig. 3.2 & Table 3.1), which retreated by approximately 6 km and 3 km respectively between 1976 and 2001, with the majority of retreat occurring prior to 1986. The western margin of NW7 also retreated during this period, coincident with the loss of a section of ice located to the west of the lateral margin of the glacier. At AG, the terminus position changed very little between 1976 and 2001 (Fig. 3.5 & Table 3.1): results show a net advance of 9 m during this interval, which equates to a rate of 0.4 m a^{-1}, and is significantly less than the frontal position error. Three distinct phases of frontal position behavior are therefore apparent at AG: i) minimal net retreat between June 1976 and July 2001; ii) very rapid retreat between July 2001 and October 2005 at 2431.4 m a^{-1} and; iii) more gradual retreat at 306.2 m a^{-1} until the end of the study period (Fig. 3.5). The vast majority of retreat on AG and on the other study glaciers occurred from 2001 onwards.

3.3.2. Atmospheric and oceanic forcing

Mean annual surface air temperatures at Kitsissorsuit increased by almost 8 ˚C between 1990 and 2010 (Fig. 3.4B), which equates to a linear warming trend of 0.29 ˚C per year (R^2 = 0.79). This trend concurs with substantial increases in air temperature observed at nearby meteorological stations during the past two decades [*Carr et al.*, 2013]. Summer (JJA) air temperatures showed a similar warming trend of 0.20 ˚C per year (R^2 = 0.68) between 1990 and 2010, which was particularly marked from 1996 onwards (Fig. 3.4B). The number of positive degree days (PDDs) at Kitsissorsuit were very high in 1995 and then showed a strong positive trend between 1996 and 2001, followed by a further period of warming between 2004 and 2009 (Fig. 3.4B).

Glacier	Total retreat (m) (1993–2010)	Retreat rate (m a^{-1}) (1993–2010)	Retreat rate (m a^{-1}) (1976–2001)	Retreat rate (m a^{-1}) (2001-2010)	Glacier velocity (winter 00-01)	Glacier velocity (winter 05-06)	Velocity change (winter 00/01 to 05/06)	Ice front advance rate (winter 05/06)
NW7	749	42	-	-	1090	950	-140	212
NW6	665	37	6	63	800	670	-130	422
NW5	1,152	64	30	60	90	100	+10	-
HA	1,768	98	7	106	2160	2070	-90	1353
NW4	668	37	7	53	850	830	-20	814
NW3	1,925	107	10	179	1060	1050	-10	1025
NW2	196	11	121	15	2710	2480	-230	675
NW1	5,317	295	263	551	390	450	+60	653
AG	11,575	643	0	1227	1800	2840	+1040	2687
IGD	824	46	+3	108	2680	2760	+80	1136

Table 3.1*. Summary of glacier retreat rates for January 1993 to January 2010, April 1976 to June 2001 and June 2001 to January 2010. Glaciers are ordered by location, from north to south (see Fig. 3.1) and abbreviations are as follows: AG (Alison Glacier); HA (Hayes Glacier) and; Igdlugdlip Sermia (IGD). The total mean error in frontal position is 28.9 m, equating to a mean error in retreat rate of 1.6 m a^{-1}. Ice velocities are shown for winter 2000-01 and 2005-06 and are used to calculate change in glacier velocity between the two time periods. Velocities were obtained the MEaSUREs ice-sheet-wide velocity maps (Joughin et al., 2010b). Winter ice front advance rates are shown for 2005-06 and were calculated from glacier frontal position data. Note the markedly higher retreat rates on AG and NW1 in comparison to the other study glaciers.*

Mean summer (JJA) and autumn (SON) sea ice concentrations showed a decreasing trend from 1997 to 2004 and then increased between 2004 and 2007, before declining once more from 2007 to 2009 (Fig. 3.4C). The glacier fjords became seasonally ice free during the summers of 2000 to 2003, 2005 and 2009, with the number of ice free months peaking in 2001, 2003 and 2009 (Fig 3.4D). MODIS SST data show warming between 2000 and 2002, followed by cooling of approximately 1 °C between 2002 and 2008 (Fig. 3.4E). SSTs then increased by 1.5 °C between 2009 and 2010. The Reynolds SST data show no net trend between 1990 and 1995, followed by warming of almost 2 °C between 1996 and 1999. SSTs cooled gradually until 2005 and then

warmed between 2008 and 2010 (Fig. 3.4E). The two SST datasets follow a similar overall pattern, but the MODIS values are consistently cooler than the Reynolds data (Fig. 3.4E).

3.4. Discussion

All glaciers underwent net retreat during the study period, but despite comparable glacier sizes and forcing, the magnitude, pattern and rate of retreat varied dramatically between individual glaciers (Table 3.1, Figs. 3.1 & 3.4). We first discuss glacier response to atmospheric and oceanic forcing at seasonal timescales, in order to investigate the factors influencing calving rates and net frontal position, and then consider these relationships at interannual to decadal timescales, before assessing the role of glacier-specific factors.

3.4.1. Influence of atmospheric and oceanic forcing on seasonal glacier behavior

3.4.1.1. Alison Glacier

Between 2004 and 2007, seasonal variations in frontal position at AG corresponded closely to changes in sea ice concentrations within the glacier fjord at the start and the end of the calving season (Fig. 3.3A). This is exemplified by its behavior in 2005, when summer sea ice concentrations were particularly low and the transition between fast ice and ice free conditions was particularly rapid (Fig. 3.3A). Seasonal retreat began from 26th June 2005, coincident with sea ice reducing from 100 % to 10 % between 20th June and 4th July (Fig. 3.3A). Conversely, sea ice concentrations reached 100 % by 21st November 2005, which was rapidly followed by the onset of winter advance from 29th November 2005 (Fig. 3.3A).

The onset of seasonal retreat/advance shows a similar coincidence with sea ice loss/formation during each calving season between 2004 and 2007 (Fig. 3.3A), suggesting that sea ice may be a primary control on seasonal frontal position variations at AG during this period. This is supported by comparison of ice velocities and terminus

advance rates for winter 2005-06 (Table 3.1), which suggest that the calving front advanced at approximately 95% of the glacier flow speed and that winter calving was therefore minimal. These results agree with findings from elsewhere on the GrIS, which suggest that sea ice may suppress winter calving rates by up to a factor of six by forming a weak seasonal ice shelf, or mélange, which inhibits calving from the terminus [*Amundson et al.*, 2010; *Joughin et al.*, 2008b; *Sohn et al.*, 1998]. In contrast, spring-time disintegration of the mélange may promote retreat by allowing high summer calving rates to commence [*Ahn and Box*, 2010; *Amundson et al.*, 2010; *Howat et al.*, 2010; *Joughin et al.*, 2008b]. Thus, sea ice is likely to be an important control on the frontal position and calving rate of AG at seasonal timescales.

The onset of seasonal retreat at AG also partially coincided with the seasonal increase in air temperatures to above 0 ˚C, although with a delay of approximately three to four weeks (Fig. 3.3B). In spring 2005, for example, SATs first exceeded 0 ˚C on 17th May, prior to terminus retreat on 26th June (Fig. 3.3B). In general, air temperatures at AG rose above 0 ˚C between mid-May and mid-June and glacier retreat began in late June (Fig. 3.3B). The seasonal increase in air temperatures could promote retreat via a number of mechanisms[*Carr et al.*, 2013], including: i) meltwater enhanced crevassing at the glacier terminus [*Andersen et al.*, 2010; *Sohn et al.*, 1998; *Vieli and Nick*, 2011]; ii) melting of sea ice/ice mélange; and iii) enhancement of submarine melt rates by subglacial plume flow [*Motyka et al.*, 2003; *Motyka et al.*, 2011; *Straneo et al.*, 2011]. The lack of available data precludes investigation of the latter mechanism, but the first two processes are supported by the presence of numerous water-filled crevasses and supraglacial lakes close to AG's terminus during summer, as observed from satellite imagery (Fig. 3.1), and by the strong correlation between SATs and sea ice ($r = 0.72$). At the end of the calving season, air temperatures at AG fall below freezing approximately 1.5 to 2.5 months before the onset of winter advance (Fig. 3.3B). This is exemplified by winter 2005/06, when air temperatures were below freezing by 18th September, but seasonal retreat persisted until 29th November (Fig. 3.3B). These

observations suggest that air temperatures may contribute to seasonal retreat at AG, but their influence on seasonal advance may be limited, which is consistent with previous findings from Jakobshavn Isbrae (JI), west Greenland [*Sohn et al.*, 1998].

Between 2004 and 2007, SST warming from June onwards was coincident with the onset of seasonal retreat at AG (Fig. 3.3C). However, the most rapid retreat did not coincide with peak SSTs: in 2005, for example, the warmest SSTs occurred in August, yet the glacier front advanced slightly between 6th and 29th August (Fig. 3.3C). Similarly, in 2006, peak SSTs in July and August were coincident with a small terminus advance between 23rd July and 5th September (Fig. 3.3C). This suggests that the frontal position responds to SST warming, as opposed to peak SSTs, which may result from the relationship between SSTs and sea ice concentrations. SST warming early in the season would melt sea ice at the glacier terminus and could thus promote retreat, given the apparent sensitivity of AG to sea ice concentrations. In contrast, peak SSTs would have a lesser affect, as sea ice has largely melted by this point in the season (Fig. 3.3A). This mechanism is supported by the moderate correlation between SSTs and sea ice at AG ($r = 0.52$) and the coincidence of SST warming with the seasonal disintegration of fast ice (i.e. 100 %) at the glacier front (Fig. 3.3). The limited correspondence between peak SSTs and retreat rates also suggests that undercutting at the waterline [*Benn et al.*, 2007; *Vieli et al.*, 2002] due to SST warming is not a primary driver of retreat.

At present, sub-surface oceanographic data are not available from AG's fjord and the only data available for the region are model outputs from the Hadley Centre EN3 quality controlled sub-surface ocean temperature and salinity dataset [*Ingleby and Huddleston*, 2007]. As noted, these data only provide information on water temperature on the continental shelf and are therefore unlikely to be representative of conditions at the glacier front. However, the modeled depth profile sampled from the continental shelf, immediately offshore of the study region, suggests that warm water is present at depth (~100 to 150m) and underlies cooler surface water (Fig. 3.8). This profile is

consistent with empirical data from central-west Greenland [*Holland et al.*, 2008] and previous studies have shown that warm Atlantic Water (AW) can access Greenland outlet glacier fjords from the continental shelf at depth [*Christoffersen et al.*, 2011; *Holland et al.*, 2008; *Johnson et al.*, 2011; *Mayer et al.*, 2000; *Straneo et al.*, 2011; *Straneo et al.*, 2010]. Given that high summer submarine melt rates have been linked to seasonal mass loss in central-west Greenland [*Rignot et al.*, 2010], it is possible that similar processes may influence seasonal glacier behaviour at AG. This is supported by estimated submarine melt rates of 0.26 m d^{-1} at AG, which may account for a significant portion of ice volume loss {Enderlin, 2013 #379}. However, the current lack of data from within the fjord precludes a more detailed assessment of this potential control on seasonal behaviour. It is clear therefore, that there is an urgent need for sub-surface measurements of ocean temperature at AG and other Greenland outlet glacier fjords. Such data are required for numerical models that incorporate oceanic forcing and would also allow a more detailed assessment of the influence of meltwater plumes on submarine melt rates: subglacial discharge may increase melting by forming a plume of cool, buoyant water at the terminus and promoting a compensatory inflow of warmer ocean water at depth [*Motyka et al.*, 2003; *Motyka et al.*, 2011; *Straneo et al.*, 2011]. This interaction is currently poorly understood [*Straneo et al.*, 2011], but may be significant at AG, given the very dramatic warming observed during the past two decades (Fig. 3.4B).

In summary, we suggest that seasonal retreat at AG may be initiated by a combination of spring-time sea ice loss and meltwater-enhanced crevassing. Winter sea ice formation may slow calving rates and promote seasonal advance and air temperatures and SSTs may indirectly influence frontal position, via their relationship with sea ice concentrations. These results indicate that multiple atmospheric and oceanic forcing factors influence seasonal frontal position variations at AG, but that their relative contribution varies during the year.

3.4.1.2. Additional study glaciers

In contrast to the close correspondence observed at AG, the relationship between sea ice and glacier frontal position is less apparent on the other study glaciers. NW1 and IGD show a pattern of response to seasonal forcing that was representative of the other glaciers within the study region (Fig. 3.3). At both glaciers, the onset of seasonal retreat and advance sometimes coincided with sea ice clearance and re-formation, respectively, but it also pre-dated it on a number of occasions and instead often showed a closer correspondence to periods when air temperatures rose above freezing. At NW1, for example, retreat began between 6th and 31st May 2005, which significantly pre-dated sea ice clearance between 20th June and 4th July (Fig. 3.3D) and coincided with air temperatures rising above freezing on 17th May in 2005 (Fig. 3.3E). Similarly, IGD retreated between 14th April and 28th June 2009, but sea ice clearance did not occur until 22nd June – 7th July (Fig. 3.3G).

Although the onset of winter advance at NW1 and IGD was generally concurrent with winter sea ice formation and occurred substantially after air temperatures fell below zero (Fig. 3.3), this was not always the case. In winter 2009, for example, terminus advance began at both glaciers between 31st August and 8th October and therefore pre-dated winter sea ice formation between 23rd November and 7th December (Figs. 3.3D & G). Furthermore, comparison of winter advance rates and ice velocities (Table 3.1) indicates that calving does not cease entirely at IGD, suggesting that winter sea ice formation may exert a weaker influence on seasonal glacier advance than at AG. In contrast to AG, the onset of seasonal retreat at NW1 and IGD frequently preceded SST warming (Figs. 3.3F & I). This differing response may reflect the weaker influence of sea ice at NW1 and IGD, which may reduce the contribution of SSTs to frontal retreat via sea ice melt.

These observations indicate that seasonal frontal position variations at NW1, IGD and the other study glaciers are influenced by both air temperatures and sea ice. However, sea ice concentrations and SSTs may be a less significant control than at AG,

suggesting that glacier-specific factors may be modulating the response to seasonal forcing. In contrast to the other study glaciers, AG initially terminated in a floating ice tongue and a number of lines of evidence suggest that this tongue was near to floatation between 2004 and 2007. First, it calved several large, tabular icebergs (Fig. 3.2), which are only thought to occur from floating termini [*Amundson et al.*, 2010]. Second, the tabular icebergs often calved back to large rifts (Fig. 3.2), which are associated with near-floating ice [*Joughin et al.*, 2008a]. Third, the tongue's surface elevation profile was very flat [*McFadden et al.*, 2011]. The presence of a floating ice tongue may account for AG's greater sensitivity to seasonal sea ice forcing, and hence to SSTs, as basal shear stresses would be low over areas close to floatation, meaning that the relative contribution of longitudinal stresses to the force balance would increase [*Echelmeyer et al.*, 1994] and that variations in longitudinal stresses associated with changes in sea ice buttressing may have had a greater influence on retreat rates. This is supported by AG's behavior subsequent to 2007, when evidence suggests that the terminus began to re-ground and the correspondence between seasonal sea ice disintegration and the onset of retreat became less pronounced, with retreat pre-dating sea ice clearance in 2009 (Fig. 3.3A). These results suggest that the seasonal response of the study glaciers to atmospheric and oceanic forcing varies according to terminus type and that this relationship may change as the glacier terminus evolves during retreat.

3.4.2. Interannual glacier behavior and atmospheric and oceanic controls

All glaciers in the study area retreated between 1993 and 2010 (Figs. 3.1 & 3.4), coincident with declining summer (JJA) and autumn (SON) sea ice concentrations and a dramatic air temperature increase of almost 8˚C (Fig. 3.4). Given the influence of sea ice and air temperatures on seasonal glacier behaviour within the study region, we suggest that these factors are likely to also be primary controls at interannual timescales, via their influence on net frontal position and calving rates.

At AG, retreat followed increased air temperatures and sea ice decline, with peak retreat rates occurring within one year of minimum sea ice concentrations in 2003 (Fig. 3.4). Seasonal results suggest that sea ice is a key control on the timing of retreat/advance at AG (Fig. 3.3A) and so early disintegration/late formation of sea ice may have triggered net terminus retreat by extending the duration of seasonally high summer calving rates, as proposed for other Greenland outlet glaciers [e.g. *Howat et al.*, 2010; *Joughin et al.*, 2008b]. This is consistent with the pattern of interannual retreat at AG (Fig. 3.4A), where very large seasonal retreats in 2004 and 2005, totaling almost 6 km, followed a prolonged decline in sea ice concentrations and substantial increase in the duration of ice free conditions (Fig. 3.3A). The very strong increase in air temperatures may also have contributed to net retreat at AG, potentially via meltwater enhanced crevassing at the terminus [*Sohn et al.*, 1998; *Vieli and Nick*, 2011], increased sea ice melting and/or enhanced submarine melt rates due to increased subglacial discharge. These observations are in agreement with previous results from the Uummannaq region of west Greenland [*Howat et al.*, 2010] and JI [*Joughin et al.*, 2008b; *Vieli and Nick*, 2011], which suggest that extension of the seasonal calving cycle through reduced sea ice concentrations and/or increased air temperatures may be sufficient to trigger rapid interannual retreat.

Output from the EN3 model indicates that ocean temperatures at depth increased substantially between 1998 and 1999 at the continental shelf (Fig. 3.8), which is broadly consistent with the sudden increase in subsurface ocean temperatures recorded on the central-west Greenland continental shelf between 1997 and 1998 {Holland, 2008 #41}. However, the modeled warming substantially predates the onset retreat at AG (Fig. 3.4). Moreover, estimated melt rates at AG showed no clear trend between 2002 and 2007 {Enderlin, 2013 #379}, whereas glacier retreat rates varied dramatically during this period (Fig. 3.4A). This is consistent with previous results, which found no statistically significant relationship between estimated melt rate and either glacier retreat or velocity at AG {Enderlin, 2013 #379}. The very limited available

evidence shows no clear relationship between subsurface oceanic warming, submarine melt rates and glacier retreat at AG. However, very little information is available and detailed subsurface oceanographic measurements from within the fjord would be required to investigate the potential influence of subsurface ocean warming on AG.

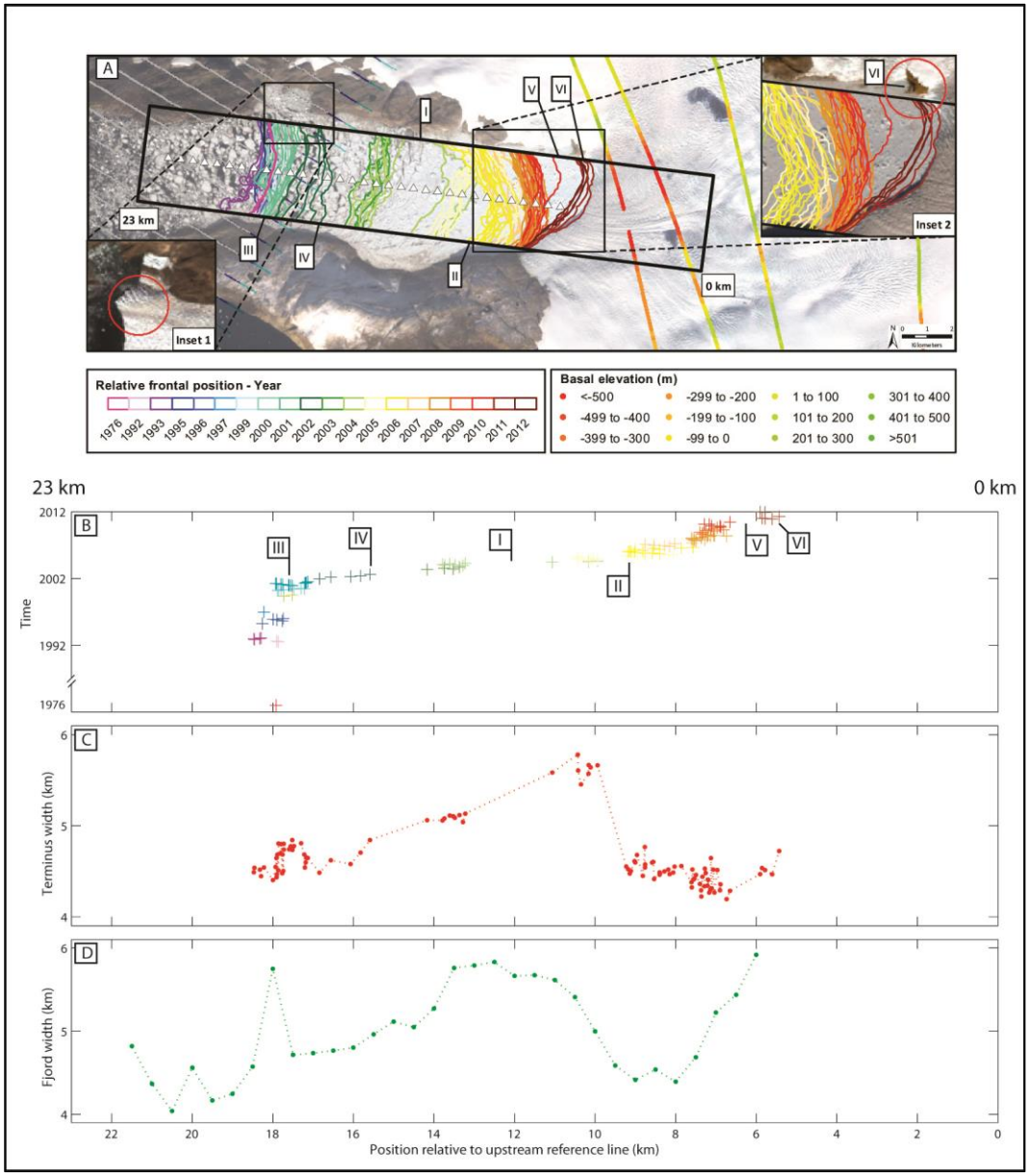

Figure 3.5. *Frontal position of Alison Glacier in relation to basal elevation, fjord width parallel to the glacier terminus, and fjord width perpendicular to the centre-line. (A): AG frontal position over time (colored lines) in relation to ice-bottom elevations from CReSIS radar depth sounder flightlines, color-coded from green (high elevation) to red (low elevation). Labeled positions are discussed in the text. Base image: Landsat scene acquired 11th September 2011 and provided by USGS GLOVIS. (B) AG frontal position over time (colored crosses), relative to upstream reference line (C) Fjord width parallel to the glacier terminus for each available frontal position.*

(D) Fjord width perpendicular to the centre-line at 500 m intervals from the upstream reference line (sample locations indicated by white triangles in A).

The MODIS and Reynolds SST data follow a similar interannual pattern (Fig. 3.4), although MODIS values are consistently cooler than the Reynolds dataset. We attribute this difference to the greater spatial resolution of the MODIS data, which allows SSTs to be sampled closer to the glacier termini. Consequently, glacial meltwater discharge and icebergs from the termini would have a greater influence on the MODIS SSTs and would thus give cooler values. The MODIS data indicate that SSTs warmed by 1 °C between 2000 and 2002, which was coincident with the onset of retreat at AG, low summer sea ice concentrations and an extended duration of ice-free conditions (Fig. 3.4). Based on relationships observed at seasonal timescales, warmer SSTs may have initiated retreat by causing early sea ice loss and thus extending the duration of high summer calving rates. However, the MODIS data then show a cooling between 2002 and 2008 and the Reynolds data demonstrate little trend during this period, despite AG continuing to retreat rapidly (Fig. 3.4). Furthermore, significant SST warming occurred in 1996-1999 and 2008-2010, yet the front exhibited little change. This suggests that AG's response to SST changes is non-linear, so that the magnitude of retreat does not depend only on the magnitude of forcing. A similar non-linearity is evident in the relationship with sea ice and air temperature trends. This was particularly notable in 2009 when sea ice concentrations and duration were comparable to 2001 and JJA SATs and PDDs reached their maximum for the study period, yet retreat rates remained low (Fig. 3.4). Together, this evidence indicates that the response of AG to these potential controls was modulated by glacier-specific factors.

Interannual retreat of the other study glaciers was also coincident with sea ice decline and atmospheric warming (Fig. 3.4), which is consistent with controls operating at seasonal timescales. However, despite being subject to very similar forcing, the magnitude and rate of retreat differed dramatically between individual glaciers (Table 3.1, Figs. 3.1 & 3.4). These results agree with previous findings from western

Greenland, which found no consistent relationship between marine-terminating outlet glacier behavior and atmospheric or oceanic forcing [*McFadden et al.*, 2011]. Furthermore, the pattern of retreat varied markedly across the study region: net retreat at AG and NW1 largely occurred via very large seasonal retreats with limited seasonal readvance (Figs. 3.3A, 3.3D & 3.4A), whereas the other glaciers retreated more gradually, with limited variation in the magnitude of seasonal frontal position variations (Figs. 3.3G & 3.4A). This contrasting behavior suggests that the study glaciers reacted very differently to external forcing and that factors specific to each glacier are a key determinate of their response.

On the majority of the study glaciers, retreat rates were substantially higher during the past decade than between 1976 and 2001 (Table 3.1 & Figs. 3.5 & 3.6) and this is consistent with a previous study which identified a large episode of mass loss in north-west Greenland between 2005 and 2010 [*Kjær et al.*, 2012]. It has also been proposed that north-west Greenland underwent an earlier event between 1985 and 1993, during which dynamic mass loss exceeded that between 2005 and 2010. Furthermore, AG was highlighted as an area of rapid thinning between 1985 and 2005 [*Kjær et al.*, 2012]. Our results suggest that the majority of the study glaciers showed limited net retreat between 1976 and 2001 (Table 3.1 & Fig. 3.6) and AG in particular showed very little change during this period (Fig. 3.5 & Table 3.1). This contrasts dramatically with observed retreat rates of almost 2.5 km a^{-1} between 2001 and 2005 at AG (Fig. 3.5). We therefore suggest that the observed thinning at AG between 1985 and 2005 was a response to rapid retreat and loss of the floating tongue between 2001 and 2005, as opposed to an earlier mass loss event. Furthermore, we highlight recent retreat rates at AG as exceptional since at least 1976. Our data record substantial retreats on NW1 and NW2 (Fig. 3.7 & Table 3.1), but the vast majority of these changes occurred prior to 1986 and therefore predate the proposed dynamic event. At NW7, retreat largely occurred on the western portion of the terminus and was coincident with the loss of a section of ice adjoining the lateral margin of the glacier. We therefore suggest that

retreat at NW7 was a response to the reduction in buttressing associated with this ice loss, as opposed to a direct dynamic response to changes in atmospheric or oceanic forcing at its terminus. Consequently, we do not observe substantial and widespread changes in frontal position within our study region at the time of the proposed discharge event.

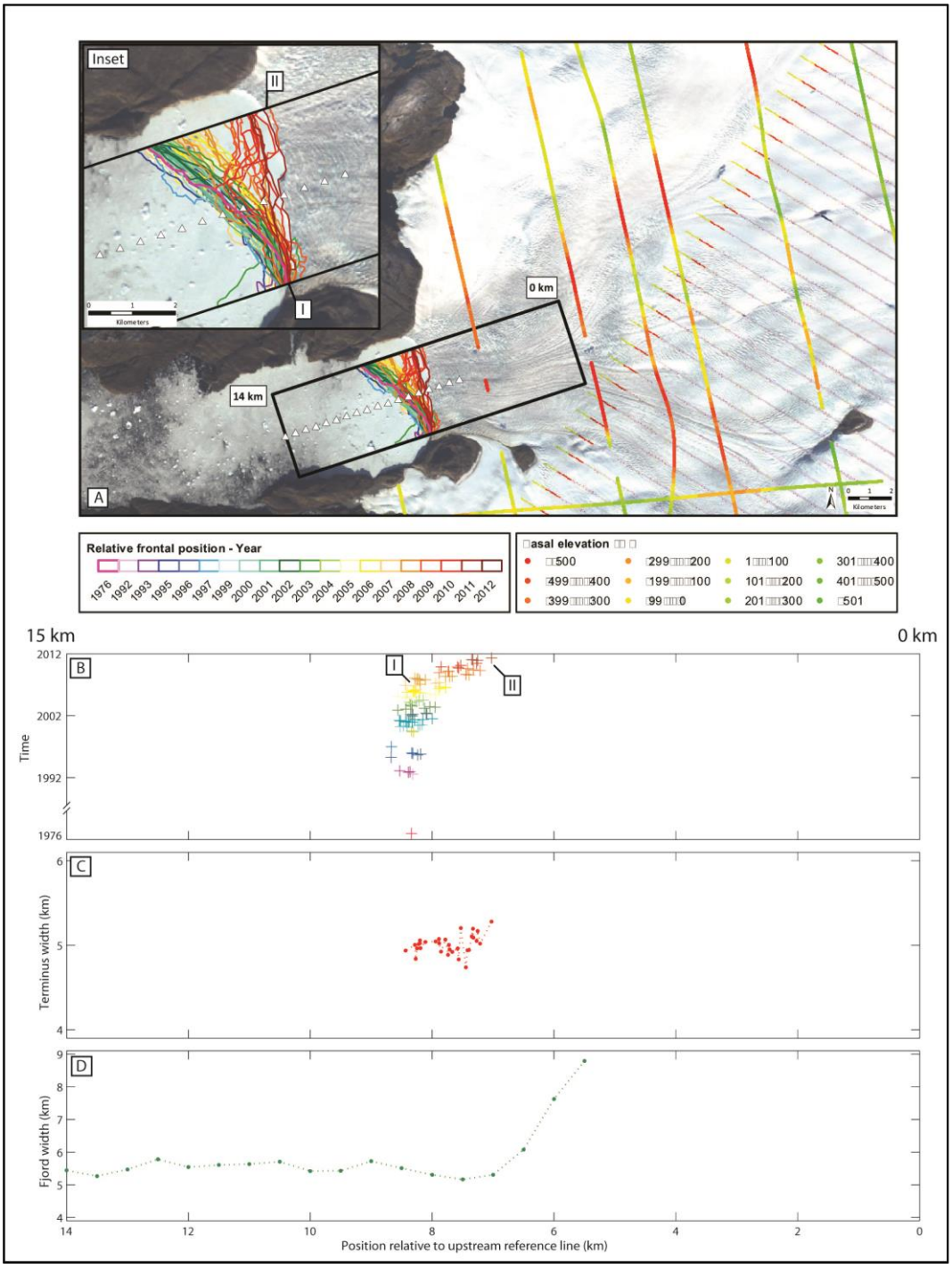

Figure 3.6. *Frontal position of Igdlugdlip Sermia in relation to basal elevation, fjord width parallel to the glacier terminus, and fjord width perpendicular to the centre-line. (A): IGD frontal*

position over time (colored lines) in to ice-bottom elevations from CReSIS radar depth sounder flightlines, color-coded from green (high elevation) to red (low elevation). Labeled positions are discussed in the text. Base image: Landsat scene acquired 11th September 2011 and provided by USGS GLOVIS. (B) IGD frontal position over time (colored crosses), relative to upstream reference line. (C) Fjord width parallel to the glacier terminus, for each available frontal position. (D) Fjord width perpendicular to the centre-line (sample locations indicated by white triangles in A).

3.4.3. Role of glacier-specific factors

We examined retreat rates in relation to a number of glacier-specific factors, including initial glacier width, ice velocity, bed topography, fjord geometry and terminus type. We found no statistically significant relationship between the mean glacier retreat rate for 1993 to 2010 and either initial glacier terminus width in January 1993 (r = -0.085) or with initial ice velocity in winter 2000-01 (r = -0.080). However, our results suggest that along-flow variations in fjord width may play an important role in ice dynamics within the study region, via their influence on lateral stresses.

The pattern of retreat at AG suggests that along-flow variations in fjord width and, potentially basal pinning points may be important controls on retreat. Peak retreat rates immediately followed terminus recession into a comparatively wide section of its fjord from July 2004 onwards (Fig. 3.5; Point I) and persisted until the calving front reached a lateral constriction in late August 2005 (Fig. 3.5; Point II). At this point, retreat slowed dramatically and the terminus position remained comparatively stable until July 2010. Narrowing of the glacier fjord may have temporarily slowed retreat via two mechanisms [*Jamieson et al.*, 2012]: i) due to the principle of mass conservation, the glacier needs to thicken and the surface slope to steepen in order to maintain the same ice flux , which would reduce thinning rates and the vulnerability of the ice to full thickness fracture, thus decreasing calving rates and slowing retreat [*O'Neel et al.*, 2005] and; ii) lateral stresses tend to increase with reducing width [*Raymond*, 1996], thus increasing resistance to flow and promoting deceleration, thickening and slower retreat.

Furthermore, a number of lines of evidence suggest that AG's terminus began to ground at this point: i) the substantial reduction in the magnitude of seasonal frontal position variation, particularly seasonal retreat, from winter 2005 onwards (Fig. 3.3A), ii) the change in calving style from tabular to capsizing icebergs; iii) the increased occurrence of glacial earthquakes, which are associated with grounded termini [*Veitch and Nettles*, 2012] and; iv) the development of a steeper surface profile near the terminus from 2006 onwards [*McFadden et al.*, 2011]. Although grounding is unconfirmed, it may have produced further positive feedbacks between glacier thickening, increased basal stresses and reduced frontal retreat rates [*Schoof*, 2007; *Vieli et al.*, 2001].

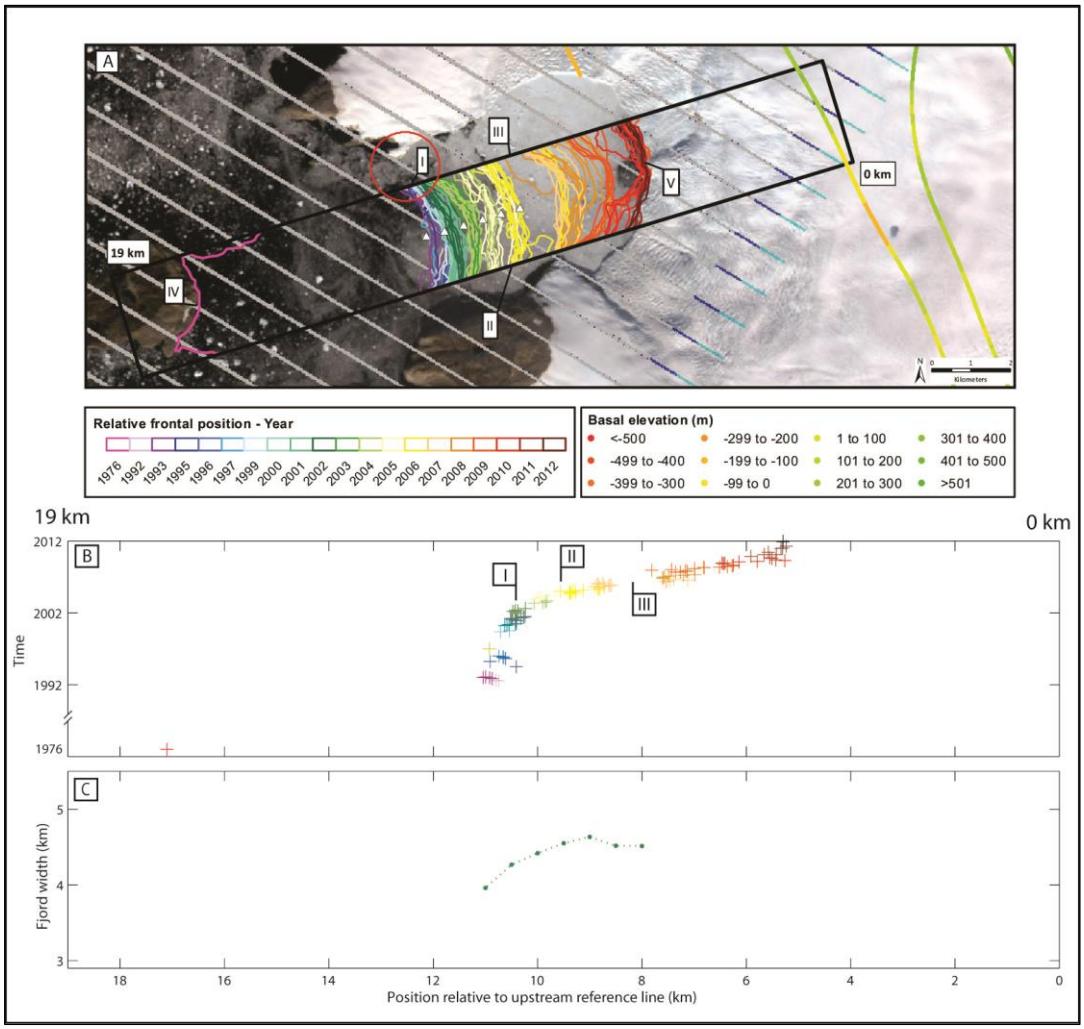

Figure 3.7. *Frontal position of NW1 in relation to basal elevation and fjord width parallel to the glacier terminus. (A) NW1 frontal position over time (colored lines) in relation to ice-bottom elevations from CReSIS radar depth sounder flightlines, color-coded from green (high elevation)*

to red (low elevation). Labeled positions are discussed in the text. Base image: Landsat scene acquired 11th September 2011 and provided by USGS GLOVIS. (B) NW1 frontal position over time (colored crosses), relative to upstream reference line. (C) Fjord width perpendicular to the centre-line at 500 m intervals from the upstream reference line (sample locations indicated by white triangles in A).

Based on these observations, we suggest that the comparative stability of AG's floating tongue between 1976 and 2001 (Fig. 3.5; Point III) was also facilitated by the relatively narrow width of the fjord and/or the presence of basal pinning points. Although fjord bathymetry data are currently unavailable, a bedrock island and a possible ice rumple are apparent at the northern margin of AG (Fig. 3.5; Inset 1). Terminus retreat past this feature and into a wider section of the fjord immediately preceded the first phase of rapid retreat at AG (Fig. 3.5: Point IV), providing empirical support for the contribution of basal and lateral pinning points to the comparative stability of AG's terminus between 1976 and 2001. These findings agree with empirical results from southern Greenland, which highlighted the role of fjord topography, particularly lateral pinning points, in determining glacier frontal position and modulating glacier response to climatic forcing [*Warren and Glasser*, 1992] and with recent numerical modeling studies, which have highlighted the influence of variations in trough width on ice stream retreat [*Jamieson et al.*, 2012]. The presence of a floating tongue at AG may have further contributed to its rapid retreat, as it would be vulnerable to basal crevassing [*van der Veen*, 1998] and positive feedbacks associated with dynamic thinning, once the glacier had been dislodged from its lateral/basal pinning points [*Meier and Post*, 1987; *Schoof*, 2007; *Vieli and Nick*, 2011].

Our data suggest that width may also have influenced the rate and pattern of retreat at NW1. The glacier occupied a fairly constant position between 1992 and 2001 and retreat rates were low (24.8 m a^{-1}) (Fig. 3.7; Point I). During this period, the terminus was located in a relatively narrow section of the fjord and the northern margin was in contact with a lateral pinning point (Fig. 3.7; Point I), which together would promote

slower retreat. Retreat rates then increased substantially as the glacier front moved through a wider section of fjord between June 2001 and July 2006 (Fig. 3.7; Point II), as observed at AG. NW1 underwent the most rapid retreat of the study period between 3rd July and 9th September 2006, when the central portion of the front retreated inland of the rock islands that had previously bounded the terminus, which would have significantly reduced lateral stresses and promoted dynamic thinning and retreat [*Jamieson et al.*, 2012; *O'Neel et al.*, 2005; *Raymond*, 1996]. The central section continued to retreat rapidly and formed a large, concave bay by the end of the study period (Fig. 3.7). The influence of the islands on the frontal position of NW1 is further supported by its earlier behavior: in 1976, NW1 terminated on a rock island (Fig. 3.7; Point IV) and then retreated by 6 km by 1986, at which point the terminus reached the narrow section between the rock islands (Fig. 3.7; Point I). Although the exact timing and pattern of retreat is unknown, this suggests that the front may have retreated rapidly after losing contact with the outer island. The most recent data from NW1 show that retreat has slowed (Fig. 3.7) and the retreat pattern indicates that the terminus may have reached a basal pinning point and/or shallower section (Fig. 3.7; Point V), although bathymetric data would be needed to confirm whether this is the case.

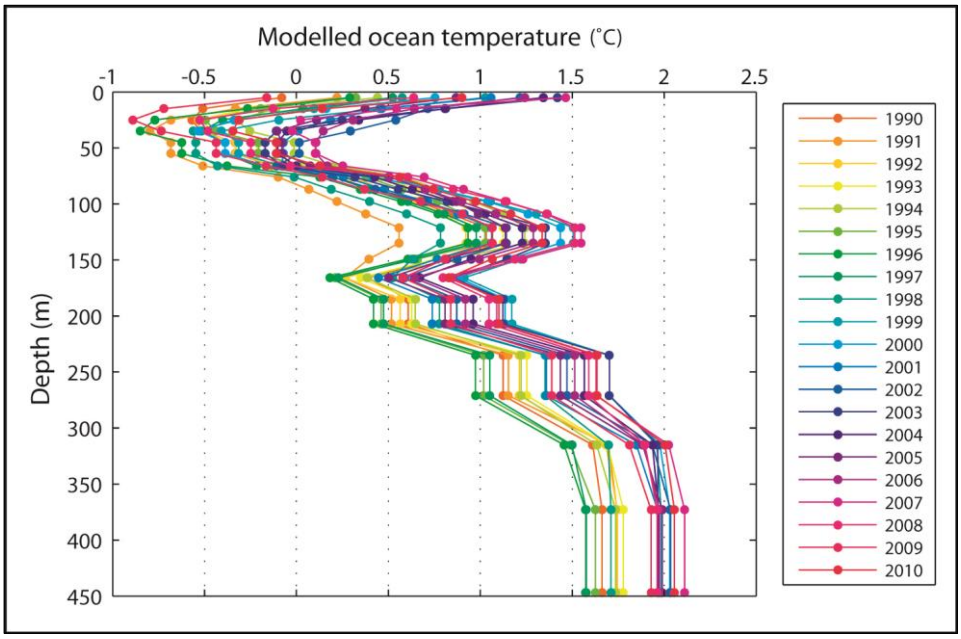

Figure 3.8. Mean annual ocean temperature profile from Hadley Centre EN3 reanalysis data. Profiles area color-coded according to year.

The termini of most of the other study glaciers were bounded laterally by rock islands, as at NW1, but they did not retreat beyond these lateral constraints during the study period (Fig. 3.1). The exception to this was IGD, which had a similar fjord configuration to AG (Fig. 3.1). However, IGD's terminus occupied a relatively narrow section of fjord for the majority of the study period (Fig. 3.6; Inset; Point I). The variation in fjord width in the along-flow direction was much less at IGD (10%) than at AG (17%), within the section over which the termini retreated (Figs. 3.5 & 3.6), and this would limit the contribution of variations in lateral stresses to retreat. On the basis of these observations, we suggest that differences in lateral topography may largely account for the high retreat rates observed at AG and NW1 and for their differing dynamic response to atmospheric and oceanic forcing. The lateral/basal topography at AG and NW1 imply that even a comparatively small additional seasonal retreat, in response to external forcing, may be sufficient to move the termini into a position where rapid retreat can occur via a series of positive feedbacks. In contrast, the other study glaciers did not retreat beyond the confines of their bounding islands and/or undergo significant changes in fjord width, thus minimizing variations in resistive stresses during retreat. Consequently, sea ice decline and/or atmospheric warming may not yet be sufficient to initiate rapid retreat on the majority of the study glacier termini.

3.4.4. Summary and future outlook

Our results suggest that the response of individual glaciers to atmospheric and oceanic forcing is substantially modulated by variations in fjord width, terminus type and, potentially, basal pinning points. Based on the observed relationships, the following factors are likely to predispose outlet glaciers to rapid retreat: the loss of contact with lateral/basal pinning points; significant widening of the fjord during retreat; and/or the presence of a floating ice tongue. Our findings are in accordance with previous results from western Greenland, which found no consistent relationship between glacier retreat and initial glacier width [*McFadden et al.*, 2011]. However, in contrast to McFadden et al [2011], who used a single measurement of glacier width prior to the onset of retreat,

our data suggest that even subtle variations in the along-flow width of the constraining fjord may be a primary controlling factor on glacier retreat rates, once retreat has been initiated [c.f. *Jamieson et al.*, 2012].

The role of fjord geometry may be particularly significant in the near-future in the study region, as data suggest that IGD and AG may be close to retreating inland of their fjords and into areas of comparatively deep basal topography (Figs. 3.5 & 3.6). This is supported by the most recent data from AG, which show that its northern margin retreated by 2.3 km between July 2010 and September 2011 (Fig. 3.5; Point V) but then halted at another lateral constriction, formed by a rock outcrop (Fig. 3.5; Point VI & Inset 2), where it remained until the last-available image in May 2012. This suggests that the lateral pinning point may have temporarily halted retreat and highlights the potentially strong influence of variations in fjord width on the pattern of retreat at AG. Importantly, no further lateral constrictions are visible at the northern margin of AG and the ice flow appears to diverge markedly upglacier (Fig. 3.5). Basal data suggest that the area inland of the current terminus is up to 700 m deep (Fig. 3.5). This deeper area may initially facilitate rapid retreat via buoyancy driven feedbacks [e.g. *Joughin et al.*, 2008b; *Vieli and Nick*, 2011], once the terminus ice has thinned sufficiently to remove it from its current lateral pinning point. However, the basal topography becomes shallower approximately 6 km inland and may therefore eventually promote slower retreat.

Following decades of minimal variation in terminus position, IGD began to retreat in winter 2008 and may also be close to moving inland of the lateral margins of its fjord (Fig. 3.6; Inset; Point II). Bed depths inland of the present terminus reach up to 600 m and the combined effects of the terminus moving beyond the constraints of its fjord and into an area of deep topography could facilitate rapid retreat. However, two channels of up to 800 m depth begin approximately 7 km inland of the front (Fig. 3.6). Dependant on their detailed geometry, these channels could promote lower retreat rates, once the terminus retreats into them, by constraining flow and increasing resistive stresses. The

other glaciers within the study region currently terminate on a series of rock outcrops (Fig. 3.1). Based on observations from NW1, these glaciers may also begin to retreat rapidly if future atmospheric and oceanic forcing is sufficient to force the termini beyond the constraining influence of these islands.

3.5. Conclusions

Our results suggest that marine-terminating outlet glacier behavior is influenced by a combination of atmospheric, oceanic and glacier-specific controls within the study region. At seasonal timescales, sea ice and air temperatures appear to be the primary external controls on frontal position. The response to seasonal forcing varies between study glaciers and can evolve during retreat, with AG showing a greater sensitivity to sea ice when its floating tongue existed. All of the study glaciers underwent net retreat between 1993 and 2010, coincident with marked sea ice decline and almost 8˚C of atmospheric warming. Retreat at AG reached rates of almost 2.5 km a^{-1} between 2001 and 2005, prior to which the terminus had occupied a very similar position since at least 1976. The magnitude, rate and pattern of retreat varied substantially between individual glaciers, with retreat rates at AG and NW1 far exceeding the regional average. This suggests that glacier-specific factors play an important role in determining outlet glacier response to external forcing and we identify variations in fjord width and terminus type as key factors. Fjord geometry may be a key control on the near-future evolution of AG and IGD, as both glaciers are close to retreating beyond the confining influence of their fjord margins and the inland basal topography may significantly influence their future pattern of retreat. We highlight the need for very high temporal resolution data and *in situ* measurements, particularly of fjord water conditions, in order to fully understand the relative importance of each forcing factor and the role of feedbacks such as plume-enhanced submarine melting. Furthermore, high-resolution information on subglacial topography and fjord bathymetry is needed to further assess the influence of fjord geometry on outlet glacier behavior. Our results underscore the importance of glacier-specific factors in determining the response of

marine-terminating outlet glaciers to atmospheric and oceanic forcing and we highlight the need to consider these factors when interpreting outlet glacier retreat rates and forecasting future behavior.

Acknowledgments

This work was supported by a Durham Doctoral Studentship, granted to J.R. Carr. Envisat and ERS Image Mode Precision scenes were provided by the European Space Agency (ESA). We acknowledge the use of data and/or data products from CReSIS generated with support from NSF grant ANT-0424589 and NASA grant NNX10AT68G. We thank T. Benham, A. Luckman, D. Small and I. Joughin for their helpful comments, and three anonymous reviewers.

3.6. References

Ahn, Y., and J. E. Box (2010), Glacier velocities from time-lapse photos: technique development and first results from the Extreme Ice Survey (EIS) in Greenland, *Journal of Glaciology*, *198*, 723-734.

Alley, R. B. (1991), Sedimentary processes may cause fluctuations of tidewater glaciers, *Annals of Glaciology*, *15*, 119-124.

Amundson, J. M., M. Fahnestock, M. Truffer, J. Brown, M. P. Lüthi, and R. J. Motyka (2010), Ice mélange dynamics and implications for terminus stability, Jakobshavn Isbræ, Greenland, *Journal of Geophysical Research*, *115*, F01005, doi:10.1029/2009JF001405.

Andersen, M. L., et al. (2010), Spatial and temporal melt variability at Helheim Glacier, East Greenland, and its effect on ice dynamics, *Journal of Geophysical Research*, *115*, F04041.

Benn, D. I., C. R. Warren, and R. H. Mottram (2007), Calving processes and the dynamics of calving glaciers, *Earth Science Reviews*, *82*, 143-179.

Bevan, S. L., A. J. Luckman, and T. Murray (2012), Glacier dynamics over the last quarter of a century at Helheim, Kangerdlugssuaq and 14 other major Greenland outlet glaciers, *The Cryosphere*, *6*, 923–937.

Cappelen, J. (2011), Technical Report 11-05: DMI Monthly Climate Data Collection 1768-2010, Denmark, The Faroe Islands and Greenland *Rep.*, Danish Meteorological Institute, Copenhagen.

Carr, J. R., C. R. Stokes, and A. Vieli (2013), Recent progress in understanding marine-terminating Arctic outlet glacier response to climatic and oceanic forcing: Twenty years of rapid change, *Progress in Physical Geography*, *37*(4), 435 - 466.

Carstensen, L. S., and B. V. Jørgensen (2011), Weather and climate data from Greenland 1958-2010., *Techincal Report*, *11-10*.

Christoffersen, P., R. Mugford, K. J. Heywood, I. Joughin, J. Dowdeswell, J. P. M. Syvitski, A. Luckman, and T. J. Benham (2011), Warming of waters in an East Greenland fjord prior to glacier retreat: mechanisms and connection to large-scale atmospheric conditions, *The Cryosphere*, *5*, 701-714.

Echelmeyer, K. A., W. D. Harrison, C. Larsen, and J. E. Mitchell (1994), The role of the margins in the dynamics of an active ice stream, *Journal of Glaciology*, *40*(136), 527-538.

Holland, D. M., R. H. D. Y. Thomas, B., M. H. Ribergaard, and B. Lyberth (2008), Acceleration of Jakobshavn Isbræ triggered by warm subsurface ocean waters, *Nature Geoscience*, *1*, 1-6.

Howat, I. M., Y. Ahn, I. Joughin, M. van den Broeke, J. Lenaerts, and B. Smith (2011), Mass balance of Greenland's three largest outlet glaciers, 2000–2010, *Geophysical Research Letters*, *38*, L12501.

Howat, I. M., J. E. Box, Y. Ahn, A. Herrington, and E. M. McFadden (2010), Seasonal variability in the dynamics of marine-terminating outlet glaciers in Greenland, *Journal of Glaciology*, *56*(198), 601-613.

Howat, I. M., and A. Eddy (2011), Multi-decadal retreat of Greenland's marine-terminating glaciers, *Journal of Glaciology*, *57*(203), 389-396.

Howat, I. M., I. Joughin, M. Fahnestock, B. E. Smith, and T. Scambos (2008), Synchronous retreat and acceleration of southeast Greenland outlet glaciers 2000-2006; Ice dynamics and coupling to climate, *Journal of Glaciology*, *54*(187), 1-14.

Ingleby, B., and M. Huddleston (2007), Quality control of ocean temperature and salinity profiles - historical and real-time data., *Journal of Marine Systems*, *65*, 158-175, doi:10.1016/j.jmarsys.2005.11.019.

IPCC (2007), *The Physical Science Basis. Contribution of Working Group I to the Fourth Assessment Report of the Intergovernmental Panel on Climate Change*, Cambridge Univ. Press, Cambridge and New York.

Jacob, T., J. Wahr, W. T. Pfeffer, and S. Swenson (2012), Recent contributions of glaciers and ice caps to sea level rise, *Nature*, *428*, 514–518.

Jamieson, S. S. R., A. Vieli, S. J. Livingstone, C. Ó Cofaigh, C. R. Stokes, C.-D. Hillenbrand, and J. Dowdeswell (2012), Ice stream stability on a reverse bed slope, *Nature Geoscience*, *5*, 799-802.

Johnson, H. L., A. Münchow, K. K. Falkner, and H. Melling (2011), Ocean circulation and properties in Petermann Fjord, Greenland, *Journal of Geophysical Research*, *116*, C01003.

Joughin, I., I. M. Howat, R. B. Alley, G. Ekström, M. Fahnestock, T. Moon, NettlesM., M. Truffer, and V. C. Tsai (2008a), Ice-front variation and tidewater behaviour on Helheim and Kangerdlugssuaq Glaciers, Greenland, *Journal of Geophysical Research*, *113*, F01004, doi:10.1029/2007JF000837.

Joughin, I., I. M. Howat, M. Fahnestock, B. Smith, W. Krabill, R. B. Alley, H. Stern, and M. Truffer. (2008b), Continued evolution of Jakobshavn Isbrae following its rapid speedup, *Journal of Geophysical Research*, *113*, F04006, doi:10.1029/2008JF001023.

Joughin, I., B. Smith, I. M. Howat, T. Scambos, and T. Moon (2010a), Greenland flow variability from ice-sheet-wide velocity mapping, *Journal of Glaciology*, *56*(197), 415-430.

Joughin, I., B. E. Smith, I. Howat, and T. Scambos (2010b), MEaSUREs Greenland Ice Sheet Velocity Map from InSAR Data, *Boulder, Colorado, USA: National Snow and Ice Data Center. Digital media.*

Joughin, I., B. E. Smith, I. M. Howat, D. Floricioiu, R. B. Alley, M. Truffer, and M. Fahnestock (2012), Seasonal to decadal scale variations in the surface velocity of Jakobshavn Isbrae, Greenland: Observation and model-based analysis, *Journal of Geophysical Research*, *117*, F02030, doi:10.1029/2011JF002110.

Khan, S. A., J. Wahr, M. Bevis, I. Velicogna, and E. Kendrick (2010), Spread of ice mass loss into northwest Greenland observed by GRACE and GPS, *Geophysical Research Letters*, *37*, L06501.

Kjær, K. H., et al. (2012), Aerial photographs reveal late–20th-Century dynamic ice loss in northwestern Greenland, *Science*, *337*, 596-573.

Mayer, C., N. Reeh, F. Jung-Rothenhäusler, P. Huybrechts, and H. Orter (2000), The subglacial cavity and implied dynamics under Nioghalvfjerdsfjorden Glacier, NE-Greenland, *Geophysical Research Letters*, *27*(15), 2289-2292.

McFadden, E. M., I. M. Howat, I. Joughin, B. Smith, and Y. Ahn (2011), Changes in the dynamics of marine terminating outlet glaciers in west Greenland (2000–2009), *Journal of Geophysical Research*, *116*, F02022.

Meier, M. F., and A. Post (1987), Fast tidewater glaciers, *Journal of Geophysical Research*, *92*, 9051–9058.

Moon, T., and I. Joughin (2008), Changes in ice-front position on Greenland's outlet glaciers from 1992 to 2007, *Journal of Geophysical Research*, *113*, F02022, doi:10.1029/2007JF000927.

Moon, T., I. Joughin, B. E. Smith, and I. M. Howat (2012), 21st-Century evolution of Greenland outlet glacier velocities, *Science*, *336*(6081), 576-578.

Motyka, R. J., L. Hunter, K. Echelmeyer, and C. Connor (2003), Submarine melting at the terminus of a temperate tidewater glacier, LeConte Glacier, Alaska, U.S.A., *Annals of Glaciology*, *36*, 57-65.

Motyka, R. J., M. Truffer, M. Fahnestock, J. Mortensen, S. Rysgaar, and I. M. Howat (2011), Submarine melting of the 1985 Jakobshavn Isbræ floating tongue and the triggering of the current retreat, *Journal of Geophysical Research*, *166*, F01007.

Murray, T., et al. (2010), Ocean regulation hypothesis for glacier dynamics in southeast Greenland and implications for ice sheet mass changes, *Journal of Geophysical Research*, *115*, F03026, doi:10.1029/2009JF001522.

Nick, F. M., A. Vieli, I. M. Howat, and I. Joughin (2009), Large-scale changes in Greenland outlet glacier dynamics triggered at the terminus, *Nature Geoscience*, *2*, 110-114.

O'Neel, S., W. T. Pfeffer, R. Krimmel, and M. Meier (2005), Evolving force balance at Columbia Glacier, Alaska, during its rapid retreat, *Journal of Geophysical Research*, *110*, F03012.

Partington, K., T. Flynn, D. Lamb, C. Bertoia, and K. Dedrick. (2003), Late twentieth century Northern Hemisphere sea-ice record from U.S. National Ice Center ice charts, *Journal of Geophysical Research*, *108*(C11), 3343, doi:10.1029/2002JC001623.

Pritchard, H. D., R. J. Arthern, D. G. Vaughan, and L. A. Edwards (2009), Extensive dynamic thinning on the margins of the Greenland and Antarctic ice sheets, *Nature*, *461*, 971-975.

Raymond, C. (1996), Shear margins in glaciers and ice sheets, *Journal of Glaciology*, *42*(140), 90-102.

Reynolds, R. W., T. M. Smith, C. Liu, D. B. Chelton, K. S. Casey, and M. G. Schlax (2007), Daily High-Resolution-Blended Analyses for Sea Surface Temperature, *Journal of Climate*, *20*(22), 5473-5496, doi:10.1175/2007jcli1824.1.

Rignot, E., J. E. Box, E. Burgess, and E. Hanna (2008), Mass balance of the Greenland ice sheet from 1958 to 2007, *Geophysical Research Letters*, *35*, L20502, doi:10.1029/2008GL035417.

Rignot, E., and P. Kanagaratnam (2006), Changes in the velocity structure of the Greenland Ice Sheet, *Science*, *311*(5763), 986–990.

Rignot, E., M. Koppes, and I. Velicogna (2010), Rapid submarine melting of the calving faces of West Greenland glaciers, *Nature Geoscience*, *3*, 187-191, doi:10.1038/NGEO765.

Rignot, E., I. Velicogna, M. Van den Broeke, A. Monaghan, and J. Lenaerts (2011), Acceleration of the contribution of the Greenland and Antarctic ice sheets to sea level rise, *Geophysical Research Letters*, *38*, L05503.

Sasgen, I., M. van den Broeke, J. Bamber, E. Rignot, L. S. Sørensen, B. Bert Wouters, Z. Martinech, A. Velicogna, and S. B. Simonseni (2012), Timing and origin of recent regional ice-mass loss in Greenland, *Earth and Planetary Science Letters*, *333-334*, 293–303.

Schoof, C. (2007), Ice sheet grounding line dynamics: steady states, stability, and hysteresis, *Journal of Geophysical Research*, *112*(F3), F03S28.

Small, D., B. Rosich, A. Schubert, E. Meier, and D. Nüesch (2004), Geometric validation of low and high-resolution ASAR imagery, *Proceedings of the 2004 Envisat & ERS Symposium, Salzburg, Austria, 6-10 September 2004*.

Sohn, H. G., K. C. Jezek, and C. J. van der Veen (1998), Jakobshavn Glacier, West Greenland: 30 years of Spacebourne observations, *Geophysical Research Letters*, *25*(14), 2699-2702.

Straneo, F., R. G. Curry, D. A. Sutherland, G. S. Hamltion, C. Cenedese, K. Våge, and L. A. Stearns (2011), Impact of fjord dynamics and glacial runoff on the circulation near Helheim Glacier, *Nature Geoscience*, *4*, 322-327.

Straneo, F., G. S. Hamilton, D. A. Sutherland, L. A. Stearns, F. Davidson, M. O. Hammill, G. B. Stenson, and A. R. Asvid (2010), Rapid circulation of warm subtropical waters in a major glacial fjord in East Greenland, *Nature Geoscience*, *3*, 182-186, doi:10.1038/NGEO764.

Thomas, R. H., E. Frederick, W. Krabill, S. Manizade, and C. Martin (2009), Recent changes on Greenland outlet glaciers, *Journal of Glaciology*, *55*(189), 147-162.

van den Broeke, M., J. Bamber, J. Ettema, E. Rignot, E. Schrama, W. J. van de Berg, E. van Meijgaard, I. Velicogna, and B. Wouters (2009), Partitioning Recent Greenland Mass Loss, *Science*, *326*, 984-986.

van der Veen, C. J. (1998), Fracture mechanics approach to penetration of bottom crevasses on glaciers, *Cold Regions Science and Technology*, *27*, 213- 223.

Veitch, S. A., and N. Nettles (2012), Spatial and temporal variations in Greenland glacial-earthquake activity, 1993--2010, *Journal of Geophysical Research*, *117*, F04007.

Vieli, A., M. Funk, and H. Blatter (2001), Flow dynamics of tidewater glaciers: a numerical modelling approach, *Journal of Glaciology*, *47*(159), 595-606.

Vieli, A., J. A. Jania, and K. Lezek (2002), The retreat of a tidewater glacier: observations and model calculations on Hansbreen, Spitsbergen, *Journal of Glaciology*, *48*(163), 592-600.

Vieli, A., and F. M. Nick (2011), Understanding and modelling rapid dynamic changes of tidewater outlet glaciers: issues and implications, *Surveys in Geophysics*, *32*, 437-485.

Warren, C. R., and N. F. Glasser (1992), Contrasting response of south Greenland glaciers to recent climatic change, *Arctic and Alpine Research*, *24*(2), 124-132.

Weertman, J. (1974), Stability of the junction of an ice sheet and an ice shelf, *Journal of Glaciology*, *13*(67), 3-11.

Chapter 4: Recent retreat of major outlet glaciers on Novaya Zemlya, Russian Arctic, influenced by fjord geometry and sea-ice conditions

Carr, J.R., Stokes, C.R. and Vieli, A., in press. *Journal of Glaciology*, 60 (219), 155-170

Outline: Results showed rapid retreat on marine-terminating outlet glaciers on Novaya Zemlya, Russian High Arctic (Fig. 1.1), which were an order of magnitude greater than on those observed on land-terminating glaciers. However, despite rapid retreat on marine-terminating glaciers, dynamic thinning rates showed no statistical difference between marine- and land-terminating basins, which strongly contrasted with observations from the GrIS [e.g. *Pritchard et al.*, 2009; *Thomas et al.*, 2011]. Retreat rates on marine-terminating glaciers accelerated from 2000 onwards and closely corresponded to variations in sea ice concentrations. Overall, retreat rates were higher on the Barents Sea coast than the Kara Sea, potentially due to difference in sea ice regime, but there was large variation between individual glaciers, suggesting that glacier-specific controls strongly influenced retreat rates. The paper demonstrates a statistically significant relationship between retreat rate and fjord width variation and defines the first empirical categories of this relationship.

Motivation: The motivation for selecting this study area was two-fold: i) it is rapidly losing mass, but has been little-studied and; ii) it provides an excellent natural experiment for assessing controls on outlet glacier behaviour. NVZ has undergone rapid mass loss during the past decade [*Moholdt et al.*, 2012], but little is known about the contribution of ice dynamics to this deficit or the causes of recent changes in outlet glacier behaviour. Improving our understanding of glacier dynamics is therefore crucial for accurately forecasting the potential contribution of NVZ to sea level rise. NVZ also affords an important opportunity to assess the respective influence of external forcing and fjord width variability, on glacier behaviour, as the Barents and Kara Sea coasts are subject to different climatic and oceanic regimes [*Zeeberg and Forman*, 2001] and NVZ has a broad range of fjord geometries [*Kotlyakov*, 2006].

Contribution: In this paper, I carried out the GIS and data analysis tasks (e.g. image processing, data acquisition and data processing), wrote the text, created the figures and lead the paper development. My co-authors provided editorial input and guidance on the development of the research.

Abstract

Substantial ice loss has occurred in the Russian High Arctic during the past decade, predominantly on Novaya Zemlya, yet the region has undergone relatively little study. Consequently, the factors forcing mass loss and the relative contribution of ice dynamics versus surface melt are poorly understood. Here we evaluate the influence of atmospheric/oceanic forcing and variations in fjord width on the behaviour of 38 glaciers on the northern ice cap, Novaya Zemlya. We compare retreat rates on land- versus marine-terminating outlets and on the Kara versus Barents Sea coasts. Between 1992 and 2010, 90% of the study glaciers retreated and retreat rates were an order of magnitude higher on marine-terminating outlets (52.1 m a^{-1}) than on land-terminating glaciers (4.8 m a^{-1}). We identify a post-2000 acceleration in marine-terminating glacier retreat, which corresponded closely to changes in sea ice concentrations. Retreat rates were higher on the Barents Sea coast, which we partly attribute to lower sea ice concentrations, but varied dramatically between individual glaciers. We use empirical data to categorise changes in along-flow fjord width and demonstrate a significant relationship between fjord width variability and retreat rate. Results suggest that variations in fjord width exert a major influence on glacier retreat.

4.1. Introduction

Glaciers and ice caps have dominated the recent cryospheric contribution to sea level rise and losses are forecast to continue during the 21st century [*Gardner et al.*, 2013; *IPCC*, 2007; *Meier et al.*, 2007]. In recent years, substantial mass deficits have been documented on the major Arctic archipelagos, including the Russian Arctic [*Kotlyakov et al.*, 2010; *Moholdt et al.*, 2012; *Sharov et al.*, 2009], Svalbard [*Moholdt et al.*, 2010; *Nuth et al.*, 2010], and the Canadian Arctic [*Gardner et al.*, 2012; *Gardner et al.*, 2011;

Lenaerts et al., 2013], highlighting their potential vulnerability to near-future warming. However, the mass budget of the Russian Arctic has received less scientific attention than other regions [*Bassford et al.*, 2006] despite accounting for 20% of Arctic glaciation outside of the Greenland Ice Sheet (GrIS) [*Dowdeswell et al.*, 1997] and containing an estimated 17,778 km^3 of ice [*Radić et al.*, 2013]. Recent estimates from ICESat laser altimetry and GRACE gravimetry data suggest that the Russian Arctic lost mass at a rate of between 9.1 ± 2.0 Gt a^{-1} [*Moholdt et al.*, 2012] and 11 ± 4 Gt a^{-1} for the period 2003 to 2009 [*Gardner et al.*, 2013], which equate to a sea level rise of between 0.025 mm a^{-1} and 0.033 mm a^{-1} respectively. Novaya Zemlya (NVZ) was identified as the dominant source of this mass deficit, accounting for 80% of observed losses [*Moholdt et al.*, 2012]. Moreover, the Russian Arctic has been identified as a primary source of 21st century ice volume loss using surface mass balance modelling, with the estimated contribution ranging between 20 ± 8 mm SLE and 28 ± 8 mm SLE, dependant on emission scenario [*Radić et al.*, 2013].

Evidence from the GrIS [e.g. *Enderlin and Howat*, 2013; *Howat et al.*, 2008; *Moon et al.*, 2012; *Nick et al.*, 2013; *Rignot et al.*, 2008] and other Arctic ice masses [*Burgess and Sharp*, 2008] has highlighted changes in marine-terminating outlet glacier dynamics as a key contributor to contemporary mass deficits and the response of Arctic ice masses to climate change. This dynamic response can produce rapid mass loss via accelerated ice discharge and currently accounts for approximately half of the total mass loss from GrIS, with the remainder being attributed to negative surface mass balance [*van den Broeke et al.*, 2009]. Despite its potential importance, however, the dynamic component of mass loss from NVZ, and elsewhere in the Russian Arctic, is poorly quantified [*Sharov*, 2005]. Studies suggest that marine-terminating outlet glaciers on NVZ retreated relatively rapidly (>300 m a^{-1}) during the first half of the 20th Century, consistent with Little Ice Age warming [*Zeeberg and Forman*, 2001]. However, there is substantial uncertainty over recent glacier behaviour, with some studies documenting glacier stabilisation or moderate retreat between 1964 and 1993 [*Zeeberg*

and Forman, 2001]. In contrast, others record substantial reductions in both ice volume [*Kotlyakov et al.*, 2010] and the length of ice coast [*Sharov*, 2005] between the 1950s and 2000s and a reduction in the aerial extent of certain marine-terminating outlets by up to 5 km^2 between circa 1990 and 2000 [*Kouraev et al.*, 2006]. Furthermore, potential differences in the response of land- and marine-terminating glaciers on NVZ to recent forcing have not been extensively assessed. Moholdt and others (2012) reported no significant difference in frontal thinning rates on marine- and land-terminating outlets. This is similar to results from the Canadian Arctic [*Gardner et al.*, 2011], but differs markedly from the GrIS, where thinning rates were far higher on marine-terminating outlets than their land-terminating counterparts [*Sole et al.*, 2008]. Assessment of NVZ glacier behaviour in relation to atmospheric and oceanic forcing has also been limited in comparison to other Arctic regions, although evidence suggests that reduced retreat between the 1960s and 1990s coincided with decreased winter air temperatures, increased precipitation, and elevated sea surface temperatures (SSTs) in the Barents Sea [*Zeeberg and Forman*, 2001]. Large uncertainties therefore remain over the magnitude of contemporary glacier retreat on NVZ, its contribution to mass loss and the factors driving this behaviour.

Here we investigate frontal position variations on 38 outlet glaciers, located on the northern ice cap, NVZ (Fig. 4.1). We focus specifically on the northern ice cap because it contains all of NVZ's major marine-terminating outlet glaciers and represents 95% of its total ice covered area [*Dowdeswell and Williams*, 1997; *Sharov*, 2005]. Our study glaciers comprise 10 land-terminating and 28 marine-terminating outlets, which enables us to explore the influence of terminus type on retreat rates (Figs. 4.1 & 4.2). Furthermore, we assess differences between the Barents and Kara Sea coasts (Figs. 4.1 & 4.2), which are characterised by different climatic, oceanic and topographic conditions [*Kotlyakov*, 1978; 2006; *Zeeberg and Forman*, 2001]. The three glaciers previously observed during the active surge phase [*Grant et al.*, 2009] were excluded from the assessment and represent approximately 6% of the total number of marine-

terminating outlet glaciers on the northern ice cap (n = 38). We first quantify NVZ outlet glacier retreat rates between 1992 and 2010 and assess changes in relation to terminus type and location. We then evaluate the influence of atmospheric and oceanic controls on frontal position change (the term 'oceanic' includes forcing associated with sea ice and sea surface temperatures). Sub-surface ocean temperature data are very limited for NVZ and are therefore only discussed briefly. Finally, we investigate the influence of variations in fjord width and provide a new empirical framework for assessing its influence on glacier frontal position change.

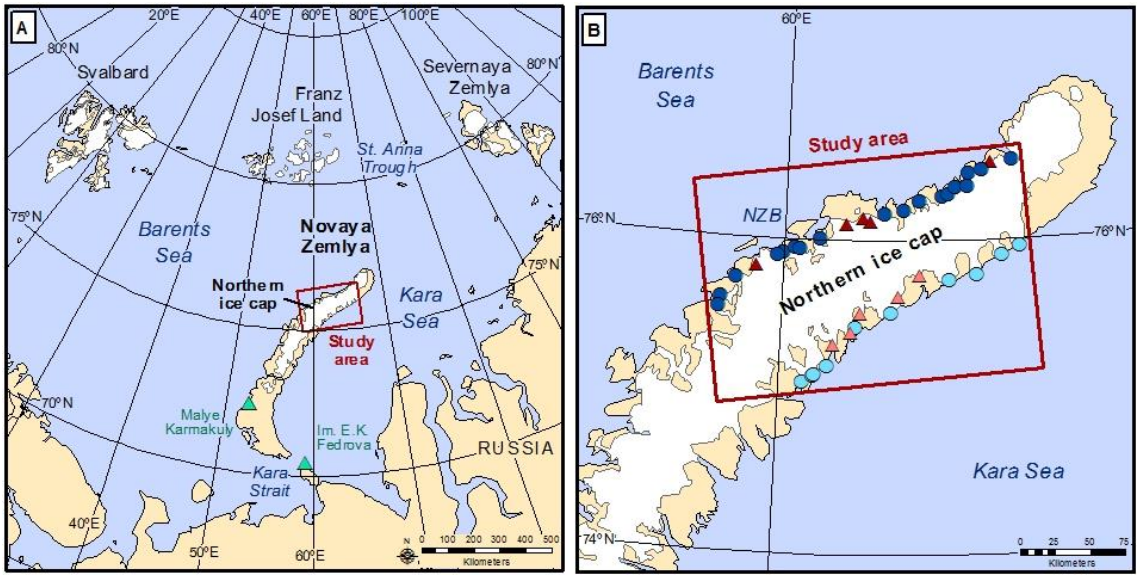

Figure 4.1. *Location map of Novaya Zemlya, showing the study area and studied glaciers. A) Location of Novaya Zemlya and the northern ice cap within the Russian High Arctic. Location of study area (red box), meteorological stations (green triangles) and water masses discussed in the text. B) Location of Novaya Zemlya Bank (NVZB) and study glaciers, symbolised according to coast and terminus type as follows: Barents Sea / marine-terminating (dark blue circles), Kara Sea / marine-terminating (light blue circles), Barents Sea / land-terminating (dark red triangles), Kara Sea / land-terminating (light red triangles).*

4.2. Methods

4.2.1. Frontal position data

Outlet glacier frontal positions were obtained primarily from Synthetic Aperture Radar (SAR) Image Mode Precision data. Imagery was supplied by the European Space

Agency (ESA), acquired as part of the ERS1, ERS2 and ENVISAT missions. Following Carr *et al.* (2014), data were processed by applying precise orbital state vectors and radiometric calibration was applied. Images were then multi-looked to reduce speckle and terrain corrected using Version 2 of the 30 m resolution Advanced Spaceborne Thermal Emission and Reflection Radiometer (ASTER) Global Digital Elevation Model (GDEM). Due to the higher geolocation accuracy of the ENVISAT data, ERS images were coregistered with corresponding ENIVSAT scenes. SAR imagery was supplemented with visible Landsat imagery, where possible, which was provided by the USGS Global Visualisation Viewer (http://glovis.usgs.gov/). For both imagery types, scenes were selected as close as possible to the end of the calendar month, to allow for comparison with monthly means of atmospheric and oceanic data. Landsat imagery was provided at a spatial resolution of 30 m and the SAR imagery was output with a cell size of 37.5 m.

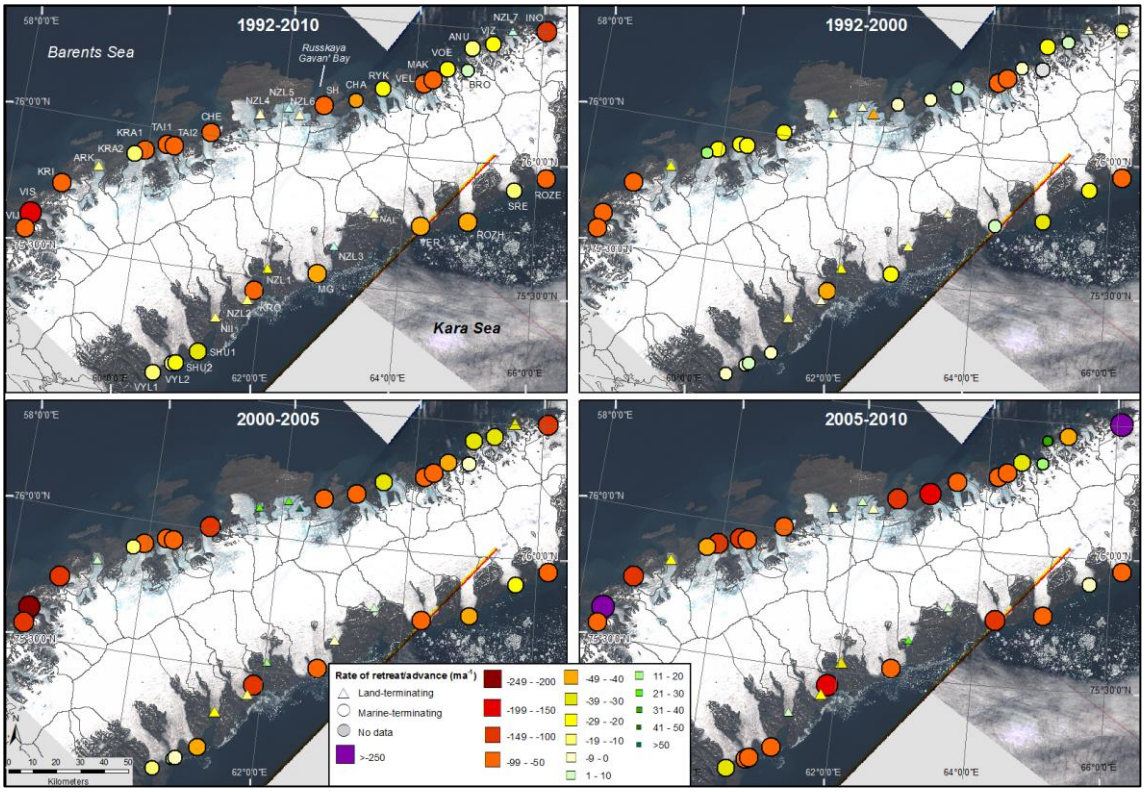

***Figure 4.2**. Outlet glacier retreat rates on the Northern Ice Cap, Novaya Zemlya for the periods A) 1992-2010, B) 1992–2000, C) 2000-2005 and D) 2005–2010. Retreat rates are symbolised according to terminus type: land-terminating (triangles) and marine-terminating (circles). The*

magnitude of frontal position change is symbolised according to colour (purple through to yellow = retreat; greens = advance) and symbol size (larger symbols = higher retreat rate). Note that the colour and size scales are non-linear (see legend). Outlet glacier catchments are shown in dark grey: data were provided by G. Moholdt (2012) and are part of the Randolph Glacier Inventory (Arendt and others, 2012). Glacier abbreviations were derived from the World Glacier Inventory, where names were available, and split termini were numbered sequentially (1 = main terminus, 2 = secondary terminus). Unnamed, land-terminating glaciers were given the prefix 'NZL' and numbered sequentially. Abbreviations of glacier names are as follows (from south to north): ***Barents Sea coast****: VIS: Vil'kitskogo Sev.; VIJ: Vil'kitskogo Juz; KRI: Krivosheina; ARK: Arkhangelskolgu; KRA2: Kraynij 2; KRA1: Kraynij 1; TAI1: Taisija 1; TAI2: Taisija 1; CHE: Chernysheva; SH: Shokalskogo; CHA: Chaveva; RYK: Rykachova; VEL: Vel'Kena; MAK: Maka; VOE: Voejkova; BRO: Brounova; ANU: Anuchina; VIZ: Vize; and INO: Inostrantseva.* ***Kara Sea coast:*** *VYL1: Vylki 1; VYL2: Vylki 2; SHU2: Shury 2 ; SHU1: Shury 1; NII; Niiga; KRO:Kropotkina; MG: Moshnyj; NAL: Nalli; NII: Niiga; VER: Vershinskogo; ROZH: Rozhdestvenskogo; SRE: Srednij; and ROZE: Roze. (A): Location of study area and meteorological stations*

Frontal position variations were measured using a previously employed method, whereby the glacier terminus was repeatedly digitised within a fixed reference box [e.g. *Carr et al.*, 2013b; *Howat et al.*, 2010; *McFadden et al.*, 2011; *Moon and Joughin*, 2008]. The box was aligned approximately parallel to the ice flow direction at the glacier terminus and extended from an arbitrary upstream reference line. The terminus was then digitised from successive images and the change in area was divided by the width to calculate the change in frontal position. Retreat rates were calculated relative to the frontal position between 24th June and 8th July 1992, with the exact date depending on data availability. Glaciers for which frontal positions were available for multiple images during this time period showed no discernible change. We first calculated total retreat rates for the study period (1992 – 2010). We then divided the period into three approximately equal portions, within the constraints of data availability, in order to investigate changes in retreat rates over time. Retreat rates were therefore calculated for the following time periods: 1992–2000, 2000–2005 and 2005-2010.

Frontal position data were obtained at a monthly to annual resolution, as image availability varied between glaciers.

The mean error in marine-terminating outlet glacier frontal position was evaluated by repeatedly digitising 16 sections of rock coastline from a sub-sample of five ERS, five ENVISAT and five Landsat images, where there should be no discernible change in coastline position between scenes [*Carr et al.*, 2013b]. The resultant total mean error in frontal position was 25.3 m for marine outlets, which can be primarily attributed to manual digitising errors and accounts for errors in image geolocation and coregistration. Frontal positions for land-terminating outlets are subject to an additional error source, which results from the comparative difficulty of identifying land-based termini from radar imagery, as the land/ice boundary is less distinct than the ocean/ice interface. Consequently, we assessed this additional error source by repeatedly digitising the same termini from the same image, for a sub-sample of five ERS and five ENVISAT images. The resultant additional error was 67.8 m and the total error for land-terminating outlets was 72.4 m.

4.2.2. Atmospheric and oceanic data

Atmospheric and oceanic data were obtained from a variety of sources and used to calculate seasonal and annual mean values for individual glaciers and for each coast. Surface air temperature data were obtained from Malye Karmaku (52° 43' 34 "E, 72° 20' 50"N) and Im.E.K. Fedrova (59° 3' 13"E, 70° 27' 8"N) meteorological stations (Fig. 4.1). Data were provided at a monthly temporal resolution by the Hydrometeorological Information, World Data Center Baseline Climatological Data Sets (http://meteo.ru/english/climate/cl_data.php). Meteorological station data are sparse on NVZ and Malye Karmaku and Im E. K Fedrova are the only stations with sufficient data to assess interannual air temperature trends during the study period. However, these stations are located approximately 400 and 525 km from the study glaciers, respectively, and we therefore also used monthly air temperature data products from

NCEP/NCAR Reanalysis 1 [*Kalnay et al.*, 1996] and ERA-Interim reanalysis data [*Dee et al.*, 2011].

NCEP/NCAR reanalysis data have a spatial resolution of 2.5° (~230 x 280 km at 76 °N) and were provided by the NOAA/OAR/ESRL PSD, Boulder, Colorado, USA (http://www.esrl.noaa.gov/psd/data/gridded/data.ncep.reanalysis.html). ERA-Interim data were produced by the European Centre for Medium-Range Weather Forecasts (ECWMF) and have a spatial resolution of 0.75° (~70 x 80 km at 76 °N). In both cases, we used air temperature data from the 700 mb geopotential height, as opposed to 2 m height, as these values correlate better with ground station data elsewhere in the Arctic (A. Gardener, pers. comm., 2013) and limit the influence of SSTs on surface temperatures [*Moholdt et al.*, 2012]. Air temperature values were extracted from all grid squares containing the study glaciers and mean annual and mean summer (Jun-Aug) values were calculated. The pattern of air temperature variation was very similar between the two data products, which were strongly correlated ($r = 0.90$, $p < 0.01$), and differences in absolute values most likely result from their differing spatial resolution. Due to the location of meteorological stations and the spatial resolution of the reanalysis data, differences in air temperatures between the Barents Sea and Kara Sea coasts could not be assessed.

Sea ice data were obtained from the National/Naval Ice Centre charts http://www.natice.noaa.gov/), which are compiled from a range of data sources and have a spatial resolution of up to 50 m. Data were sampled at each glacier terminus, within a polygon extending 50 m perpendicular to the terminus and along its entire width. Mean seasonal values were calculated for each coast by averaging data from all study glaciers on that coast. The standard deviation in mean monthly sea ice concentrations was 0.67% on the Barents Sea coast and 2.34 % on the Kara Sea coast. Coastal averages were also used to calculate the number of ice-free months per year.

SST (sea surface temperature) data were obtained from Version 2 of the Reynolds SST analysis dataset [*Reynolds et al.*, 2007]. The SST products have been developed using optimum interpolation (OI) of satellite, ship and buoy data, with correction for biases between *in-situ* and satellite data. We use the monthly resolution product, which has a spatial resolution of 0.25° (~23 x 28 km at 76 °N) [*Reynolds et al.*, 2007]. SST values were extracted from the grid squares closest to the study glacier termini, to ensure that data were as representative as possible of conditions at the calving front. The data are used to investigate surface ocean temperatures and are not necessarily representative of deeper ocean conditions. The sea ice field within the dataset was used to identify months with minimal sea ice concentrations, as significant sea ice coverage would result in incorrect SST values. Mean values were therefore calculated for Jul-Sep, as these months had minimal sea ice concentrations on both coasts for all years.

4.2.3. Glacier width, fjord geometry , catchment size and bathymetry

Fjord width was measured perpendicular to the glacier flowline: lines were drawn perpendicular to the flowline, at intervals of 100 m from the upstream reference line, and width was measured where the lines intersected with the fjord walls at sea level, as determined from satellite imagery. Fjord width variability was quantified by digitising both fjord walls at sea level from the most recent satellite image and calculating the length of each fjord wall between the least and most extensive frontal positions. These lengths were divided by the straight-line distance between their respective start and end points to give the width variation for each wall and these values were then used to calculate the mean fjord width variability. Consequently, a fjord width variability value of 1 would indicate a fjord with straight walls, whilst higher values indicate a fjord with greater variability in width. Width variability was only calculated for glaciers with continuous fjord walls and not for those which retreated across sections of open water (e.g. between two islands). Qualitative categories of along-flow variation in fjord width during retreat were defined using satellite imagery and frontal position data from all of

the study glacier fjords. We identified eight different categories of fjord shape on NVZ, which are shown in the top panel of Table 4.1. The penultimate category gives the percentage of the glacier front which terminates on land. The final category identifies glaciers which appear to have bathymetric pinning points, either in the form of rock islands visible at the terminus or a pattern of retreat which suggests that bathymetric highs are present. This initial assessment has been carried out on the basis of visible satellite imagery and is not extensively discussed, due to the lack of detailed bathymetric data.

Catchments were provided by G. Moholdt and form part of the global Randolph Glacier inventory project [*Arendt et al.*, 2012]. Catchments were manually digitised from satellite imagery obtained between 2000 and 2010 during the summer. SPIRIT SPOT5 scenes [*Korona et al.*, 2009] were the primary data source for Novaya Zemlya and were supplemented with Landsat data. We verified the catchment data against Landsat and radar imagery and catchments containing multiple termini (e.g. KRA1 & KRA 2) were not included when testing for a statistical relationship between catchment size and retreat rate. Regional bathymetry was assessed using 1:200,000 scale topographic maps dating from 1974 and provided by www.topmap.narod.ru. Maps were georeferenced for comparison with other data sources.

.

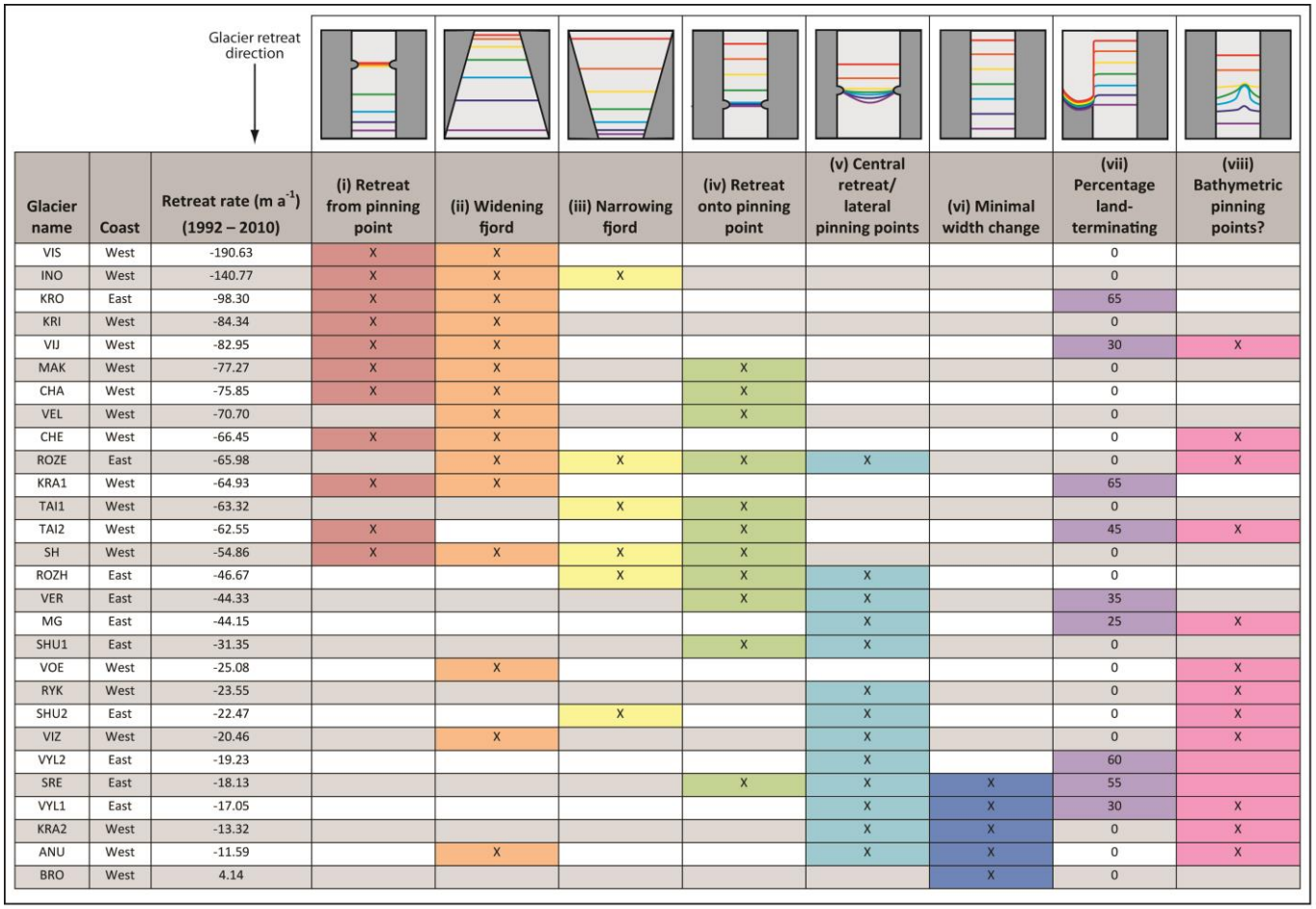

Glacier name	Coast	Retreat rate (m a^{-1}) (1992 – 2010)	(i) Retreat from pinning point	(ii) Widening fjord	(iii) Narrowing fjord	(iv) Retreat onto pinning point	(v) Central retreat/ lateral pinning points	(vi) Minimal width change	(vii) Percentage land-terminating	(viii) Bathymetric pinning points?
VIS	West	-190.63	X	X					0	
INO	West	-140.77	X	X	X				0	
KRO	East	-98.30	X	X					65	
KRI	West	-84.34	X	X					0	
VIJ	West	-82.95	X	X					30	X
MAK	West	-77.27	X	X		X			0	
CHA	West	-75.85	X	X		X			0	
VEL	West	-70.70		X		X			0	
CHE	West	-66.45	X	X					0	X
ROZE	East	-65.98		X	X	X	X		0	X
KRA1	West	-64.93	X	X					65	
TAI1	West	-63.32			X	X			0	
TAI2	West	-62.55	X			X			45	X
SH	West	-54.86	X	X	X	X			0	
ROZH	East	-46.67			X	X	X		0	
VER	East	-44.33				X	X		35	
MG	East	-44.15					X		25	X
SHU1	East	-31.35				X	X		0	
VOE	West	-25.08		X					0	X
RYK	West	-23.55					X		0	X
SHU2	East	-22.47			X		X		0	X
VIZ	West	-20.46		X			X		0	X
VYL2	East	-19.23					X		60	
SRE	East	-18.13				X	X	X	55	
VYL1	East	-17.05					X	X	30	X
KRA2	West	-13.32					X	X	0	X
ANU	West	-11.59		X			X	X	0	X
BRO	West	4.14						X	0	

Table 4.1. Categorisation of fjord width change in relation to total glacier retreat rate (1992-2010). Top row shows idealised cartoons of frontal position change in relation to changes in fjord width during retreat, going from the oldest measurement (red) to the most recent (purple). For each glacier, the types of width change observed during retreat are marked with an 'x'. The percentage of the glacier which terminates on land is given in the penultimate column. Frontal retreat indicative of bathymetric pinning points is recorded in the final column. The table is ordered according to glacier retreat rate (1992-2010) from highest to lowest (column 3).

4.2.4. Statistical analysis

Regression analysis was used to assess whether there was a significant difference between mean retreat rates on marine- and land-terminating outlets and between the Kara and Barents Sea coasts for the period 1992-2010. The data were divided into four groups: (i) land-Kara, (ii) marine-Kara, (iii) land-Barents and (iv) marine-Barents. For each group, we plotted relative frontal position against time (Fig. 4.3) and fitted a series of curves of varying complexity to each group of data: quadratic, fractional polynomial, cubic spline and lowess smoothing. This was done to assess whether the choice of curve resulted in a significant change in the goodness of fit of the curve to the data. The goodness of fit varied little with the choice of curve and a quadratic curve was therefore used. To further assess the goodness of fit, the residuals for each group were plotted and no pattern was apparent, suggesting that the quadratic functions adequately describe the curve of the data.

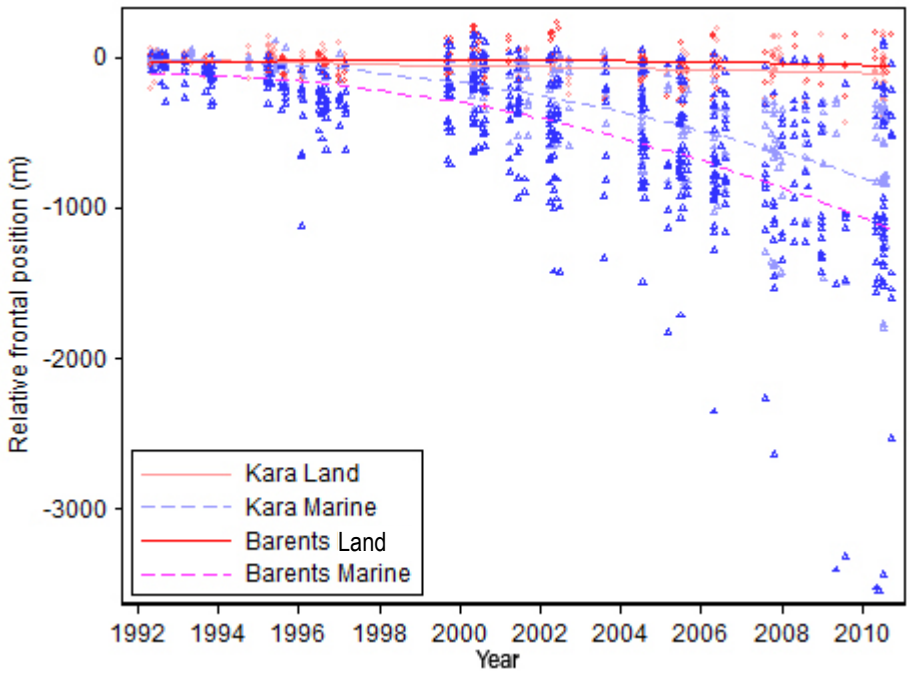

Figure 4.3. *Regression model for relative frontal position against time. Quadratic curves and individual data points are shown for each group. Data points are colour-coded as follows: Barents/marine-terminating (dark blue triangle); Kara/marine-terminating (light blue triangle); Barents/land-terminating (dark red triangle) and; Kara/land-terminating (light red triangle).The overall R2 value for the regression model was 0.51.*

In the first regression model, we regressed frontal position against time for each of the four groups using a quadratic function (Fig. 4.3). The overall R^2 value for the model was 0.51 and the RMSE 318 m. These values apply to the model as a whole and include all four curves: the R^2 value is a measure of how well the four curves together describe their respective groups of data and the RMSE value describes how far, on average, a given point would lie from its curve. Output from the model, specifically the t and p> |t| values, were used to compare the curve for land-Kara with the curves for the other three groups for each component of the quadratic equation (Table 4.2). The quadratic equation can be written in the form:

$$Y = b_0 + b_1 X + b_2 x^2$$

Following this, the first set of t and p> |t| values refer to B_0 (i.e. the intercept), the second set to B_1 (i.e. the slope) and the third to B_2 (i.e. the curvature). The t value is calculated by dividing the coefficient by the standard error and tests whether the coefficient is significantly different from zero, given the variability in the data. The value p> |t| tests the probability of getting a value that is at least as extreme as the observed value if the null hypothesis is true (i.e. the coefficient value is zero). We use a p>|t| value of 0.05 (i.e. a 95% confidence interval), meaning that a given coefficient is significantly different from zero when the p> |t| value is < 0.05. An additional regression model was then used to compare marine-Barents with marine-Kara data, in order to assess whether there was a significant difference in marine-terminating outlet glacier retreat rates between the two coasts (Table 4.3).

	Group	Coefficient	Standard Error	t	P>|t|
Intercept(B_o)		-51.69	33.39	-1.55	0.12
Date(B_1)		-0.01	0.01	-1.28	0.20
Date^2(B_2)		-2.62E-08	5.52E-06	0.00	0.99
Group (B_o)	Land-Barents	33.00	48.04	0.69	0.49
	Marine-Barents	-246.35	39.12	**-6.3**	**0.00**
	Marine-Kara	-116.36	45.63	**-2.55**	**0.01**
Group,	Land-Barents	0.013	0.02	0.78	0.43

Date(B_1)	Marine-Barents	-0.12	0.01	**-8.59**	**0.00**
	Marine-Kara	-0.09	0.02	**-6.11**	**0.00**
Group, Date^2 (B_2)	Land-Barents	-2.10E-06	8.47E-06	-0.25	0.81
	Marine-Barents	-2.2E-05	6.60E-06	**-3.34**	**0.00**
	Marine-Kara	-1.8E-05	7.35E-06	**-2.46**	**0.01**

Table 4.2. *Regression model of glacier retreat over time using quadratic curves and grouping data according to coast and terminus type. The first three rows show the model output for the group Kara-Land for each component of the quadratic equation. The subsequent outputs compare the curves for each data group with Kara-land for each component of the regression model (B_o, B_1 and B_2). The 'coefficient' gives the value for predicting the dependant variable from the independent variable and 'standard error' provides the standard errors associated with the coefficients. 't' tests whether the coefficient is significantly different from zero and is calculated by (coefficient / standard error). p> |t| gives two-tailed p-values which test the probability of getting a value as great or greater than the observed value if the null hypothesis is true (i.e. the coefficient value is zero). A p>|t| value of 0.05 was used to identify results that were statistically significant, which are in bold.*

	Group	Coefficient	Standard Error	t	P>|t|
Intercept(B_o)		-168.05	37.93	-4.43	0.00
Date(B_1)		-0.11	0.01	-8.16	0.00
Date^2(B_2)		-0.00	5.92E-06	-3.06	0.002
Group (B_o)	Marine-Barents	-129.00	45.36	**-2.87**	**0.004**
Group, Date(B_1)	Marine-Barents	-0.02	0.02	-1.44	0.15
Group, Date^2 (B_2)	Marine-Barents	-3.94E-06	7.38E-06	-0.53	0.593

Table 4.3. *As in Table 3, but including only the groups Kara-marine and Barents-marine in the regression model.*

4.3. Results

4.3.1. Frontal position

Between 1992 and 2010, 90% of the study glaciers underwent net retreat (Fig. 4.2). During this period, retreat rates were an order of magnitude greater on marine-terminating outlets (51.2 m a^{-1}) than on their land-terminating counterparts (4.8 m a^{-1})

(Figs. 4.3 & 4.4). Retreat rates on land-terminating outlets were therefore comparable to error values: the mean frontal position error was 72.4 m, which equates to an error in retreat rate of 4.0 m a^{-1} for the period 1992 to 2010. Our results also show that mean retreat rates for marine- terminating outlets, were significantly higher on the Barents Sea coast (61.7 m a^{-1}) than on the Kara Sea (40.8 m a^{-1}) during the study period (Figs 4.2 & 4.3). Although the pattern of retreat was similar for glaciers located on the same coast, the magnitude and rate of retreat varied markedly between individual glaciers (Figs 4.2 & 4.3). Indeed, neighbouring glaciers demonstrated very different retreat rates. This was most marked on VIS and VIJ, where retreat rates for the period 2005-2010 averaged 343.9 m a^{-1} on VIS, compared to 84.6 m a^{-1} on the neighbouring VIJ (Fig. 4.2).

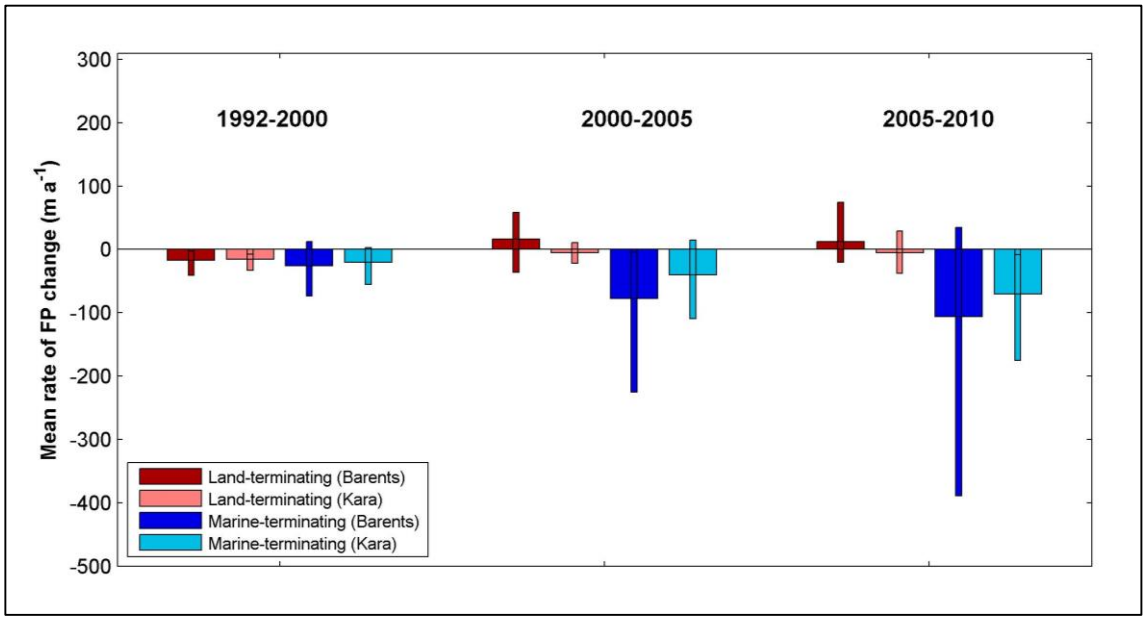

Figure 4.4. *Mean retreat rates for study glaciers on the Northern Ice Cap, Novaya Zemlya. Retreat rates are calculated for three time periods: 1992-2000, 2000-2005 and 2005-2010. Retreat rates are calculated separately for marine- and land-terminating glaciers and for glaciers located on the Kara and Barents Sea coasts of Novaya Zemlya. Thick bars show mean rate of frontal position change for each category and thin bars show the range (min-max) of values.*

Seasonal frontal position variations on marine-terminating outlets were of the order of 100 m and were only distinguishable where high temporal resolution data were

available (Fig. 4.5A). Seasonal variations were comparable to interannual retreat rates on certain study glaciers, but were significantly less on rapidly retreating outlets such as VIS. Intrannual changes in the frontal position on land-terminating outlets were indistinguishable from the errors in frontal position.

In addition to spatial variations, the temporal pattern of retreat also differed according to terminus type and coast. Comparison of retreat rates for three time periods (1992-2000, 2000-2005 and 2005-2010) showed little change on land-terminating glaciers, whereas retreat rates on marine-terminating glaciers increased substantially between each interval (Fig. 4.4). For the period 1992-2000, the difference in retreat rates between the four groups was small (Fig. 4.4). Subsequently, retreat rates increased substantially on marine-terminating outlets and this was particularly marked on the Barents Sea coast, where retreat rates for the period 2000-2005 were three times greater than those for 1992-2000 (Fig. 4.4). Mean retreat rates then further increased by approximately 30 m a^{-1} on both coasts between 2000-2005 and 2005-2010, to reach values of 106.5 m a^{-1} and 70.2 m a^{-1} on the Barents and Kara Sea coasts, respectively (Fig. 4.4). In addition to the increase in mean values on marine-terminating glaciers, the range of retreat rates also increased markedly between each time step. This was particularly notable on the Barents Sea coast, where the range underwent a five-fold increase from 86 m a^{-1} in 1992-2000 to 424 m a^{-1} in 2005-2010. On the Kara Sea coast, the range increased by almost a factor of three, from 57.8 m a^{-1} in 1992-2000 to 166.7 m a^{-1} in 2005-2010 (Fig. 4.4).

Regression analysis was used to further assess differences in retreat rates according to terminus type and coast. The first regression model was used to compare the curve for the group Land-Kara with the three other groups for each component of the regression equation (B_0, B_1 and B_2) (Fig. 4.3 and Table 4.2). Results demonstrated no significant difference between the curves for the two land groups (Fig. 4.3 and Table 4.2), In contrast, the curves for the two groups of marine-terminating glaciers (marine-Barents and marine-Kara), were statistically different from the curve for Land-Kara for

all components of the regression equation (Fig. 4.3 and Table 4.2). Taken together this indicates that: i) retreat rates on land-terminating glaciers on the Barents and Kara Sea coasts were not significantly different from each other and; ii) retreat rates on marine-terminating glaciers on both the Barents and Kara Sea coasts were statistically different from retreat rates on land-terminating glaciers on both coasts.

The first regression model demonstrated that there was no significant difference between land-terminating glaciers located on different coasts (Table 4.2). We therefore used a second model to assess the coastal difference in retreat rates for marine terminating outlets only (Table 4.3). Results show a significant difference in terms of the intercept (B_0), but not in terms of the slope (B_1) or the curvature (B_2) (Table 4.3). This indicates that the magnitude of retreat on marine-terminating outlets was significantly different between the coasts, but that the rate (B_1) and acceleration (B_2) were not significantly different (Table 4.3 & Fig. 4.3).

4.3.2. Atmospheric and oceanic forcing

On the Barents Sea coast, sea ice concentrations during all seasons were high between 1997 and 1999 (Fig. 4.5B). Sea ice concentrations decreased markedly in 2000 and 2001 (Fig. 4.5B) and the mean duration of ice free conditions increased to five months (Fig. 4.5C). Summer and autumn sea ice concentrations were relatively high between 2002 and 2004 (Fig. 4.5B) and the number of ice free months reduced to two (Fig. 4.5C). From 2005 onwards, sea ice concentrations were generally very low (>5%) during summer and autumn (Fig. 4.5B), which resulted in ice free conditions persisting for approximately six months of the year (Fig. 4.5C). Winter and spring sea ice values also declined markedly between 2004 and 2008 (Fig. 4.5B).

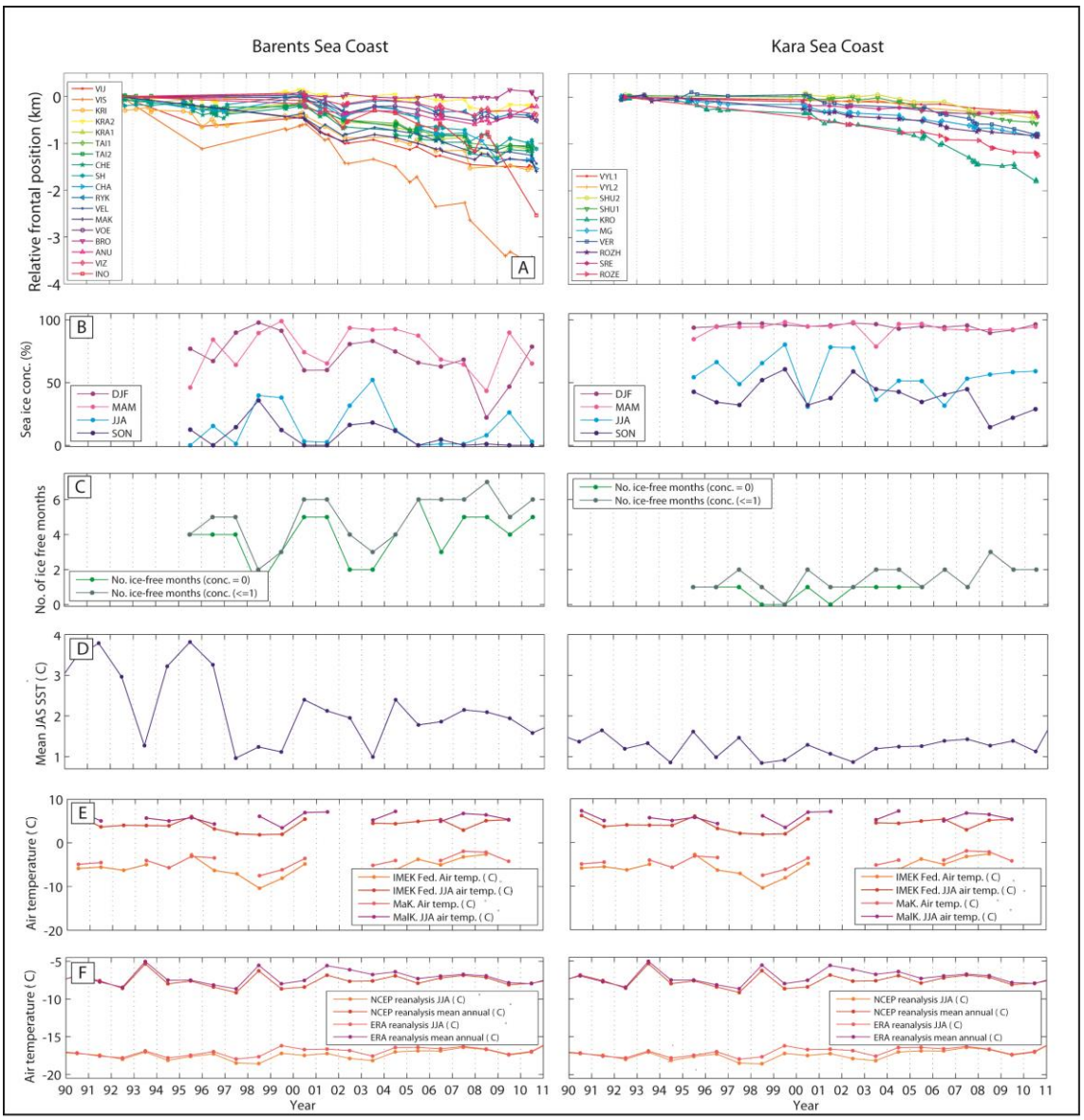

Figure 4.5. *Relative glacier frontal position and atmospheric / oceanic forcing factors for the Barents Sea coast (left-hand column) and Kara Sea coast (right-hand column). (A) Frontal position for all glaciers, relative to Jul/Aug 1992, colour-coded according to glacier and ordered south to north. (B) Mean seasonal sea ice concentrations for the periods Dec–Feb (DJF), Mar-May (MAM), Jun-Aug (JJA) and Sep-Nov (SON). (C) Number of months of ice-free conditions. (D) Mean sea surface temperatures for Jun-Sep (JAS). (E) Mean annual and mean summer (JJA) air temperatures from Malye Karmaku and Im E. K Fedrova meteorological stations (location shown in Fig 1A). (F) Mean annual and mean summer (JJA) air temperatures from NCEP/NCAR and ERA-Interim reanalysis data at 700mb geopotential height.*

On the Kara Sea coast, winter and spring sea ice concentrations remained close to 100% throughout the study period (Fig. 4.5B). Summer and autumn concentrations increased

between 1997 and 1999, followed by a rapid decrease in 2000 (Fig. 4.5B) and an increase in the number of ice free months (Fig. 4.5C). Sea ice concentrations remained high during the summers of 2001 and 2002, before decreasing markedly in 2003 and remaining at approximately 50% thereafter (Fig. 4.5B). From 2003 onward, the average number of ice free months was two and reached a peak of three months in 2008 (Fig. 4.5C), when autumn sea ice concentrations also decreased significantly (Fig. 4.5B).

SSTs in the Barents Sea peaked in 1991 and 1995, followed by a comparatively cool period between 1997 and 1999 (Fig. 4.5D). SSTs warmed again by 2000, decreased substantially in 2003 and warmed again by 2004 (Fig. 4.5D). Temperatures then warmed gradually until 2007 and decreased slowly thereafter. On the Kara Sea coast, SSTs varied considerably between 1990 and 1998, with peaks occurring in 1991, 1995 and 1997 (Fig. 4.5D). Temperatures were comparatively warm in 2000 and then cooled until 2002. Thereafter, SSTs increased gradually until 2007 and cooled slightly in 2008 and 2010 (Fig. 4.5D). SSTs generally varied in a similar pattern to summer and autumn sea ice concentrations (Fig. 4.5).

Air temperatures showed no statistically significant interannual trend at Malye Karmaku, Im E. K Fedrova or in the reanalysis data (Fig. 4.5E & F). Furthermore, no trend was apparent in summer (JJA) mean values in any of the datasets. Using both reanalysis datasets, a paired t-test was used to evaluate whether there was a significant difference in mean annual air temperatures before and after the onset of retreat on the Barents Sea coast in 2000 and on the Kara Sea coast in 2003 (Fig. 4.5E & F). Results demonstrate that there was no significant difference in mean annual air temperatures for either period.

4. 3.3. Catchment area and fjord width variation

We found no correlation between outlet glacier retreat rate and catchment area (R^2 = 0.08). The relationship between fjord width variation and glacier retreat was assessed by comparing the value for fjord width variability (see Section 2.3) with total retreat rate

(1992-2010) for all marine-terminating glaciers with continuous fjord walls (n = 20) (Fig. 4.6). First, we calculated the Pearson's correlation coefficient between width variability and total retreat rate, which gave a value of r = 0.80 at a confidence level of >0.01 (99%) and demonstrates a strong positive correlation between the two variables. Simple linear regression of width variability versus total retreat rate gave an R^2 value of 0.65 and polynomial regression, using a quadratic curve, resulted in an R^2 value of 0.75 (Fig. 4.6). Together these results show a statistical relationship between fjord with variability and glacier retreat rates within the study region.

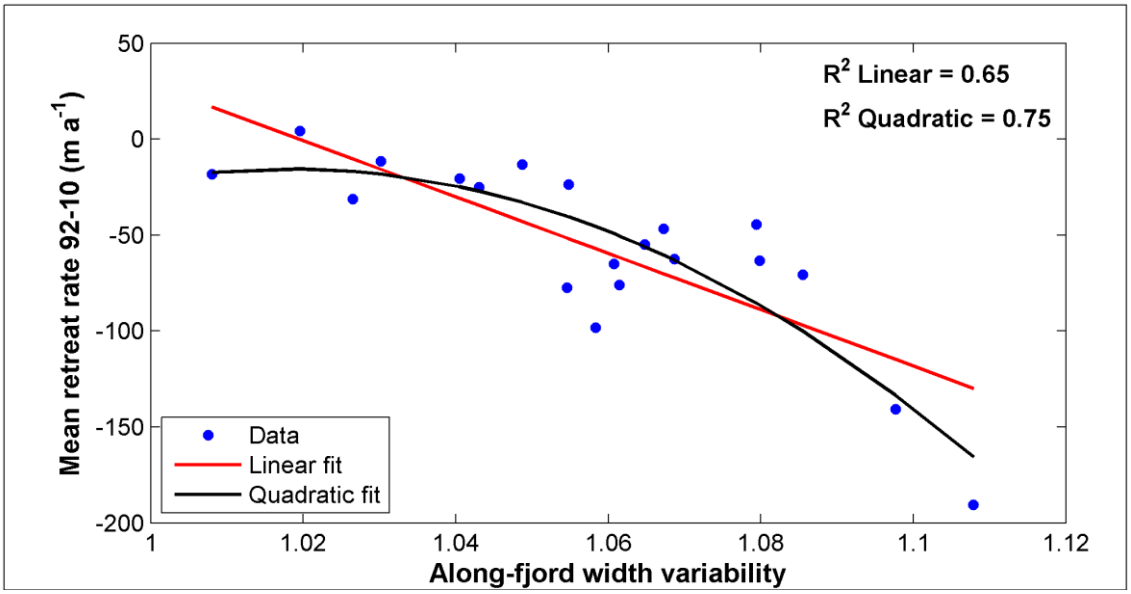

Figure 4.6. *Scatter plot of along-fjord width variability versus mean rate of frontal position change between 1992 and 2010. This shows the relationship between outlet glacier retreat rate, for all study glaciers with continuous fjord walls, and width variability between the least and most advanced position reached by the glacier terminus during the study period. A value of 1 indicates a straight fjord wall, with increasing values related to increasing variability. Linear (black line) and quadratic (red line) fits were applied to the data.*

4.4. Discussion

4.4.1. Glacier retreat

Our data demonstrate that the vast majority (90%) of outlet glaciers on NVZ retreated between 1992 and 2010 (Figs. 4.2 & 4.4). This concurs with the substantial mass deficit recently reported by *Moholdt et al.* [2012] and highlights the potential

contribution of glacier retreat to mass loss from NZ. The vast majority of retreat occurred on marine-terminating outlets and losses increased over time (Figs. 4.3 & 4.4), in contrast to land-terminating glaciers where retreat rates were comparable to frontal position errors. The order of magnitude difference in retreat rates between marine- and land-terminating outlets is consistent with previous results from the GIS [*Moon and Joughin*, 2008; *Pritchard et al.*, 2009; *Sole et al.*, 2008] and Austfonna Ice Cap, Svalbard [*Dowdeswell et al.*, 2008]. However, it contrasts with the pattern of surface elevation change recently reported for NVZ using ICESat laser altimetry data (Fig. 4.7), which found no significant difference in frontal thinning rates between marine- and land-terminating glaciers [*Moholdt et al.*, 2012]. We suggest that this difference may reflect i) the spatial coverage of the surface elevation data and/or; ii) a delay between terminus retreat and dynamic thinning on marine-terminating outlets. The location of the ICESat tracks results in comparatively sparse data coverage close to the termini of marine terminating outlets (Fig. 4.7), where we would expect dynamic thinning in response to recent frontal retreat to be greatest. Consequently, the data may not fully account for near-terminus thinning and may thus underestimate thinning rates on marine-terminating outlets. Alternatively, recent glacier retreat may not yet have initiated dynamic thinning on marine-terminating glaciers, potentially due to slower glacier response times on NVZ in comparison to areas such as the GrIS. If so, recent retreat may result in substantial near-future mass loss from NVZ once the dynamic response begins. This longer-term dynamic component has been highlighted as a potential primary source of future mass loss from the GrIS, where it may account for >75% of 21st century losses [*Price et al.*, 2011], although dynamic changes may be self-limiting on 200-year timescales [*Goelzer et al.*, 2013]. Our data therefore suggest that we may be underestimating the contribution of ice dynamics to recent and/or near-future mass losses on NVZ.

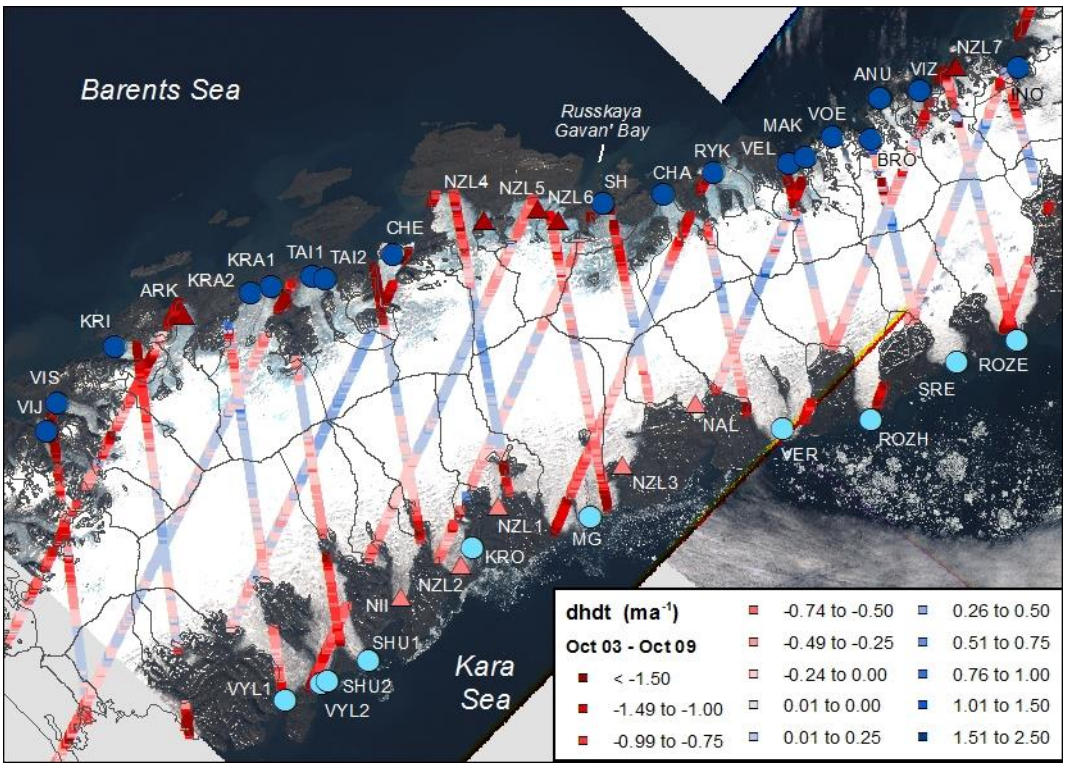

Figure 4.7. Rate of elevation change along ICESat laser altimetry tracks for the period Oct 2003 – Oct 2009. Data provided by G. Moholdt (Moholdt et al., 2012). Study glaciers are symbolised according to coast and terminus type as follows: Barents Sea / marine-terminating (dark blue circles), Kara Sea / marine-terminating (light blue circles), Barents Sea / land-terminating (dark red triangles), Kara Sea / land-terminating (light red triangles).

4.4.2. Glacier response to atmospheric and oceanic forcing

4.4.2.1. Sea ice controls

The marked difference in retreat rates between land- and marine- terminating glaciers suggests that factors operating at the calving front are the primary control on glacier retreat rates on NVZ. Our data show a close correspondence between NVZ glacier frontal position, sea ice concentrations and the number of ice free months (Fig. 4.5). On the Barents Sea coast, outlet glaciers advanced from 1997 until 2000, when sea ice concentrations were high during all seasons in comparison to the rest of the study period and the number of ice-free months was low (Fig. 4.5). Subsequent retreat between 2000 and 2002 was coincident with sea ice decline and retreat slowed once again between 2002 and 2004, when sea concentrations increased, particularly during the summer (JJA) (Fig. 4.5). The main period of retreat occurred between 2004 and

2008, when fjords were largely ice-free in summer and autumn (SON) and sea ice concentrations in winter (DJF) and spring (MAM) also declined markedly. Thereafter, retreat rates reduced from 2008, concurrent with an upward trend in winter and spring sea ice concentrations. A similar correspondence between sea ice concentrations and frontal position is apparent on the Kara Sea coast, where a brief reduction in sea ice concentrations in 2000 was coincident with the first phase of marked glacier retreat (Fig. 4.5). In 2001 and 2002, summer sea ice concentrations increased markedly and the glaciers underwent limited retreat or even advance. The main retreat phase from 2003 onwards began with a substantial reduction in summer and autumn sea ice concentrations and was concurrent with an increase in the number of ice free months (Fig. 4.5).

Sea ice concentrations have been identified as a key control on outlet glacier retreat rates in Greenland [*Amundson et al.*, 2010; *Carr et al.*, 2013a; *Carr et al.*, 2013b; *Howat et al.*, 2010; *Joughin et al.*, 2008] and Antarctica [*Miles et al.*, 2013] via their control on calving rates. Formation of winter sea ice is thought to suppress calving by up to a factor of six, whereas seasonal disintegration allows high summer calving rates to commence [*Amundson et al.*, 2010; *Joughin et al.*, 2008; *Sohn et al.*, 1998]. Consequently, we suggest that years characterised by late formation and/or early disintegration of sea ice, resulting in a longer seasonal duration of ice-free conditions, promoted higher summer calving rates and net retreat on NVZ. Conversely, years of higher sea ice concentrations and/or shorter duration of open water conditions would reduce calving rates, thus lowering retreat rates. On this basis, we suggest sea ice concentrations are an important control on outlet glacier retreat rates on NVZ. Furthermore, sea ice conditions may partly account for the difference in retreat rates between the two coasts: on the Barents Sea coast, fjords become seasonally ice free for up to six months of the year, in comparison to a maximum of three months on the year on the Kara Sea (Fig. 4.5). Consequently, higher summer calving rates can persist

for longer on the Barents Sea coast and could therefore produce higher mean retreat rates.

4.4.2.2. Ocean temperatures

Changes in SSTs corresponded with both variations in sea ice concentrations and the number of ice free months (Fig. 4.5). This was particularly marked on the Barents Sea coast, where comparatively cool SSTs in 1998-1999 and 2003 were concurrent with increased sea ice concentrations during all months. Conversely, periods of warmer SSTs were characterised by lower sea ice concentrations, as observed in 2000 and 2004 (Fig. 4.5). This indicates a relationship between SSTs and sea ice concentrations: warmer SSTs may cause sea ice melt and lower sea ice concentrations may promote warmer SSTs. Together these factors may facilitate retreat, as reduced sea ice concentrations [*Amundson et al.*, 2010; *Joughin et al.*, 2008] and/or undercutting at the waterline due to increased SSTs [*Benn et al.*, 2007; *Vieli et al.*, 2002], which may increase calving rates. Thus, periods of warmer SSTs are likely to promote glacier retreat on NVZ. Previous studies have documented mass gains on NVZ during periods of warmer Barents SSTs due to increased accumulation, which has been linked to positive phases of the North Atlantic Oscillation (NAO) and increased winter precipitation [*Zeeberg and Forman*, 2001]. However, our data suggest that warmer SSTs may also promote retreat, which may partly offset the surface mass balance gains during positive phases of the NAO.

In addition to surface changes, warmer SSTs during positive phases of the NAO are thought to reflect the increased advection of warm Atlantic Water (AW) into the Barents Sea [*Hurrell*, 1995; *Loeng*, 1991]. This has important implications for submarine melt rates and glacier behaviour on NVZ: SSTs are unlikely to cause significant mass loss through glacial melt, whereas warming at depth can result in rapid submarine melting [*Motyka et al.*, 2003; *Motyka et al.*, 2011; *Rignot et al.*, 2010]. As outlined above, oceanic warming may also cause retreat via waterline melting and undercutting of the terminus [*Benn et al.*, 2007; *Vieli et al.*, 2002]. Topographic maps indicate that fjord

depths around NVZ are of the order of 100-200 m deep near the glacier termini, meaning that they are considerably shallower than major outlet glacier fjords in Greenland and likely to only be close to flotation at the calving front. Furthermore, calving generally occurs via small icebergs (<200 m), rather than large tabular bergs, further indicating that the glaciers do not have extensive floating sections. As a consequence of the limited floating sections and comparatively shallow grounding line depths, the relative contribution of undercutting at the waterline to ocean-induced mass loss maybe more significant on NVZ than in areas with deeper fjords, such as the GrIS.

Previous studies have highlighted the distribution and properties of AW as a potentially key control on Greenland glacier dynamics and have demonstrated that it can penetrate to the calving front [*Andresen et al.*, 2012; *Christoffersen et al.*, 2011; *Holland et al.*, 2008; *Murray et al.*, 2010; *Straneo et al.*, 2011]. On the Barents Sea coast, modified AW is present on the Novaya Zemlya Bank (Fig. 4.1), within the West Novaya Zemlya Current [*Årthun et al.*, 2011; *Ivanov and Shapiro*, 2005; *Pfirman et al.*, 1994], and the study glacier fjords are comparatively short and open to the ocean (Fig. 4.2). Very few direct measurements of oceanographic conditions are available from NVZ glacier fjords, meaning that little is known about fjord circulation and/or the potential for the offshore AW to reach the glacier termini. However, subsurface ocean temperatures have been measured in Russkaya Gavan' Bay (Fig. 4.2), at points located 3.5 and 9.6 km from the terminus of Shokalskogo glacier (SH) [*Politova et al.*, 2012]. Water temperatures of almost 3.5 ºC were recorded between depths of 30 and 65 m, providing empirical evidence that warm water can access at least some Barents Sea fjords. These temperatures are warmer than those recorded at the same depth in the fjords of Helheim, Kangerdlugssuaq and Jakobshavn Isbrae, Greenland, and are comparable to values recorded in deeper water masses (>200 m) within these fjords, which are thought to be of Atlantic origin [*Christoffersen et al.*, 2011; *Holland et al.*, 2008; *Straneo et al.*, 2010].

In the Kara Sea, Atlantic-derived water masses enter at three points: via the Kara Strait in the south, via the passage between Franz Josef Land and NVZ and through the St. Anna Trough in the north (Fig. 4.1) [*Karcher et al.*, 2003; *Pavlov and Pfirman*, 1995]. Near to the Kara Strait, surface ocean temperatures of up to 9 °C have been recorded during late summer, with warming thought to extend to depths of up to 60 m [*Pavlov and Pfirman*, 1995]. In the northern Kara Sea, water temperatures of approximately 1.5 °C have been measured at the St. Anna Canyon (depth ~ 300 m) [*Hanzlick and Aagaard*, 1980] and offshore of the northern tip of NVZ (depth ~ 125 m) [*Karcher et al.*, 2003]. The latter area is characterised by late freezing and thin sea ice, in comparison to the rest of the Kara Sea, and previous studies have highlighted the potential link between AW and sea ice conditions in the region [*Hanzlick and Aagaard*, 1980]. This evidence suggests that Atlantic-derived water has the potential to influence glacier behaviour on the Kara Sea coast, via submarine melting and/or sea ice controls, and that differences in oceanographic conditions may contribute to the coastal difference in glacier retreat rates. However, detailed oceanographic measurements would be required on both coasts to assess the extent to which oceanic changes are transmitted to the glacier front and their influence on glacier behaviour. We therefore highlight this as an important area for future research, given the rapid recent retreat of marine-terminating outlets on NVZ, their apparent sensitivity to changes at the ocean boundary and the potential for rapid connections between the glacier termini and warm continental shelf waters.

4.4.2.3. Atmospheric forcing

Previous studies have identified a number of different mechanisms by which air temperatures may drive marine-terminating outlet glacier retreat: i) hydrofracture of crevasses at the terminus/lateral margins [*Andersen et al.*, 2010; *Sohn et al.*, 1998; *Vieli and Nick*, 2011]; ii) sea ice melting and/or; iii) enhanced submarine melting due to subglacial meltwater plumes [*Motyka et al.*, 2003; *Motyka et al.*, 2011; *Sohn et al.*, 1998]. From visual inspection of satellite imagery, we see no evidence of significant

areas of water-filled crevasses during the melt season and calving generally occurs via small icebergs (<200 m), rather than large tabular bergs. This indicates that the glacier termini do not have extensive floating sections and would therefore be less vulnerable to full thickness fracture via meltwater enhanced crevassing. Moreover, our data show no clear correspondence between variations in air temperature and sea ice (Fig. 4.5). Instead, sea ice variability corresponded with changes in SSTs, suggesting that they may be a more significant influence on sea ice concentrations than air temperatures. Meltwater plumes have been highlighted as a potentially important control on outlet glacier behaviour elsewhere in the Arctic [*Christoffersen et al.*, 2011; *Motyka et al.*, 2003; *Motyka et al.*, 2011; *Seale et al.*, 2011; *Straneo et al.*, 2011] and turbid meltwater plumes are evident at the glacier termini. However, very limited oceanographic data are available from NVZ glacial fjords, which precludes a detailed assessment of this mechanism.

Our results show limited correspondence between air temperatures and frontal position variations on NVZ. During the study period, no statistically significant trend was evident in any of our air temperature data sets, in contrast to the acceleration in marine-terminating glacier retreat, and we find no statistical difference in air temperatures before and after the onset of retreat on either coast (Figs. 4.3 & 4.5). Although previous findings from the GrIS suggest that the response of marine-terminating glaciers to forcing at the terminus is rapid [*Vieli and Nick*, 2011], we also calculated air temperature trends from the 1950s to present using reanalysis data, in order to identify any longer-term forcing to which glacier dynamics might be responding. During this time period, we found no significant trend in mean annual or mean summer (JJA) air temperatures in any of the datasets and mean annual values showed marked interannual and interdecadal variability. Although comparison of meteorological station data with retreat rates is limited by data availability, the pattern of retreat on the Kara Sea coast showed little correspondence to air temperature variations at either meteorological station (Fig. 4.5). On the Barents Sea coast, the onset of retreat in 2000

followed two years of atmospheric warming, but temperatures were equally warm at other points during the study period when retreat rates were lower (Fig. 4.4). Previous studies have suggested that a longitudinal temperature gradient exists across NVZ [*Zeeberg and Forman*, 2001], which could potentially contribute to the difference in retreat rates between the Barents and Kara Sea coasts This potential coastal difference cannot be assessed, due to lack of data. However, our results provide no evidence for a change in air temperatures that coincided with glacier retreat, suggesting that they are not a primary driver of marine-terminating glacier retreat on NVZ.

4.4.3. Fjord width variation

Although mean retreat rates were somewhat higher on the Barents Sea coast than on the Kara Sea (Figs. 4.3 & 4.4), there were large variations in retreat rates between glaciers located on the same coast and even between neighbouring glaciers (Figs. 4.2 & 4.3), despite being subject to comparable forcing. Together, this evidence suggests that factors specific to each glacier can modulate its response to forcing. A number of potential glacier-specific controls have been identified to date, including catchment area, glacier width and basal topography [*Carr et al.*, 2013a]. We found no correlation between outlet glacier retreat rate and catchment area (R^2 = 0.08). However, our data suggest that along-flow variations in fjord width are an important control and we demonstrate a statistical relationship between fjord width variability and glacier retreat across the study region. We suggest that along-flow width variations may influence retreat rates via two mechanisms: i) due to the principle of mass conservation, widening of the fjord would mean that the glacier needs to thin and the surface slope needs to reduce in order to maintain the same ice flux, which would make the ice more vulnerable to thinning and eventually to floatation, thus increasing calving rates and promoting retreat [*O'Neel et al.*, 2005] and; ii) lateral resistive stresses tend to decrease with increasing width, which would reduce resistance to flow and promote further dynamics thinning and retreat [*Raymond*, 1996].

In addition to the relationship between retreat rates and width variability, we assessed the relative importance of specific types of width variation (Table 4.1). Based on the hypothesis outlined above, widening of the fjord in the along-flow direction, either rapidly (Class I) or gradually (Class II), is likely to promote retreat and acceleration (Table 4.3). Conversely, narrowing of the fjord, either at pinning points (Class III) or progressively (Class IV), would be expected to reduce retreat rates and ice velocities (Table 4.3). These changes are likely to occur more rapidly where pinning points are present (Classes I & IV) than where changes in fjord width are gradual (Classes II & III). Glaciers undergoing minimal along-flow width variation (Class VI) would experience limited changes in surface slope, thickness and/or resistive stresses over time, meaning that these factors would have a minimal effect on glacier retreat rates and/or ice velocities.

Our results demonstrate that rapid retreat was associated with widening fjords and was particularly marked where glaciers retreated from pinning points (Table 4.1). This was exemplified by VIS, located on the Barents Sea coast (Fig. 4.2), which exhibited the highest mean retreat rate between 1992 and 2010 and its fjord width varied by 16% between the most and least extended frontal positions. Between Jan 1996 and Aug 2001, the glacier front occupied a very similar position at a comparatively narrow point of the fjord and its southern margin was attached to a prominent pinning point (Fig. 4.8; Point I). The glacier then retreated rapidly from Apr 2002, as the southern margin retreated from the pinning point and the front moved into a wider section of the fjord (Fig. 4.8; Point II). Retreat persisted until May 2009, when the fjord narrowed (Fig. 4.8; Point III). This relationship between frontal retreat, pinning points and variations in fjord width is consistent with previous empirical results from Greenland [*Carr et al.*, 2013b;

Warren and Glasser, 1992] and numerical modelling studies [*Jamieson et al.*, 2012].

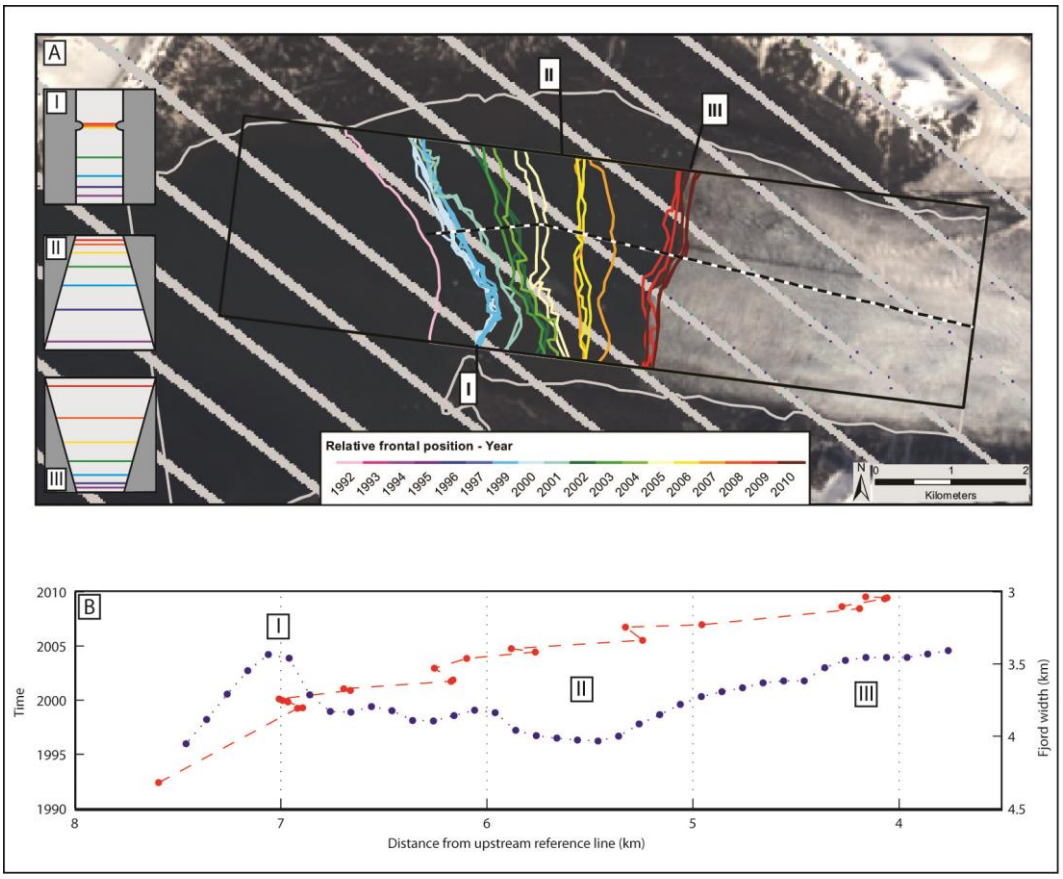

Figure 4.8. *Frontal position of Vil'kitskogo Sev. (VIS) in relation to fjord width perpendicular to the glacier centre-line (A): VIS frontal position over time (colour-coded by year), glacier centreline (black dashed line) and fjord margins as sea level (light-grey line). Labelled positions are discussed in the text. Base image: Landsat scene acquired 7th Jul 2010 and provided by USGS Global Visualisation Viewer. (B) Fjord width perpendicular to the centre-line (blue), in relation to glacier frontal position (red).*

Our results also demonstrate that the glaciers exhibiting the lowest retreat rates have a relatively uniform width along their retreat path and their termini were generally located at narrow points within the fjord (Table 4.1). This is illustrated by BRO, which underwent the least retreat during the study period. The fjord width varied very little (2.5%) between the minimum and maximum frontal positions and the terminus occupied a comparatively narrow section of fjord throughout this period (Fig. 4.9). However, the fjord widens upstream of the current terminus position (Fig. 4.9), which may facilitate retreat in the future, if forcing is sufficient to move the front into this wider

section. BRO is located on the Barents Sea coast, approximately 195 km north of VIS. Despite this latitudinal difference, sea ice concentrations at these two glaciers varied by only 4%, whereas the absolute change in frontal position was 48 times greater on VIS than BRO, with VIS retreating by 190 m a^{-1} and BRO advancing by 4 m a^{-1} during the study period (Table 4.1). A similar pattern is evident along the Barents Sea coast, where the variation in mean monthly sea ice concentrations was small (SD = 0.67%), but total retreat rate varied markedly, ranging between +4 m a^{-1} and 190 m a^{-1} (SD = 47.35 m a^{-1}) (Fig. 4.4 & Table 4.1). On the Kara Sea coast, total retreat rates also showed substantial variation (SD = 25.75 m a^{-1}) and variability in sea ice concentrations was limited, although slightly higher than on the Barents Sea coast (SD = 2.34%). Thus, evidence indicates that there is high variation in retreat rates on both coasts between individual glaciers, but limited variation in forcing and we suggest that variations in fjord width contribute substantially to these differences.In addition to the two extreme cases described above, a number of study glaciers experienced retreat only at the central portion of the terminus, whilst the margins remained on lateral pinning points (Table 4.1). This mainly occurred on the relatively wide outlet glaciers located on the Kara Sea coast, from Moshnyij (MG) northwards (Fig. 4.2), and is exemplified by the pattern of retreat on MG (Fig. 4.10). Although detailed bathymetric data are unavailable, topographic maps indicate that the area immediately offshore of these glaciers is shallow and gently sloping, and previous studies suggest that glaciers on the Kara Sea coast terminate in shallow water [*Kotlyakov*, 2006]. Due to the comparatively shallow and wide fjords, ice close to the lateral margins is more likely to be grounded and retreat may therefore be limited to the central portion, where water depths are sufficient to bring the termini close to floatation. Consequently, contemporary forcing may be insufficient to dislodge the glacier termini from their lateral pinning points. This contrasts with fjords located on the Barents Sea coast and those further south on the Kara Sea, which are narrower and possibly deeper, as indicated by previous results [*Kotlyakov*, 2006] and bathymetric data from the topographic maps. Narrower fjords are likely to result in a greater contribution of lateral

stresses to the force budget and deeper fjords may allow the terminus to reach near-floatation, which could then facilitate rapid retreat via a series of positive feedbacks once the terminus has moved beyond a pinning point. As a result, differences in fjord geometry may also contribute to the coastal difference in mean retreat rates, as the majority of the wide, shallow fjords are located on the northern Kara Sea coast. A number of the marine-terminating study glaciers also have a portion of their ice front which is land-terminating and this is particularly notable within the northern section of the Kara Sea (Table 4.1). However, this characteristic appears to bear little relationship to glacier retreat rate during the study period (Table 4.1).

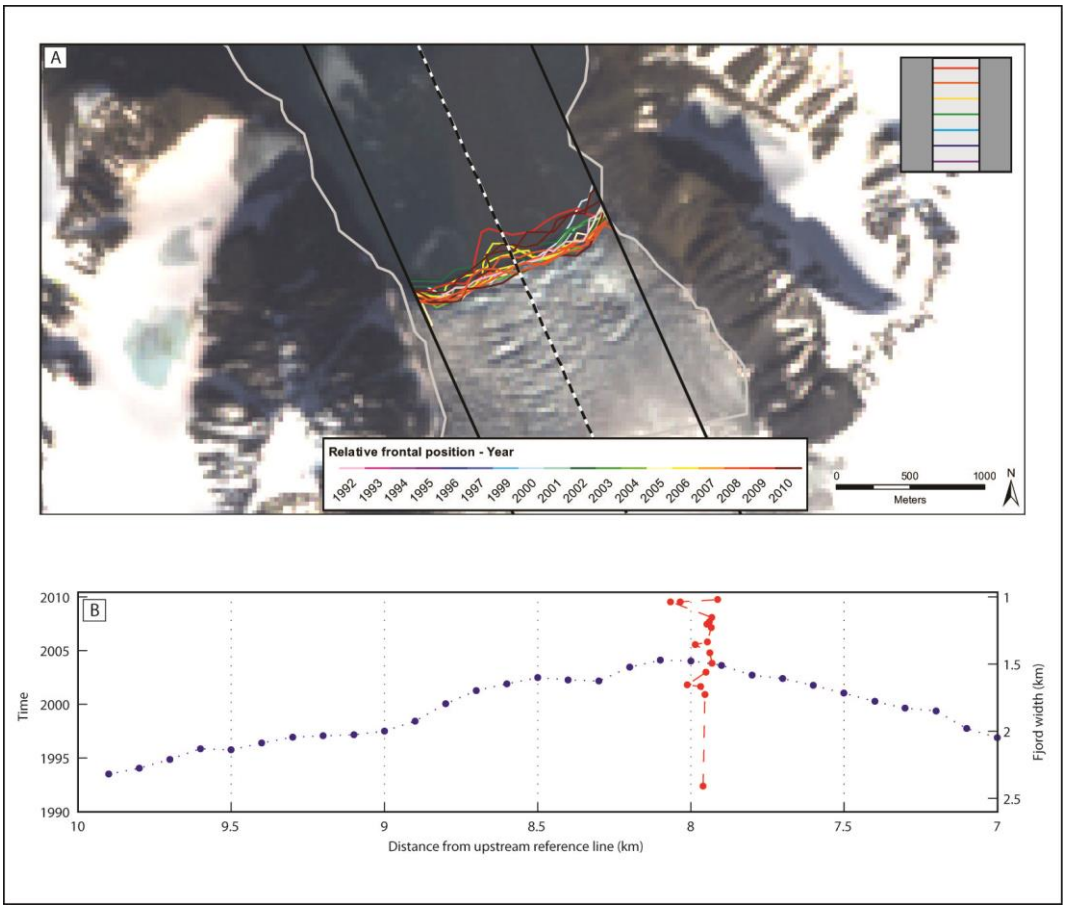

Figure 4.9. *Frontal position of Brounova (BRO) in relation to fjord width perpendicular to the glacier centre-line (A): BRO frontal position over time (colour-coded by year), glacier centreline (black dashed line) and fjord margins as sea level (light-grey line). Labelled positions are discussed in the text. Base image: Landsat scene acquired 13th Aug 2011 and provided by USGS Global Visualisation Viewer. (B) Fjord width perpendicular to the centre-line (blue), in relation to glacier frontal position (red).*At present, no data are available on the subglacial

topography of NVZ outlet glaciers and bathymetric information within the fjords is limited. Our results suggest that fjord bathymetry may influence the pattern and magnitude of glacier retreat on the northern section of the Kara Sea coast, where fjords may be comparatively shallow. Retreat rates vary spatially along the fronts of these glaciers (Fig. 4.10), which may reflect local variations in basal topography and/or bathymetry. Furthermore, rock islands are visible at the calving of a number of the study glaciers (e.g. KRI and CHE), which may promote retreat as the terminus recedes and ungrounds from these pinning points. It has been suggested that loss of contact with basal pinning points contributed to the dramatic retreat of Jakobshavn Isbrae, west Greenland [*Thomas et al.*, 2003]. Basal topography has been identified as a potentially important control on outlet glacier dynamics in other Arctic regions [*Meier and Post*, 1987; *Nick et al.*, 2009; *Thomas et al.*, 2009] and our results underscore the influence of fjord geometry on glacier retreat rates. Thus, basal topographic and bathymetric data in NVZ are urgently needed to fully understand the factors controlling outlet glacier behaviour and modulating their response to forcing.

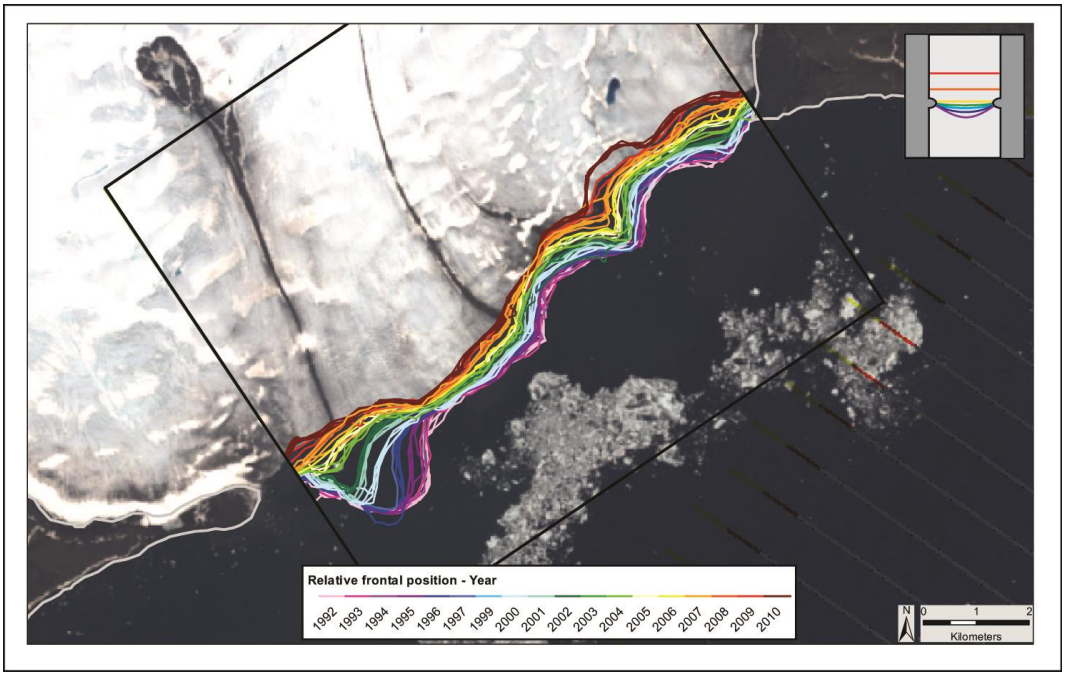

Figure 4.10. *Frontal position of Moshnyj (MG) in relation to fjord width perpendicular to the glacier centre-line (A): MG frontal position over time (colour-coded by year), glacier centreline*

(black dashed line) and fjord margins as sea level (light-grey line). Labelled positions are discussed in the text. Base image: Landsat scene acquired 13th Aug 2011 and provided by USGS Global Visualisation Viewer. (B) Fjord width perpendicular to the centre-line (blue), in relation to glacier frontal position (red).

4.5. Conclusions

Major outlet glaciers on Novaya Zemlya have retreated rapidly between 2000 and 2010. Retreat rates were an order of magnitude greater on marine-terminating outlets than on land-terminating glaciers. Marine-terminating glacier retreat has accelerated over time and the temporal pattern of retreat corresponded closely to changes in sea ice concentration. Retreat rates were significantly higher on the Barents Sea coast than on the Kara Sea coast, mostly likely due to the differences in sea ice concentrations and duration. Despite a consistent overall retreat trend, however, there was a large range in retreat rates between outlet glaciers located on the same coast, which far exceeded variations in forcing. We identify fjord width variability as a key factor modulating glacier response to forcing and show a significant relationship between this factor and total glacier retreat rates. Using empirical evidence, we categorise the influence of fjord width and highlight lateral pinning points as an important control. We suggest that these qualitative criteria encompass the primary classes of glacier response to fjord width variation and may therefore prove a useful framework for interpreting and assessing observations of marine-terminating outlet glacier retreat in other regions. Future work should measure subsurface ocean conditions (temperature and salinity) within outlet glacier fjords, given the apparent sensitivity of NVZ glaciers to changes at the calving front. Information on fjord bathymetry and subglacial topography is also required, as fjord geometry appears to be a key control on NVZ outlet glacier retreat rates but the influence of basal topography in this region has yet to be quantified. Our data indicate that variations in fjord width can strongly influence the behaviour of a large sample of study glaciers and we highlight the danger of extrapolating retreat rates without due consideration of these local factors. We underscore the need to consider

the dynamic component of mass loss from Novaya Zemlya, in order to accurately forecast near-future losses.

Acknowledgments

This work was supported by a Durham Doctoral Scholarship, granted to J.R. Carr. ENVISAT and ERS Image Mode Precision scenes were provided by the European Space Agency (ESA). We thank N.J. Cox, G. Moholdt and A. Gardner for their helpful comments, and Mauri Pelto and Michael Willis for their thoughtful reviews.

4.6. References

Amundson, J. M., M. Fahnestock, M. Truffer, J. Brown, M. P. Lüthi, and R. J. Motyka (2010), Ice mélange dynamics and implications for terminus stability, Jakobshavn Isbræ, Greenland, *Journal of Geophysical Research*, *115*, F01005, doi:10.1029/2009JF001405.

Andersen, M. L., et al. (2010), Spatial and temporal melt variability at Helheim Glacier, East Greenland, and its effect on ice dynamics, *Journal of Geophysical Research*, *115*, F04041.

Andresen, C. S., et al. (2012), Rapid response of Helheim Glacier in Greenland to climate variability over the past century, *Nature Geoscience*, *5*, 37-41.

Arendt, A., et al. (2012), Randolph Glacier Inventory [v2.0]: A Dataset of Global Glacier Outlines. Global Land Ice Measurements from Space*Rep.*, Boulder Colorado, USA, Digitial Media.

Årthun, M., R. B. Ingvaldsen, L. H. Smedsrud, and C. Schrum (2011), Dense water formation and circulation in the Barents Sea, *Deep Sea Research Part I: Oceanographic Research Papers*, *58*(8), 801-817, doi:http://dx.doi.org/10.1016/j.dsr.2011.06.001.

Bassford, R. P., M. J. Siegert, and J. Dowdeswell (2006), Quantifying the Mass Balance of Ice Caps on Severnaya Zemlya, Russian High Arctic. II: Modeling the Flow of the Vavilov Ice Cap under the Present Climate, *Arctic, Antarctic and Alpine Research*, *38*(1), 13-20.

Benn, D. I., C. R. Warren, and R. H. Mottram (2007), Calving processes and the dynamics of calving glaciers, *Earth Science Reviews*, *82*, 143-179.

Burgess, D. O., and M. J. Sharp (2008), Recent changes in thickness of the Devon Island ice cap, Canada, *Journal of Geophysical Research*, *113*, B07204.

Carr, J. R., C. R. Stokes, and A. Vieli (2013a), Recent progress in understanding marine-terminating Arctic outlet glacier response to climatic and oceanic forcing: Twenty years of rapid change, *Progress in Physical Geography*, *37*(4), 435 - 466.

Carr, J. R., A. Vieli, and C. R. Stokes (2013b), Climatic, oceanic and topographic controls on marine-terminating outlet glacier behavior in north-west Greenland at seasonal to interannual timescales, *Journal of Geophysical Research*, *118*(3), 1210-1226.

Christoffersen, P., R. Mugford, K. J. Heywood, I. Joughin, J. Dowdeswell, J. P. M. Syvitski, A. Luckman, and T. J. Benham (2011), Warming of waters in an East Greenland fjord prior to glacier retreat: mechanisms and connection to large-scale atmospheric conditions, *The Cryosphere*, *5*, 701-714.

Dee, D. P., et al. (2011), The ERA-Interim reanalysis: configuration and performance of the data assimilation system, *Quarterly Journal of the Royal Meteorological Society*, *137*(656), 553-597, doi:10.1002/qj.828.

Dowdeswell, J., T. J. Benham, T. Strozzi, and J. M. Hagen (2008), Iceberg calving flux and mass balance of the Austfonna ice cap on Nordaustlandet, Svalbard, *Journal of Geophysical Research*, *113*, F03022.

Dowdeswell, J., et al. (1997), The Mass Balance of Circum-Arctic Glaciers and Recent Climate Change, *Quaternary Research*, *48*, 1-14.

Dowdeswell, J., and M. Williams (1997), Surge-type glaciers in the Russian High Arctic identified from digital satellite imagery, *Journal of Glaciology*, *43*(145), 489-494.

Enderlin, E. M., and I. M. Howat (2013), Submarine melt rate estimates for floating termini of Greenland outlet glaciers (2000-2010), *Journal of Glaciology*, *59*(213), 67-75, doi:10.3189/2013JoG12J049.

Gardner, A., G. Moholdt, A. Arendt, and B. Wouters (2012), Accelerated contributions of Canada's Baffin and Bylot Island glaciers to sea level rise over the past half century, *The Cryosphere*, *6*, 1103-1125, doi:10.5194/tc-6-1103-2012.

Gardner, A., et al. (2013), A Reconciled Estimate of Glacier Contributions to Sea Level Rise: 2003 to 2009, *Science*, *340*(6134), 852-857, doi:10.1126/science.1234532.

Gardner, A., G. Moholdt, B. Wouters, G. J. Wolken, D. O. Burgess, M. J. Sharp, J. G. Cogley, C. Braun, and C. Labine (2011), Sharply increased mass loss from glaciers and ice caps in the Canadian Arctic Archipelago, *Nature*, *473*, 357-360.

Goelzer, H., P. Huybrechts, J. J. Fürst, M. L. Andersen, T. L. Edwards, X. Fettweis, F. M. Nick, A. J. Payne, and S. Shannon (2013), Sensitivity of Greenland ice sheet projections to model formulations, *Journal of Glaciology*, *59*(216), 733-749.

Grant, K. L., C. R. Stokes, and I. S. Evans (2009), Identification and characteristics of surge-type glaciers on Novaya Zemlya, Russian Arctic, *Journal of Glaciology*, *55*(194), 960-972.

Hanzlick, D., and K. Aagaard (1980), Freshwater and Atlantic water in the Kara Sea, *Journal of Geophysical Research: Oceans*, *85*(C9), 4937-4942, doi:10.1029/JC085iC09p04937.

Holland, D. M., R. H. D. Y. Thomas, B., M. H. Ribergaard, and B. Lyberth (2008), Acceleration of Jakobshavn Isbræ triggered by warm subsurface ocean waters, *Nature Geoscience*, *1*, 1-6.

Howat, I. M., J. E. Box, Y. Ahn, A. Herrington, and E. M. McFadden (2010), Seasonal variability in the dynamics of marine-terminating outlet glaciers in Greenland, *Journal of Glaciology*, *56*(198), 601-613.

Howat, I. M., I. Joughin, M. Fahnestock, B. E. Smith, and T. Scambos (2008), Synchronous retreat and acceleration of southeast Greenland outlet glaciers 2000-2006; Ice dynamics and coupling to climate, *Journal of Glaciology*, *54*(187), 1-14.

Hurrell, J. W. (1995), Decadal trends in the North Atlantic Oscillation: Regional temepratures and precipitation, *Science*, *269*, 676-679.

IPCC (2007), *The Physical Science Basis. Contribution of Working Group I to the Fourth Assessment Report of the Intergovernmental Panel on Climate Change*, Cambridge Univ. Press, Cambridge and New York.

Ivanov, V. V., and G. I. Shapiro (2005), Formation of a dense water cascade in the marginal ice zone in the Barents Sea, *Deep Sea Research Part I: Oceanographic Research Papers*, *52*(9), 1699-1717, doi:http://dx.doi.org/10.1016/j.dsr.2005.04.004.

Jamieson, S. S. R., A. Vieli, S. J. Livingstone, C. Ó Cofaigh, C. R. Stokes, C.-D. Hillenbrand, and J. Dowdeswell (2012), Ice stream stability on a reverse bed slope, *Nature Geoscience*, *5*, 799-802.

Joughin, I., I. M. Howat, M. Fahnestock, B. Smith, W. Krabill, R. B. Alley, H. Stern, and M. Truffer. (2008), Continued evolution of Jakobshavn Isbrae following its rapid speedup, *Journal of Geophysical Research*, *113*, F04006, doi:10.1029/2008JF001023.

Kalnay, E., et al. (1996), The NCEP/NCAR 40-Year Reanalysis Project, *Bulletin of the American Meteorological Society*, *77*(3), 437-471, doi:10.1175/1520-0477(1996)077<0437:tnyrp>2.0.co;2.

Karcher, M., M. Kulakov, S. Pivovarov, U. Schauer, F. Kauker, and R. Schlitzer (2003), Atlantic Water flow to the Kara Sea - comparing model results with observations, in *Siberian River Runoff in the Kara Sea: Characterisation, Quantification, Variability and*

Environmental Significance, edited by F. Stein, Fütterer, Galimov, Elsevier, Proceedings in Marine Science, pp. 47-69

Korona, E. J.Berthier, M. Bernard, F. Rèmy, and E. Thouvenot (2009), SPIRIT. SPOT 5 stereoscopic survey of Polar Ice Reference Images and Topographies during the fourth International Polar Year (2007-2009) ISPRS *ISPRS Journal of Photogrammetry and Remote Sensing*, *64*, 204-212.

Kotlyakov, V. M. (Ed.) (1978), *Katalog Lednikov SSSR: Tom 3, Severnyj Kraj,Chast' 2 Novaja Zemlya [Catolgue of Glaciers of USSR: Volume 3, Northern Area, Part 2, Novaya Zemlya.*, Hydrometeoizdat [In Russian], Leningrad.

Kotlyakov, V. M. (Ed.) (2006), *Oledenenie Severnoj I Central'noj Evrazii V Sovremennuju Epochu [Glaciation in North and Central Eurasia at present time]*, Russain Academy of Sciences, Institute of Geography, Moscow, Nauka.

Kotlyakov, V. M., A. F. Glazovskii, and I. E. Frolov (2010), Glaciation in the Arctic, *Herald of the Russian Academy of Sciences*, *80*(2), 155–164.

Kouraev, A. V., B. Legrésy, and F. Remy (2006), Northern Novaya Zemlya outlet glaciers: 1990-2000 changes.

Lenaerts, J. T. M., J. H. van Angelen, M. R. van den Broeke, A. S. Gardner, B. Wouters, and E. van Meijgaard (2013), Irreversible mass loss of Canadian Arctic Archipelago glaciers, *Geophysical Research Letters*, *40*(5), 870-874, doi:10.1002/grl.50214.

Loeng, H. (1991), Features of the physical oceanographic conditions of the Barents Sea, *Polar Research*, *10*(1), 5-18.

McFadden, E. M., I. M. Howat, I. Joughin, B. Smith, and Y. Ahn (2011), Changes in the dynamics of marine terminating outlet glaciers in west Greenland (2000–2009), *Journal of Geophysical Research*, *116*, F02022.

Meier, M. F., M. B. Dyurgerov, U. K. Rick, S. O'Neel, W. T. Pfeffer, R. S. Anderson, S. P. Anderson, and A. F. Glazovsky (2007), Glaciers Dominate Eustatic Sea-Level Rise in the 21st Century. , *Science*, *317*, 1064-1067.

Meier, M. F., and A. Post (1987), Fast tidewater glaciers, *Journal of Geophysical Research*, *92*, 9051–9058.

Miles, B. W. J., C. R. Stokes, A. Vieli, and N. J. Cox (2013), Rapid, climate-driven changes in outlet glaciers on the Pacific coast of East Antarctica, *Nature*, *500*(7464), 563-566, doi:10.1038/nature12382

http://www.nature.com/nature/journal/v500/n7464/abs/nature12382.html#supplementary-information.

Moholdt, G., C. Nuth, J. O. Hagen, and J. Kohler (2010), Recent elevation changes of Svalbard glaciers derived from ICESat laser altimetry, *Remote Sensing of Environment*, *114*, 2756–2767.

Moholdt, G., B. Wouters, and A. S. Gardner (2012), Recent mass changes of glaciers in the Russian High Arctic, *Geophysical Research Letters*, *39*, L10502.

Moon, T., and I. Joughin (2008), Changes in ice-front position on Greenland's outlet glaciers from 1992 to 2007, *Journal of Geophysical Research*, *113*, F02022, doi:10.1029/2007JF000927.

Moon, T., I. Joughin, B. E. Smith, and I. M. Howat (2012), 21st-Century evolution of Greenland outlet glacier velocities, *Science*, *336*(6081), 576-578.

Motyka, R. J., L. Hunter, K. Echelmeyer, and C. Connor (2003), Submarine melting at the terminus of a temperate tidewater glacier, LeConte Glacier, Alaska, U.S.A., *Annals of Glaciology*, *36*, 57-65.

Motyka, R. J., M. Truffer, M. Fahnestock, J. Mortensen, S. Rysgaar, and I. M. Howat (2011), Submarine melting of the 1985 Jakobshavn Isbræ floating tongue and the triggering of the current retreat, *Journal of Geophysical Research*, *166*, F01007.

Murray, T., et al. (2010), Ocean regulation hypothesis for glacier dynamics in southeast Greenland and implications for ice sheet mass changes, *Journal of Geophysical Research*, *115*, F03026, doi:10.1029/2009JF001522.

Nick, F. M., A. Vieli, M. L. Andersen, I. Joughin, A. J. Payne, T. L. Edwards, F. Pattyn, and R. S. W. van de Wal (2013), Future sea-level rise from Greenland's main outlet glaciers in a warming climate, *Nature*, *497*(7448), 235-238, doi:10.1038/nature12068.

Nick, F. M., A. Vieli, I. M. Howat, and I. Joughin (2009), Large-scale changes in Greenland outlet glacier dynamics triggered at the terminus, *Nature Geoscience*, *2*, 110-114.

Nuth, C., G. Moholdt, J. Kohler, J. O. Hagen, and A. Kääb (2010), Svalbard glacier elevation changes and contribution to sea level rise, *Journal of Geophysical Research*, *115*, F01008, doi:10.1029/2008JF001223.

O'Neel, S., W. T. Pfeffer, R. Krimmel, and M. Meier (2005), Evolving force balance at Columbia Glacier, Alaska, during its rapid retreat, *Journal of Geophysical Research*, *110*, F03012.

Pavlov, V. K., and S. L. Pfirman (1995), Hydrographic structure and variability of the Kara Sea: Implications for pollutant distribution, *Deep Sea Research Part II: Topical Studies in Oceanography*, *42*(6), 1369-1390, doi:http://dx.doi.org/10.1016/0967-0645(95)00046-1.

Pfirman, S. L., D. Bauch, and T. Gammelsrød (1994), The Northern Barents Sea: Water Mass Distribution and Modification, *The Polar Oceans and Their Role in Shaping the Global Environment Geophysical Monograph*, *85*, 77-94.

Politova, N. V., V. P. Shevchenko, and V. V. Zernova (2012), Distribution, Composition, and Vertical Fluxes of Particulate Matter in Bays of Novaya Zemlya Archipelago, Vaigach Island at the End of Summer, *Advances in Meteorology*, *2012*, 15, doi:10.1155/2012/259316.

Price, S., A. J. Payne, I. M. Howat, and B. Smith (2011), Committed sea-level rise for the next century from Greenland ice sheet dynamics during the past decade, *Proceedings of the National Academy of Sciences*, *108*(22), 8978-8983.

Pritchard, H. D., R. J. Arthern, D. G. Vaughan, and L. A. Edwards (2009), Extensive dynamic thinning on the margins of the Greenland and Antarctic ice sheets, *Nature*, *461*, 971-975.

Radić, V., A. Bliss, A. C. Beedlow, R. Hock, E. Miles, and J. G. Cogley (2013), Regional and global projections of twenty-first century glacier mass changes in response to climate scenarios from global climate models, *Climate Dynamics*, 1-22, doi:10.1007/s00382-013-1719-7.

Raymond, C. (1996), Shear margins in glaciers and ice sheets, *Journal of Glaciology*, *42*(140), 90-102.

Reynolds, R. W., T. M. Smith, C. Liu, D. B. Chelton, K. S. Casey, and M. G. Schlax (2007), Daily High-Resolution-Blended Analyses for Sea Surface Temperature, *Journal of Climate*, *20*(22), 5473-5496, doi:10.1175/2007jcli1824.1.

Rignot, E., J. E. Box, E. Burgess, and E. Hanna (2008), Mass balance of the Greenland ice sheet from 1958 to 2007, *Geophysical Research Letters*, *35*, L20502, doi:10.1029/2008GL035417.

Rignot, E., M. Koppes, and I. Velicogna (2010), Rapid submarine melting of the calving faces of West Greenland glaciers, *Nature Geoscience*, *3*, 187-191, doi:10.1038/NGEO765.

Seale, A., P. Christoffersen, R. Mugford, and M. O'Leary (2011), Ocean forcing of the Greenland Ice Sheet: Calving fronts and patterns of retreat identified by automatic satellite monitoring of eastern outlet glaciers, *Journal of Geophysical Research*, *116*(F3), F03013.

Sharov, A. I. (2005), Studying changes of ice coasts in the European Arctic, *Geo-Marine letters*, *25*, 153–166.

Sharov, A. I., W. Schöner, and P. R. (2009), Spatial features of glacier changes in the Barents-Kara Sector, *EGU General Assembly*, *11*, EGU2009-3046.

Sohn, H. G., K. C. Jezek, and C. J. van der Veen (1998), Jakobshavn Glacier, West Greenland: 30 years of Spacebourne observations, *Geophysical Research Letters*, *25*(14), 2699-2702.

Sole, A., T. Payne, J. Bamber, P. Nienow, and W. Krabill (2008), Testing hypotheses of the cause of peripheral thinning of the Greenland Ice Sheet: is land-terminating ice thinning at anomalously high rates?, *The Cryosphere Discussions*, *2*, 673–710.

Straneo, F., R. G. Curry, D. A. Sutherland, G. S. Hamltion, C. Cenedese, K. Våge, and L. A. Stearns (2011), Impact of fjord dynamics and glacial runoff on the circulation near Helheim Glacier, *Nature Geoscience*, *4*, 322-327.

Straneo, F., G. S. Hamilton, D. A. Sutherland, L. A. Stearns, F. Davidson, M. O. Hammill, G. B. Stenson, and A. R. Asvid (2010), Rapid circulation of warm subtropical waters in a major glacial fjord in East Greenland, *Nature Geoscience*, *3*, 182-186, doi:10.1038/NGEO764.

Thomas, R. H., W. Abdalati, E. Frederick, W. Krabill, S. Manizade, and K. Steffen (2003), Investigation of surface melting and dynamic thinning on Jakobshavn Isbrae, Greenland, *Journal of Glaciology*, *49*(165), 231-239.

Thomas, R. H., E. Frederick, W. Krabill, S. Manizade, and C. Martin (2009), Recent changes on Greenland outlet glaciers, *Journal of Glaciology*, *55*(189), 147-162.

van den Broeke, M., J. Bamber, J. Ettema, E. Rignot, E. Schrama, W. J. van de Berg, E. van Meijgaard, I. Velicogna, and B. Wouters (2009), Partitioning Recent Greenland Mass Loss, *Science*, *326*, 984-986.

Vieli, A., J. A. Jania, and K. Lezek (2002), The retreat of a tidewater glacier: observations and model calculations on Hansbreen, Spitsbergen, *Journal of Glaciology*, *48*(163), 592-600.

Vieli, A., and F. M. Nick (2011), Understanding and modelling rapid dynamic changes of tidewater outlet glaciers: issues and implications, *Surveys in Geophysics*, *32*, 437-485.

Warren, C. R., and N. F. Glasser (1992), Contrasting response of south Greenland glaciers to recent climatic change, *Arctic and Alpine Research*, *24*(2), 124-132.

Zeeberg, J., and S. L. Forman (2001), Changes in glacier extent on north Novaya Zemlya in the Twentieth Century, *The Holocene*, *11*(2), 161-175.

Chapter 5: Basal topographic controls on rapid retreat of Humboldt Glacier, northern Greenland

Carr, J.R., Vieli, A., Stokes, C.R., Jamieson, S.S.R , Palmer, S., Christoffersen, P., Dowdeswell, J.A., Blankenship. D. and Young, D. *To be submitted to Geophysical Research Letters*.

Outline: Humboldt Glacier, northern Greenland, retreated rapidly from 1999 onwards, coincident with atmospheric warming and sea ice decline. However, retreat rates were an order of magnitude greater on the northern section of the terminus than the southern section, despite the same initial forcing. This was attributed to the presence of a large subglacial trough beneath the northern section, which extends up to 72 km inland. Numerical modelling experiments suggest that this order of magnitude difference in retreat between the two sections of the terminus persists when sea ice buttressing is reduced and for moderate air temperature warming related increases in crevasse water depth. If present retreat rates persist, the northern section of the terminus will remain in the trough for approximately 170 years and may therefore facilitate substantial and sustained ice loss during the 21st Century and beyond.

Motivation: Humboldt Glacier was chosen to investigate the impact of basal topography on glacier dynamics, as it provides an excellent natural experiment to evaluate this control: the two sections of its terminus are subject to the same external forcing and are part of the same glacier system, but have very different basal topographies. Furthermore, Humboldt Glacier is very wide and so the influence of fjord width variation on retreat rates is likely to be minimal [*Raymond*, 1996]. This allows us to separate the influence of basal topography from fjord width variability, which is often difficult on smaller outlet glaciers. Finally, Humboldt Glacier is one of the major Greenland outlet glaciers, but comparatively little is known about its contemporary behaviour, making it important to quantify its recent retreat and potential contribution to future mass loss.

Contribution: My contribution to this paper was to complete the GIS and data analysis tasks (e.g. image processing, data acquisition and data processing), write the text, create the figures and lead the paper development. I also carried out the numerical modelling experiments, with technical assistance from S. Jamieson and A. Vieli. Basal topographic data was provided by S. Palmer, P. Christofferson and J. Dowdeswell and was processed originally by D. Blakenship and D. Young. At this stage, editorial input and guidance on the development of the research was provided by some co-authors (C. Stokes, S. Jamieson, A. Vieli, S. Palmer and J. Dowdeswell). For the purposes of this thesis, the paper draft has been modified and the 'Supplementary Information' associated with the paper has been integrated into the body text.

Abstract

Accelerated discharge from marine-terminating outlet glaciers accounts for approximately half of the contemporary mass loss from the Greenland Ice Sheet. However, the factors driving this dynamic response are not fully understood and contribute significantly to uncertainties surrounding ice sheet response to climate change and its contribution to near-future sea level rise. Here we assess the climatic and basal topographic controls on the behaviour of Humboldt Glacier (HG), northern Greenland, which is the widest glacier on the Greenland Ice Sheet and is a major outlet of its northern sector. Thinning and mass loss were observed on HG during the 1990s, but its contemporary dynamics and the factors driving its behaviour have yet to be investigated. We demonstrate that HG retreated rapidly from 1999, coincident with an atmospheric warming trend of 0.1 °C per year summer and sea ice decline. Significantly, retreat rates were an order of magnitude greater on the northern section of the terminus, where response to forcing was strongly modulated by a major basal trough. Radar echo-sounding data shows that this trough extends up to 72 km inland, highlighting the potential for sustained and substantial mass loss and retreat during the 21st century and beyond. Moreover, sensitivity experiments using numerical modelling demonstrate that the northern section shows an order of magnitude greater response

to reduced sea ice buttressing and to increases in crevasse water depth (which approximates the influence of atmospheric warming and increased meltwater input, via enhanced hydrofracture of crevasses) than the southern section. Results therefore demonstrate the potential for basal troughs to generate order of magnitude differences in retreat rates and dynamic response to external forcing on major Greenland outlet glaciers.

5.1. Introduction

The Greenland Ice Sheet (GrIS) has rapidly lost mass during the past decade [*Jacob et al.*, 2012], with approximately half of the deficit being attributed to accelerated discharge from marine-terminating outlet glaciers [*Rignot et al.*, 2008; *van den Broeke et al.*, 2009]. Consequently, identifying the dominant controls on marine-terminating outlet glacier dynamics is critical for accurate prediction of 21st century sea level rise [*IPCC*, 2013]. However, substantial uncertainty remains over the drivers of observed changes [*IPCC*, 2007], with air temperatures, ocean temperatures and sea ice concentrations being identified as potential forcing factors [e.g. *Carr et al.*, 2013a; *Holland et al.*, 2008; *Howat et al.*, 2008; *Vieli and Nick*, 2011].

Recent studies have demonstrated that Greenland outlet glaciers can retreat rapidly in response to external forcing [e.g. *Howat et al.*, 2008; *Joughin et al.*, 2008a; *Moon et al.*, 2012] and have also underscored the role of local factors, particularly basal topography and fjord width variations, in modulating their response [*Carr et al.*, 2014; *Carr et al.*, 2013a; *Enderlin et al.*, 2013; *Jamieson et al.*, 2012; *Moon et al.*, 2012]. These topographic factors can produce substantial variations in local retreat rates at a range of timescales, from seasonal to internnual changes [e.g. *Carr et al.*, 2013b; *Enderlin et al.*, 2013] through to major still-stands and periods of potentially catastrophic retreat during deglaciation [E.g. *Hughes*, 1986; *Mercer*, 1968; *Warren and Hulton*, 1990]. This highlights the danger of extrapolating patterns of behaviour from a small number of study glaciers [*Carr et al.*, 2014; *McFadden et al.*, 2011; *Moon et al.*, 2012].

The potential impact of basal topography on the dynamics of marine-terminating glacier and ice sheets has long been recognised [e.g. *Meier and Post*, 1987; *Weertman*, 1974] and has been proposed as a potential mechanism for collapse of the West Antarctic Ice Sheet (WAIS) during the last interglacial [*Mercer*, 1968]. However, its influence on the recent and future response of contemporary Arctic outlet glaciers has not been extensively assessed, due to the limited availability of high-resolution subglacial topographic data.

Here we investigate the multi-decadal behaviour of Humboldt Glacier (HG) (Fig. 5.1), northern Greenland, in relation to basal topography and atmospheric and oceanic forcing (the term 'oceanic' includes sea ice and sea surface temperatures). HG is the widest marine-terminating outlet glacier in Greenland, with a calving front width of ~90 km [*Weidick*, 1995] and drains approximately 3 % of the ice sheet [*Rignot and Kanagaratnam*, 2006]. Previous studies reported negative mass balance, grounding line retreat and thinning during the 1990s [*Abdalati et al.*, 2001; *Joughin et al.*, 1999; *Rignot et al.*, 2001]. However, HG's recent dynamics and the factors driving its behaviour have yet to be investigated. Moreover, ice thickness profiles indicate that the bedrock is substantially deeper beneath the northern portion of its terminus, in comparison to the southern section [*Joughin et al.*, 1999], which enables us to assess the impact of this varying basal topography on HG's response to forcing.

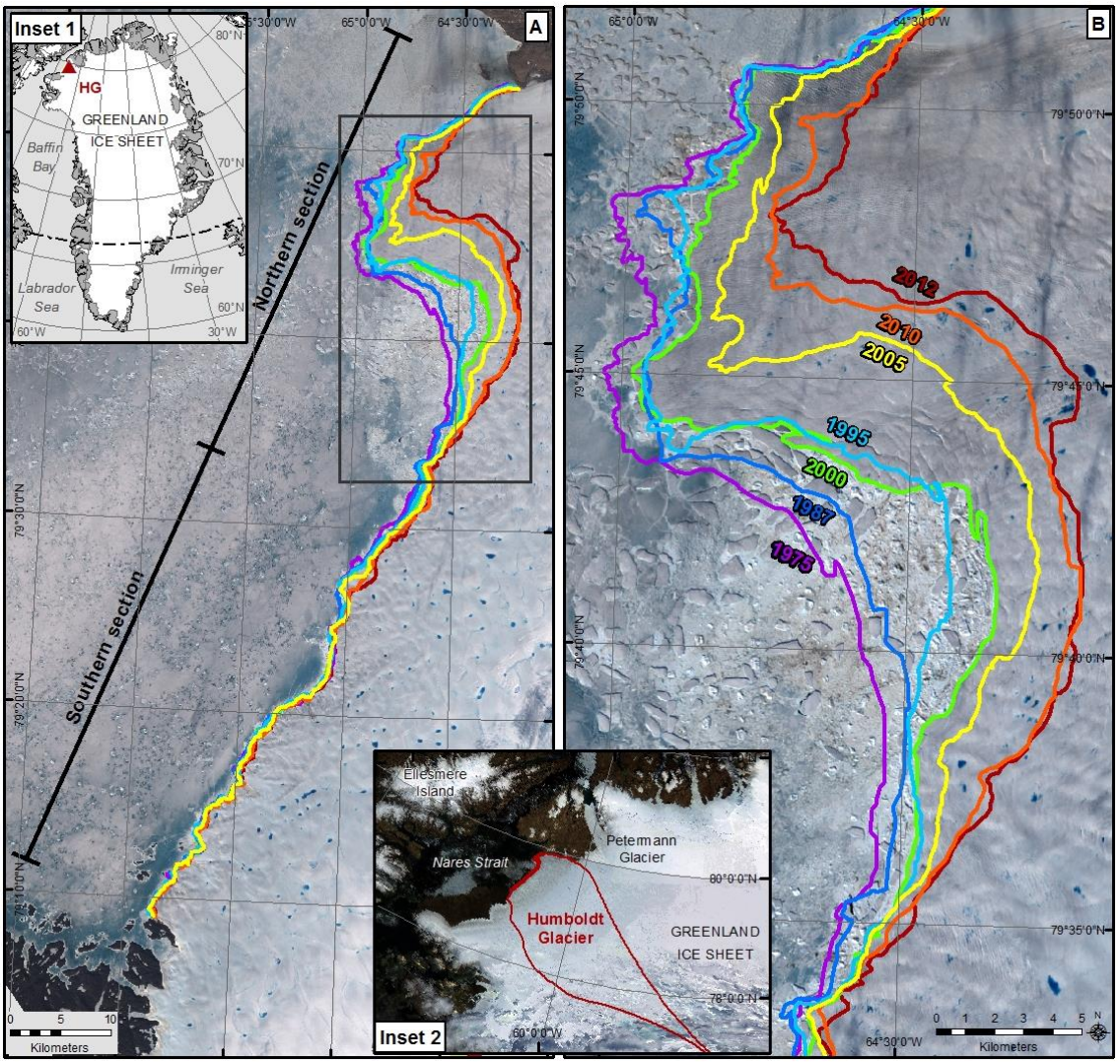

Figure 5.1. *Frontal retreat of Humboldt Glacier between 1975 and 2012. Frontal positions are displayed for selected years between 1975 and 2012 for (a) the entire terminus and (b) the northern section of the terminus. Frontal positions are coloured-coded according to year and were selected as close as possible to 31st July for each year. All frontal position measurements are shown in Fig. 5.2. Image source: Landsat, acquired 28th June 2000, provided by USGS GLOVIS. Inset 1: Location of Humboldt Glacier (HG) on the Greenland Ice Sheet. Inset 2: Location of Humboldt Glacier catchment in relation to surrounding topography and glacial features. Image source: MODIS Aqua, acquired 5th August 2012, provided by USGS GLOVIS.*

5.2. Methods

We use a range of remotely sensed datasets to assess frontal retreat at HG in relation to atmospheric and oceanic forcing and basal topography. Numerical modelling was used to further investigate glacier sensitivity to the primary controls identified from the

remotely sensed data, specifically air temperatures and sea ice. The data required for this assessment were available for the period 1975 to 2012 and were compiled at a monthly to decadal resolution, dependant on availability.

5.2.1. Frontal position data

Frontal positions were manually digitised from Synthetic Aperture Radar (SAR) Image Mode Precision imagery, provided by the European Space Agency (ESA) (1992 to 2012), and from Landsat data obtained from the USGS GLOVIS (http://glovis.usgs.gov/) (1975 to 2012). Following previous studies [*Carr et al.*, 2013b; *McFadden et al.*, 2011; *Moon and Joughin*, 2008], frontal positions were digitised from sequential images, within a reference box of fixed width and upstream extent (Fig. 5.2). The mean change in frontal position was calculated by dividing the change in the area of the reference box by its width. This improves upon the use of a single reference point at the centreline, as it accounts for uneven retreat rates across the terminus and is therefore more representative measure of frontal position change [*Howat et al.*, 2008; *Moon and Joughin*, 2008]. Retreat was calculated relative to 6th August 1975. Frontal position errors were evaluated by repeatedly digitising sections of rock coastline from a subset of 15 SAR and Landsat images. The resultant mean error in frontal position was 42.4 m.

5.2.2. Atmospheric and oceanic data

Surface air temperature (SAT) data were obtained from Qaanaaq (69°13'W 77°28'N) and Qaanaaq Mittarfik (69°23'W 77°29'N) meteorological stations, which are located 190 km from HG. Data were provided by the Danish Meteorological Institute at a temporal resolution of three hours [*Carstensen and Jørgensen*, 2011]. Data were filtered to account for missing values and were only used in the calculation of monthly/annual averages if the following criteria were met [Cappelen, 2011]: i) no more than two consecutive records were missing in a day; ii) no more than three records in total were missing in a day; iii) daily averages were available for 22 or more days per month and; iv) monthly averages were available for all months of the year. In order to extend the temporal coverage of the data, records were used from Qaanaaq between

Jan 1996 and Aug 2001 and from Qaanaaq Mittarfik between Sept 2001 and Dec 2010. The two stations are located 1.9 km apart. The variation between the two stations was assessed by comparing mean monthly values for the period of data overlap (Aug 2001 – Oct 2004) and the average difference was 0.28 °C. Data were then used to calculate mean summer (JJA) and mean annual air temperatures and the number of positive degree days per year.

Meteorological data were not available for the entire study period and Qannaaq is located 190 km from HG. Thus, reanalysis data were also used to assess air temperature changes. These were obtained from NCEP/NCAR Reanalysis 1, which has a spatial resolution of 2.5° (~230 km x 280 km at 76 °N) [*Kalnay et al.*, 1996] and ERA-Interim reanalysis, which has a spatial resolution of 0.75° (~70 km x 80 km at 76 °N) [*Dee et al.*, 2011]. In both cases, air temperature values from the 700 mb geopotential height were used, as their correlation with meteorological station data is better than values from 2 m height (A. Gardner, pers. comm., 2013) and the influence of SSTs on air temperature values is reduced [*Moholdt et al.*, 2012]. Trends in mean annual air temperatures were calculated from both reanalysis datasets

Sea ice data were extracted from charts provided by the National/Naval Ice Centre (NIC) (http://www.natice.noaa.gov/), which are compiled from a range of remotely sensed and directly-measured data sources and have a spatial resolution of up to 50 m. Sea ice values were sampled from a polygon extending the full width of the glacier terminus, as defined in the land mask of the sea ice product, and 50 m perpendicular to it. These values were then used to calculate seasonal means.

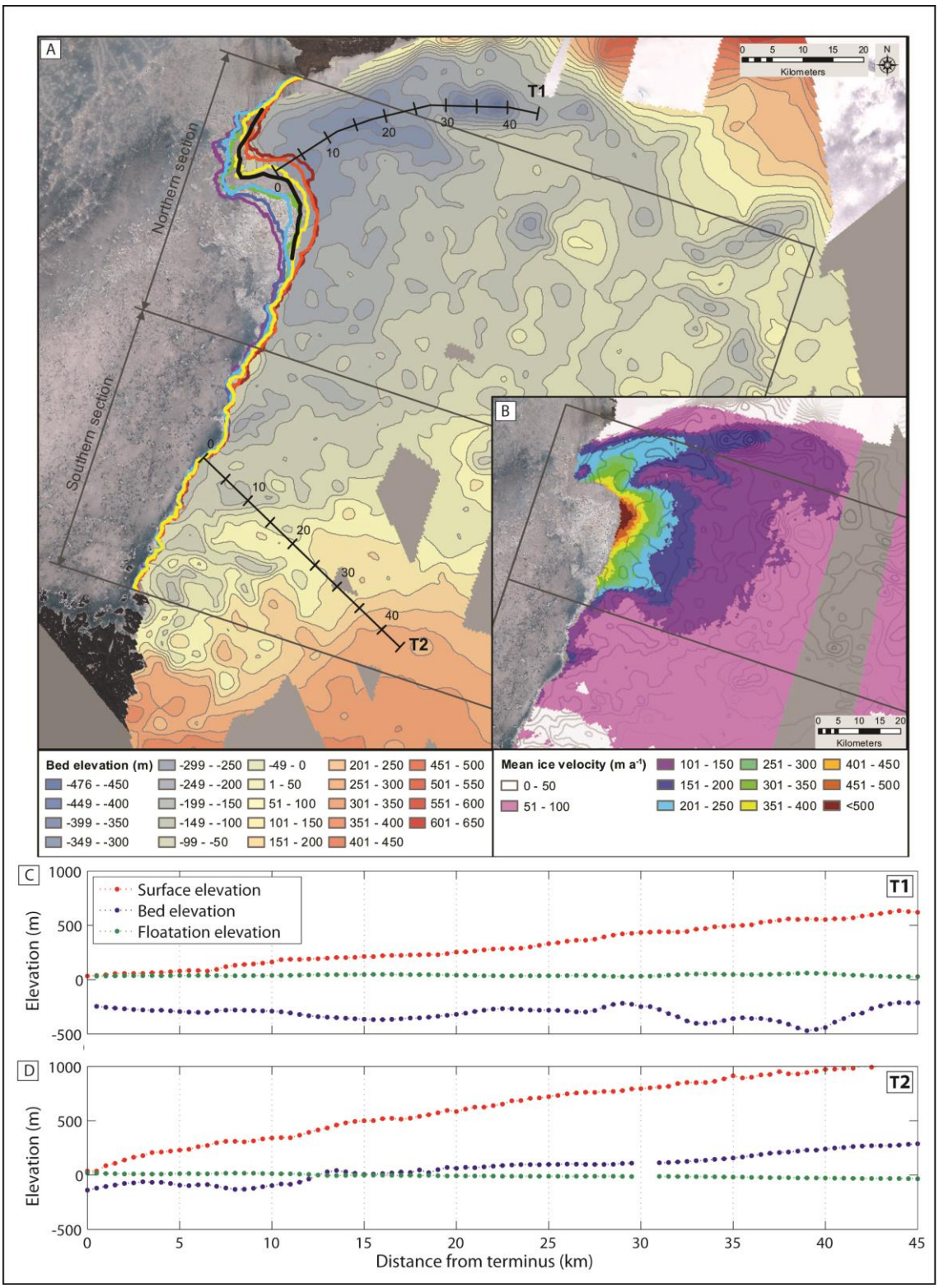

Figure 5.2. *Basal topography and surface elevation profiles for Humboldt Glacier. A) Basal topography of HG. Frontal positions are colour-coded as in Fig. 5.1 and transects are shown in black, with distance markers in km. The section of terminus used to calculate potential future mass loss is shown by the thick black line. Reference boxes used to repeatedly digitise frontal positions are shown in dark grey and the northern and southern sections of the terminus are marked. B) Mean ice velocity field for HG (colour scale), overlain* on basal topography

(greyscale). Mean velocities were calculated from all available MEaSUREs winter ice velocity grids [*Joughin et al.*, 2010b]. *Surface elevation, basal topography and floatation elevation for transects along C) the fast-flowing section of the northern terminus and* ***D)*** *the southern terminus. Elevation data were sampled at 500 m intervals from the 2007 glacier terminus and transects followed the approximate flow direction.*

Sea Surface Temperature (SST) data were obtained from two sources: i) monthly SST climatology products acquired by MODIS (Moderate Resolution Imaging Spectroradiometer) (spatial resolution 5 km), which were provided by the NASA Ocean Color Project (http://oceancolor.gsfc.nasa.gov/); and ii) the Reynolds SST analysis data set Version 2 (spatial resolution 0.25°), provided by NOAA [*Reynolds et al.*, 2007]. SST values were sampled from all grid squares within 25 km of the terminus of HG from the MODIS data. Due to the comparatively coarse resolution of the Reynolds data, SSTs were sampled from the grid squares closest to HG's terminus.

For all atmospheric and oceanic forcing data, the statistical significance of trends was evaluated using the t-statistic. The t-statistic is used to evaluate whether the coefficient associated with a given independent variable is significantly different from zero, given the variation in the data, and it is calculated by dividing the coefficient by the standard error. In this case, the t-statistic is used to evaluate whether the trend in a given forcing factor (e.g. mean annual air temperatures) over time is significantly different from zero, taking into account the variations in individual values of that forcing factor. The t-statistic is associated with a p-value, which tests the probability of obtaining a value of the t-statistic that is at least as extreme as the one observed, if the null hypothesis true. We use a significance interval of 0.05 (i.e. a confidence interval of 95%), meaning that p-values of less than or equal to 0.05 shows that the coefficient is significantly different from zero.

5.2.3. Basal topography, surface elevation and ice velocity data

Basal topographic data were acquired by the Greenland Outlet Glacier Geophysics (GrOGG) project using airborne laser altimetry (Palmer et al., in prep). Data were

acquired in May 2012 using the High-Capability Radar Sounder (HiCARS, Peters et al., 2005). Survey lines were flown parallel to the ice flow direction, at a constant height of 800 m above the ice surface, and perpendicular to the ice flow direction, at a constant altitude for each perpendicular survey line. Ice thickness measurements from previous airborne surveys conducted by CReSIS [*Gogineni et al.*, 2001] and NASA's Operation IceBridge [*Koenig et al.*, 2010] were incorporated to improve data coverage. Ice surface elevations were supplemented with data from the Greenland Ice Mapping Project (GIMP) DEM [*Howat et al.*, 2012]. Bed elevations were calculated by interpolating all ice thickness data onto a 500 m grid, removing areas more than 5 km from any survey line and then subtracting them from the combined laser-altimeter/GIMP ice surface DEM, also resampled to 500 m (Palmer et al., in prep).

Surface elevation data were obtained from the Greenland Mapping Project (GIMP) Digital Elevation Model (DEM) [*Howat et al.*, 2012]. The DEM is constructed from ASTER and SPOT-5 DEMs for the study area. The data are registered to ICESat elevations for 2003 to 2009 and the DEM therefore has a nominal date of 2007. The root-mean-squared error across the ice sheet, relative to ICESat, is ±10 m. This ranges from approximately ± 1 m over most ice surfaces to ± 30 m in areas of high relief [*Howat et al.*, 2012]. Given the nominal date of the DEM, surface profiles were taken from the closest frontal position to mid-summer in 2007 (24th July 2007), in order to avoid including sea ice in the elevation profile. Surface elevations were sampled at 500 m intervals from the 2007 terminus, along transects following the approximate ice flow direction [*Howat et al.*, 2012].

Surface and basal elevations were sampled at 500 m intervals from the calving front, along two along-flow transects that were representative of the two sections of the terminus (Fig. 5.2), with the northern section (T1) being underlain by the basal trough (Fig. 5.2). Basal and surface elevations were used to calculate floatation elevations along each transect, assuming a value for ice density of 0.910 kg km^3 [*Cuffey and Paterson*, 2010] and 1.028 kg km^3 for ocean density. Ice surface velocity data were

obtained from the winter ice-sheet-wide velocity maps for the GrIS, developed as part of the MEaSUREs program [*Joughin et al.*, 2010b]. A mean velocity field for HG was calculated using all available velocity maps (winter 2000/01, 2005/06, 2006/07, 2007/08 and 2008/09).

5.2.4. Numerical modelling

5.2.4.1. Model description

We use a 1-dimensional flowline model for the numerical modelling experiments, which is described in detail in *Nick et al.* [2010] and has previously been used to investigate the behaviour of large Greenland outlet glaciers and their response to external forcing [*Nick et al.*, 2012; *Nick et al.*, 2013; *Vieli and Nick*, 2011]. It is used to calculate the evolution of the ice surface, ice flow and stress field for the two along-flow transects detailed above (Fig. 5.2). The model calculates width- and depth-averaged stresses, where the driving stress (τ_d) is balanced by resistive stresses from the base (τ_b) and lateral margins (τ_{lat}) and by the along-flow stress gradients, $\frac{\partial \tau_{xx}}{\partial x}$, in the ice flow direction (x):

$$\frac{\partial \tau_{xx}}{\partial x} + \tau_b + \tau_{lat} = \tau_d \quad (1)$$

We assume a non-linear sliding relation [*Weertman*, 1957] that is a function of the effective pressure at the bed (N). The stress balance (Equation 1) gives the following expression for depth- and width-averaged ice flow (u), for an ice thickness of (H) and half-width (W):

$$2\frac{\partial}{\partial x}\left(Hv\frac{\partial u}{\partial x}\right) - \beta\left(\frac{u}{N}\right)^{1/m} + \frac{H}{W}\left(\frac{5u}{2AW f_{lat}}\right)^{1/n} = \rho_i g H \frac{\partial S}{\partial x} \quad (2)$$

Where ρ_I is ice density (910 kg m^{-3}), g is gravitational acceleration, S is the ice surface, β is the basal sliding coefficient [*Weertman*, 1957], *n* and *m* are the exponents for ice

flow and sliding relations, respectively, and are set as 3, and f_{lat} is the buttressing factor. *A* is the flow rate factor [*Glen*, 1955] that relates to ice rheology and is set to a value of 1.16 x10^{-18} Pa^{-3} a^{-1}, which equates to an ice temperature of -30 °C. Equation (2) is solved for the width-averaged ice flow *(u)* by iterating for effective viscosity (*v):*

$$v = A^{-1/n} \left| \frac{\partial u}{\partial x} \right|^{\frac{1-n}{n}} \tag{3}$$

Variations in surface accumulation (*a*) and width with distance along flow (W) are explicitly accounted for in calculations of surface elevation change along the flow line:

$$\frac{\partial H}{\partial t} = a - \frac{1}{W} \frac{\partial (uHW)}{\partial x} \tag{4}$$

The model allows the glacier terminus to move freely using a physically based calving model [*Nick et al.*, 2010] and the approach to simulating grounding line motion is consistent with boundary layer theory [*Schoof*, 2007] and thus overcomes previous issues relating to model numerics [*Vieli and Payne*, 2005]. The horizontal grid resolution adjusts with each time step, meaning that the grounding line position can be accurately tracked over time [*Vieli and Payne*, 2005]. The model includes a dynamic calving model, which is the best currently available and is based on the depth of both surface and basal crevasses: calving occurs when surface and basal crevasses penetrate the full ice thickness [*Nick et al.*, 2010]. Using this calving criterion, the terminus is not necessarily at floatation, but instead can be above floatation. Where the glacier is at floatation, which is usually the case very close to the calving front, the velocity boundary condition at the calving front is calculated from the longitudinal stress that balances the difference in hydrostatic pressure between the ice front and the ocean [*Vieli and Payne*, 2005], and is given by:

$$\left.\frac{\partial u}{\partial x}\right|_f = f_s A\left[\frac{\rho_i g}{4}\left(1-\frac{\rho_w}{\rho_i}\right)\right]^n H_f^n \quad (5)$$

where horizontal velocity gradient with along-flow distance x is evaluated at the terminus. The parameter ρ_w is the density of ocean water (1028 kg m^{-3}) and H_f is ice thickness at the terminus, D_f is the ice thickness below the water line (water depth at the terminus when grounded). The parameter f_s is used to scale the rate factor (A) in the perturbation experiments described in Section 5.2.4.3. It is used to simulate sea-ice-induced changes in longitudinal strain rates and is set to 1 in the reference state, where no perturbation is applied [*Nick et al.*, 2013].

5.2.4.2. Model input data and initial setup

The modelling undertaken here does not aim to reproduce nor to predict in detail the evolution of Humboldt Glacier but instead aims to explore differences in the sensitivity of the two profiles defined on the northern and southern sections of the terminus to external forcing factors. Thus, we have set up approximate geometries of these two profiles, using data on basal topography, surface elevation and terminus retreat. Remotely sensed data from the two transects defined above (Fig. 5.2) were used as initial input for the numerical model, to build up initial states for the perturbation experiments. The data source for each initial parameter required by the model is given in Table 5.1. These values were calculated separately for each transect, e.g. surface mass balance was calculated across the area draining into the northern and southern sections respectively. In order to calculate the width for each section, the drainage basin extent for HG from *Joughin et al.* [1999] was used to delineate the outer margins of the northern and southern catchments. The divide between the two sections was then determined from a combination of the surface DEM and Landsat imagery (Table 5.1). For each transect, the width was calculated at 500 m intervals along the transect, at the sample locations used to extract the surface and basal elevations (Section 5.2.3).

This was done by calculating the distance between the outer margin and inner divide perpendicular to the transect at the sample point. For each transect, the model was run with these input parameters for 2,000 years. The initial grid resolution was 500 m. The basal sliding coefficient was then adjusted so that modelled retreat rates approximately fitted rates observed at each transect between 1976 and 1999. This was taken as the 'initial state' prior to rapid retreat from 1999 onwards. Perturbation experiments were then applied to these initial reference states.

Parameter	**Data source**
1. Bed elevation	Palmer et al. In prep and Cresis/IceBridge flightline data
2. Ice surface elevation	GIMP DEM [*Howat et al.*, 2012]
3.Ice thickness	1 and 2
4.Ice velocity	MEaSURES velocity grids [*Joughin et al.*, 2010b]
5. Glacier width	Defined using GIMP DEM [*Howat et al.*, 2012] and Landsat imagery [USGS GLOVIS]
6. Ablation	RACMO modelled melt [*van den Broeke et al.*, 2009]
7. Accumulation	Greenland Ice Sheet Snow Accumulation Grids [*Burgess et al.*, 2010]
8. Surface mass balance	6 & 7

Table 5.1. *Input parameters and data sources for numerical modelling experiments*

5.2.4.3. Perturbation experiments

To the initial reference states we applied perturbations associated with changes in atmospheric and sea-ice forcing, which our observations suggest are primary controls (Fig. 5.3). Air temperature warming is approximated by increasing the water-level parameter within crevasses and hence the increasing the crevasse depth [*Nick et al.*, 2010; *Nick et al.*, 2013]. This approach has been used in numerous previous studies that employed the model to assess outlet glacier response to air temperature warming [*Nick et al.*, 2012; *Nick et al.*, 2010; *Nick et al.*, 2013; *Vieli and Nick*, 2011] and is the best method currently available for applying this perturbation [*Nick et al.*, 2010].

Following *Nick et al.* [2013], changes in the potential buttressing effect of sea-ice, which could result from weakening and/or thinning of the sea ice, are applied by altering the rate factor (A, here 1.16 x10^{-18} Pa^{-3} a^{-1}) using the parameter f_s (Equation 5). Initially, f_s is set to a value of 1, when no perturbations are applied. Higher values of f_s increase the longitudinal strain-rate at the terminus and thus simulate a reduction in sea ice buttressing [*Nick et al.*, 2013].

Step-changes in crevasse water depth and sea-ice buttressing were applied to each transect after an initial phase of 100 years with no perturbation: crevasse water depth was increased by 5, 10, 15, 20 and 25 m and reduced sea ice buttressing was simulated by increasing the factor (f_s) by 1.05, 1.1, 1.2, 1.5 and 2.0. Physically, f_s = 2.0 increases the terminus longitudinal strain-rate by a factor of two [*Nick et al.*, 2013]. The model was then run for a further 100 years. Crevasse water depth is very difficult to estimate and so we use values of up to 10 m as potentially realistic estimates [cf. *Cook et al.*, 2012] and then explore more extreme values. Note that we assess the differing sensitivity of the two sections to the same perturbation, rather than predicting the response of a single profile to forcing of a particular magnitude, meaning that the absolute perturbation values selected should have minimal impact on results.

SSTs showed no significant change during the study period and are therefore unlikely to be a primary control on retreat, so were not included in the numerical modelling experiments. The lack of sub-surface ocean temperature data and presence of subglacial meltwater plumes at HG makes it difficult to realistically model the impact of sub-surface warming on retreat rates. This control is therefore not evaluated here, but is highlighted as an important area for future work, both in terms of collecting the necessary sub-surface ocean data and the numerical model development to incorporate increased submarine melting from enhanced plume flow, driven by subglacial melt water.

5.3. Results

5.3.1. Frontal position, ice velocities and basal topography

Terminus-wide retreat rates at HG averaged 81 m a^{-1} between 1975 and 2012 (Figs. 5.1 & 5.3). Retreat showed two distinct phases: between 1975 and 1999 it was relatively gradual and slow (mean rate of 37 m a^{-1}), but thereafter it substantially increased (mean rate of 162 m a^{-1}) for the period 1999 to 2012 (Figs. 5.1 & 5.3). Moreover, our observations demonstrate a marked difference in the behaviour of the northern and southern sections of the terminus (Fig. 5.1). The northern section flows significantly faster (150 - 570 m a^{-1}) than the southern portion of the terminus (< 150 m a^{-1}) (Fig. 5.2B), which is consistent with the velocity pattern identified by previous studies [*Joughin et al.*, 2010a; *Rignot et al.*, 2001]. Mean retreat rates were an order of magnitude greater on the northern section of the terminus (147 m a^{-1}) than on the southern section (15 m a^{-1}) between 1975 and 2012 (Figs. 5.1 & 5.3). This spatial difference persisted between 1999 and 2012, when retreat rates averaged 289 m a^{-1} at the northern section and only 35 m a^{-1} at the southern section (Figs. 5.1 & 5.3).

The northern section of the terminus is situated in a basal trough that extends up to 72 km inland (Fig. 5.2A). Its depth is generally greater than 300m and reaches a maximum of 475 m (Fig. 5.2A). In contrast, the bedrock beneath the southern section is comparatively shallow, reaching a maximum depth of 220 m (Fig. 5.2A). On the northern transect, the terminus is close to floatation up to 6.5 km inland (Fig. 5.2C), whereas the southern section only comes close to floatation within 500 m of the ice front (Fig. 5.2D).

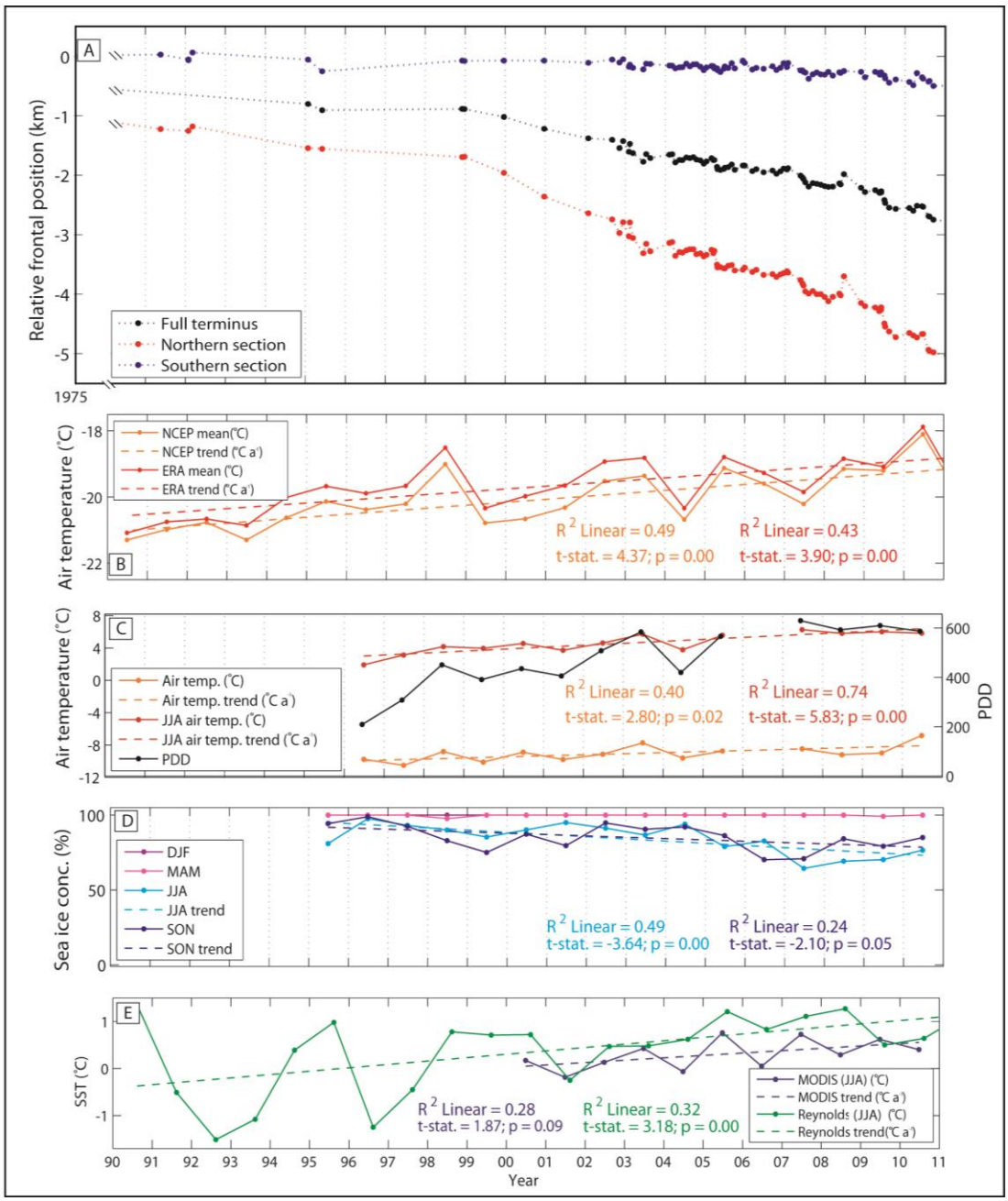

Figure 5.3. *Relative frontal position and forcing factors at HG. A) Frontal position of HG, relative to 6th August 1975 for the full terminus (black), northern section (red) and southern section (blue). B) Mean annual and mean summer (JJA) air temperatures from NCEP/NCAR and ERA-Interim reanalysis data at 700mb geopotential height. C) Mean annual and mean summer (JJA) air temperatures and number of positive degree days (PDD) at Qaanaq/ Qaanaaq Mittarfik meteorological stations. D) Mean seasonal sea ice concentrations for Dec–Feb (DJF), Mar-May (MAM), Jun-Aug (JJA) and Sep-Nov (SON). E) Sea surface temperatures from MODIS (blue) and Reynolds (green line) SST products for Jun-Aug. The statistical significance of trends in forcing factors is evaluated using the t-statistic and associated p-value: a p-value of 0.05 or less is considered to be statistically significant.*

5.3.2. Atmospheric and oceanic forcing

Frontal retreat was coincident with a linear warming trend of 0.1 °C a^{-1} in both the NCEP/NCAR (R^2 = 0.49, t-statistic = 4.37, p-value <0.01) and ERA-Interim (R^2 = 0.43, t-statistic = 3.90, p-value <0.01) reanalysis data between 1990 and 2010 (Fig. 5.3B). Trends were statistically significant at a confidence interval of 0.05. Paired t-test results showed that the mean air temperature for the ten years following the onset of retreat (1999-2008) were statistically warmer than any of the preceding ten year intervals from 1949 to 1999 at a confidence level of >0.05. Although the meteorological record is incomplete and extends only from 1996 to 2010, it shows a similar trend of 0.1 °C a^{-1} (R^2 = 0.40, p= 0.02), which is significant at the 0.05 significance interval (Fig. 5.3C). Warming was particular marked during the summer months (Jun-Aug), with air temperatures increasing by 0.2 °C a^{-1} between 1996 and 2010 (R^2 = 0.74, p< 0.01) (Fig. 5.3C). The number of positive degree days (PDDs) rose markedly during the period of rapid retreat, increasing from 208 in 1996 to 597 in 2010 (Fig. 5.3C). Interannual data demonstrate that the onset of seasonal retreat closely followed air temperatures increasing above freezing (Figs. 5.4A & C), with retreat generally beginning in June and air temperatures rising above freezing at the end of May.

Frontal retreat was also concurrent with reduced summer (JJA) and Autumn (SON) sea ice concentrations (Fig. 5.3A & D). Between 1995 and 2010, JJA sea ice concentrations reduced by 1.5% per year (R^2 = 0.49, t-statistic = -3.54, pvalue = 0.00) and SON values declined by 0.9% per year (R^2 = 0.24, t-statistic = -2.10, pvalue = 0.05). The largest seasonal retreats occurred during 2007 and 2009, when summer (JJA) sea ice concentrations were low (Figs. 5.4B & D). Sea surface temperatures (SSTs) from both the MODIS and Reynolds datasets showed no statistically significant trend at the 0.05 significance level during the study period (Fig. 5.3E).

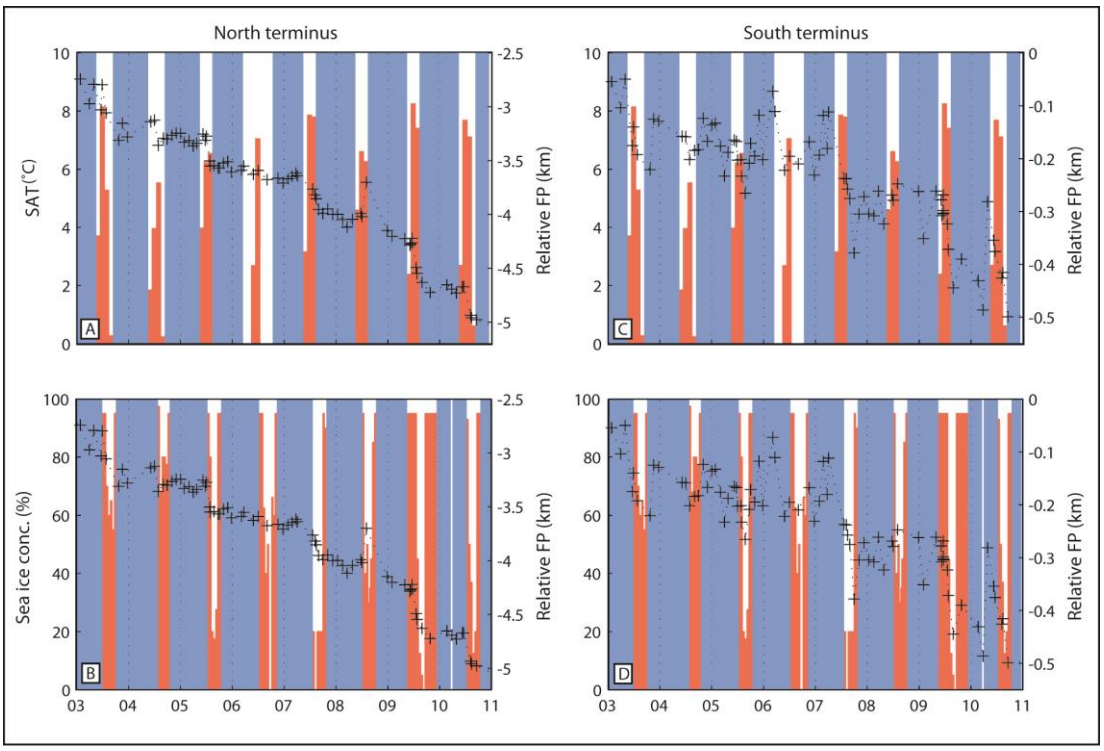

Figure 5.4*: Glacier frontal position relative to 1974 (black crosses, more negative values show retreat) and seasonal climatic/oceanic forcing factors for the northern terminus (left-hand panels) and southern section (right-hand panels). Panels A & C: Mean monthly air temperatures for Qaanaaq/ Qaanaaq Mittarfik meteorological stations, plotted in red for temperatures above 0˚C and blue for temperatures below 0˚C. Panels B & D: Mean monthly sea ice concentrations are plotted in percent, with fast ice (i.e. 100 %) in blue and all other values in red.*

5.3.3. Numerical modelling

Numerical modelling experiments were used to assess the sensitivity of glacier frontal position on both sections of the terminus to reduced sea ice concentrations and to warmer air temperatures, via increases in crevasse water depth (Fig. 5.5). Modelled retreat rates were more than an order of magnitude greater on the northern transect than on the southern, for all percentage reductions in sea ice buttressing (Fig. 5.5). For example, retreat was 13 times greater on the northern transect when buttressing was reduced by 5 or 10 % and was between 15 and 16 times greater for a reduction of 15 to 25 % (Fig. 5.5). Increasing crevasse water depth by 5 and 10 m produced retreat rates which were 15 and 16 times greater on the northern section, respectively. For larger increases in crevasse water depth, however, we note that the difference in

retreat rates between the two sections was less pronounced and ranged between 5 times greater for an increase of 15 m, and 3 times greater for a 25 m increase (Fig. 5.5).

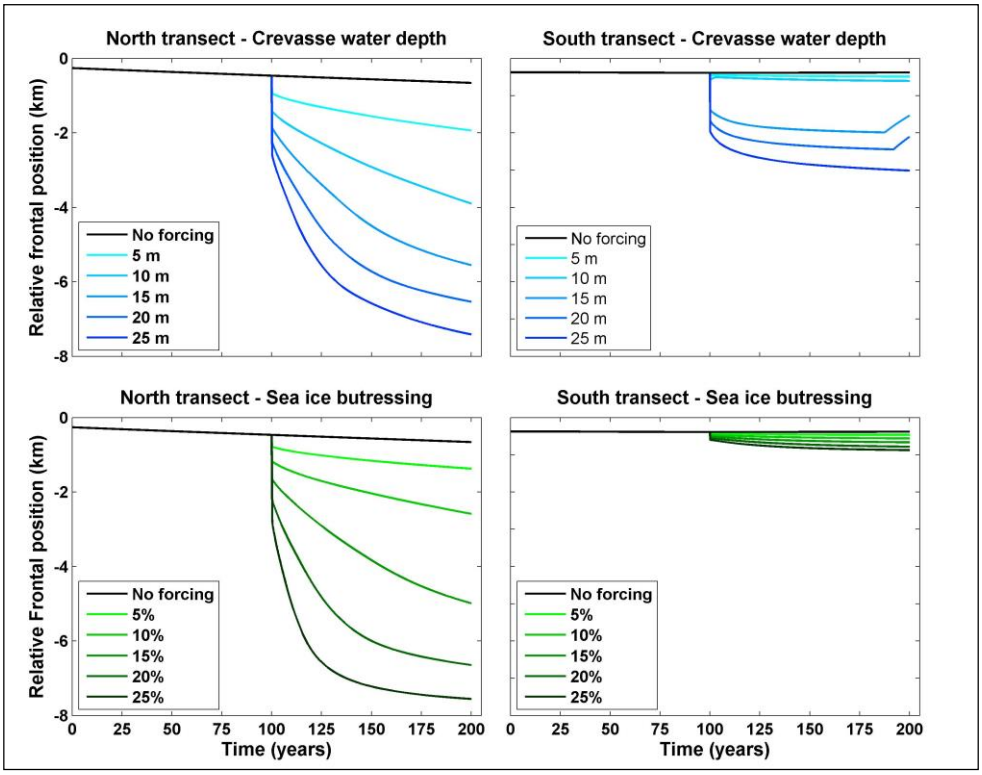

***Figure 5.5**. Numerical modelling experiments showing changes in relative frontal position over time for Transect 1 (left panels) and Transect 2 (right panels). A step increase in crevasse water depth (top panels) and a step reduction in sea ice buttressing (bottom panels) were applied after 100 years. Note that the retreat trends before the perturbations were applied were adjusted to match retreat rates between 1976 and 1999, which were taken as the 'initial state', prior to the onset of rapid retreat (see Section 5.2.4.2).*

5.4. Discussion

5.4.1. Atmospheric and oceanic controls on glacier behaviour

The association between frontal position change and atmospheric warming, particularly during summer, (Figs. 5.4A-C) suggests that increased air temperatures are linked to both seasonal and interannual retreat at HG. Increased summer air temperatures at HG would enhance meltwater availability, thus increasing the frequency of hydrofracture of terminus crevasses and would promote calving and retreat. This mechanism has been identified as a potential contributor to seasonal and interannual

retreat at Jakobshavn Isbrae, central-west Greenland [*Sohn et al.*, 1998; *Vieli and Nick*, 2011] . Evidence from satellite imagery supports this mechanism, as numerous water-filled lakes and crevasses are present within approximately 25 km of HG's northern terminus and are particularly prevalent over the lower ~ 7 km (Fig. 5.6), which is near floatation (Fig. 5.6). Notably, however, no water is observed in the large, rift-like crevasses that form with a few hundred metres of the ice front and from which the large, tabular icebergs subsequently calve (Fig. 5.6). We therefore suggest that hydrofracture may not necessarily cause the icebergs to detach from the terminus, but instead may open fractures near to the front, thus deepening crevasses and facilitating calving once the ice reaches the terminus. This is consistent with our numerical modelling results, which indicate that the northern section of HG is acutely sensitive to raising the water-level parameter within crevasses and hence the increasing the crevasse depth.

Meltwater inputs may also facilitate retreat by increasing the outflow of subglacial meltwater at the calving front. Buoyant subglacial meltwater plumes emerging at the terminus are thought to substantially increase submarine melt rates by promoting a compensatory inflow of warm water at depth [*Jenkins*, 2011; *Motyka et al.*, 2003; *Rignot et al.*, 2010; *Seale et al.*, 2011; *Straneo et al.*, 2011] and are visible at the terminus of HG in satellite imagery (Fig. 5.6). However, the lack of temperature and salinity data from HG's fjord precludes more detailed assessment of this mechanism. At present, buoyant plumes driven by subglacial meltwater outflow are not incorporated into the numerical models that are used to assess glacier response to forcing, yet evidence suggests that they may provide an important link between atmospheric warming, submarine melting and glacier response. We therefore highlight the need to incorporate plume flow into numerical models, in order to fully assess the influence of atmospheric warming on marine-terminating outlet glacier behaviour.

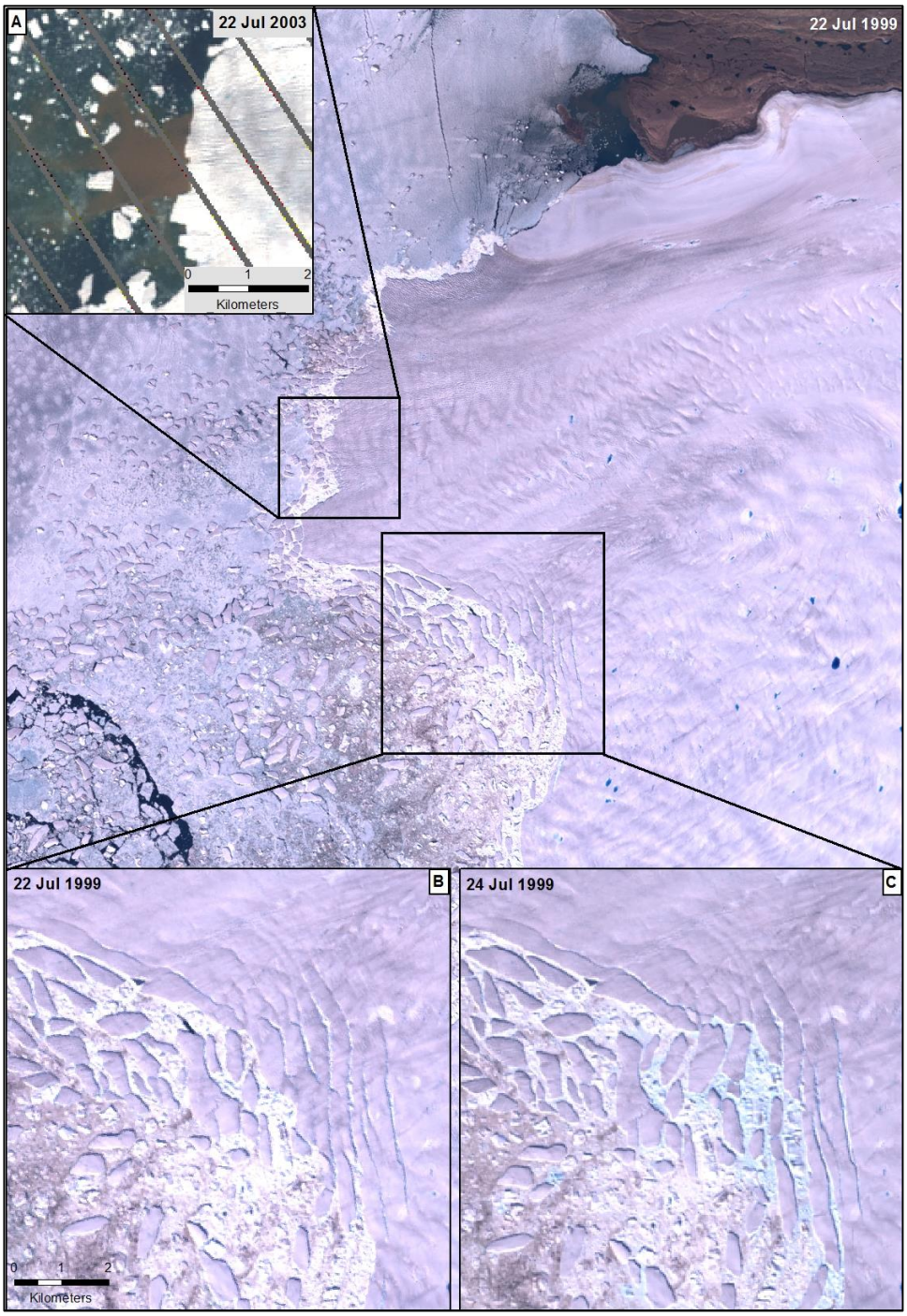

Figure 5.6: *Subglacial meltwater plume and the pattern of iceberg calving / rift formation on northern section of HG's terminus. A) Turbid meltwater plume exiting the calving front. B) & C) Large tabular icebergs calving back to rifts over a two day period.*

Retreat at HG coincided with a statistically significant negative trend in summer (JJA) sea ice concentrations of 1.5 % per year (Fig. 5.3). This indicates that sea ice decline may have contributed to retreat, potentially through extending the duration of seasonally high calving rates [*Amundson et al.*, 2010; *Howat et al.*, 2010; *Joughin et al.*,

2008b; *Seale et al.*, 2011]. The influence of sea ice on net frontal position is partly supported by interannual data, as the onset of seasonal retreat is coincident with spring-time sea ice loss in some years (e.g. 2005 & 2009), (Fig. 5.4). However, this relationship is not perennial (e.g. in 2007) and seasonal retreat persists substantially after winter sea ice formation in 2003 and 2007 (Fig. 5.4). This is supported by observations from satellite imagery which demonstrate that calving can occur whilst sea ice is present (Fig. 5.6). Moreover, comparatively large seasonal retreats occurred during years of high summer sea ice concentrations: seasonal retreat in 2003 was more than double the 2006 value, yet summer sea ice concentrations were comparable (Fig. 5.4). Despite an overall negative trend in sea ice concentrations during the rapid retreat phase, sea ice concentrations returned to pre-retreat values between 2002 and 2004, yet retreat rates remained relatively constant (Fig. 5.4). Taken together, this evidence suggests that sea ice is a significant control on net frontal position at HG, but that its influence is not straightforward and may be secondary to air temperatures.

At multi-year timescales, our numerical modelling results compare well with observations, as both indicate that reductions in sea ice concentrations result in glacier retreat (Figs. 5.3 & 5.5). However, the remotely sensed data suggest that this relationship is not linear and is complex at seasonal timescales, as calving can occur when the ice mélange is in place (Figs. 5.4 & 5.6). As our numerical modelling experiments were designed to evaluate interannual controls on HG's frontal position, they do not allow a full assessment of the interactions between sea ice and frontal position at seasonal timescales. We therefore highlight the need for further numerical modelling work at HG, which focuses specifically on the more complex seasonal-scale relationships between sea ice concentrations and glacier frontal position.

5.4.2. Differing response to forcing on the northern and southern sections

The northern and southern sections of HG exhibited very different retreat rates during the study period (Figs. 5.1 & 5.2), despite being subject to very similar initial forcing,

and we attribute this difference to the underlying basal topography (Fig. 5.2). The bed beneath the northern section is deep (max. depth = 475 m) in comparison to the southern section (max. depth = 220 m) and deepens up-glacier, whereas the southern section becomes shallower with distance inland (Fig. 5.2). Our data further indicate that the northern section is close to floatation across the lowest 6.5 km (Fig. 5.2B), in contrast to the grounded southern section (Fig. 5.2C). This is in agreement with previous ice thickness measurements [*Rignot et al.*, 2001], and is further supported by observations that on the northern section: i) calving is predominantly via large, tabular icebergs (Fig. 5.6) which are only thought to occur from floating termini [*Amundson et al.*, 2010]; ii) the terminus frequently calved back to large rifts visible on the glacier surface (Fig. 5.6), which are associated with near-floating ice [*Joughin et al.*, 2008a] and; iii) the surface profile is very flat close to the terminus (Fig. 5.2C).

Interestingly, the shape of the ice front and calving pattern on the northern section of HG (Fig. 5.1) resembles the calving bays identified by *Hughes* [2002]*Hughes* [2002]. It was proposed that these bays promoted accelerated retreat of marine-terminating sections of Quaternary ice sheets at the end of glacial cycles and may have facilitated the rapid retreat of the Hudson Strait Ice Stream into the Laurentide Ice Sheet interior towards the end of the last glacial period [*Hughes*, 2002]. The observed embayment at HG's northern terminus may therefore represent a smaller-scale example of these larger calving bays and may thus facilitate rapid retreat via similar mechanisms, specifically calving of slabs above the waterline and blocks beneath it [*Hughes*, 2002]. The near-floatation and deeper basal topography of the northern section have important implications for its response to external forcing. First, empirical studies have demonstrated a statistically significant relationship between water depth and calving rates [*Brown et al.*, 1982; *Pelto and Warren*, 1991], which is consistent with the higher rates of retreat and calving on the northern section (Fig. 5.1). Basal shear stresses are low over areas close to floatation, meaning that the relative contribution of longitudinal stresses to the force balance would increase [*Echelmeyer et al.*, 1994], given the large

width of the northern section (~45 km). This would lead to higher longitudinal stretching rates, which, together with dynamic thinning, would promote crevasse formation [*van der Veen*, 1998b]. As a result, the terminus would be more vulnerable to calving via hydrofracture and to full-thickness crevassing, as both basal and surface crevasses could form [*van der Veen*, 1998a & b]. Moreover, variations in longitudinal stresses associated with changes in sea ice buttressing would have a greater influence on retreat rates and calving.

In addition to being close to floatation, the differing response of the northern section to forcing likely stems from its deeper basal topography and greater ice thickness. If a glacier terminus is close to floatation, longitudinal stresses at the calving front increase linearly with ice thickness [*Schoof*, 2007]. As the bed is considerably deeper beneath the northern section and the ice is thicker (Fig. 5.2), the longitudinal stresses will be higher than on the southern section. This difference can also be expressed in terms of stretching rate at the terminus (Equation 6), which increases with thickness to the power of three (i.e. the exponent in Glenn's Flow Law). Due to its deeper bed and thicker ice, the northern section therefore experiences higher stretching rates and longitudinal stresses at the terminus, which would promote crevasse formation, calving and retreat.

Finally, floatation close to the terminus would also, at least temporarily, increase the area that is exposed to submarine melting. Although less significant, the grounding line of the northern section is located in deeper water than the southern section and would therefore experience subsurface temperatures which are approximately 0.11 °C warmer, due to the pressure dependence of the melting point of ice [*Rignot et al.*, 2010]. We therefore suggest that the northern section is more sensitive to forcing than the southern portion due to its deeper basal topography, which brings it closer to floatation, results in higher stretching rates at the calving front and, to a lesser extent, may increase ice loss through submarine melting.

5.4.3. Numerical modelling and glacier sensitivity to forcing

Numerical modelling results affirm the increased sensitivity of the northern section to forcing, for a range of reductions in sea ice buttressing and crevasse water depth (Fig. 5.5). For all magnitudes of reduction in sea ice buttressing, retreat rates were at least an order of magnitude greater on the northern section (Fig. 5.5). We suggest that this reflects the greater influence of changes in longitudinal stress, associated with reduced sea ice buttressing, on the northern section. As detailed above, this section is closer to floatation and longitudinal stresses are higher, due to the greater ice thickness, which together would make the northern section more sensitive to changes in longitudinal stresses.

Increasing crevasse depth by raising crevasse water levels (as a proxy for enhanced surface melt) by 5 to 10 m also resulted in an order of magnitude difference in retreat rates between the northern and the southern sections (Fig. 5.5), which corresponds closely to observed retreat patterns on HG (Figs. 5.1 & 5.4). However, the difference in response was smaller when crevasse water depth was increased by 15 m or more (Fig. 5.5). We suggest that this step-change in sensitivity of the southern section may be a consequence of the local bed and surface topography at the terminus. This could be further investigated by modelling sensitivity on additional transects on the southern section and/or applying the perturbation once the front has retreated further inland. This would allow us to establish whether this enhanced sensitivity at higher crevasse water depths is a persistent feature or a consequence of localised topography.

The strong sensitivity of HG's frontal position to crevasse water depth, via its influence on crevasse depth, in our model experiments is consistent with the results from a previous study, which also used a crevasse-depth calving criterion to model retreat at Columbia Glacier, Alaska [*Cook et al.*, 2012]. These findings demonstrated that modelled calving rates and frontal position change were strongly influenced by crevasse water depth [*Cook et al.*, 2012]. Our study affirms this sensitivity and highlights the need to further assess this relationship: model outputs are highly

dependent on the input crevasse water depth, due to its control on crevasse depth, but this parameter is very difficult to measure *in-situ* or to determine using surface mass balance modelling [*Cook et al.*, 2012]. We therefore highlight the need for further investigation of the relationship between atmospheric warming, crevasse depth, crevasse water levels and glacier calving rates. In particular, future work should investigate whether hydrofracture influences glacier behaviour via its effect on calving events at terminus and/or by deepening crevasses up to a few kilometres inland, particularly on floating sections, and thus creating weaknesses that promote calving once the ice reaches the terminus.

5.4.4. Future outlook and wider implications

The basal trough beneath the northern section of HG has important implications for its response to 21st century climate change. The trough extends up to 72 km inland and in places the bed has a reversed bed slope in the up-glacier direction (Figs. 5.2 & 5.3). The trough may therefore continue to facilitate rapid retreat and subsequent surface draw-down for a considerable period. Fitting a simple linear trend to our frontal position data gives a retreat rate of 427 m a^{-1} (R^2 = 0.95) between 1999 and 2012 for this section. Assuming this trend continues, the terminus would remain in the trough for approximately 169 years, highlighting the potential for sustained and substantial mass loss from HG during the 21st Century and beyond. However, our results demonstrate the strong influence of basal topography on retreat rates, meaning that future recession may be non-linear and could substantially exceed contemporary rates, as the bed is below sea level and reverse-sloping in certain sections (Fig. 5.2).

Results from HG demonstrate that a basal trough can potentially produce an order of magnitude difference in retreat rates, given the same initial forcing, and it is likely that many other outlet glaciers possess similar overdeepenings [*Cook and Swift*, 2012]. However, it is important to stress that the northern section of HG is substantially wider (~45 km) than the majority of Arctic outlet glacier fjords (~ 5 km). Consequently, the

relative importance of lateral stresses is likely to be greater on narrower glaciers [*Raymond*, 1996]. Furthermore, the presence of overdeepenings may have very important broader consequences for ice sheet stability and longer-term behaviour. Evidence suggests that the WAIS may have collapsed catastrophically during the last interglacial, or was at least much less extensive, due to its ice stream grounding lines being located below sea level [*Joughin and Alley*, 2011; *Mercer*, 1968]. Significant areas of the contemporary GrIS lie below sea level [*Bamber et al.*, 2013; *Morlighem et al.*, 2014], meaning that understanding the interaction between glacier behaviour and basal topography is critical for assessing ice sheet stability and potential response to future climate change. The influence of basal topography should therefore be considered in combination with fjord width, when interpreting and/or forecasting outlet glacier behaviour in other locations [*Carr et al.*, 2014; *Carr et al.*, 2013b; *Gudmundsson et al.*, 2012; *Jamieson et al.*, 2012].

5.5. Conclusions

Humboldt Glacier has retreated rapidly during the past decade, in response to increased air temperatures and, to a lesser extent, reduced sea ice concentrations. However, subglacial topography has strongly modulated its behaviour and generated retreat rates that were an order of magnitude greater on the northern section of the terminus. This area is underlain by a major basal trough (up to 475 m deep) that extends up to 72 km inland. Numerical modelling sensitivity experiments demonstrate that this differing response persists for moderate increases in crevasse water depth (as a proxy for atmospheric warming) and for reduced sea ice buttressing. We conclude that basal topography is an important influence on contemporary outlet glacier behaviour and underscore the dangers of extrapolating patterns of response to forcing without appropriate consideration of subglacial topography and variations in fjord width. Furthermore, results suggest that we cannot always assume that individual glaciers have a uniform bed topography and these internal variations need to be considered when assessing glacier response to forcing. In the case of the relatively wide Humboldt

Glacier, the overdeepening is likely to continue to facilitate high retreat rates and substantial mass loss during the 21st century. We therefore emphasise the need to acquire further data on the subglacial topography of marine-terminating outlet glaciers, in order to assess and accurately predict their response to climatic warming and their potential contribution to near-future sea level rise.

Acknowledgements

Funding for this work was provided by a Durham Doctoral Studentship to JRC. Radio-echo sounding data were acquired and processed through UK NERC grant NE/H020667 to JAD.

5.6. References

Abdalati, W., W. Krabill, E. Frederick, S. Manizade, C. Martin, J. Sonntag, R. Swift, R. H. Thomas, W. Wright, and J. Yungel (2001), Outlet glacier and margin elevation changes: Near-coastal thinning of the Greenland ice sheet, *Journal of Geophysical Research*, *106*(D24), 33,729 –733,741.

Amundson, J. M., M. Fahnestock, M. Truffer, J. Brown, M. P. Lüthi, and R. J. Motyka (2010), Ice mélange dynamics and implications for terminus stability, Jakobshavn Isbræ, Greenland, *Journal of Geophysical Research*, *115*, F01005, doi:10.1029/2009JF001405.

Bamber, J. L., et al. (2013), A new bed elevation dataset for Greenland, *The Cryosphere*, *7*(2), 499-510, doi:10.5194/tc-7-499-2013.

Brown, C. S., M. F. Meier, and A. Post (1982), The calving relation of Alaskan tidewater glaciers, with application to Columbia Glacier, *US Geological Survey Professional Paper, US Government Printing Office, Washington, DC*, *1258-C*, 13.

Burgess, E. W., R. R. Forster, J. E. Box, E. Mosley-Thompson, D. H. Bromwich, R. C. Bales, and L. C. Smith (2010), A spatially calibrated model of annual accumulation rate on the Greenland Ice Sheet (1958–2007), *Journal of Geophysical Research*, *115*, F02004, doi:10.1029/2009JF001293.

Carr, J. R., C. Stokes, and A. Vieli (2014), Recent retreat of major outlet glaciers on Novaya Zemlya, Russian Arctic, influenced by fjord geometry and sea-ice conditions, *Journal of Glaciology*, *60*, 155-170.

Carr, J. R., C. R. Stokes, and A. Vieli (2013a), Recent progress in understanding marine-terminating Arctic outlet glacier response to climatic and oceanic forcing: Twenty years of rapid change, *Progress in Physical Geography*, *37*(4), 435 - 466.

Carr, J. R., A. Vieli, and C. R. Stokes (2013b), Climatic, oceanic and topographic controls on marine-terminating outlet glacier behavior in north-west Greenland at seasonal to interannual timescales, *Journal of Geophysical Research*, *118*(3), 1210-1226.

Carstensen, L. S., and B. V. Jørgensen (2011), Weather and climate data from Greenland 1958-2010., *Techincal Report*, *11-10*.

Cook, S., and D. A. Swift (2012), Subglacial basins: their origin and importance in glacial systems and landscapes, *Earth-Science Reviews*, *115*, 332-372.

Cook, S., T. Zwinger, I. C. Rutt, S. O'Neel, and T. Murray (2012), Testing the effect of water in crevasses on a physically based calving model, *Annals of Glaciology*, *53*(60), 90-96, doi:10.3189/2012AoG60A107.

Cuffey, K. M., and W. S. B. Paterson (2010), *The Physics of Glaciers*, Elsevier.

Dee, D. P., et al. (2011), The ERA-Interim reanalysis: configuration and performance of the data assimilation system, *Quarterly Journal of the Royal Meteorological Society*, *137*(656), 553-597, doi:10.1002/qj.828.

Echelmeyer, K. A., W. D. Harrison, C. Larsen, and J. E. Mitchell (1994), The role of the margins in the dynamics of an active ice stream, *Journal of Glaciology*, *40*(136), 527-538.

Enderlin, E. M., I. M. Howat, and A. Vieli (2013), High sensitivity of tidewater outlet glacier dynamics to shape, *The Cryosphere*, *7*(3), 1007-1015, doi:10.5194/tc-7-1007-2013.

Glen, J. W. (1955), The creep of polycrystalline ice, *Proceedings of the Royal Society of London - Series A*, *228*, 519-387.

Gogineni, S., D. Tammana, D. Braaten, C. Leuschen, T. Akins, J. Legarsky, P. Kanagaratnam, J. Stiles, C. Allen, and K. Jezek (2001), Coherent radarice thickness measurements over the Greenland ice sheet, *Journal of Geophysical Research*, *106 (D24)*(33), 761-733, doi:10.1029/2001JD900183.

Gudmundsson, G. H., J. Krug, G. Durand, L. Favier, and O. Gagliardini (2012), The stability of grounding lines on retrograde slopes, *The Cryosphere Discussions*, *6*, 2597–2619.

Holland, D. M., R. H. D. Y. Thomas, B., M. H. Ribergaard, and B. Lyberth (2008), Acceleration of Jakobshavn Isbræ triggered by warm subsurface ocean waters, *Nature Geoscience*, *1*, 1-6.

Howat, I. M., J. E. Box, Y. Ahn, A. Herrington, and E. M. McFadden (2010), Seasonal variability in the dynamics of marine-terminating outlet glaciers in Greenland, *Journal of Glaciology*, *56*(198), 601-613.

Howat, I. M., I. Joughin, M. Fahnestock, B. E. Smith, and T. Scambos (2008), Synchronous retreat and acceleration of southeast Greenland outlet glaciers 2000-2006; Ice dynamics and coupling to climate, *Journal of Glaciology*, *54*(187), 1-14.

Howat, I. M., A. Negrete, T. Scambos, and T. Haran (2012), A high-resolution elevation model for the Greenland Ice Sheet from combined stereoscopic and photoclinometric data, edited, Byrd Polar Research Centre, Ohio State University.

Hughes (2002), Calving bays, *Quarternary Science Reviews*, *21*(1-3), 267-282.

Hughes, T. (1986), The Jakobshavns effect, *Geophysical Research Letters*, *13*(1), 46-48.

IPCC (2007), *The Physical Science Basis. Contribution of Working Group I to the Fourth Assessment Report of the Intergovernmental Panel on Climate Change*, Cambridge Univ. Press, Cambridge and New York.

IPCC (2013), Climate Change 2013: The Physical Science Basis. Working Group I Contribution to the IPCC 5th Assessment Report. Online unedited version.

Jacob, T., J. Wahr, W. T. Pfeffer, and S. Swenson (2012), Recent contributions of glaciers and ice caps to sea level rise, *Nature*, *428*, 514–518.

Jamieson, S. S. R., A. Vieli, S. J. Livingstone, C. Ó Cofaigh, C. R. Stokes, C.-D. Hillenbrand, and J. Dowdeswell (2012), Ice stream stability on a reverse bed slope, *Nature Geoscience*, *5*, 799-802.

Jenkins, A. (2011), Convection-Driven Melting near the Grounding Lines of Ice Shelves and Tidewater Glaciers, *Journal of Physical Oceanography*, *41*, 2279–2294.

Joughin, I., and R. B. Alley (2011), Stability of the West Antarctic ice sheet in a warming world, *Nature Geoscience*, *4*, 506-513.

Joughin, I., M. Fahnestock, R. Kwok, P. Gogineni, and C. Allen (1999), Ice flow of Humboldt, Petermann and Ryder Gletscher, northern Greenland, *Journal of Glaciology*, *45*(150), 231-241.

Joughin, I., I. M. Howat, R. B. Alley, G. Ekström, M. Fahnestock, T. Moon, NettlesM., M. Truffer, and V. C. Tsai (2008a), Ice-front variation and tidewater behaviour on Helheim and

Kangerdlugssuaq Glaciers, Greenland, *Journal of Geophysical Research*, *113*, F01004, doi:10.1029/2007JF000837.

Joughin, I., I. M. Howat, M. Fahnestock, B. Smith, W. Krabill, R. B. Alley, H. Stern, and M. Truffer. (2008b), Continued evolution of Jakobshavn Isbrae following its rapid speedup, *Journal of Geophysical Research*, *113*, F04006, doi:10.1029/2008JF001023.

Joughin, I., B. Smith, I. M. Howat, T. Scambos, and T. Moon (2010a), Greenland flow variability from ice-sheet-wide velocity mapping, *Journal of Glaciology*, *56*(197), 415-430.

Joughin, I., B. E. Smith, I. Howat, and T. Scambos (2010b), MEaSUREs Greenland Ice Sheet Velocity Map from InSAR Data, *Boulder, Colorado, USA: National Snow and Ice Data Center. Digital media.*

Kalnay, E., et al. (1996), The NCEP/NCAR 40-Year Reanalysis Project, *Bulletin of the American Meteorological Society*, *77*(3), 437-471, doi:10.1175/1520-0477(1996)077<0437:tnyrp>2.0.co;2.

Koenig, L., S. Martin, M. Stuedinger, and J. Sonntag (2010), Polar airborne observations fill gap in satellite data, *EOS*, *91*(38), 333-334.

McFadden, E. M., I. M. Howat, I. Joughin, B. Smith, and Y. Ahn (2011), Changes in the dynamics of marine terminating outlet glaciers in west Greenland (2000–2009), *Journal of Geophysical Research*, *116*, F02022.

Meier, M. F., and A. Post (1987), Fast tidewater glaciers, *Journal of Geophysical Research*, *92*, 9051–9058.

Mercer, J. H. (1968), Antarctic ice and Sangamon sea level rise, *IAHS Publ.*, *179*, 217–225

Moholdt, G., B. Wouters, and A. S. Gardner (2012), Recent mass changes of glaciers in the Russian High Arctic, *Geophysical Research Letters*, *39*, L10502.

Moon, T., and I. Joughin (2008), Changes in ice-front position on Greenland's outlet glaciers from 1992 to 2007, *Journal of Geophysical Research*, *113*, F02022, doi:10.1029/2007JF000927.

Moon, T., I. Joughin, B. E. Smith, and I. M. Howat (2012), 21st-Century evolution of Greenland outlet glacier velocities, *Science*, *336*(6081), 576-578.

Morlighem, M., E. Rignot, J. Mouginot, H. Seroussi, and E. Larour (2014), Deeply incised submarine glacial valleys beneath the Greenland ice sheet, *Nature Geosci*, *7*(6), 418-422, doi:10.1038/ngeo2167.

Motyka, R. J., L. Hunter, K. Echelmeyer, and C. Connor (2003), Submarine melting at the terminus of a temperate tidewater glacier, LeConte Glacier, Alaska, U.S.A., *Annals of Glaciology*, *36*, 57-65.

Nick, F. M., A. Luckman, A. Vieli, C. J. van der Veen, D. van As, R. S. W. van de Wal, F. Pattyn, and D. Floricioiu (2012), The response of Petermann Glacier, Greenland, to large calving events, and its future stability in the context of atmospheric and oceanic warming, *Journal of Glaciology*, *58*(208), 229 - 239.

Nick, F. M., C. J. van der Veen, A. Vieli, and D. I. Benn (2010), A physically based calving model applied to marine outlet glaciers and implications for the glacier dynamics, *Journal of Geophysical Research*, *56*(199), 781-794.

Nick, F. M., A. Vieli, M. L. Andersen, I. Joughin, A. J. Payne, T. L. Edwards, F. Pattyn, and R. S. W. van de Wal (2013), Future sea-level rise from Greenland's main outlet glaciers in a warming climate, *Nature*, *497*(7448), 235-238, doi:10.1038/nature12068.

Pelto, M. S., and C. R. Warren (1991), Relationship between tidewater glacier calving velocity and water depth at the calving front, *Annals of Glaciology*, *15*, 115-118.

Raymond, C. (1996), Shear margins in glaciers and ice sheets, *Journal of Glaciology*, *42*(140), 90-102.

Reynolds, R. W., T. M. Smith, C. Liu, D. B. Chelton, K. S. Casey, and M. G. Schlax (2007), Daily High-Resolution-Blended Analyses for Sea Surface Temperature, *Journal of Climate*, *20*(22), 5473-5496, doi:10.1175/2007jcli1824.1.

Rignot, E., J. E. Box, E. Burgess, and E. Hanna (2008), Mass balance of the Greenland ice sheet from 1958 to 2007, *Geophysical Research Letters*, *35*, L20502, doi:10.1029/2008GL035417.

Rignot, E., S. P. Gogineni, I. Joughin, and W. Krabill (2001), Contribution to the glaciology of northern Greenland from satellite radar interferometry, *Journal of Geophysical Research*, *106*, 34007-34019.

Rignot, E., and P. Kanagaratnam (2006), Changes in the velocity structure of the Greenland Ice Sheet, *Science*, *311*(5763), 986–990.

Rignot, E., M. Koppes, and I. Velicogna (2010), Rapid submarine melting of the calving faces of West Greenland glaciers, *Nature Geoscience*, *3*, 187-191, doi:10.1038/NGEO765.

Schoof, C. (2007), Ice sheet grounding line dynamics: steady states, stability, and hysteresis, *Journal of Geophysical Research*, *112*(F3), F03S28.

Seale, A., P. Christoffersen, R. Mugford, and M. O'Leary (2011), Ocean forcing of the Greenland Ice Sheet: Calving fronts and patterns of retreat identified by automatic satellite monitoring of eastern outlet glaciers, *Journal of Geophysical Research*, *116*(F3), F03013.

Sohn, H. G., K. C. Jezek, and C. J. van der Veen (1998), Jakobshavn Glacier, West Greenland: 30 years of Spacebourne observations, *Geophysical Research Letters*, *25*(14), 2699-2702.

Straneo, F., R. G. Curry, D. A. Sutherland, G. S. Hamltion, C. Cenedese, K. Våge, and L. A. Stearns (2011), Impact of fjord dynamics and glacial runoff on the circulation near Helheim Glacier, *Nature Geoscience*, *4*, 322-327.

van den Broeke, M., J. Bamber, J. Ettema, E. Rignot, E. Schrama, W. J. van de Berg, E. van Meijgaard, I. Velicogna, and B. Wouters (2009), Partitioning Recent Greenland Mass Loss, *Science*, *326*, 984-986.

van der Veen, C. J. (1998a), Fracture mechanics approach to penetration of bottom crevasses on glaciers, *Cold Regions Science and Technology*, *27*, 213- 223.

van der Veen, C. J. (1998b), Fracture mechanics approach to penetration of surface crevasses on glaciers *Cold Regions Science and Technology*, *27*(1), 31-47.

Vieli, A., and F. M. Nick (2011), Understanding and modelling rapid dynamic changes of tidewater outlet glaciers: issues and implications, *Surveys in Geophysics*, *32*, 437-485.

Vieli, A., and A. J. Payne (2005), Assessing the ability of numerical ice sheet models to simulate grounding line migration, *Journal of Geophysical Research*, *110*, F01003.

Warren, C. R., and N. R. J. Hulton (1990), Topographic and glaciological controls on Holocene ice sheet margin dyanmics, central west Greenland, *Annals of Glaciology*, *14*, 307-310.

Weertman, J. (1957), On the sliding of glaciers, *Journal of Glaciology*, *3*, 33-38.

Weertman, J. (1974), Stability of the junction of an ice sheet and an ice shelf, *Journal of Glaciology*, *13*(67), 3-11.

Weidick, A. (1995), Satellite Image Atlas of Glaciers of the World, Greenland, *USGS Professional Paper 1386-C, United States Government Printing Office, Washington.*

Chapter 6: Pan-Arctic controls on marine-terminating Arctic outlet glacier retreat rates

J.R. Carr, C.R. Stokes and A. Vieli. *To be submitted to Nature Geoscience*.

Outline: Outlet glacier retreat in the Atlantic sector of the Arctic has been widespread and rapid during the past two decades and accelerated between 1992-2000 and 2000-2010. The highest retreat rates were concentrated in northern, north- and central-western and south eastern Greenland. Despite some correspondence between mean regional retreat rates and atmospheric warming in western and south-eastern Greenland between 1990 and 1999, no simple pattern of response was apparent in these areas between 2000 and 2010 nor was any relationship evident in the other study regions. Sea ice decline may have contributed to retreat in north- and central-west Greenland, Spitzbergen and NVZ. Despite overall regional trends, retreat rates varied dramatically between individual glaciers, which are attributed to glacier-specific factors. Results suggest that fjord width variability is an important control on glacier behaviour across the Atlantic Arctic and is most marked in areas where outlet glaciers are constrained by rock fjords.

Motivation: This paper compares outlet glacier retreat rates and response to forcing across the study area and thus allowed the project aim to be fully addressed. Furthermore, the paper enabled evaluation of fjord width variation as a widely-applicable control on glacier behaviour. Thus, this chapter contributes significantly to our understanding of two of the key limitations identified in Chapter 3, namely the spatial variation in forcing factors and retreat and the role of glacier-specific factors.

Contribution: In this paper, I carried out the GIS and data analysis tasks (e.g. image processing, data acquisition and data processing), wrote the text, created the figures and lead the paper development. My co-authors provided editorial input and guidance on the development of the research. For the purpose of this thesis, this chapter has been written in the form of a long-format journal article, but will be later prepared for submission to Nature Gesocience.

Abstract

Arctic ice masses have lost mass rapidly during the past two decades, coincident with dramatic climate change in the region. A primary component of these losses has been accelerated ice discharge through marine-terminating outlet glaciers. However, substantial uncertainties exist over the spatial variation in outlet glacier retreat rates and response to various forcings across the Arctic. Here we use remotely sensed data to quantify recent (1992-2010) retreat rates of major ocean-terminating outlet glaciers across the entire Atlantic sector of the Arctic and to evaluate the relative influence of air temperature, sea ice, sea surface temperature, and fjord width variation. Results demonstrate rapid and widespread retreat across the study region, which increased five-fold between 1992-2000 (23.6 m a^{-1}) and 2000-2010 (107.2 m a^{-1}). Retreat rates were highest in northern, western and south-eastern Greenland for the period 2000-2010, and also increased substantially on Novaya Zemlya and Spitzbergen between 1992-2000 and 2000-2010. Atmospheric warming coincided with retreat in western and south-eastern Greenland between 1990 and 1999, but showed limited correspondence to retreat rates between 2000 and 2010 or to the pattern of retreat elsewhere in the study region. Sea ice declined markedly in central- and north-west Greenland, suggesting that it contributed to glacier retreat within these regions. Despite overall regional trends, however, there were large variations in retreat rates within regions and between individual glaciers, with the areas exhibiting the highest retreat rates also showing the greatest variability. Importantly, our results demonstrate a widespread statistical relationship between fjord width variability and glacier retreat rate on study glaciers located across the Atlantic Arctic. This relationship was strongest in areas where glaciers are constrained by mountainous topography. We underscore the role of glacier-specific factors in modulating glacier response to forcing and highlight the need to consider these controls when interpreting and/or forecasting glacier response to climate change.

6.1. Introduction

Arctic warming is expected to far exceed the global average and to reach between 2.2 and 8.3 °C by 2100 [*IPCC*, 2013]. As a result, Arctic ice masses are expected to undergo rapid mass loss and contribute substantially to 21st century sea level rise. During the past two decades, ice deficits in the Arctic have been dramatic, with the Greenland Ice Sheet (GrIS) losing an estimated 142 ± 49 Gt a^{-1} between 1992 and 2011 and contributing 0.39 ± 0.14 mm a^{-1} to sea level rise [*Shepherd et al.*, 2012]. Substantial mass deficits have also been recorded on other Arctic ice masses between 2003 and 2009, specifically in northern Arctic Canada (–33 ± 4 Gt a^{-1}), southern Arctic Canada (–27 ± 4 Gt a^{-1}), Alaska (–50 ± 17 Gt a^{-1}), Russian Arctic (–11 ± 4 Gt a^{-1}) and Svalbard (–5 ± 2 Gt a^{-1}) [*Gardner et al.*, 2013].

Recent ice loss has occurred via two primary mechanisms: negative surface mass balance (SMB) and accelerated ice discharge from marine-terminating outlet glaciers. Losses due to negative SMB reflect an excess of surface melting in comparison to accumulation and evidence from the GrIS [*Rignot et al.*, 2008; *Rignot et al.*, 2011; *van den Broeke et al.*, 2009; *Zwally et al.*, 2011] and Canadian High Arctic [*Gardner et al.*, 2011] suggests that this has largely resulted from an increase in melt rates. Marine-terminating outlet glaciers have also been highlighted as a key mechanism for rapid ice loss and studies from the GrIS have recorded retreat rates of kilometres per year on major outlet glaciers [e.g. *Howat et al.*, 2008; *Joughin et al.*, 2008a; *Moon and Joughin*, 2008]. These ‘dynamic’ losses currently account for approximately half of the total ice loss from the GrIS, with the other half resulting from negative SMB [*Rignot et al.*, 2008; *van den Broeke et al.*, 2009]. Although some studies suggest that the relative importance of dynamic losses from the GrIS may slow at centennial timescales [*Goelzer et al.*, 2013], recent results suggest that they are likely to contribute substantially to 21st Century sea level rise [*IPCC*, 2013; *Nick et al.*, 2013]. For the GrIS increases due to dynamic changes are forecast to be between 20 and 85 mm (RCP [Representative Concentration Pathway] scenario 8.5) and 14 and 63 mm (all other

RCP scenarios) by 2100 [*IPCC*, 2013; *Nick et al.*, 2013], whilst losses through negative SMB balance are expected to range between 90 ± 40 mm (RCP 8.5) and 40 ± 20 mm (RCP 4.5) [*Fettweis et al.*, 2013].

Despite its apparent importance, the contribution of ice dynamics to Arctic ice loss outside of the GrIS has not been extensively investigated and the spatial variation in glacier retreat rates across the region has yet to be assessed. Moreover, our understanding of the factors controlling these dynamic losses and glacier retreat rates remains incomplete [*IPCC*, 2013]. Sea ice, air and ocean temperatures have been identified as key external controls [e.g. *Carr et al.*, 2013a; *Straneo et al.*, 2013; *Vieli and Nick*, 2011], whilst basal topography and fjord width variation have the capacity to strongly modulate the response of individual glaciers to external forcing [*Carr et al.*, 2014; *Carr et al.*, 2013b; *Enderlin et al.*, 2013; *Howat and Eddy*, 2011; *Jamieson et al.*, 2012; *Moon et al.*, 2012]. The these local factors are thought to influence glacier behaviour at interannual [e.g. *Carr et al.*, 2014; *Moon et al.*, 2012], decadal [*Warren and Glasser*, 1992] and glacial/interglacial [*Hughes*, 1986; *Warren and Hulton*, 1990] timeframes. They have also been identified as potential mechanisms for ice sheet collapse during the Quaternary [*Hughes*, 2002; *Hughes*, 1986; *Mercer*, 1968], highlighting their relevance for understanding contemporary ice sheet stability. Much of our understanding of the factors controlling outlet glacier dynamics comes from a limited number of study sites and so little is known about how the relative importance of these controls varies across the Arctic and which factors, if any, can be taken as indicators for potentially rapid retreat at regional or pan-Arctic scales.

Here we evaluate glacier frontal position changes on 321 major marine-terminating outlet glaciers, located across the Atlantic sector of the Arctic, on the Greenland Ice Sheet (GrIS), Svalbard (SVB), Novaya Zemlya (NVZ) and Franz Josef Land (FJL) (Fig. 6.1). Glaciers previously identified as surge type [e.g. *Blaszczyk et al.*, 2009; *Grant et al.*, 2009; *Hamilton and Dowdeswell*, 1996; *Weidick*, 1995] were excluded from the analysis. The GrIS was divided into regions following *Moon and Joughin* [2008] (Fig.

6.1). The study region was chosen to encompass the Atlantic sector of the Arctic, i.e. the region that is potentially influenced by water of North Atlantic origin. It incorporates a very wide range of climatic, oceanic and glaciological conditions and therefore allows us to assess spatial variations in external and glacier-specific controls along these gradients. Moreover, the region includes the majority of large, ocean-terminating Arctic outlet glaciers. We first assess marine-terminating outlet glacier retreat rates between and within each study region. Next, we evaluate retreat in relation to climatic and oceanic changes (here the term 'oceanic' refers to sea ice and sea surface temperatures) across the study region. Finally, we investigate the impact of fjord width variability on retreat rates.

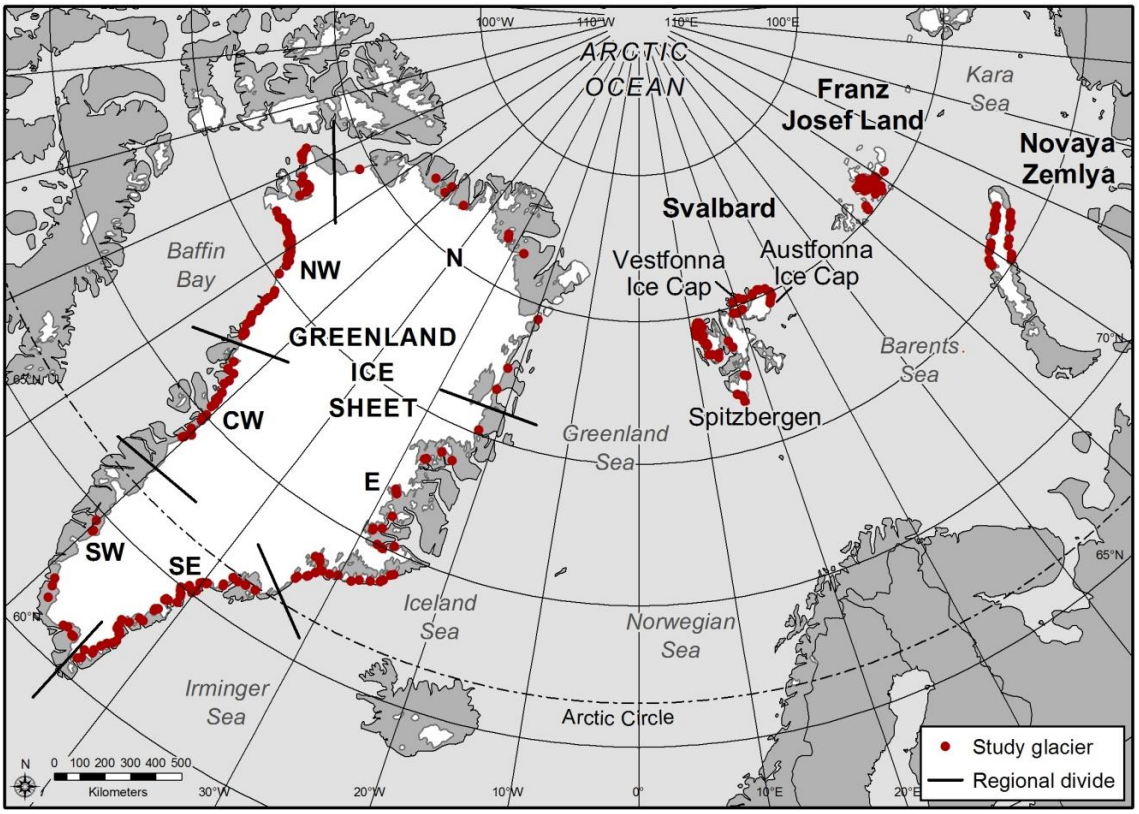

Figure 6.1. *Location map, showing major ice masses, study regions, and study glaciers (red dots). The Greenland Ice Sheet is sub-divided into regions, following [Moon and Joughin, 2008].*

6.2. Methods

6.2.1. Glacier frontal position

Following the approach employed in previous studies [*Carr et al.*, 2014; *Carr et al.*, 2013b], marine-terminating outlet glacier frontal positions were obtained from a

combination of Synthetic Aperture Radar (SAR) Image Mode Precision data, provided by the European Space Agency (ESA), and visible Landsat imagery, provided by the USGS Global Visualisation Viewer (http://glovis.usgs.gov/). SAR imagery was processed following the method [*Carr et al.*, 2013b]: i) apply precise orbital state vectors; ii) apply radiometric calibration; iii) multi-look to reduce speckle and; iv) terrain correct using the Advanced Spaceborne Thermal Emission and Reflection Radiometer (ASTER) Global Digital Elevation Model (GDEM) version 2, which has a 30 m resolution. SAR images acquired by the ERS1, ERS2 and ENVISAT missions were used and ERS images were coregistered with corresponding ENVISAT scenes, due to the higher geolocation accuracy of ENIVSAT data. Scenes were obtained for the years 1992, 2000 and 2010, and were acquired as close as possible to 31st July to minimise the impact of seasonal variations on interannual trends. The spatial resolution of the imagery is 30 m for Landsat scenes and 37.5 m for the SAR data, following processing.

Changes in glacier frontal position were measured using the reference box approach [e.g. *Carr et al.*, 2013b; *McFadden et al.*, 2011; *Moon and Joughin*, 2008]. A reference box was defined that is aligned approximately parallel to the main ice flow direction at the terminus and extends in land by an arbitrary distance. Frontal positions were then digitised from successive images and the change in area between each time step was calculated. This was divided by the reference box width, to give the terminus position relative to the upstream reference line, which was then used to calculate frontal position change between 1992-2000 and 2000-2010. The mean error in frontal position was calculated by repeatedly digitising sections of rock coastline for a sub-sample of ten ERS, ten ENVISAT and ten Landsat images, which should show no discernible change between successive images [*Carr et al.*, 2014; *Carr et al.*, 2013b]. The total frontal position error was 27.1 m and results primarily from manual digitising errors. This equates to an error in retreat rates of approximately 1.5 m a^{-1}, at the decadal timescales evaluated here.

6.2.2. Atmospheric and oceanic data

Air temperature data were acquired from selected meteorological stations located across the Arctic [*Carr et al.*, 2013a]. Stations were chosen on the basis that data were available for the entire study period (1990-2010) and that data gaps were minimal. Data were obtained from a variety of different sources, which are detailed in Table 6.1. The temporal resolution of the available data ranged between three-hourly and monthly. Data were filtered to account for missing values, using the following criteria: three-hourly data were used only if (1) no more than two consecutive records were missing in a day; and (2) no more than three records in total were missing in a day. Daily data were only used if values were available for 22 or more days per month and monthly values were used only if data were available for all months of the year [*Cappelen*, 2011]. Linear trends were then calculated from mean annual air temperature series for the periods 1990-1999 and 2000-2010. The length of the air temperature records enabled us to calculate trends for two time periods (1990-1999 and 2000-2010). This was not possible for sea ice and SSTs, as the datasets were too short to calculate statistically significant trends for both periods.

Sea ice data were acquired from the National/Naval Ice Centre Charts (http://www.natice.noaa.gov/). The charts are compiled from a wide range of remotely sensed and directly measured data sources and have a spatial resolution of up to 50 m. Sea ice values were sampled at the terminus of each study glacier, within a polygon extending 50 m perpendicular to the terminus and along its entire width. Linear trends in sea ice concentrations where then calculated for the period 1995 to 2010.

Sea surface temperature (SST) data were obtained from the Reynolds SST analysis dataset (Version 2) and were provided by the National Oceanic and Atmospheric Administration (NOAA) (http://www.esrl.noaa.gov/psd/data/gridded/data.noaa.oisst.v2.html). The dataset was compiled from a range of satellite, ship and buoy data, which was then corrected for known biases between the different data types [*Reynolds et al.*, 2007]. The data have a spatial resolution of 0.25° and the monthly-

averaged product was used. The data were used to calculate a mean SST field for July-September for the years 1990 and 2010. These months were selected as sea ice concentrations are minimal across the study region during this time period. The mean values were then used to calculate the change in summer (Jul-Sep) SSTs between 1990 and 2010.

Dataset	Data source	URL / Reference
Weather and climate Data from Greenland 1958–2010	Danish Meteorological Institute	[*Carstensen and Jørgensen*, 2011]
Eklima climate database	Norwegian Meteorological Institute	www.eklima.no
Climate Explorer	Royal Netherlands Meteorological Institute	http://climexp.knmi.nl/start.cgi?id=someone@somewhere
National Climate Data and Information Archive	Canadian Daily Climate Data	http://climate.weather.gc.ca
World Data Center – Baseline Climatological Data Sets	Scientific Research Institute of Hydrometeorological Information	http://meteo.ru/english/climate/cl_data.php

Table 6.1. *Meteorological datasets used to calculate air temperature trends during the study period.*

6.2.3. Fjord width variability

Following *Carr et al.* [2014], fjord width variability was measured by digitising both fjord walls at sea level from the most recent satellite imagery. This was done between the least and most extensive frontal positions occupied by each study glacier between 1992 and 2010. The length of each fjord wall was then divided by the straight line distance between its start and end points and a mean value for fjord width variability was calculated for each glacier from these values. A value of 1 for fjord width variability

therefore indicates that the fjord walls are comparatively straight, whilst higher values indicate greater fjord width variation. Fjord width variability was calculated only for glaciers with continuous fjord walls and glaciers retreating across stretches of open water (e.g. between two islands) were not included. Only glaciers that underwent net retreat, not net advance, were included in the analysis, which resulted in a total of 216 glaciers out of 321 study glaciers.

6.2.4. Statistical analysis

In order to assess changes in air temperatures and sea ice concentrations over time, simple linear regression was used. This gives a value for the trend (i.e. the slope of the fitted line) and an R^2 value, which describes how well the fitted line describes the data: if the R^2 value is equal to 1 then all points are located on the line; if the R^2 is equal to zero then the points are randomly distributed around the line. In order to assess the statistical significance of these trends, the F-statistic and its associated p-value were used. The F-statistic tests the significance of a regression model and components of the model, using the analysis of variance approach (ANOVA). The F-statistic is used in preference to the t-statistic, so that a single measure of statistical significance could be used for both linear and polynomial regression. The F-statistic is accompanied by p-value, which gives the probability of obtaining a value of the F-statistic that is at least as extreme as the one obtained, if the null hypothesis is true. We use a significance level of 0.05 (i.e. 95% confidence interval), meaning that results with a p value of less than or equal to 0.05 are considered to be statistically significant.

In order to assess the relationship between fjord width variability and total (1992-2010) retreat rate, we used linear and polynomial (quadratic) regression, as visual inspection of the data indicated that there was some non-linearity in this relationship. As with the air temperature and sea ice data, the p-value associated with the F-statistic was used to assess whether or not the relationship between these two variables was significant, using a significance level of 0.05. The Pearson's Correlation Coefficient (r) was also used to asses this relationship and provides a measure of the linear correlation

between two variables, with a value of 1 being total positive correlation and 0 being no correlation. The p-value associated with the Pearson's correlation coefficient was used to assess its statistical significance, at a significance interval of 0.05.

6.3. Results

6.3.1. Frontal position

6.3.1.1. Regional patterns

During the study period, there was a pan-Arctic retreat trend on marine-terminating outlet glaciers (Fig. 6.3). Mean retreat rates and the number of glaciers retreating increased substantially between the two time steps. Between 1992 and 2000, 77% of the study glaciers retreated, at a mean rate of 23.6 m a^{-1} (Table 6.2). This subsequently increased to a rate of 107.2 m a^{-1} for the period 2000-2010 when 95 % of the study glaciers retreated (Table 6.2). The highest regional retreat rates (mean ~400 m a^{-1}) occurred in northern Greenland between 2000 and 2010, followed by south-east, central-west and north-west Greenland (Fig. 6.3, Table 6.2). Retreat rates were lowest in east Greenland, Vestfonna and Spitzbergen for the period 1992-2000 and in Vestfonna, Austfonna and FJL between 2000 and 2010 (Fig. 6.3, Table 6.2). Austfonna was the only region where retreat rates were lower in 2000-2010 (-28.8 m a^{-1}) than 1992-2000 (-23.1 m a^{-1}).

For the period 2000 to 2010, the regions with the highest retreat rates also showed the largest standard deviation in retreat rate between individual glaciers (Fig. 6.2 & 6.3, Table 6.2). Simple linear regression of retreat rate versus standard deviation in retreat rate gave an R^2 value of 0.98 and the p-value was substantially less than the significance interval of 0.05 (Fig. 6.2), demonstrating that the relationship is statistically significant. In contrast, there was no statistically significant relationship between the mean regional retreat rate and standard deviation in retreat rate between individual glaciers between 1992 and 2000 (Fig. 6.2). The standard deviation in retreat rate was highest in northern Greenland for both time periods and was generally higher on the

GrIS than in other regions (Fig. 6.2, Table 6.2). The spatial variation within the each regions (i.e. between single glaciers) is evaluated in the following subsections.

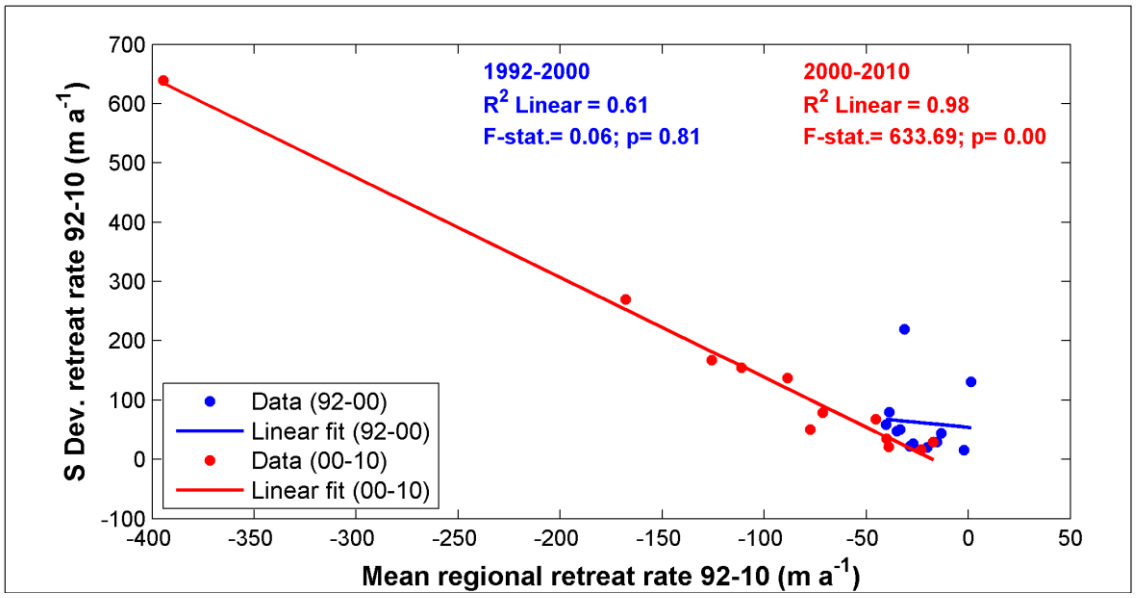

Figure 6.2. *Linear regression of mean regional retreat rate (m a^{-1}) versus the standard deviation (S Dev.) in retreat rate (m a^{-1}) between individual glaciers within that region, for the periods 1992-2000 (blue) and 2000-2010 (red). The values for the F-statistic and the associated p-values are given and a significance level of 0.05 is used (i.e. p-values less than or equal to 0.05 demonstrate a statistically significant relationship).*

		1992-2000				2000-2010			
Region	**No. of glaciers**	**% Retreat**	**% Advance**	**Mean retreat rate (m a^{-1})**	**SD retreat rate (m a^{-1})**	**% Retreat**	**% Advance**	**Mean retreat rate (m a^{-1})**	**SD retreat rate (m a^{-1})**
N GrIS	12	67	33	-31.2	219.8	75	25	-394.6	639.0
NW GrIS	72	88	22	-33.5	50.5	95	5	-111.2	154. 6
CW GrIS	37	84	16	-38.6	80.0	95	5	-168.0	269.6
SW GrIS	10	80	20	-35.1	48.1	60	40	-45.3	68.1
E GrIS	34	69	31	+0.1	130.9	97	3	-86.7	138.1
SE GrIS	47	77	23	-40.3	58.9	94	6	-125.7	167.2
NVZ (B)	18	82	18	-27.1	26.2	100	0	-77.4	50.0
NVZ (K)	10	80	20	-20.3	19.8	90	10	-40.0	34.9
FJL	29	76	24	-15.5	29.6	100	0	-39.0	21.2
Spitzbergen	30	73	27	-13.2	44.2	100	0	-71.5	78.8
AF	10	80	20	-28.8	22.4	100	0	-23.1	16.7
VF	8	63	37	-2.1	15.6	88	12	-17.2	29.7
ALL	**321**	**77**	**23**	**-23.6**	**86.1**	**95**	**5**	**-107.2**	**202.0**

Table 6.2. *Overview of glacier retreat statistics by region for the periods 1992-2000 and 2000-2010.The number of study glaciers within each region is given in the second column. For each region, the following retreat statistics are given for each time period: the percentage of glaciers retreating/advancing, the mean retreat rate for all glaciers within the study region (m a^{-1}) and the standard deviation in retreat rate between individual glaciers within a given region (m a^{-1}).*

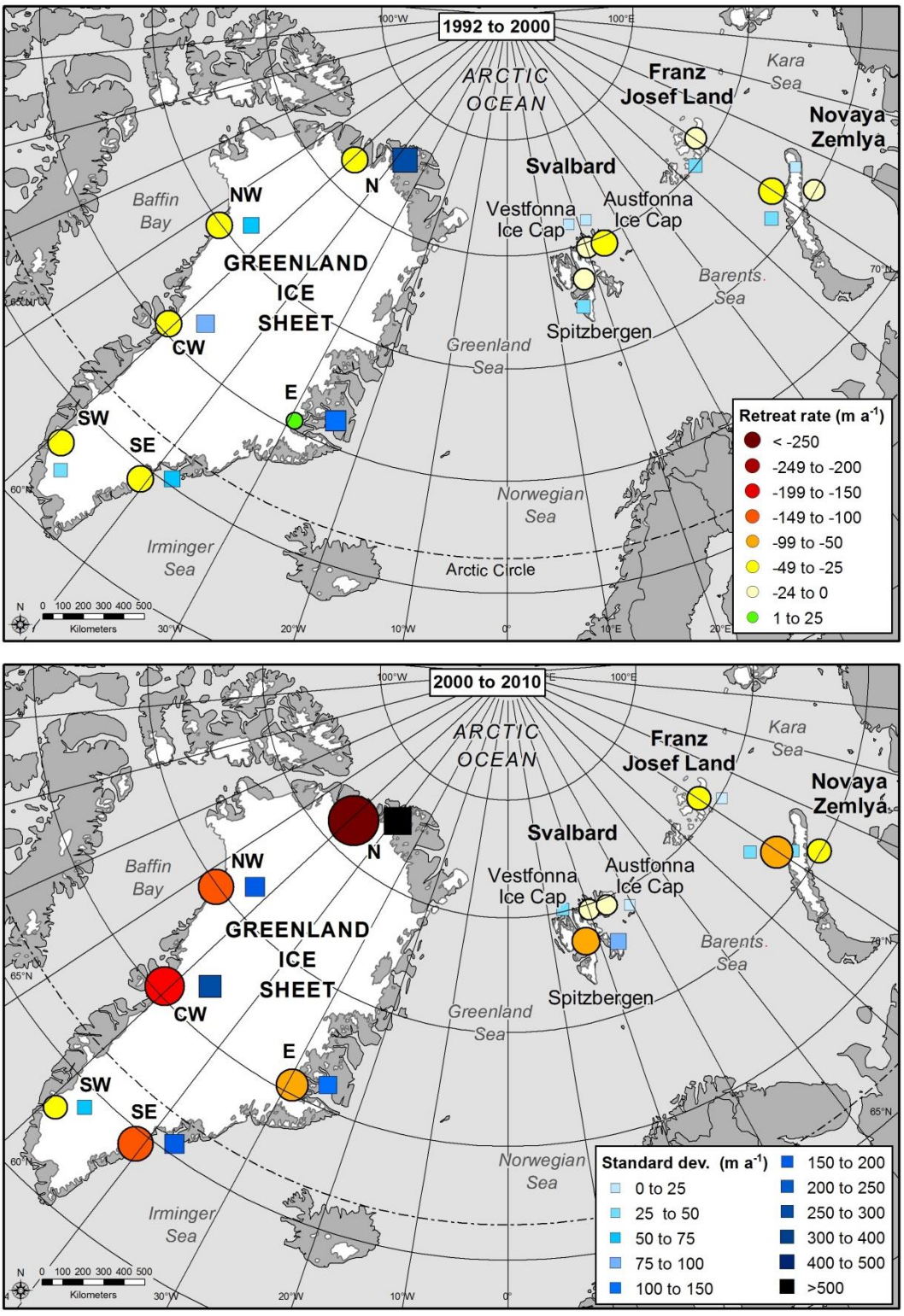

Figure 6.3 *Mean regional marine-terminating outlet glacier retreat rates for the periods 1992-2000 and 2000-2010. Symbol colour shows the magnitude of glacier retreat (yellow through red circles) and standard deviation in retreat rates (blue squares) between 1992 and 2010. In both cases, symbol size shows the R^2 value of the relationship: a larger symbol represents a larger R^2 value and therefore the trend line better fits the data. The spatial extend of the GrIS regions are shown in Figure 1 and follow moon and Joughin (2008).*

6.3.1.2. Greenland Ice Sheet

During the study period, marine-terminating outlets on the GrIS underwent widespread and dramatic retreat (Fig. 6.4, Table 6.2). Between 1992 and 2000, 78 % of all study glaciers retreated, compared to 97 % between 2000 and 2010 (Fig. 6.4, Table 6.2).

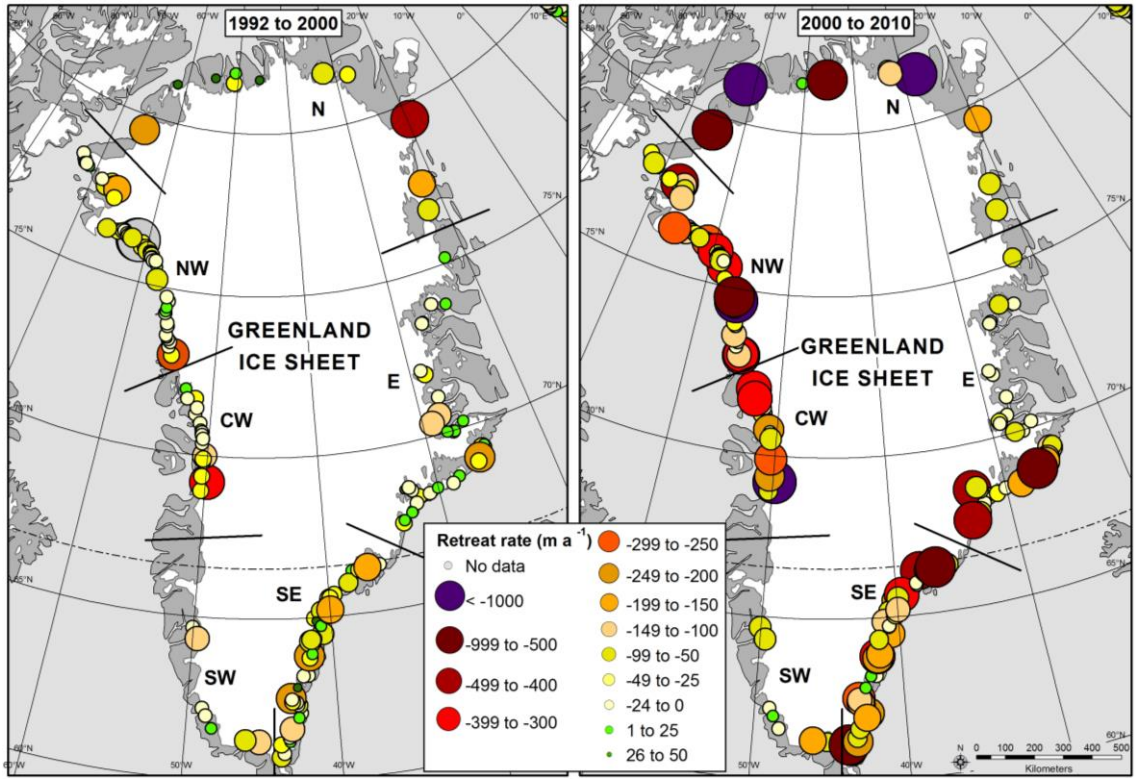

Figure 6.4. *Mean marine-terminating outlet glacier retreat rates for the Greenland Ice Sheet, for the periods 1992-2000 and 2000-2010. Retreat rate is symbolised by colour and size, with larger symbols indicating more rapid retreat*

Mean retreat rates increased markedly over time, from 30.2 m a^{-1} in 1992-2000 to 133.2 m a^{-1} in 2000-2010. Between 2000 and 2010, the highest retreat rates occurred in northern-Greenland, although two major outlet glaciers in the region underwent notable advance, namely Ryder Glacier (+ 0.9 km) and Steenstrup (+3. km). In north-west, central-west and south-east GrIS, glaciers underwent moderate retreat between 1992 and 2000 (33.5 to 40.3 m a^{-1}), which more than trebled to reach 111.2 to 168.0 m a^{-1} by 2000-2010 (Fig. 6.4, Table 6.2). Retreat rates changed little in south-west Greenland between the two time periods and the area showed the lowest retreat rates on the GrIS between 2000 and 2010. Between 1992 and 2000, 41 % of east Greenland

glaciers underwent net advance, resulting in no significant change in frontal position (0.1 m a^{-1}). This changed markedly in 2000-2010, when 97% of glaciers underwent net retreat, at an average retreat rate of 88.7 m a^{-1} (Fig. 6.4, Table 6.2).

The standard deviation in retreat rates was higher in northern Greenland than any other region of the ice sheet for both 1992-2000 (219.8 m a^{-1}) and 2000-2010 (639.0 m a^{-1}) (Figs. 6.2-6.4, Table 6.2). Similar to retreat rates, variability trebled in N, NW, CW and SE Greenland between 1992-2000 and 2000-2010, but showed little change in east Greenland. Variability in retreat rates was consistently lower in SW Greenland than any other region of the ice sheet (Figs. 6.2 -6.4, Table 6.2).

6.3.1.3. Svalbard

Marine-terminating outlet glacier retreat was widespread across Svalbard during the study period (Fig. 6.5, Table 6.2). The number of glaciers undergoing net retreat increased from 73% in 1992-2000 to 98% in 2000-2010, when just one glacier advanced (Fig. 6.5, Table 6.2).

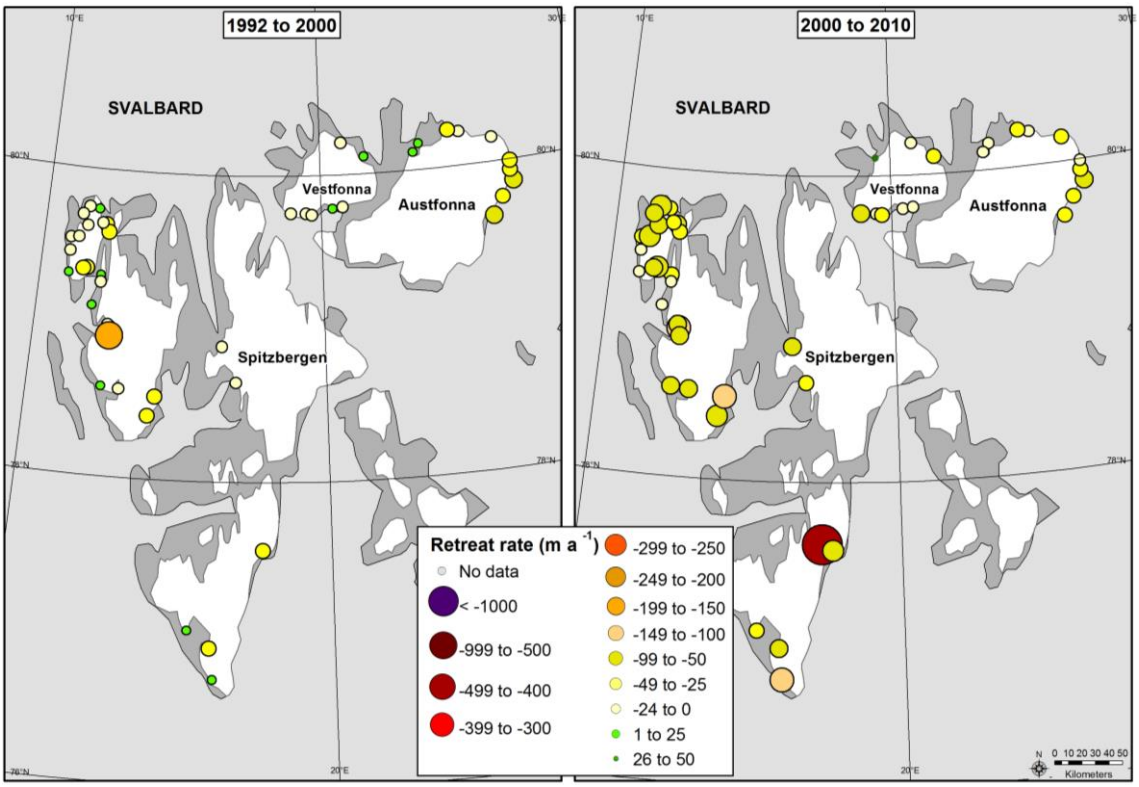

Figure 6.5. *Mean marine-terminating outlet glacier retreat rates for the Svalbard, for the periods 1992-2000 and 2000-2010. Retreat rate is symbolised by colour and size, with larger symbols indicating more rapid retreat*

Focusing on specific regions within Svalbard, between 2000 and 2010 retreat rates were substantially higher on Spitzbergen (71.5 m a^{-1}) than on either Vestfonna (VF) (17.2 m a^{-1}) or Austfonna (AF) (23.1 m a^{-1}). However, this may reflect the very high retreat rates on a single glacier (Strongbreen), which exceeded the regional average by a factor of six (Fig. 6.5). Retreat rates on Spitzbergen also showed by far the largest change between the two time periods, increasing five-fold from 13.2 m a^{-1} in 1992-2000 to 71.5 m a^{-1} in 2000-2010. The marine-terminating outlets on VF demonstrated the lowest retreat rates in the region and these did not increase substantially between 1992-2000 (2.1 m a^{-1}) and 2000-2010 (17.2 m a^{-1}) (Fig. 6.5, Table 6.2). AF was the only study region where retreat rates decreased between 1992-2000 (28.8 m a^{-1}) and 2000-2010 (23.1 m a^{-1}) (Fig. 6.5, Table 6.2). The standard deviation in retreat rates on Spitzbergen was more than double that on AF or VF for both time periods (Figs. 6.3 & 6.5, Table 6.2).

6.3.1.4. Novaya Zemlya

Marine-terminating outlet glaciers on NVZ underwent widespread retreat between 1992 and 2010 (Fig. 6.6, Table 6.2). Mean retreat rates almost trebled between 1992-2000 (24.6 m a^{-1}) and 2000-2010 (64.0 m a^{-1}), with only one glacier advancing during the latter period (Fig. 6.6, Table 6.2). Retreat rates were significantly higher on the Barents Sea coast (61.7 m a^{-1}) than the Kara Sea (40.8 m a^{-1}). Variability in ocean-terminating outlet glacier retreat rates was higher on the Barents Sea than the Kara Sea during both time periods (Figs. 6.2 & 6.6) and doubled on both coasts between 1992-2000 and 2000-2010 (Figs. 6.2 & 6.6, Table 6.2).

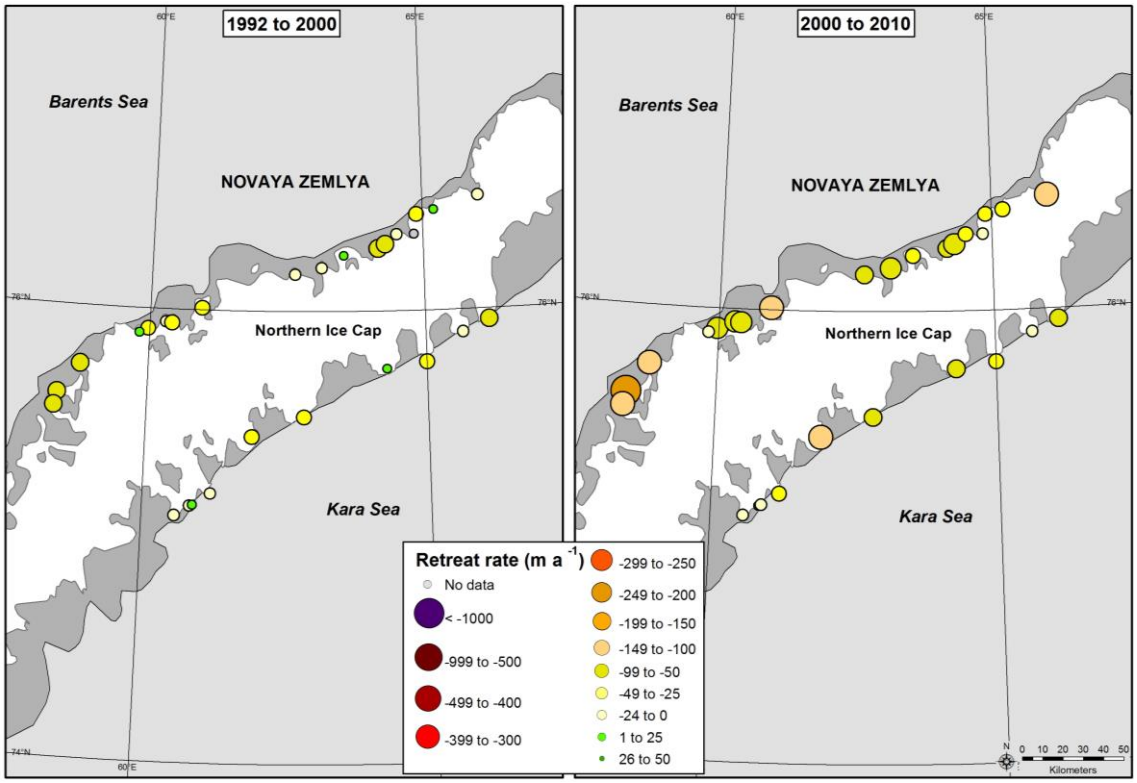

Figure 6.6. *Mean marine-terminating outlet glacier retreat rates for the NVZ, for the periods 1992-2000 and 2000-2010. Retreat rate is symbolised by colour and size, with larger symbols indicating more rapid retreat*

6.3.1.5. Franz Josef Land

FJL marine-terminating outlet glaciers retreated substantially between 1992 and 2010 (Fig. 6.7, Table 6.2). Between 1992 and 2000, 76 % of glaciers retreated at a mean rate of 15.5 m a^{-1} (Fig. 6.7, Table 6.2). This subsequently increased to 39.0 m a^{-1} for the period 2000-2010, when all glaciers underwent net retreat (Fig. 6.7, Table 6.2). The standard deviation in retreat rates reduced from 29.6 m a^{-1} in 1992-2000 to 21.2 m a^{-1} in 2000-2010 (Figs. 6.2 & 6.7, Table 6.2).

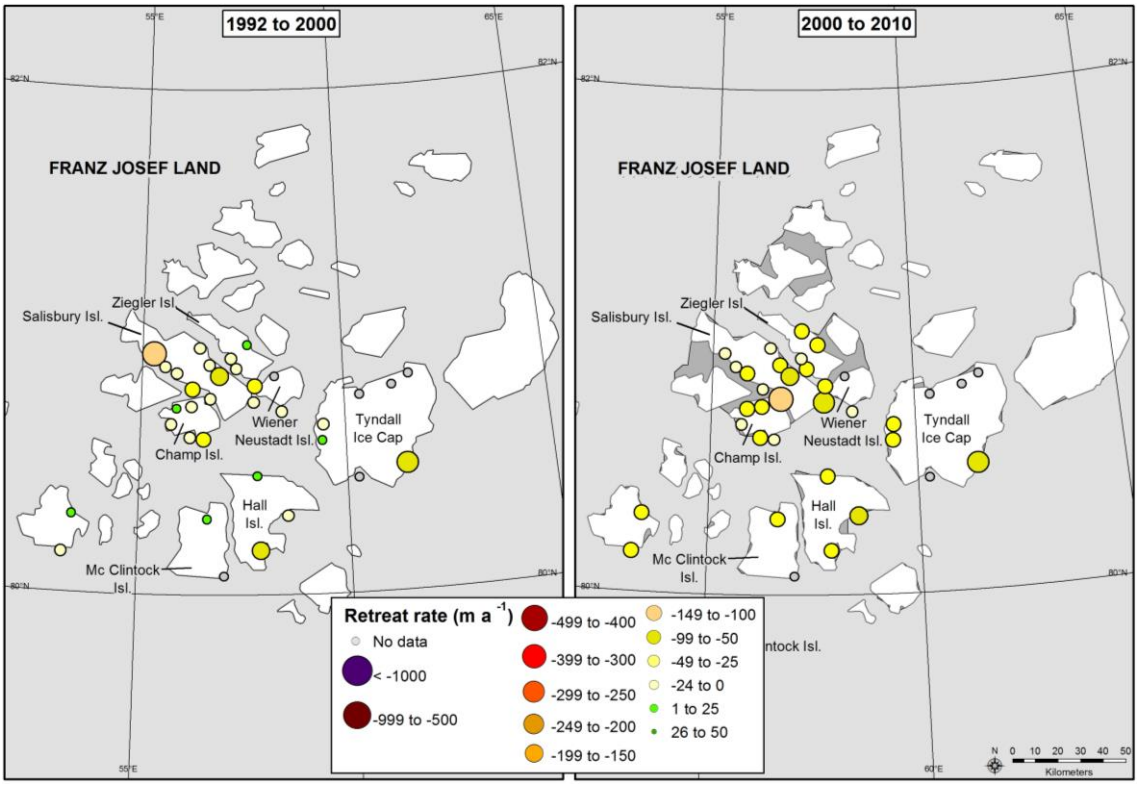

Figure 6.7. *Mean marine-terminating outlet glacier retreat rates for the FJL, for the periods 1992-2000 and 2000-2010. Retreat rate is symbolised by colour and size, with larger symbols indicating more rapid retreat.*

6.3.2. Air temperatures

Statistically significant warming trends occurred along the west Greenland coast between 1990 and 1999, with air temperatures increasing at a rate of up to 0.3 °C per year (Fig. 6.8). Stations surrounding Baffin Island and certain stations in south-eastern Greenland also showed significant warming (Fig. 6.8). Between 2000 and 2010, warming occurred in the Canadian High Arctic, including Baffin Bay and Ellesmere Island, at certain stations in south-eastern Greenland and at stations located on the Kara Sea (Fig. 6.8). No statistically significant air temperature trends were observed on the northern or north-eastern Greenland coast, on Svalbard or in the Russian High Arctic during either time period (Fig. 6.8).

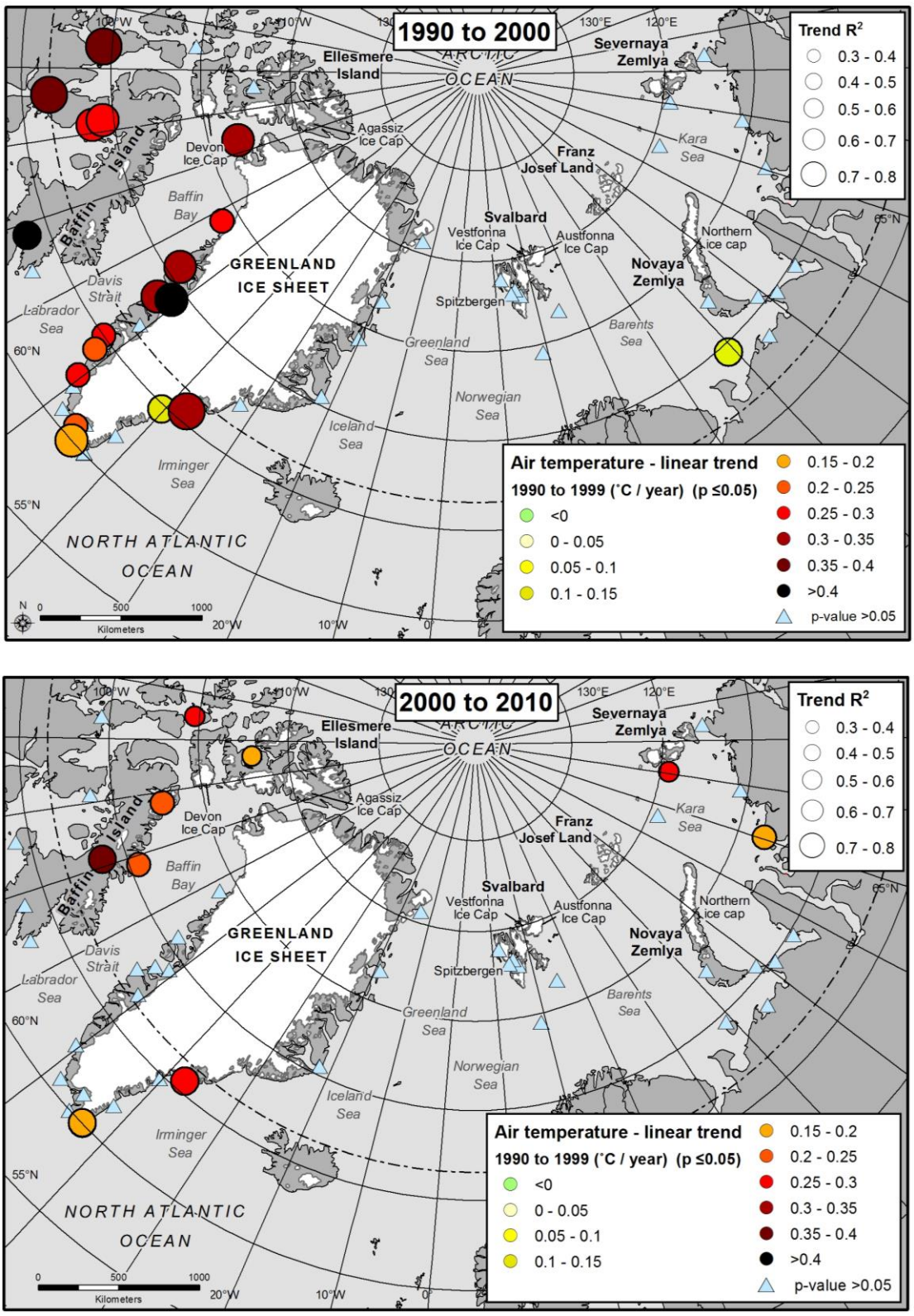

Figure 6.8. *Linear trend in mean annual air temperatures between 1990 and 2010 for selected Arctic meteorological stations. Symbol colour shows the magnitude of the linear trend in ºC per year between 1990 and 2010. Symbol size shows the R^2 value of the relationship. Trends are shown only for locations where the p-value associated with the F-statistic was ≤ 0.05, i.e. locations where the trend was statistically significant.*

6.3.3. Sea ice

Changes in mean annual sea ice concentrations varied substantially across the study region (Fig. 6.9). Statistically significant negative trends occurred in north- and central-west Greenland, FJL and at certain glaciers on the west Spitzbergen coast. Maximum rates of sea ice decline occurred at the termini of glaciers located on FJL and NW GrIS, where the trend approached 2 % per year (Fig. 6.9). Sea ice decline was particularly marked and widespread in north-west Greenland, where the rate of reduction in sea ice concentrations exceeded 1% per year at the majority of the study glacier termini (Fig. 6.9). No statistically significant trends in sea ice concentrations were found on the northern or eastern coasts of Greenland, on Vestfonna, Austfonna or on NVZ (Fig. 6.9).

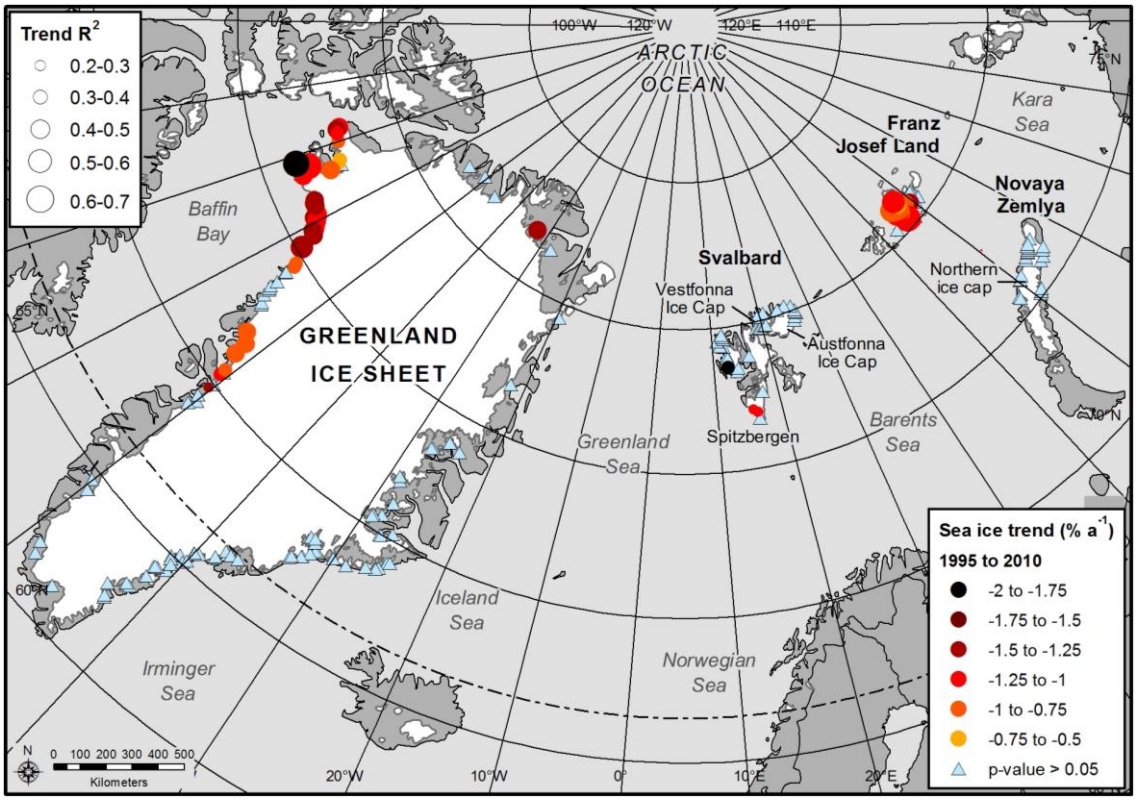

Figure 6.9. *Linear trend in mean annual sea ice concentrations over time between 1995 and 2010 at the study glacier termini. Symbol colour shows the magnitude of the linear trend in percent per year between 1995 and 2010. Symbol size shows the R^2 value of the relationship. Trends are shown only for locations where the p-value associated with the F-statistic was ≤ 0.05, i.e. locations where the trend was statistically significant.*

6.3.4. Sea surface temperatures

Between 2000 and 2010, marked SST warming occurred in the Labrador and Irminger Seas (Fig. 6.10), offshore of south-east and south-west Greenland. SSTs increased substantially in south-west Baffin Bay, with the greatest warming occurring at the central-west Greenland coast. Offshore of east Greenland, SST increases extended north of the Denmark Strait, to approximately 72 ºN (Fig. 6.10). Warming also occurred to the north and east of FJL and was particularly marked in the western Kara Sea. In contrast, cooling occurred across the Barents Sea, particularly to the south and west of NVZ. Slight cooling occurred on the north-east Greenland coast, north of 72 ºN, and to the south and west of Svalbard (Fig. 6.10).

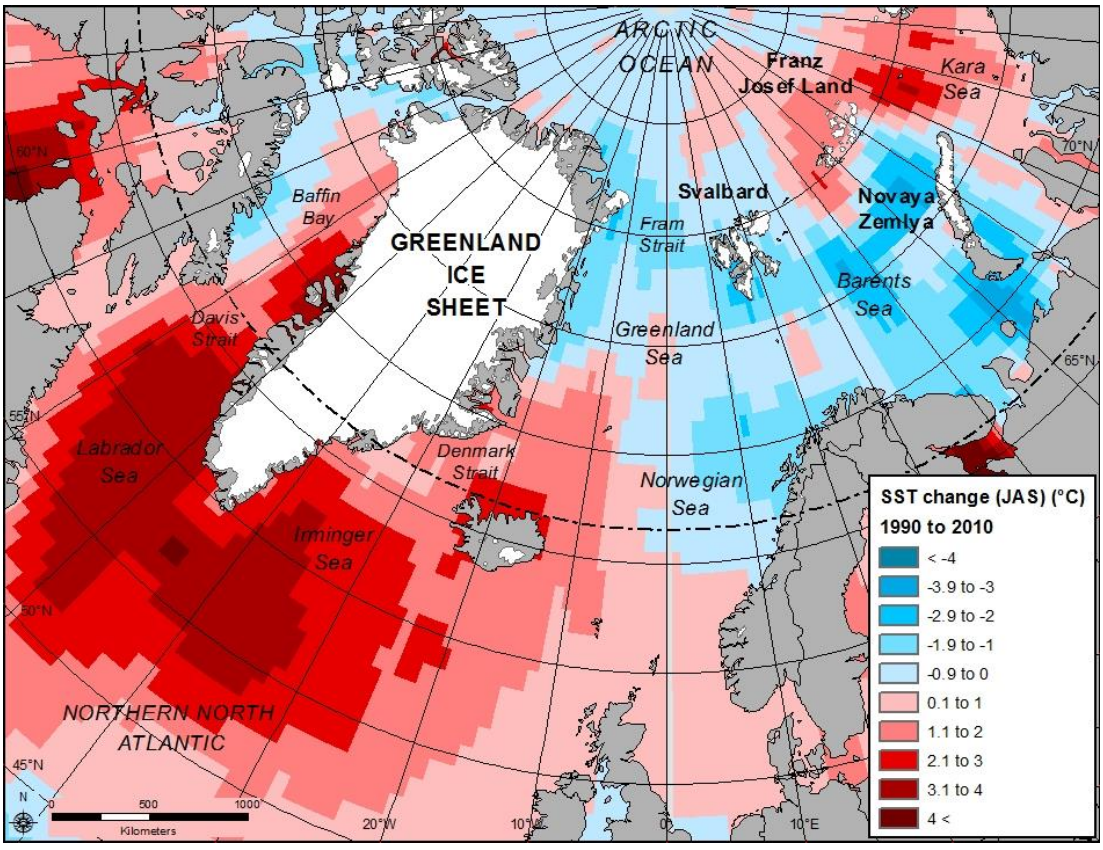

Figure 6.10. *Total change in mean summer (July-September) sea surface temperatures between 2000 and 2010 for the study region.*

6.3.5. Fjord width variation

In the majority of the study regions, there was a statistically significant relationship between along-fjord width variability and total retreat rate (1992-2010) for study

glaciers with continuous fjord walls (Fig. 6.11). Specifically, glaciers which experienced higher along-fjord width variability along their retreat path underwent more rapid retreat.

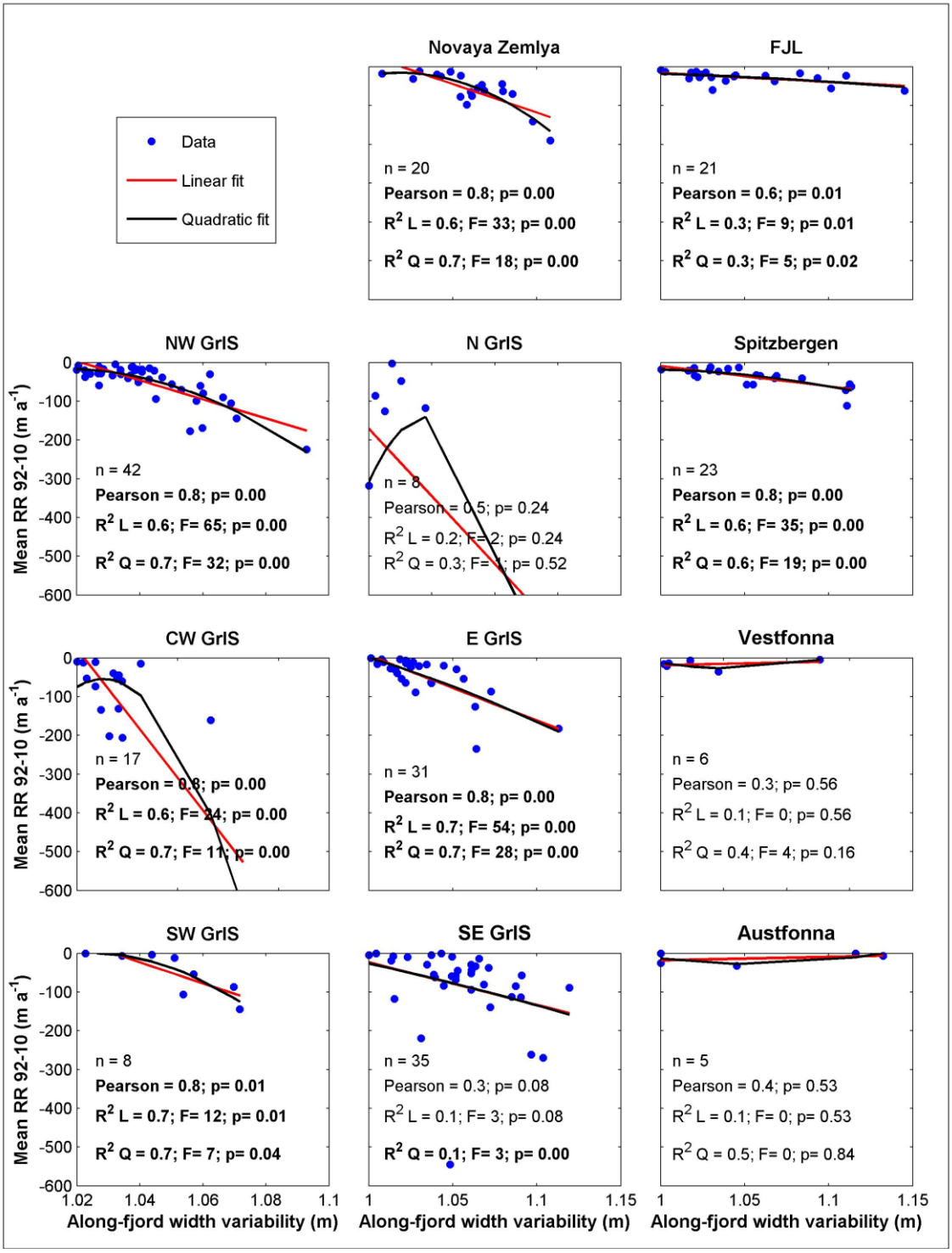

Figure 6.11. *Scatter plots of along-fjord width variability versus mean retreat rate (m a^{-1}) between 1992 and 2010. Plots are divided according to region and each plot includes all study glaciers within that region with continuous fjord walls (top left). This encompasses approximately 75 % of the total number of study glaciers. Width variability was measured between the least*

and most advanced position reached by the glacier terminus during the study period. Linear (red line) and quadratic (black line) fits were applied to the data (blue dots).

A statistically significant relationship was observed along the west Greenland coast (NW, CW and SW), in East Greenland, Novaya Zemlya, Spitzbergen and FJL, which together accounts for 162 glaciers out of the total of 216 glaciers with continuous fjord walls (Fig. 6.11). In west Greenland, East Greenland, NVZ and Spitzbergen, the values for the Pearson's correlation coefficient were ~0.8 and the associated p-value was substantially less than the significance level of 0.05 (Fig. 6.11). This demonstrates that there was a statistically significant linear correlation between along-fjord width variability and total retreat rate in these regions. The R^2 values for linear regression of along-fjord width variability against total retreat rate ranged between 0.6 and 0.7 and polynomial regression gave an R^2 of ~0.7 (Fig. 6.11). The p-value associated with the F-statistic for both linear and polynomial regression was below the 0.05 significance level and, most often, below the 0.01 significance level. This shows that the regression models are statistically significant (i.e. there is a statistically significant relationship between the two variables).

There was a statistically significant relationship between along-fjord width variability and total retreat rate on FJL, but the values for the Pearson's correlation coefficient (0.6), linear R^2 (0.3) and polynomial R^2 (0.3) are low compared to the regions discussed above (Fig. 6.11). The lower value for the Pearson's correlation coefficient suggests that the linear correlation between fjord-width variability and retreat rate is less strong and the lower R^2 values for linear and polynomial regression demonstrate that the data have a greater spread around the fitted lines.

In south-east Greenland, the relationship between fjord width variability and total retreat rate was not statistically significant and the values of r and R^2 were comparatively low (Fig. 6.11). However, these values are strongly influenced by four glaciers in the region, which show a marked deviation from the general pattern of more rapid retreat with higher fjord-width variability. These were Helheim, Fenris and

Midgård glaciers, which drain into the same fjord system, and an unnamed glacier which we term SE5. Helheim Glacier underwent rapid retreat between 2000 and 2010, but experienced little variation in fjord width along its retreat path (Fig 6.12A) and Midgård and SE5 exhibited similar behaviour. Conversely, Fenris Glacier experienced large changes in fjord width but showed comparatively low retreat rates. If these four glaciers are removed from the analysis, then the relationship between fjord width variability and total retreat rate in south-east Greenland becomes statistically significant and the Pearson's correlation coefficient and R^2 values are comparable to central-west Greenland.

6.4. Discussion

6.4.1. Marine-terminating outlet glacier retreat and dynamic change

The widespread and rapid retreat of marine-terminating outlet glaciers we observe in the Atlantic sector of the Arctic is consistent with the near world-wide glacier recession reported in the IPCC Fifth Assessment Report [*IPCC*, 2013]. It also concurs with the rapid and often accelerating ice loss recorded on Arctic masses during the past two decades [e.g. *Gardner et al.*, 2013; *Lenaerts et al.*, 2013; *Moholdt et al.*, 2012; *Rignot et al.*, 2011; *Shepherd et al.*, 2012]. Our findings therefore affirm that the Atlantic sector of the Arctic is an area undergoing rapid dynamic change and marine outlet glacier retreat.

Our results demonstrate that ocean-terminating outlet glacier retreat is widespread on all ice masses within the Atlantic sector of the Arctic (Fig. 6.3, Table 6.2). Retreat rates have increased notably on Spitzbergen and the Barents Sea coast of NVZ during the past two decades (Figs. 6.3, 6.5 & 6.6, Table 6.2), but little is known about the potential impact of this retreat on ice dynamics and near-future mass loss. On the basis of previous studies on the GrIS, marine-terminating outlet glacier retreat has the capacity to rapidly initiate widespread and substantial thinning, as well as contributing directly to sea level rise through the loss of grounded ice [*Howat et al.*, 2008; *Pritchard et al.*, 2009; *Thomas et al.*, 2011; *Zwally et al.*, 2011]. It is therefore imperative to assess the

committed ice loss and thinning due to recent retreat on other Arctic ice masses and to evaluate the timescales of this dynamic response to retreat, in order to accurately forecast near-future Arctic ice loss.

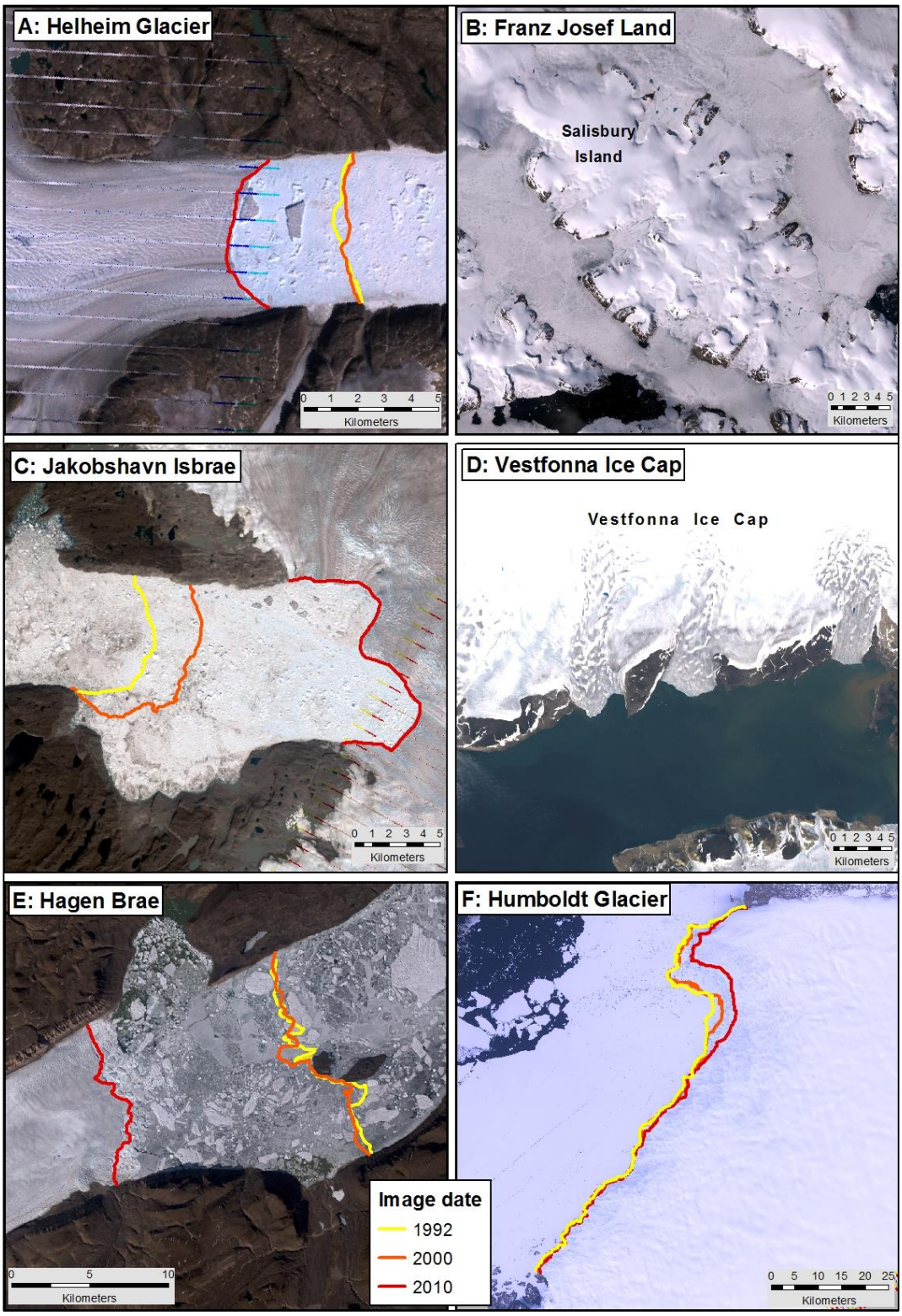

Figure 6.12. *Relationship between marine-terminating outlet glacier retreat (1992, 200 &, 2010) and fjord width variation for selected glaciers: A) Helheim Glacier, south-east Greenland; B)*

Marine-terminating outlet glaciers of Salisbury Island, Franz Josef Land (fjords mostly filled by sea-ice); C) Jakobshavn Isbrae, central-west Greenland; D) Marine-terminating outlet glaciers on southern Vestfonna Ice Cap; E) Hagen Brae, north Greenland; and F) Humboldt Glacier, northern Greenland. Images are Landsat, provided by the USGS GLOVIS.

The need to further investigate the contribution of ice dynamics to deficits outside of the GrIS is exemplified by recent results from NVZ [*Carr et al.*, 2014; *Moholdt et al.*, 2012]. Retreat rates were an order of magnitude higher on marine-terminating outlet glaciers, in comparison to those terminating on land, yet no significant difference in thinning has been observed between the two types of basin [*Carr et al.*, 2014; *Moholdt et al.*, 2012]. These results suggest that we may be underestimating contemporary dynamic losses from the region and/or that dynamic response may contribute substantially to future ice loss [*Carr et al.*, 2014]. In either scenario, we need to improve our understanding of dynamic losses and glacier response times on NVZ, and other large Arctic ice masses outside of the GrIS, in order to accurately forecast their contribution to near-future sea level rise.

Focusing specifically on the GrIS, rapid retreat occurred in north- and central-west Greenland between 2000 and 2010 (Fig. 6.4, Table 6.2). This is consistent with previously reported changes in the region: GRACE results showed accelerated ice loss from 2005 onwards [*Khan et al.*, 2010] and large increases in flow speed occurred between 2005 and 2010 [*Moon et al.*, 2012]. Furthermore, estimates suggest that between 2003 and 2008, approximately half of the mass loss from the central- and north-west of the GrIS was dynamic in origin [*van den Broeke et al.*, 2009]. Despite an overall retreat trend, however, there was large variability in retreat rates between individual glaciers (Fig. 6.4, Table 6.2). This agrees with the highly non-uniform pattern of glacier acceleration previously reported for north-west Greenland [*Moon et al.*, 2012]. Our results demonstrate a similar pattern of behaviour in south-east Greenland, whereby retreat rates were high, but varied substantially between individual outlets (Fig. 6.3 & 6.4, Table 6.2). This agrees with previous findings [*Howat et al.*, 2008; *Moon*

and Joughin, 2008; *Murray et al.*, 2010] and with the large spatial variation in glacier velocities observed in the region between 2000 and 2010 [*Moon et al.*, 2012]. In contrast to north-west Greenland, however, a number of south-east Greenland glaciers decelerated between 2005 and 2010 [*Moon et al.*, 2012]. Although it is very difficult to forecast future response, these trends suggest that at a regional scale, central- and north-west Greenland may be very important, but highly spatially variable, sources of near-future dynamic ice loss and that their contribution may exceed that of south-eastern Greenland.

Northern Greenland was the area of most rapid glacier retreat between 2000 and 2010 (Figs. 6.3 & 6.4, Table 6.2). Substantial mass balance anomalies have not been recorded in the region, either in data from GRACE [e.g. *Khan et al.*, 2010] or through comparison of discharge and SMB [*van den Broeke et al.*, 2009]. Furthermore, previous results suggest that the contribution of changes in ice discharge to mass loss between 2003 and 2008 was small [*van den Broeke et al.*, 2009]. This apparently limited dynamic response to retreat contrasts markedly with observations from other areas of the GrIS [e.g. *Howat et al.*, 2008; *Pritchard et al.*, 2009; *Thomas et al.*, 2011; *Zwally et al.*, 2011]. Moreover, the impact of glacier retreat on ice dynamics appears to vary substantially across northern Greenland [*Moon et al.*, 2012; *Nick et al.*, 2012]. For example, Hagen Brae retreated very rapidly (1279.6 m a^{-1}) between 2000 and 2010 (Fig. 6.4), which coincided with its dramatic acceleration between 2000 and 2007 [*Moon et al.*, 2012]. In contrast, C.H. Ostenfeld Glacier retreated at a rate of 766.1 m a^{-1} during the past decade (Fig. 6.4), but showed no significant change in flow velocity [*Moon et al.*, 2012]. Similarly, the recent loss of a large section of Peterman Glacier's ice tongue had little impact on ice velocities [*Nick et al.*, 2012].

The very high regional retreat rates in northern GrIS may result from the fact that many glaciers terminate in substantial floating ice tongues, which are rare elsewhere on the GrIS and in other regions of the Atlantic sector of the Arctic. The nature of calving differs from other areas of the GrIS due to these floating sections, which usually

produce very large tabular icebergs that are trapped close to the ice front for years to decades by semi-permanent fast ice [*Higgins*, 1989; 1990; *Reeh*, 1994]. Consequently, when ice is removed from the calving front, the magnitude of retreat can be very large (Figs. 6.3 and 6.4). Differences in the properties of these ice tongues may also explain the strong variation in dynamic response of northern Greenland glaciers to frontal retreat. At both Peterman and C.H. Ostenfeld Glacier, the ice tongues were thin and the latter was heavily fractured prior to retreat [*Joughin et al.*, 2010; *Moon and Joughin*, 2008; *Nick et al.*, 2012]. Consequently, the lateral resistance to flow provided by the tongues is likely to have been small and so loss of substantial floating sections had limited impact on ice velocities [*Nick et al.*, 2012]. In contrast, it is thought that Hagen Brae lost grounded ice during retreat and that its tongue receded from a pinning point within its fjord, which together would have substantially reduced resistive stresses and thus may have caused glacier acceleration [*Joughin et al.*, 2010]. In light of the highly variable retreat rates in northern Greenland (Figs. 6.3 & 6.4) and the strong variation in dynamic response to these episodes of retreat, we underscore the need for further research into the influence of these floating sections on glacier behaviour. Furthermore, northern Greenland outlet glaciers are very large, can retreat very rapidly and have the potential to contribute very substantially to sea level rise through loss of grounded ice / dynamic draw-down. However, their highly variable behaviour makes it difficult to forecast their contribution to near-future sea level rise and so we highlight the region as a priority for future research.

6.4.2. Atmospheric and oceanic controls

6.4.2.1. Air temperatures

For the period 1990 to 1999, statistically significant warming trends along the western and south-eastern coasts of Greenland coincided with regional outlet glacier retreat rates of between 33.5 and 40.3 m a^{-1} (Figs. 6.4 & 6.8, Table 6.2). These retreat rates exceeded the average for the Atlantic Arctic (23.6 m a^{-1}) and for regions where atmospheric warming was limited, specifically East Greenland, Svalbard and the

Russian High Arctic. This indicates that elevated air temperatures may have contributed to observed retreat (Figs. 6.4 & 6.8, Table 6.2). This is consistent with previous results from western Greenland, which suggested that warming may have promoted retreat at Alison Glacier, north-west Greenland. [*Carr et al.*, 2013b] and that increased water levels in terminus and/or lateral crevasses may have contributed to rapid retreat at Jakobshavn Isbrae, central-west Greenland [*Sohn et al.*, 1998; *van der Veen et al.*, 2011; *Vieli and Nick*, 2011]. In addition to meltwater enhanced crevassing, elevated air temperatures may also cause glacier retreat via sea ice melt: the presence of sea ice in glacier fjords is thought to substantially influence calving and hence the magnitude of seasonal retreat [e.g. *Amundson et al.*, 2010; *Joughin et al.*, 2008b; *Sohn et al.*, 1998], meaning that a reduction in sea ice due to atmospheric warming could promote net glacier retreat. This mechanism is supported by the coincidence of sea ice loss and atmospheric warming in central- and north-western Greenland (Figs. 6.8 & 6.9). Previous results from Jakobshavn Isbrae [*Motyka et al.*, 2011], central-west Greenland [*Rignot et al.*, 2010] and numerical modelling studies [*Jenkins*, 2011; *Xu et al.*, 2012] suggest that increased air temperatures may also contribute to glacier retreat by enhancing subglacial plume flow and thus increasing submarine melt rates. However, little is known about the relative importance of this mechanism at regional scales, as oceanic data are available for only a limited number of glacier fjords and accurate measurement of submarine melt rates is very challenging [*Straneo et al.*, 2013].

Despite a correspondence between marine-terminating outlet glacier retreat and atmospheric warming between 1990 and 1999, no relationship is apparent in western and south-eastern Greenland between 2000 and 2010. In north and central-west Greenland, no statistically significant trend in air temperatures was recorded between 2000 and 2010, yet regional retreat rates were up to four times greater than 1990-1999 (Figs. 6.4 & 6.8, Table 6.2). Similarly, in south-eastern Greenland, atmospheric warming trends were stronger during the period1990-1999 than during 2000-2010, yet

retreat rates were three times higher during the later period (Figs. 6.4 & 6.8, Table 6.2). This suggests that there is no straightforward, linear relationship between atmospheric warming and mean regional retreat rates in these regions. Furthermore, despite an overall regional correspondence between atmospheric warming and glacier retreat in western and south-eastern Greenland between 1990 and 1999, there was large variability in individual glacier retreat rates (Fig. 6.4, Table 6.2). This indicates that no simple relationship exists between air temperature increases and individual glacier response, even in areas which appear to show a regional-scale sensitivity to warming.

In other study regions, specifically northern Greenland, Spitzbergen and Novaya Zemlya, there was no statistically significant trend in air temperatures during either time period (Fig. 6.8). However, our results recorded rapid marine-terminating outlet glacier retreat in these areas and mean regional retreat rates increased substantially between 1992-2000 and 2000-2010 (Fig. 6.3, Table 6.2). On the basis of observed rapid retreat despite there being no significant atmospheric warming trend, we suggest that increased air temperatures are not the primary driver of retreat in these regions during the past two decades. However, it has previously been suggested that a warming of a few degrees would be sufficient to melt fast-ice in northern Greenland, thus making the ice tongues unsustainable [*Reeh et al.*, 1999]. This is supported by radio carbon dating of marine sediments, which suggested that northern Greenland ice tongues collapsed several times during the Holocene Climatic Optimum [*Reeh et al.*, 1999; *Weidick et al.*, 1994], which was a period approximately 9,000 to 6,000 years ago when temperatures were considerably warmer than present and the GrIS margins thinned substantially [*Vinther et al.*, 2009]. This indicates that northern Greenland glaciers may be sensitive to future air temperature increases, if warming is sufficient to overstep the potential stability thresholds suggested for this region, but that other factors are driving contemporary retreat.

It should also be noted that even if atmospheric warming did occur in regions such as northern Greenland, its impact on glacier retreat rates may not be comparable to

locations in southern Greenland, as the climate is comparatively cool. This is exemplified by comparison of mean annual air temperatures at Henrik Krøyer Holme, located in the north-east of Greenland (-12.4 °C), and at Angisoq, at the southern tip of Greenland (+0.9 °C). As temperatures as Henrik Krøyer Holme are far below freezing, a small increase in air temperatures would have limited effect on meltwater production, where as their impact could be substantial at Angisoq. As such, the impact of given amount of warming will have a differing impact on melt rates and glacier retreat, dependant on the climatic regime in which it is situated.

6.4.2.2. Sea ice

Strong and statistically significant trends in sea ice loss occurred in central- and north-west Greenland (Fig. 6.9). This coincides with rapid glacier retreat (Fig. 6.4, Table 6.2) and suggests that sea ice may be a primary forcing factor in these regions. This is consistent with previous studies, which identified sea ice as an important control on the dynamics of Jakobshavn Isbrae [*Amundson et al.*, 2010; *Joughin et al.*, 2008b; *Sohn et al.*, 1998], Alison Glacier [*Carr et al.*, 2013b] and glaciers located in the Uummannaq region of central-west Greenland [*Howat et al.*, 2010]. Sea ice is thought to influence glacier behaviour by determining the timing of calving events [*Amundson et al.*, 2010; *Joughin et al.*, 2008b; *Sohn et al.*, 1998]. In winter, sea ice binds together icebergs within the fjord to form an ice mélange, which can strongly supress calving, whereas in the summer, seasonal loss of the mélange allows seasonally high calving rates to commence [*Amundson et al.*, 2010; *Joughin et al.*, 2008b; *Sohn et al.*, 1998]. Consequently, a reduction in sea ice concentrations can promote internnual retreat, by extending the duration of seasonally high calving rates [*Carr et al.*, 2013b; *Howat et al.*, 2010; *Joughin et al.*, 2008b; *Seale et al.*, 2011]. Given the marked changes in sea ice recently observed in north-west Greenland, along with the rapid glacier retreat (Fig. 6.4), glacier acceleration [*Moon et al.*, 2012] and ice loss [*Khan et al.*, 2010] during the past decade, we highlight the region as a key site for future research.

Marked sea ice decline occurred on FJL, coincident with a moderate increase in glacier retreat rates during the study period, which suggests that sea ice may be a significant control on retreat within the region (Figs. 6.7 & 6.9). However, retreat rates on FJL are much lower than in other regions that experienced a similar sea ice reduction, such as north-western Greenland (Fig. 6.9). We suggest that this may reflect differences in fjord topography: FJL outlet glaciers generally terminate on small rock islands (Fig. 6.12B), whereas north-west Greenland outlet glaciers occupy comparatively well-defined rock fjords. Consequently, the ice mélange may be much less extensive on FJL, as it does not have a large, sheltered fjord in which to form, and so may have a lesser influence on calving rates and glacier frontal position. Sea ice loss at FJL also coincides with marked SST warming (Fig. 6.10), suggesting that this may have contributed to sea ice decline. FJL has received very little scientific attention to date, but the dramatic changes in sea ice and SSTs we observe during the past two decades highlight the need to conduct further research in the region.

Sea ice has been previously identified as an important control on NVZ marine-terminating outlet glacier retreat rates and changes in frontal position show a close correspondence to sea ice concentrations at annual timescales [*Carr et al.*, 2014]. However, at the decadal timescales investigated here, this relationship is not apparent: marine-terminating NVZ outlet glaciers retreated substantially between 1995 and 2010 (Fig. 6.6), but sea ice concentrations showed no statistically significant trend (Fig. 6.9). This most likely reflects the very substantial interannual variability in sea ice concentrations observed on NVZ [*Carr et al.*, 2014]. Due to this high variability, no significant trend is apparent at decadal time periods, but instead, years of anomalously low sea ice concentrations may trigger outlet glacier retreat [*Carr et al.*, 2014]. This exemplifies the need to utilise high temporal resolution datasets when investigating the controls on glacier behaviour in areas where forcing factors show substantial temporal variation, such as NVZ

.6.4.2.3 Sea surface temperatures

Sea surface temperature warming was most marked in south-western and south-eastern Greenland and in south-west Baffin Bay (Fig. 6.10). This agrees with previous studies, which noted that widespread glacier retreat in south-eastern Greenland during the early 2000s coincided with elevated SSTs [*Murray et al.*, 2010] and that interannual retreat in the Uummunaq region occurred in response to SST warming and sea ice reductions in 2003 [*Howat et al.*, 2010]. Furthermore, our results show a marked difference in retreat rates between glaciers located to the north and the south of the Denmark Strait on the east Greenland coast (Fig. 6.4). The northerly extent of the higher retreat rates coincides with spatial extent of the SST warming (Figs. 6.4 & 6.10), suggesting that increased SSTs may have contributed to this retreat. This is supported by the limited change in ice velocities north of ~69 ºN during the past decade, in contrast to substantial acceleration in south-eastern Greenland, which has been attributed to the comparatively cool surface and sub-surface ocean temperatures in the northern section [*Moon et al.*, 2012; *Seale et al.*, 2011].

Although elevated SSTs may promote retreat through melting at the water line [*Benn et al.*, 2007; *Vieli et al.*, 2002] and/or through sea ice loss, their impact on submarine melt rates is limited compared to deeper ocean temperatures. Furthermore, SSTs do not necessarily provide any indication of sub-surface temperature changes. Previous studies have highlighted the potentially large contribution of submarine melting to the mass loss from marine-terminating outlets [*Enderlin and Howat*, 2013; *Motyka et al.*, 2011; *Rignot et al.*, 2010], yet little is known about how this control varies across the Arctic, due to very limited data availability. This may be particularly important for interpreting recent changes in northern Greenland and for assessing future behaviour, as basal melting from the ice tongues is a primary mass loss mechanism in the region [*Reeh*, 1994; *Reeh et al.*, 1999]. For example, on Peterman Glacier, mass conservation calculations suggest that submarine melting across the floating tongue accounts for up to 80% of ice loss and that deep channels formed during the melting process may have

important implications for ice shelf vulnerability to climate change [*Rignot and Steffen*, 2008]. We therefore highlight the need to collect detailed salinity and temperature data from major Arctic outlet glacier fjords, in order to improve our understanding of the role of sub-surface ocean temperatures in driving marine-terminating outlet glacier retreat.

6.4.3. Fjord width variation

Although some regional-scale patterns in marine-terminating outlet glacier retreat rates were apparent, there was large variability between individual glaciers and within regions (Figs. 6.4 to 6.7, Table 6.2). This indicates that glacier-specific factors significantly influenced glacier retreat rates and substantially modulated the response of individual glaciers to external forcing. Our results show a statistically significant relationship between along-fjord width variability and total retreat rate (1992-2010) in western Greenland (NW, CW, SW), East Greenland, NVZ, Spitzbergen and FJL (Fig. 6.11). We suggest that along-flow fjord width variability may influence glacier retreat via two mechanisms. First, as a glacier moves into a wider section of its fjord, it would need to thin in order to conserve mass, which would make the ice more vulnerable to full-thickness fracture and bring it close to floatation, which in turn would increase calving rates and promote retreat [*O'Neel et al.*, 2005]. Second, lateral stresses have an inverse relationship with width, meaning that resistance to flow from the sidewalls was reduced in wider sections of the fjord, thus promoting further acceleration, dynamic thinning and retreat [*Raymond*, 1996]. On the basis of the strong statistical relationship observed in western Greeenland, East Greenland, NVZ and Spitzbergen (Fig. 6.11), fjord width variability may provide a widely-applicable indicator of glaciers with the potential to undergo rapid retreat in these regions.

This is consistent with observations over longer (glacial/interglacial) time frames, which have demonstrated the strong influence of lateral topography on the pattern and rate of retreat. This is exemplified by the recession of the Marguerite Bay Ice Stream, Antarctica, following the Last Glacial Maximum (LGM), which was highly non-linear and underwent a series of temporary still-stands that were associated narrow sections of its

trough, even on areas of reverse sloping bed [*Jamieson et al.*, 2012]. Similarly, evidence from the West Greenland Ice Sheet suggests that retreat was forced by climatic warming following the LGM, but that the pattern of terminus recession and the location of temporary periods of frontal stability were determined by the fjord topography [*Warren and Hulton*, 1990]. Finally, it has been suggested that development of a large, calving embayment, which followed the retreat of the grounding line of the Hudson Strait Ice Stream beyond its constraining topography, allowed the ice stream to migrate rapidly into the interior of the Laurentide Ice Sheet [*Hughes*, 2002]. Taken together, this highlights the strong influence of fjord width variations on glacier behaviour at a range of temporal and spatial scales.

There was a strong relationship between fjord width variation and glacier retreat in the majority of regions and for most of the study glaciers, but some spatial variation was apparent (Fig. 6.11). The influence of fjord width variation was most marked in areas where ocean-terminating outlet glaciers discharge through well-defined fjords that strongly constrain their flow. This is the case for the majority of marine-terminating glaciers in Greenland, NVZ and Spitzbergen and hence the vast majority of our study glacier population. One notable example is Jakobshavn Isbrae, which exhibited very high retreat rates between 2000 and 2010 (1160.7 m a^{-1}) and large fjord width variability along its retreat path (5064.5 m) (Fig. 6.12C). In contrast, in areas such as Austfonna and Vestfonna, the topography is much less mountainous [*Hagen et al.*, 2003; *Moholdt et al.*, 2010; *Nuth et al.*, 2010] and marine-terminating outlet glaciers are less constrained by their topography (Fig. 6.12D). Here, many of the outlet glaciers resemble small ice streams that are laterally bounded by slower-moving ice, as opposed to rock walls (Fig. 6.12D) [*Dowdeswell*, 1986]. As a result, there are less likely to be sharp changes in fjord width along the retreat path, such as pinning points, and so variations in lateral stresses are likely to be lower than on glaciers bounded by bedrock. On FJL, some outlet glaciers are bounded by fjords and others by slower moving ice (Fig. 6.12B). This may explain the statistically significant but comparatively

weak relationship between fjord width variability and total retreat rate on the archipelago: fjord width variations may influence glacier behaviour more strongly on the outlets which have more substantial fjords.

Northern Greenland represents a notable exception to the strong relationship between fjord width variability and total retreat observed elsewhere in the study area (e.g. Fig. 6.12E). This may result from the presence of substantial floating sections at many of the glacier termini and the large variations in the characteristics of these ice tongues, as detailed above. For example, Hagen Brae demonstrated very rapid retreat and large along-flow width variability (Fig. 6.12E), whereas NFG and Humboldt Glacier both underwent substantial retreat but yet experienced no significant change in width (Fig. 6.12F). Given that lateral resistive stresses reduce with increasing width [*Raymond*, 1996], we suggest that their influence on glacier retreat would be limited on the very wide glaciers found in northern Greenland, such as Humboldt (width = ~90 km) and NFG (width = ~34 km), but could become more significant in smaller outlets such as Hagen Brae (width = ~10km). Furthermore, the influence of fjord width variation on glacier dynamics may vary substantially, due to the differing characteristics of glacier ice tongues within the region. As discussed above, the tongues of Peterman and C.H. Ostenfeld Glacier were both thin and provided limited lateral resistance prior to retreat [*Joughin et al.*, 2010; *Moon and Joughin*, 2008; *Nick et al.*, 2012]. As a consequence, changes in the lateral stresses acting on the tongue, associated with variations in fjord width along the retreat path, would have a limited effect on glacier dynamics. This further highlights the need for additional research in northern Greenland, as our results demonstrate very rapid and highly variable retreat rates (Figs. 6.3. & 6.4, Table 6.2), no clear primary external control(s) (Figs. 6.8-6.10) and large variations in response to fjord width variability.

Our results highlight the importance of fjord geometry in determining retreat rates on individual marine-terminating outlet glaciers. Fjord width variability has emerged as a widespread and important control and is comparatively easier to measure. However,

we underscore the need to combine this information with basal topographic data, in order to fully quantify the impact of fjord geometry on outlet glacier retreat rates and response to climate change. The potential for basal overdeepenings to facilitate rapid mass loss from major marine-terminating Arctic outlet glaciers has been previously recognised [e.g. *Meier and Post*, 1987; *Nick et al.*, 2009; *Vieli et al.*, 2001] and recent results from Humboldt Glacier have demonstrated that bedrock troughs can produce order of magnitude differences in retreat rates [*Carr et al.*, in prep.]. The need to integrate information on basal topography and fjord width variation is exemplified by Helheim Glacier, south east Greenland. The glacier retreated along a relatively straight fjord (Fig. 6.12A), indicating that the contribution of fjord width variability to retreat was limited, but previous studies suggested that it retreated into a basal overdeepening, which may have facilitated its rapid retreat [e.g. *Howat et al.*, 2007; *Nick et al.*, 2009],. At present, detailed information on bed topography is limited, particularly outside of the GrIS. Given the potential for fjord geometry to strongly modulate glacier response to forcing, we highlight the need to acquire basal topographic data from major marine-terminating Arctic outlet glaciers.

6.5. Conclusions

Widespread and rapid marine-terminating outlet glacier retreat has occurred across the Atlantic sector of the Arctic during the past two decades. Mean retreat rates for the study region increased five-fold between 1992-2000 (23.6 m a^{-1}) and 2000-2010 (-107.2 m a^{-1}), with 95% of all study glaciers undergoing net retreat during the latter time period. Retreat rates were highest on the GrIS, specifically in the north, central- and north-west and south-east. There was large variability in retreat rates within regions and between individual glaciers. Strong atmospheric warming in western and south-eastern Greenland coincided with glacier retreat between 1990 and 1999, but this relationship was less apparent between 2000 and 2010. Results suggest that marked sea ice decline may have contributed to glacier retreat in central- and north-west Greenland. Despite some regional patterns, however, there is no one forcing factor

which is clearly dominant, suggesting that glacier sensitivity to forcing varies both between and within regions. Furthermore, the different forcing factors are often intrinsically linked, making it difficult to separate out the influence of any single factor. We demonstrate a statistically significant relationship between total glacier retreat rate (1992-2010) and along-flow fjord width variability in the majority of our study regions. This relationship was strongest in areas where fjords strongly constrain glacier flow, such as western Greenland, Spitzbergen and Novaya Zemlya, and was less marked in areas of flatter relief, particularly Austfonna and Vestfonna. These results indicate that fjord width variation is an important control on marine-terminating Arctic outlet glacier behaviour and suggests that it may provide an indicator of glaciers with the potential for rapid retreat. We underscore the need to acquire information on subglacial topography and fjord bathymetry for major Arctic ice masses, in order to accurately forecast their response to forcing. Overall, our results show some regional patterns of glacier retreat and response to external forcing, but demonstrate that retreat rates on individual glaciers are highly variable and strongly influenced by fjord geometry.

6.6. References

Amundson, J. M., M. Fahnestock, M. Truffer, J. Brown, M. P. Lüthi, and R. J. Motyka (2010), Ice mélange dynamics and implications for terminus stability, Jakobshavn Isbræ, Greenland, *Journal of Geophysical Research*, *115*, F01005, doi:10.1029/2009JF001405.

Benn, D. I., C. R. Warren, and R. H. Mottram (2007), Calving processes and the dynamics of calving glaciers, *Earth Science Reviews*, *82*, 143-179.

Blaszczyk, M., J. A. Jania, and J. M. Hagen (2009), Tidewater glaciers of Svalbard: Recent changes and estimates of calving fluxes, *Polish Polar Resarch*, *30*(2), 85–142.

Cappelen, J. (2011), Technical Report 11-05: DMI Monthly Climate Data Collection 1768-2010, Denmark, The Faroe Islands and Greenland *Rep.*, Danish Meteorological Institute, Copenhagen.

Carr, J. R., C. Stokes, and A. Vieli (2014), Recent retreat of major outlet glaciers on Novaya Zemlya, Russian Arctic, influenced by fjord geometry and sea-ice conditions, *Journal of Glaciology*, *60*, 155-170.

Carr, J. R., C. R. Stokes, and A. Vieli (2013a), Recent progress in understanding marine-terminating Arctic outlet glacier response to climatic and oceanic forcing: Twenty years of rapid change, *Progress in Physical Geography*, *37*(4), 435 - 466.

Carr, J. R., A. Vieli, and C. R. Stokes (2013b), Climatic, oceanic and topographic controls on marine-terminating outlet glacier behavior in north-west Greenland

at seasonal to interannual timescales, *Journal of Geophysical Research*, *118*(3), 1210-1226.

Carr, J. R., A. Vieli, C. R. Stokes, S. S. R. Jamieson, S. Palmer, P. Christoffersen, J. A. Dowdeswell, D. Blankenship, and D. Young (in prep.), Basal topographic controls on rapid retreat of Humboldt Glacier, northern Greenland.

Carstensen, L. S., and B. V. Jørgensen (2011), Weather and climate data from Greenland 1958-2010., *Techincal Report*, *11-10*.

Dowdeswell, J. (1986), Drainage basin characteristics of Nordaustlandet ice caps, Svalbard, *Journal of Glaciology*, *32*(10), 31-38.

Enderlin, E. M., and I. M. Howat (2013), Submarine melt rate estimates for floating termini of Greenland outlet glaciers (2000-2010), *Journal of Glaciology*, *59*(213), 67-75.

Enderlin, E. M., I. M. Howat, and A. Vieli (2013), High sensitivity of tidewater outlet glacier dynamics to shape, *The Cryosphere*, *7*(3), 1007-1015, doi:10.5194/tc-7-1007-2013.

Fettweis, X., B. Franco, M. Tedesco, J. H. van Angelen, J. T. M. Lenaerts, M. R. van den Broeke, and H. Gallée (2013), Estimating the Greenland ice sheet surface mass balance contribution to future sea level rise using the regional atmospheric climate model MAR, *The Cryosphere*, *7*(2), 469-489, doi:10.5194/tc-7-469-2013.

Gardner, A., et al. (2013), A Reconciled Estimate of Glacier Contributions to Sea Level Rise: 2003 to 2009, *Science*, *340*(6134), 852-857, doi:10.1126/science.1234532.

Gardner, A., G. Moholdt, B. Wouters, G. J. Wolken, D. O. Burgess, M. J. Sharp, J. G. Cogley, C. Braun, and C. Labine (2011), Sharply increased mass loss from glaciers and ice caps in the Canadian Arctic Archipelago, *Nature*, *473*, 357-360.

Goelzer, H., P. Huybrechts, J. J. Fürst, M. L. Andersen, T. L. Edwards, X. Fettweis, F. M. Nick, A. J. Payne, and S. Shannon (2013), Sensitivity of Greenland ice sheet projections to model formulations, *Journal of Glaciology*, *59*(216), 733-749.

Grant, K. L., C. R. Stokes, and I. S. Evans (2009), Identification and characteristics of surge-type glaciers on Novaya Zemlya, Russian Arctic, *Journal of Glaciology*, *55*(194), 960-972.

Hagen, J. O., J. Kohler, K. Melvold, and J.-G. Winther (2003), Glaciers in Svalbard: mass balance, runoff and freshwater flux, *Polar Research*, *22*(2).

Hamilton, G. S., and J. Dowdeswell (1996), Controls on glacier surging in Svalbard, *Journal of Glaciology*, *42*, 157-168.

Higgins, A. K. (1989), North Greenland ice islands, *Polar Record*, *25*(154), 209-212.

Higgins, A. K. (1990), North Greenland glacier velocities and calf ice production, *Polarforschung*, *60*(1), 1-23.

Howat, I. M., J. E. Box, Y. Ahn, A. Herrington, and E. M. McFadden (2010), Seasonal variability in the dynamics of marine-terminating outlet glaciers in Greenland, *Journal of Glaciology*, *56*(198), 601-613.

Howat, I. M., and A. Eddy (2011), Multi-decadal retreat of Greenland's marine-terminating glaciers, *Journal of Glaciology*, *57*(203), 389-396.

Howat, I. M., I. Joughin, M. Fahnestock, B. E. Smith, and T. Scambos (2008), Synchronous retreat and acceleration of southeast Greenland outlet glaciers

2000-2006; Ice dynamics and coupling to climate, *Journal of Glaciology*, *54*(187), 1-14.

Howat, I. M., I. Joughin, and T. A. Scambos (2007), Rapid changes in ice discharge from Greenland outlet glaciers, *Science*, *315*(5818), 1559-1561.

Hughes (2002), Calving bays, *Quarternary Science Reviews*, *21*(1-3), 267-282.

Hughes, T. (1986), The Jakobshavns effect, *Geophysical Research Letters*, *13*(1), 46-48.

IPCC (2013), Climate Change 2013: The Physical Science Basis. Working Group I Contribution to the IPCC 5th Assessment Report. Online unedited version.

Jamieson, S. S. R., A. Vieli, S. J. Livingstone, C. Ó Cofaigh, C. R. Stokes, C.-D. Hillenbrand, and J. Dowdeswell (2012), Ice stream stability on a reverse bed slope, *Nature Geoscience*, *5*, 799-802.

Jenkins, A. (2011), Convection-Driven Melting near the Grounding Lines of Ice Shelves and Tidewater Glaciers, *Journal of Physical Oceanography*, *41*, 2279–2294.

Joughin, I., I. M. Howat, R. B. Alley, G. Ekström, M. Fahnestock, T. Moon, NettlesM., M. Truffer, and V. C. Tsai (2008a), Ice-front variation and tidewater behaviour on Helheim and Kangerdlugssuaq Glaciers, Greenland, *Journal of Geophysical Research*, *113*, F01004, doi:10.1029/2007JF000837.

Joughin, I., I. M. Howat, M. Fahnestock, B. Smith, W. Krabill, R. B. Alley, H. Stern, and M. Truffer. (2008b), Continued evolution of Jakobshavn Isbrae following its rapid speedup, *Journal of Geophysical Research*, *113*, F04006, doi:10.1029/2008JF001023.

Joughin, I., B. Smith, I. M. Howat, T. Scambos, and T. Moon (2010), Greenland flow variability from ice-sheet-wide velocity mapping, *Journal of Glaciology*, *56*(197), 415-430.

Khan, S. A., J. Wahr, M. Bevis, I. Velicogna, and K. E. (2010), Spread of ice mass loss into northwest Greenland observed by GRACE and GPS, *Geophysical Research Letters*, *37*, L06501, doi:10.1029/2010GL042460.

Lenaerts, J. T. M., J. H. van Angelen, M. R. van den Broeke, A. S. Gardner, B. Wouters, and E. van Meijgaard (2013), Irreversible mass loss of Canadian Arctic Archipelago glaciers, *Geophysical Research Letters*, *40*(5), 870-874, doi:10.1002/grl.50214.

McFadden, E. M., I. M. Howat, I. Joughin, B. Smith, and Y. Ahn (2011), Changes in the dynamics of marine terminating outlet glaciers in west Greenland (2000–2009), *Journal of Geophysical Research*, *116*, F02022.

Meier, M. F., and A. Post (1987), Fast tidewater glaciers, *Journal of Geophysical Research*, *92*, 9051–9058.

Mercer, J. H. (1968), Antarctic ice and Sangamon sea level rise, *IAHS Publ.*, *179*, 217–225

Moholdt, G., C. Nuth, J. O. Hagen, and J. Kohler (2010), Recent elevation changes of Svalbard glaciers derived from ICESat laser altimetry, *Remote Sensing of Environment*, *114*, 2756–2767.

Moholdt, G., B. Wouters, and A. S. Gardner (2012), Recent mass changes of glaciers in the Russian High Arctic, *Geophysical Research Letters*, *39*, L10502.

Moon, T., and I. Joughin (2008), Changes in ice-front position on Greenland's outlet glaciers from 1992 to 2007, *Journal of Geophysical Research*, *113*, F02022, doi:10.1029/2007JF000927.

Moon, T., I. Joughin, B. E. Smith, and I. M. Howat (2012), 21st-Century evolution of Greenland outlet glacier velocities, *Science*, *336*(6081), 576-578.

Motyka, R. J., M. Truffer, M. Fahnestock, J. Mortensen, S. Rysgaar, and I. M. Howat (2011), Submarine melting of the 1985 Jakobshavn Isbræ floating tongue and the triggering of the current retreat, *Journal of Geophysical Research*, *166*, F01007.

Murray, T., et al. (2010), Ocean regulation hypothesis for glacier dynamics in southeast Greenland and implications for ice sheet mass changes, *Journal of Geophysical Research*, *115*, F03026, doi:10.1029/2009JF001522.

Nick, F. M., A. Luckman, A. Vieli, C. J. van der Veen, D. van As, R. S. W. van de Wal, F. Pattyn, and D. Floricioiu (2012), The response of Petermann Glacier, Greenland, to large calving events, and its future stability in the context of atmospheric and oceanic warming, *Journal of Glaciology*, *58*(208), 229 - 239.

Nick, F. M., A. Vieli, M. L. Andersen, I. Joughin, A. J. Payne, T. L. Edwards, F. Pattyn, and R. S. W. van de Wal (2013), Future sea-level rise from Greenland's main outlet glaciers in a warming climate, *Nature*, *497*(7448), 235-238, doi:10.1038/nature12068.

Nick, F. M., A. Vieli, I. M. Howat, and I. Joughin (2009), Large-scale changes in Greenland outlet glacier dynamics triggered at the terminus, *Nature Geoscience*, *2*, 110-114.

Nuth, C., G. Moholdt, J. Kohler, J. O. Hagen, and A. Kääb (2010), Svalbard glacier elevation changes and contribution to sea level rise, *Journal of Geophysical Research*, *115*, F01008, doi:10.1029/2008JF001223.

O'Neel, S., W. T. Pfeffer, R. Krimmel, and M. Meier (2005), Evolving force balance at Columbia Glacier, Alaska, during its rapid retreat, *Journal of Geophysical Research*, *110*, F03012.

Pritchard, H. D., R. J. Arthern, D. G. Vaughan, and L. A. Edwards (2009), Extensive dynamic thinning on the margins of the Greenland and Antarctic ice sheets, *Nature*, *461*, 971-975.

Raymond, C. (1996), Shear margins in glaciers and ice sheets, *Journal of Glaciology*, *42*(140), 90-102.

Reeh, N. (1994), Calving from Greenland glaciers: Observations, balance estimates of calving rates, calving laws, in *Workshop on the calving rate of West Greenland glaciers in response to climate change, 13-15 September 1993, Copenhagen Denmark*, edited by N. Reeh, pp. 85-102, Danish Polar Center.

Reeh, N., C. Mayer, H. Miller, H. H. Thomsen, and A. Weidick (1999), Present and past climate control on fjord glaciations in Greenland: implications for IRD-deposition in the sea, *Geophysical Research Letters*, *26*(8), 1039-1042.

Reynolds, R. W., T. M. Smith, C. Liu, D. B. Chelton, K. S. Casey, and M. G. Schlax (2007), Daily High-Resolution-Blended Analyses for Sea Surface Temperature, *Journal of Climate*, *20*(22), 5473-5496, doi:10.1175/2007jcli1824.1.

Rignot, E., J. E. Box, E. Burgess, and E. Hanna (2008), Mass balance of the Greenland ice sheet from 1958 to 2007, *Geophysical Research Letters*, *35*, L20502, doi:10.1029/2008GL035417.

Rignot, E., M. Koppes, and I. Velicogna (2010), Rapid submarine melting of the calving faces of West Greenland glaciers, *Nature Geoscience*, *3*, 187-191, doi:10.1038/NGEO765.

Rignot, E., and K. Steffen (2008), Channelized bottom melting and stability of floating ice shelves, *Geophysical Research Letters*, *35*, L02503.

Rignot, E., I. Velicogna, M. Van den Broeke, A. Monaghan, and J. Lenaerts (2011), Acceleration of the contribution of the Greenland and Antarctic ice sheets to sea level rise, *Geophysical Research Letters*, *38*, L05503.

Seale, A., P. Christoffersen, R. Mugford, and M. O'Leary (2011), Ocean forcing of the Greenland Ice Sheet: Calving fronts and patterns of retreat identified by automatic satellite monitoring of eastern outlet glaciers, *Journal of Geophysical Research*, *116*(F3), F03013.

Shepherd, A., et al. (2012), A Reconciled Estimate of Ice-Sheet Mass Balance, *Science*, *338*(6111), 1183-1189, doi:10.1126/science.1228102.

Sohn, H. G., K. C. Jezek, and C. J. van der Veen (1998), Jakobshavn Glacier, West Greenland: 30 years of Spacebourne observations, *Geophysical Research Letters*, *25*(14), 2699-2702.

Straneo, F., et al. (2013), Challenges to Understanding the Dynamic Response of Greenland's Marine Terminating Glaciers to Oceanic and Atmospheric Forcing, *Bulletin of the American Meteorological Society*, *94*(8), 1131-1144, doi:10.1175/bams-d-12-00100.1.

Thomas, R. H., E. Frederick, J. Li, W. Krabill, S. Manizade, J. Paden, J. Sonntag, R. Swift, and J. Yungel (2011), Accelerating ice loss from the fastest Greenland and Antarctic glaciers, *Geophysical Research Letters*, *38*, L10502.

van den Broeke, M., J. Bamber, J. Ettema, E. Rignot, E. Schrama, W. J. van de Berg, E. van Meijgaard, I. Velicogna, and B. Wouters (2009), Partitioning Recent Greenland Mass Loss, *Science*, *326*, 984-986.

van der Veen, C. J., J. C. Plummer, and L. A. Stearns (2011), Controls on the recent speed-up of Jakobshavn Isbræ, West Greenland, *Journal of Glaciology*, *57*(204), 770–782.

Vieli, A., M. Funk, and H. Blatter (2001), Flow dynamics of tidewater glaciers: a numerical modelling approach, *Journal of Glaciology*, *47*(159), 595-606.

Vieli, A., J. A. Jania, and K. Lezek (2002), The retreat of a tidewater glacier: observations and model calculations on Hansbreen, Spitsbergen, *Journal of Glaciology*, *48*(163), 592-600.

Vieli, A., and F. M. Nick (2011), Understanding and modelling rapid dynamic changes of tidewater outlet glaciers: issues and implications, *Surveys in Geophysics*, *32*, 437-485.

Vinther, B. M., et al. (2009), Holocene thinning of the Greenland ice sheet, *Nature*, *461*(7262), 385-388, doi:http://www.nature.com/nature/journal/v461/n7262/suppinfo/nature08355_S1.html.

Warren, C. R., and N. F. Glasser (1992), Contrasting response of south Greenland glaciers to recent climatic change, *Arctic and Alpine Research*, *24*(2), 124-132.

Warren, C. R., and N. R. J. Hulton (1990), Topographic and glaciological controls on Holocene ice sheet margin dyanmics, central west Greenland, *Annals of Glaciology*, *14*, 307-310.

Weidick, A. (1995), Satellite Image Atlas of Glaciers of the World, Greenland, *USGS Professional Paper 1386-C, United States Government Printing Office, Washington.*

Weidick, A., H. Andreasen, H. Oerter, and N. Reeh (1994), Neoglacial glacier changes around Storstrømmen, North-east Greenland, *Polarforschung*, *64*(3), 95-108.

Xu, Y., E. Rignot, D. Menemenlis, and M. N. Koppes (2012), Numerical experiments on subaqueous melting of Greenland tidewater glaciers in response to ocean warming and enhanced subglacial discharge, *Annals of Glaciology*, *53*(60), 229–234.

Zwally, H. J., et al. (2011), Greenland ice sheet mass balance: distribution of increased mass loss with climate warming; 2003–07 versus 1992–2002, *Journal of Glaciology*, *57*(201), 88-102.

Chapter 7: Discussion

The following chapter summarises the main findings of the thesis, highlights key limitations and sets out primary directions for future research.

7.1. Outlet glacier retreat

A primary finding of the thesis is that widespread and rapid marine-terminating outlet glacier retreat has occurred across the Atlantic sector of the Arctic during the past two decades (Chapter 6). Retreat has accelerated, increasing five-fold between 1992-2000 and 2000-2010 (Chapter 6), and is consistent with the dramatic mass losses observed across the Arctic during the past decade [*Gardner et al.*, 2013; *Shepherd et al.*, 2012]. Arctic outlet glacier retreat has important implications for contemporary and near-future sea level rise, as it can contribute immediately through the loss of grounded ice, and at annual to decadal timescales via dynamic thinning. The importance of dynamic losses has been demonstrated by previous results from the Greenland Ice Sheet (GrIS) [e.g. *Howat et al.*, 2008; *Nick et al.*, 2013; *Pritchard et al.*, 2009; *Thomas et al.*, 2011; *Zwally et al.*, 2011], but little is known about its contribution to mass loss in other Arctic ice masses. This is highlighted by results from NVZ (Chapter 4), where retreat rates during the past decade have been an order of magnitude higher on marine-terminating outlets than on those which are land-terminating, yet no significant difference in thinning rates has been observed between the two types of basin. This suggests that we may be underestimating contemporary dynamic loss and/or that substantial loss may occur in the near-future, once dynamic loss begins (Chapter 4).

With the data currently available for NVZ, it is not possible to ascertain whether the lack of observed difference in thinning rates between marine- and land-terminating outlets is due to limited data coverage near glacier termini (where dynamic thinning would be greatest) or a result of limited and/or delayed response to retreat (Chapter 4). In order to distinguish between the two possible explanations and to fully investigate the dynamic response of NVZ outlet glaciers to frontal retreat, a number of approaches should be used. First, stereo-photogrammetry should be employed to construct digital

elevation models from satellite image pairs, in order to provide an independent and spatially comprehensive estimate of surface elevation change. Second, changes in outlet glacier velocities should be investigated, using either feature tracking or synthetic aperture radar interferometry, in order to identify any acceleration following retreat, which could then lead to dynamic thinning. Finally, a 3D numerical model should be used to simulate the response of land- and marine-terminating glaciers on NVZ to the observed frontal retreat. Thus, the timescale and magnitude of response of these glaciers to observed retreat could be quantified. This would allow for differentiation between the two possible explanations for the lack of observed dynamic response and would improve our capacity to forecast the contribution of ice losses from NVZ to near future sea level rise.

The rapid retreat observed across the Atlantic sector of the Arctic between 1992 and 2010 (Chapter 6) and the large uncertainties over the dynamic response of NVZ (Chapter 4) highlight the need to improve our understanding of the relative contribution of ice dynamics to mass loss outside of the GrIS. Numerical modelling should therefore be used to evaluate the time-scales required for glaciers located across the Atlantic Arctic to respond to forcing, both in terms of retreat and dynamic thinning, and the potential duration and magnitude of this response. This should be assessed for a range of glacier geometries and catchment areas, in order to investigate how glacier response times and the impact of changes in glacier dynamics varies between different Arctic ice masses. Furthermore, the committed contribution to sea level rise from recent glacier retreat should be evaluated. Together, this would help to predict the timing, pattern and magnitude of future sea level rise, resulting from changes in Arctic outlet glacier dynamics.

7.2. Spatial variation in external forcing factors

The project aim was to quantify marine-terminating outlet glacier retreat rates in the Atlantic sector of the Arctic between 1992 and 2010 and to evaluate the spatial variation in the primary factors controlling this retreat (Chapter 1). Results from the

specific study regions, namely north-west Greenland, Novaya Zemlya and Humboldt Glacier, provided some insight into the varying importance of different forcing factors. In north-west Greenland, both sea ice and air temperatures were identified as important controls on outlet glacier behaviour and results suggested that glacier sensitivity to forcing can evolve over time as the terminus transitions from floating to grounded (Chapter 3). Sea ice was identified as the predominant control on frontal positions on NVZ and retreat rates showed no correspondence to air temperatures (Chapter 4). In contrast, results from Humboldt Glacier suggest that the influence of sea ice is more limited and more complex, and that air temperatures were the dominant control (Chapter 5).

At the scale of the entire study region, certain patterns of retreat and response to forcing were apparent. Rapid glacier retreat in north- and central-west Greenland corresponded to marked sea ice decline (Chapter 6). The observed dramatic changes in forcing factors, rapid glacier retreat (Chapter 6), ice acceleration [*Moon et al.*, 2012] and mass loss [*Khan et al.*, 2010] in north-west Greenland during the past decade highlight the region as a key area for future study. In NVZ, changes in marine-terminating outlet glacier frontal position corresponded closely with interannual variations in sea ice concentrations (Chapter 4). However, no significant trend was apparent at decadal timescales, suggesting that glaciers are responding to years with anomalously low sea ice concentrations as opposed to a longer-term trend (Chapter 6). These results highlight the need to use high temporal resolution data when assessing the controls on marine-terminating outlet glacier behaviour in areas where forcing factors show substantial variation at interannual timescales.

Despite some regional-scale patterns, the relationship between regional forcing and regional retreat rates was not straightforward. For example, atmospheric warming was marked in western Greenland between 1990 and 1999, but no significant trends were apparent between 2000-2010, yet outlet glacier retreat rates were up to four time greater during the later period (Chapter 6). In NVZ, there was an overall mean

difference in retreat between the Kara (40.8 m a^{-1}) and Barents Sea (61.7 m a^{-1}) coasts between 1992 and 2010, but this was relatively small, given the large differences in climatic and oceanic conditions between the two coasts (Chapter 5). FJL experienced large changes in sea ice and sea surface temperatures, yet retreat rates were low compared to other regions (Chapter 6). In contrast, northern Greenland exhibited the highest and most variable retreat rates, despite no observed change in external forcing (Chapter 6). Furthermore, there was marked variability in the response of individual glaciers to forcing, even in areas which showed an overall trend, such as central- and north-west Greenland and Novaya Zemlya (Chapters 3, 4 & 6). Taken together, these results suggest that some regional-scale patterns of glacier response to external forcing are apparent, but that these relationships are far from universal and in certain areas, such as northern Greenland and FJL, the primary controls on outlet glacier retreat have yet to be identified. This highlights the need for further research in these regions, particularly northern Greenland, given its potential for rapid retreat and substantial ice loss (Chapter 6).

A key limitation that has emerged from all elements of the project is the lack of detailed oceanographic data from major outlet glacier fjords, both on the GrIS (Chapters 3 & 5) and other Arctic ice masses (Chapters 4 & 6). This results in substantial uncertainties over the influence of deeper ocean temperatures on glacier behaviour, including: i) the relative contribution of sub-surface warming and submarine melting to glacier retreat in different regions of the Arctic; ii) the access of Atlantic water to outlet glacier termini; and iii) the potential feedbacks between enhanced submarine melting, plume flow and glacier runoff. Significant progress has been made in understanding these controls in recent years, through a combination of numerical modelling and direct observations [*Jenkins*, 2011; *Motyka et al.*, 2011; *Rignot et al.*, 2010; *Straneo et al.*, 2011; *Straneo et al.*, 2010; *Straneo et al.*, 2013; *Xu et al.*, 2013]. However, data are presently only available for a limited number of Greenland outlet glacier fjords and for a very short time period. Consequently, our knowledge of how the influence of sub-surface warming

varies between different oceanographic settings, different glacier geometries and different fjord shapes is limited. Given its potentially strong influence on glacier behaviour, there is an urgent need to collect detailed oceanographic data from outlet glacier fjords and to integrate this information into numerical models.

Atmospheric circulation and storm events provide potentially important links between oceanic and atmospheric warming and outlet glacier behaviour, but have received comparatively little consideration to date. Previous work has demonstrated that these factors may influence sea ice extent [*Parkinson and Comiso*, 2013], access of warm AW into glacier fjords [e.g. *Straneo et al.*, 2011; *Straneo et al.*, 2010] and ice sheet mass balance [e.g. *Hanna et al.*, 2014], which all have the potential to influence outlet glacier dynamics. However, our ability to fully investigate the impact of storms and wind patterns at the scale of individual glaciers or groups of glaciers is currently limited by data availability, with the main data sources being meteorological stations of climate re-analysis data. The former offer high temporal resolution information at particular locations, but stations are usually sparsely distributed, particularly in inaccessible regions such as the Russian High Arctic, and there are significant issues with extrapolating beyond their local topographic and climatic setting. Re-analysis data provide comprehensive spatial coverage, but have a coarse spatial resolution that does not adequately capture the complex wind patterns that would occur over the ice sheet [*Gorter et al.*, 2014] and within the complex topography of Arctic outlet glacier fjords.

Regional Climate Models, such as the Regional Atmospheric Climate Model version 2.1 (RACMO2) (11 km resolution) [*Van Meijgaard et al.*, 2008], Modèle Atmosphérique Régional (MAR) (25 km resolution) [*Franco et al.*, 2013], and the Polar MM5 (24 km resolution) [*Box et al.*, 2009] offer a higher spatial resolution alternative and should therefore be used in future work to investigate the potential impact of winds and storms on outlet glacier behaviour. However, it should be noted that the spatial resolution of these models ranges between 11 and 25 km, which is still relatively coarse in comparison to the width of Arctic outlet glaciers fjords, which is usually in the order of a

few kilometres. Consequently, even higher resolution, glacier specific models may be needed in order to fully quantify the complex interaction of atmospheric circulation and storms with fjord topography, fjord water properties and glacier dynamics.

One possible approach to assessing outlet glacier response to external forcing is the use of multivariate statistics to determine statistically significant relationships between glacier retreat and multiple controls. However, this is complicated by a number of factors. First, data availability means that, on a given glacier, data on forcing factors and glacier frontal positions area rarely available for exactly the same period or on the same date. Equally, data availability and acquisition dates vary between individual glaciers and regions and over time, with frontal position data in particular becoming increasingly sparse further back in history. These inconsistencies in acquisition dates and the spatial and temporal data coverage require that interpolation is carried out prior to the application of multivariate statistics, but this is complex and potentially inappropriate for data series such as glacier frontal position, which is likely to fluctuate at a variety of timescales.

Further to issues relating to data availability, frontal position at a given point in time is a function of previous forcing, but it is difficult to establish the time scale over which a given forcing factor and even a specific mechanism impacts on glacier behaviour. For example, air temperature warming may influence frontal position via meltwater enhanced hydrofracture and the effects may be immediate (e.g. by water draining into a crevasse proximal to the terminus and thus causing a calving event), at seasonal to interannual timescales (e.g. by opening an inland crevasse, which forms a weakness and calves once the ice reaches the terminus) or even decadal timescales (e.g. if hydrofracture moves the terminus beyond a stable position and initiates a series of positive feedbacks). This makes any statistical analysis very complex, as it would need to assess the statistical relationship between glacier frontal position at a given point in time with previous forcing at a wide range of timescales. Finally, each forcing factor is interlinked, meaning that it may not always be possible to identify a dominant cause

statistically. For example, if subglacial meltwater plume outflow were the main driver of retreat, we would expect glacier frontal position to correlate with air temperatures (via increased meltwater inputs), ocean temperatures (due to the ambient water temperature) and sea ice (which could be melted by the plume).

As a consequence of the complications associated with the data, a new method of time series analysis would need to be developed in order to evaluate the relationship between forcing factors and frontal position using a multivariate statistical approach. However, even if this technique were developed, a fundamental limitation is that correlation does not equate to causality and it does not provide information on the mechanisms by which a given factor causes frontal position change. As a result, a better approach to understanding the causes of outlet glacier retreat may be to use observational data and basic statistical analysis to identify potential relationships, which can then be further evaluated via the use of numerical modelling, which allows the processes involved to be investigated.

7.3. Glacier-specific factors

Results from all sections of the project demonstrated large variability in retreat rates at all spatial scales, ranging from a single glacier in the case of Humboldt Glacier (Chapter 5), to variability within regions (Chapters 3, 4 & 6) and finally variation across the Atlantic sector of the Arctic (Chapter 6). Results indicate that this variability resulted from glacier-specific factors (Chapters 3 to 6), particularly fjord width variation and basal topography. A primary conclusion of the project was that these local controls can strongly modulate the response of individual glaciers to external forcing. This has very important implications, as it suggests that glacier behaviour cannot be forecast on the basis of climatic or oceanic change alone, but instead glacier-specific factors must also be considered.

This project demonstrated the strong influence of fjord width variability on glacier retreat rates, both within specific study regions (Chapters 3 & 5) and across the Atlantic

sector of the Arctic (Chapter 6). Consequently, results suggest that fjord width variability may provide a widely-applicable indicator for rapid retreat. In order to further explore this relationship, empirical categories of fjord width variability were defined using data from Novaya Zemlya (Chapter 4). It is hoped that these categories will be a useful framework for assessing glacier retreat elsewhere in the Arctic and will provide an initial insight into the different ways in which fjord width variation can influence glacier dynamics. This should be evaluated more fully in the future, using numerical models which account for stress terms in 2 horizontal dimensions [e.g. *Gudmundsson et al.*, 2012]. In this way, glacier response to forcing could be assessed for each of the categories of fjord width variation defined in Chapter 4. This could be expanded to include different magnitudes and types of perturbation (e.g. sea ice buttressing, increased crevasse water depth) and to assess the varying impact of fjord width on a range of glacier geometries. This would provide us with a more comprehensive understanding of how fjord width variation modulates glacier response to forcing and how this control varies across the Arctic.

The project highlighted the lack of detailed data on subglacial topography and fjord bathymetry for the majority of Arctic outlet glaciers as a primary limitation to our understanding of glacier-specific controls. Results from Humboldt Glacier demonstrated that the presence of a bedrock trough has the potential to cause an order of magnitude difference in glacier retreat rates and ice velocities (Chapter 5) and the potential impact of basal topography on glacier behaviour has long been recognised [*Meier and Post*, 1987; *Weertman*, 1974]. However, very little is known about the basal topography of the majority of Arctic outlet glaciers (Chapters 3, 4, & 6) and extrapolating relationships based on observations observed at only a few glaciers is potentially dangerous. This underscores the need to acquire bathymetric and basal topographic data for major outlet glaciers located on each of the main Arctic ice masses. This will help to address a number of key uncertainties relating to the influence of basal topography on outlet glacier retreat rates, including: i) its spatial

variation between different Arctic regions; ii) its importance relative to external controls and fjord width variation; and iii) its varying influence on glaciers of different sizes and geometries. Basal topographic controls should also be explored through numerical modelling and should be assessed in combination with fjord width variability, in order to identify the fjord geometries which may predispose Arctic outlet glaciers to rapid retreat.

7.4. Numerical modelling

Our capacity to model the dynamic behaviour of marine-terminating Arctic outlet glaciers has improved substantially in recent years and has contributed markedly to our understanding of their response to forcing [e.g. *Nick et al.*, 2012; *Nick et al.*, 2010; *Nick et al.*, 2013; *Nick et al.*, 2009; *Vieli and Nick*, 2011]. As a result, we can now forecast the response of major Greenland outlet glaciers to future climate change and estimate their potential sea level rise contribution [*Nick et al.*, 2013]. However, these models use highly simplified geometries (i.e. 1 horizontal dimension) and calving parametrizations, and their applications have focused on comparatively few, albeit important, outlet glaciers that are mostly located on the GrIS. Given the marked variability in glacier retreat rates and response to forcing observed from remotely sensed data (Chapters 3-6), a key direction for future research is to apply these numerical models to glaciers located in other Arctic regions. This would allow us to evaluate how glacier response to forcing varies between different ice masses, different glaciological settings and different climatic/oceanic regimes. It would therefore provide a broader understanding of the potential response of Arctic outlet glaciers to climate change.

On the basis of the limitations highlighted above, a number of areas for future numerical modelling work have emerged. First, the treatment of dynamic calving in models should be extended from the current 1-dimensional models into 2- or 3-dimensions, in order to fully represent the influence of fjord geometry and sea ice buttressing on outlet glacier dynamics. Second, numerical modelling should be used to assess glacier response times and committed thinning due to recent retreat, for a

range of glacier geometries and locations across the Arctic (Section 7.1). This will help to assess the near-future dynamic contribution of Arctic ice masses to sea level rise. Third, In order to improve our understanding of the primary forcing factors at the calving front, plume circulation and the associated submarine melting should be incorporated into flowline models (Section 7.2). This is a potentially key control on outlet glacier retreat rates [*Motyka et al.*, 2011; *Straneo et al.*, 2011; *Xu et al.*, 2013], but is not yet incorporated into the flowline models that are used to assess glacier response to forcing.

The influence of sea ice on glacier behaviour has been documented empirically [e.g. *Amundson et al.*, 2010; *Carr et al.*, 2014; *Joughin et al.*, 2008], but has not been extensively assessed for different glacier sizes, fjord configurations and/or different sea ice regimes. Future work should therefore use numerical modelling to assess the impact of changes in sea ice duration and concentration on glaciers of different sizes and with different fjord geometries. The range of values used could be constrained using remotely sensed data. As detailed in Section 7.3, fjord width variation and basal topography appear to be key controls on outlet glacier retreat rates and numerical modelling should therefore be used to evaluate which combination(s) of these factors predisposes outlet glaciers to rapid retreat. Finally, outlet glacier dynamics are not yet adequately included in ice sheet scale numerical models [*Price et al.*, 2011; *Vieli and Nick*, 2011; *Zwally et al.*, 2011], which represents a major challenge for future numerical modelling work.

7.5. References

Amundson, J. M., M. Fahnestock, M. Truffer, J. Brown, M. P. Lüthi, and R. J. Motyka (2010), Ice mélange dynamics and implications for terminus stability, Jakobshavn Isbræ, Greenland, *Journal of Geophysical Research*, *115*, F01005, doi:10.1029/2009JF001405.

Box, J. E., L. Yang, D. H. Bromwich, and L. S. Bai (2009), Greenland Ice Sheet Surface Air Temperature Variability: 1840–2007, *Journal of Climate*, *22*, 4029-4049.

Carr, J. R., C. Stokes, and A. Vieli (2014), Recent retreat of major outlet glaciers on Novaya Zemlya, Russian Arctic, influenced by fjord geometry and sea-ice conditions, *Journal of Glaciology*, *60*, 155-170.

Franco, B., X. Fettweis, and M. Erpicum (2013), Future projections of the Greenland ice sheet energy balance driving the surface melt, *The Cryosphere*, *7*(1), 1-18, doi:10.5194/tc-7-1-2013.

Gardner, A., et al. (2013), A Reconciled Estimate of Glacier Contributions to Sea Level Rise: 2003 to 2009, *Science*, *340*(6134), 852-857, doi:10.1126/science.1234532.

Gorter, W., J. H. van Angelen, J. T. M. Lenaerts, and M. R. van den Broeke (2014), Present and future near-surface wind climate of Greenland from high resolution regional climate modelling, *Climate Dynamics*, *42*(5-6), 1595-1611, doi:10.1007/s00382-013-1861-2.

Gudmundsson, G. H., J. Krug, G. Durand, L. Favier, and O. Gagliardini (2012), The stability of grounding lines on retrograde slopes, *The Cryosphere Discussions*, *6*, 2597–2619.

Hanna, E., X. Fettweis, S. H. Mernild, J. Cappelen, M. H. Ribergaard, C. A. Shuman, K. Steffen, L. Wood, and T. L. Mote (2014), Atmospheric and oceanic climate forcing of the exceptional Greenland ice sheet surface melt in summer 2012, *International Journal of Climatology*, *34*(4), 1022-1037, doi:10.1002/joc.3743.

Howat, I. M., I. Joughin, M. Fahnestock, B. E. Smith, and T. Scambos (2008), Synchronous retreat and acceleration of southeast Greenland outlet glaciers 2000-2006; Ice dynamics and coupling to climate, *Journal of Glaciology*, *54*(187), 1-14.

Jenkins, A. (2011), Convection-Driven Melting near the Grounding Lines of Ice Shelves and Tidewater Glaciers, *Journal of Physical Oceanography*, *41*, 2279–2294.

Joughin, I., I. M. Howat, M. Fahnestock, B. Smith, W. Krabill, R. B. Alley, H. Stern, and M. Truffer. (2008), Continued evolution of Jakobshavn Isbrae following its rapid speedup, *Journal of Geophysical Research*, *113*, F04006, doi:10.1029/2008JF001023.

Khan, S. A., J. Wahr, M. Bevis, I. Velicogna, and K. E. (2010), Spread of ice mass loss into northwest Greenland observed by GRACE and GPS, *Geophysical Research Letters*, *37*, L06501, doi:10.1029/2010GL042460.

Meier, M. F., and A. Post (1987), Fast tidewater glaciers, *Journal of Geophysical Research*, *92*, 9051–9058.

Moon, T., I. Joughin, B. E. Smith, and I. M. Howat (2012), 21st-Century evolution of Greenland outlet glacier velocities, *Science*, *336*(6081), 576-578.

Motyka, R. J., M. Truffer, M. Fahnestock, J. Mortensen, S. Rysgaar, and I. M. Howat (2011), Submarine melting of the 1985 Jakobshavn Isbræ floating tongue and the triggering of the current retreat, *Journal of Geophysical Research*, *166*, F01007.

Nick, F. M., A. Luckman, A. Vieli, C. J. van der Veen, D. van As, R. S. W. van de Wal, F. Pattyn, and D. Floricioiu (2012), The response of Petermann Glacier, Greenland, to large calving events, and its future stability in the context of atmospheric and oceanic warming, *Journal of Glaciology*, *58*(208), 229 - 239.

Nick, F. M., C. J. van der Veen, A. Vieli, and D. I. Benn (2010), A physically based calving model applied to marine outlet glaciers and implications for the glacier dynamics, *Journal of Geophysical Research*, *56*(199), 781-794.

Nick, F. M., A. Vieli, M. L. Andersen, I. Joughin, A. J. Payne, T. L. Edwards, F. Pattyn, and R. S. W. van de Wal (2013), Future sea-level rise from Greenland's main outlet glaciers in a warming climate, *Nature*, *497*(7448), 235-238, doi:10.1038/nature12068.

Nick, F. M., A. Vieli, I. M. Howat, and I. Joughin (2009), Large-scale changes in Greenland outlet glacier dynamics triggered at the terminus, *Nature Geoscience*, *2*, 110-114.

Parkinson, C. L., and J. C. Comiso (2013), On the 2012 record low Arctic sea ice cover: Combined impact of preconditioning and an August storm, *Geophysical Research Letters*, *40*(7), 1356-1361, doi:10.1002/grl.50349.

Price, S., A. J. Payne, I. M. Howat, and B. Smith (2011), Committed sea-level rise for the next century from Greenland ice sheet dynamics during the past decade, *Proceedings of the National Academy of Sciences*, *108*(22), 8978-8983.

Pritchard, H. D., R. J. Arthern, D. G. Vaughan, and L. A. Edwards (2009), Extensive dynamic thinning on the margins of the Greenland and Antarctic ice sheets, *Nature*, *461*, 971-975.

Rignot, E., M. Koppes, and I. Velicogna (2010), Rapid submarine melting of the calving faces of West Greenland glaciers, *Nature Geoscience*, *3*, 187-191, doi:10.1038/NGEO765.

Shepherd, A., et al. (2012), A Reconciled Estimate of Ice-Sheet Mass Balance, *Science*, *338*(6111), 1183-1189, doi:10.1126/science.1228102.

Straneo, F., R. G. Curry, D. A. Sutherland, G. S. Hamltion, C. Cenedese, K. Våge, and L. A. Stearns (2011), Impact of fjord dynamics and glacial runoff on the circulation near Helheim Glacier, *Nature Geoscience*, *4*, 322-327.

Straneo, F., G. S. Hamilton, D. A. Sutherland, L. A. Stearns, F. Davidson, M. O. Hammill, G. B. Stenson, and A. R. Asvid (2010), Rapid circulation of warm subtropical waters in a major glacial fjord in East Greenland, *Nature Geoscience*, *3*, 182-186, doi:10.1038/NGEO764.

Straneo, F., et al. (2013), Challenges to Understanding the Dynamic Response of Greenland's Marine Terminating Glaciers to Oceanic and Atmospheric Forcing, *Bulletin of the American Meteorological Society*, *94*(8), 1131-1144, doi:10.1175/bams-d-12-00100.1.

Thomas, R. H., E. Frederick, J. Li, W. Krabill, S. Manizade, J. Paden, J. Sonntag, R. Swift, and J. Yungel (2011), Accelerating ice loss from the fastest Greenland and Antarctic glaciers, *Geophysical Research Letters*, *38*, L10502.

Van Meijgaard, E., L. H. Van Ulft, W. J. Van de Berg, F. C. Bosveld, B. J. J. M. Van den Hurk, G. Lenderink, and A. P. Siebesma (2008), The KNMI regional atmospheric climate model RACMO version 2.1., *Technical Report TR-302, Royal Netherlands Meteorological Institute, De Bilt, The Netherlands*.

Vieli, A., and F. M. Nick (2011), Understanding and modelling rapid dynamic changes of tidewater outlet glaciers: issues and implications, *Surveys in Geophysics*, *32*, 437-485.

Weertman, J. (1974), Stability of the junction of an ice sheet and an ice shelf, *Journal of Glaciology*, *13*(67), 3-11.

Xu, Y., E. Rignot, I. Fenty, D. Menemenlis, and M. M. Flexas (2013), Subaqueous melting of Store Glacier, west Greenland from three-dimensional, high-resolution numerical modeling and ocean observations, *Geophysical Research Letters*, *40*(17), 4648-4653, doi:10.1002/grl.50825.

Zwally, H. J., et al. (2011), Greenland ice sheet mass balance: distribution of increased mass loss with climate warming; 2003–07 versus 1992–2002, *Journal of Glaciology*, *57*(201), 88-102.

Chapter 8: Conclusions

Results demonstrated widespread and rapid retreat on marine-terminating Arctic outlet glaciers between 1992 and 2010. In north-west Greenland, we observed very rapid retreat on Alison Glacier, which totalled almost 10 km in four years and followed 25 years of limited change. This coincided with large increases in air temperatures and marked sea ice decline, but the response of individual study glaciers varied substantially. We linked this variable response to forcing to differences in the specific characteristics of each glacier, particularly fjord width variation and basal topography. On Novaya Zemlya, Russian High Arctic, we documented rapid outlet glacier retreat, which accelerated from 2000 and coincided with reduced sea ice concentrations. Retreat rates were an order of magnitude greater on marine-terminating glaciers than on their land-terminating counterparts, but there was no significant difference in thinning rates between these two types of basin. This suggests that we may be underestimating the contribution of dynamic changes to contemporary and/or future mass loss within the region. Despite an overall trend, retreat rates varied markedly between individual glaciers and we demonstrated a statically significant relationship between fjord width variation and total retreat. Using empirical evidence from the region, we defined primary classes of the influence of fjord width variation on glacier retreat, which may be used to interpret glacier retreat rates in other regions.

The influence of basal topography on the dynamic behaviour of contemporary Arctic outlet glaciers was investigated at Humboldt Glacier, northern Greenland. Humboldt Glacier retreated rapidly from 1999 onwards, coincident with atmospheric warming and sea ice decline. However, we observed an order of magnitude difference in retreat rates between the northern and southern sections of the terminus, despite the same apparent initial forcing. We attributed this differing sensitivity to forcing to a major basal trough beneath the northern section, which extends up to 72 km inland and may therefore continue to facilitate sustained and substantial retreat from Humboldt Glacier during the 21st century. Overall, results from Humboldt Glacier demonstrated the

potential for basal topography to generate order of magnitude differences in retreat rates and ice velocities.

Finally, we documented rapid and accelerating outlet glacier retreat across the Atlantic sector of the Arctic for the period 1992 to 2010, with 95% of all study glaciers retreating between 2000 and 2010. Retreat rates were highest in northern, western and south-eastern Greenland but varied markedly between individual outlets. We observed some regional-scale correspondence between outlet glacier retreat and changes in external forcing, but this relationship was far from universal. Instead, results suggest that fjord width variability was a widespread control on outlet glacier retreat rates, particularly marked in areas where outlet glacier flow was constrained by fjord topography. Importantly, this suggests that retreat rates cannot be forecast solely from changes in external forcing factors but must be assessed in relation to glacier-specific controls.

We highlight a number of key directions for future research, namely: i) assessing the relative contribution of ice dynamics to mass loss outside of the Greenland Ice Sheet; ii) collecting temperature and salinity data from major Arctic outlet glacier fjords and incorporating plume flow into glacier models; iii) acquiring high resolution information on the basal topography and fjord bathymetry of major outlet glaciers; and iv) using numerical modelling to further our understanding of glacier response to external and glacier specific controls, both on the Greenland Ice Sheet and on other Arctic ice masses. Furthermore, we underscore the need for further study in north-west Greenland, given the dramatic climatic and glaciological changes observed in the region during the past decade, and in northern Greenland, as the area is undergoing rapid and highly variable retreat, but the factors driving these losses remain unclear. Overall, our results document rapid outlet glacier retreat across the Arctic during the past two decades and highlight the need for continuing research into the dynamic response of Arctic ice masses to climate change.